OPERATIONALLY RESPONSIVE SPACECRAFT USING ELECTRIC PROPULSION

DISSERTATION

Thomas C. Co, Captain, USAF

AFIT/DS/ENY/12-01

DEPARTMENT OF THE AIR FORCE
AIR UNIVERSITY

AIR FORCE INSTITUTE OF TECHNOLOGY

Wright-Patterson Air Force Base, Ohio

The views expressed in this dissertation are those of the author and do not reflect the official policy or position of the United States Air Force, Department of Defense, or the U.S. Government.

AFIT/DS/ENY/12-01

OPERATIONALLY RESPONSIVE SPACECRAFT USING ELECTRIC PROPULSION

DISSERTATION

Presented to the Faculty

Department of Aeronautical and Astronautical Engineering

Graduate School of Engineering and Management

Air Force Institute of Technology

Air University

Air Education and Training Command

In Partial Fulfillment of the Requirements for the

Degree of Doctor of Philosophy in Aeronautical Engineering

Thomas C. Co, MS

Captain, USAF

Sept 2012

APPROVED FOR PUBLIC RELEASE; DISTRIBUTION IS UNLIMITED

AFIT/DS/ENY/12-01

OPERATIONALLY RESPONSIVE SPACECRAFT USING ELECTRIC PROPULSION

Thomas C. Co, MS
Captain, USAF

Approved:

//SIGNED//	_____
Jonathan T. Black, PhD (Chairman)	Date
//SIGNED//	_____
Lt Col Ronald Simmons, PhD (Member)	Date
//SIGNED//	_____
Eric D. Swenson, PhD (Member)	Date
//SIGNED//	_____
David R. Jacques, PhD (Member)	Date

Accepted:

//SIGNED//	_____
M. U. THOMAS	Date
Dean, Graduate School of Engineering and Management	

Abstract

A desirable space asset is responsive and flexible to mission requirements, low-cost, and easy to acquire. Highly-efficient electric thrusters have been considered a viable technology to provide these characteristics; however, it has been plagued by limitations and challenges such that operational implementation has been severely limited. Many studies exist detailing the possible applications of the proposed responsive electric propulsion (EP) space system; however, none address the responsiveness achieved by modifying a satellite's ground track to arrive over a desired target at a user-defined time and altitude. This research develops the necessary algorithm and tools to demonstrate that EP systems can maneuver significantly in a timely fashion to overfly any target within the satellite's coverage area. An in-depth analysis of a reconnaissance mission reveals the potential the proposed spacecraft holds in today's competitive, congested, and contested environment. Using Space Mission Analysis and Design concepts along with the developed algorithm, an observation mission is designed for three conventional methods and compared to the proposed responsive system. Analysis strongly supports that such a spacecraft is capable of reliable target overflight at the same cost as non-maneuvering ones, while it is three times as responsive in terms of time-to-overflight by sacrificing one third of its mission life. An electric versus a chemical system can maneuver 5.3 times more. Its responsiveness and mission life are slightly inferior to that of a Walker constellation, but cuts total system cost by almost 70%.

To my Wife and Kids

Acknowledgments

Enormous gratitude goes to Dr. Jon Black for the countless meetings and valuable guidance to define and scope the problem. His constant push to publish my work resulted in the following document. His positive attitude pulled me through the countless low points of the past three years and his encouragement always re-energized my interest in this problem. I want to also thank Lt Col Simmons for keeping me on my toes and reminding me how "trivial" my work really is. On a more serious note, he provided the technical direction and helped me realize that the solution was already there, though I could not recognize it. I truly appreciate both mentors reading every single paper and providing valuable, constructive, and sometimes blunt feedback. Thanks also to Dr. Eric Swenson and Dr. David Jacques for their comments. My sincere appreciation goes to Costas Zagaris for working countless hours together on many of these equations, concepts, and thoughts; sharing the joy of triumph when a solution converged; and feeling defeated when the problem seemed impossible to solve.

Thomas C. Co

Table of Contents

Abstract v
Acknowledgments vii
List of Figures xii
List of Tables xv
1 Introduction 1
2 Literature Review 2-1
2.1 Continuous Thrust Maneuver 2-2
2.1.1 Electric Propulsion. 2-2
2.1.2 Cost Savings and Benefits of Electric Propulsion. 2-7
2.1.3 Maneuvering Algorithms. 2-9
2.2 Operationally Responsive Space 2-12
2.3 Impulsive Thrust 2-21
2.3.1 Survey Missions. 2-21
2.3.2 Planetary Flyby (Lunar-Gravity Assist). 2-25
2.4 Atmospheric Maneuver 2-28
2.4.1 Space Plane. 2-28
2.4.2 Aero-Assist. 2-30
3 Motivation 3-1
3.1 Newberry's Responsive Space System 3-1
3.2 Initial Modeling & Analysis 3-7
3.3 Expanding the Idea of Responsive Space Systems 3-14
4 A Taskable Space Vehicle 4-1
4.1 Introduction 4-1
4.2 Operationally Responsive Space 4-3
4.3 Meeting User Needs with a Maneuverable Asset 4-6
4.4 Concept Design and Results 4-10
4.5 Conclusion 4-12

5 Responsive Satellites through Ground Track Manipulation using Existing Technology 5-1

5.1 Introduction 5-4

5.2 System Models 5-8

Metric: Terrestrial Distance. 5-14

5.3 Model Setup 5-16

5.4 Classical Orbital Elements' Effects on Maneuverability 5-19

5.5 Maneuverability with Chemical Propulsion Systems 5-28

5.6 Maneuverability with Electric Propulsion Systems 5-32

5.7 Comparison of CP vs. EP 5-37

5.8 Application 5-39

5.9 Conclusion 5-41

6 Optimal Low Thrust Profiles for Responsive Satellites 6-1

6.1 Introduction 6-4

6.2 System Models 6-8

Defining Target Location. 6-11

6.3 Analytical Solutions 6-12

6.4 Results and Discussion 6-15

6.4.1 Scenario 1 – In-plane, Phasing Maneuver. 6-16

6.4.2 Scenario 2 – In-plane, Unrestricted Maneuver. 6-18

6.4.3 Scenario 3 – Out-of-plane, Δi Maneuver 6-20

6.4.4 Scenario 4 – Out-of-plane, $\Delta\Omega$ Maneuver. 6-22

6.4.5 Scenario 5 – Combination In-Plane and Out-of-plane Maneuver. . 6-24

6.4.6 Thrust-Coast Maneuver. 6-26

6.5 Conclusion 6-27

7 Responsiveness in Low Orbits using Electric Propulsion 7-1

7.1 Introduction 7-4

7.2 System Model 7-8

7.3 Control Algorithm 7-12

7.4 Global Reach 7-15

7.5 Affecting Arrival Time 7-17

7.6 Out-of-Plane Maneuvers 7-19

7.7 Results and Discussion 7-22

7.7.1 Thrust-Coast Period. 7-23

7.7.2 Arrival Time. 7-24

7.7.3 System Life. 7-25

7.7.4 Operational Application. 7-26

7.8 Conclusion 7-29

8 Comparison of Electric Propulsion Maneuvers to Conventional Observation Missions 8-1

8.1 Introduction 8-2

8.2 Traditional Mission vs. Electric Propulsion 8-10

8.2.1 Walker Constellation. 8-10

8.2.2 Single Non-Maneuvering Satellite. 8-13

8.2.3 Single Maneuvering Satellite (Chemical). 8-17

8.2.4 Single Maneuvering Satellite (Electric). 8-19

8.3 Compare and Contrast 8-20

8.4 Conclusion 8-27

9 Conclusion 9-1
A. Appendix A – Nomenclature A-1
B. Appendix B – 2-Body Assumption B-1
C. Appendix C – CP Reachability C-1
D. Appendix D – EP Reachability D-1
E. Appendix E – Global Coverage E-1
F. Appendix F – Target Overflight F-1
G. Appendix G – Walker Constellation G-1
H. Appendix H – Single Static Satellite H-1
I. Appendix I – Single Maneuvering CP Satellite I-1
J. Appendix J – Single Maneuvering EP Satellite J-1
Bibliography 10-1
Vita 11-1

List of Figures

Figure Page

2-1. Responsive Space Literature Review Research Areas 2-1

2-2. Delta Walker Constellations (AVM Dynamics) 2-14

2-3. High Circular and Elliptical Constellations (AVM Dynamics) 2-15

2-4. "Streets of Coverage" in Polar Orbit (Larrimore, 2005: 7) 2-19

2-5. Multi-chained, inclined "Streets of Coverage" (Larrimore, 2005: 9) 2-20

2-6. NanoEye Maneuvering, Electro-optical Satellite Concept 2-23

2-7. Diagram of Lunar Free Return (Mathur, 2010: 6) 2-27

2-8. Multiple Skip Trajectory for Two Entry Angles (Vinh, 1997: 105) 2-32

2-9. Characteristic Velocities vs. Rotation Angle (Vinh, 1997: 110) 2-34

2-10. LEO to LEO Aero-assisted Orbital Transfer (Rao, 2008) 2-35

2-11. ΔV for Aero-assisted & Impulsive Transfer vs Δi (Rao, 2008) 2-37

3-1. Time over Target (TOT) Control 3-5

3-2. TOT Performance based on Lead Time (Newberry, 2005: 49) 3-6

3-3. TOT Control vs. Time for a Circular Orbit ($e = 0$) 3-8

3-4. TOT Control vs. Time for an Eccentric Orbit ($e = 0.5$) 3-9

3-5. TOT Control vs. Time for an Eccentric orbit ($e = 0.7$) 3-10

3-6. TOT Control vs. Eccentricity 3-11

3-7. TOT Control vs. RAAN 3-12

3-8. TOT Control vs. True Anomaly 3-12

5-1. TOT Performance vs. Lead Time for Maneuvering (Newberry, 2005) 5-7

Figure Page

5-2 a-c. Distance between a Maneuvering Satellite and Reference 5-15

5-3. Effect of Varying Thrusting Period on Distance 5-21

5-4. Effect of Varying Initial Inclination on Distance 5-22

5-5 a-c. Ground Tracks of Maneuvering and Reference Satellites 5-24

5-6. Effect of Varying Initial Altitude on Distance 5-25

5-7. Effect of Varying Initial Eccentricity on Distance 5-27

5-8. Distance Regression for ΔV of 0.01 km/s CP 5-30

5-9. Distance Regression for ΔV of 0.01 km/s EP. 5-33

5-10. Distance Regression for Continuous Thrusting EP 5-36

5-11 a-c. Distance Required to Move Reference Ground Track over Target 5-40

6-1. Acceleration Vector and Control Angles 6-9

6-2. Control Inputs and States of Optimal Solution, Scenario 1 6-17

6-3. Ground Track and Target Location, Scenario 1 6-17

6-4. Control Inputs and States of Optimal Solution for Scenario 2. 6-19

6-5. Ground Track and Target Location, Scenario 2 6-19

6-6. Control Angle and States, Scenario 3 6-21

6-7. Ground Track and Final Positions, Scenario 3 6-21

6-8. Control Angle and States, Scenario 4 6-23

6-9. Ground Track and Final Positions, Scenario 4 6-23

6-10. Control Angle and States, Scenario 5 6-25

6-11. Ground Track and Final Positions, Scenario 5 6-25

7-1. Flowchart to solve for Ground Target Overflight 7-13

Figure Page

7-2. Control of Δt to Shift Ground Track 7-14

7-3. Target Overflight in a Subsequent Pass 7-16

7-4. Global Reach for EP at Different Altitudes 7-17

7-5. Arrival Times based on Opportunities 7-18

7-6. Regions of maximum RAAN Change from Out-of-plane Thrusting 7-21

7-7. RAAN Change vs. Thrusting Time 7-21

7-8. Longitudinal Change due to Maneuvering & Geopotential 7-25

7-9. Semi-major Axis vs. Time for 10-Target Campaign 7-27

7-10. Propellant Consumption vs. Time for 10-Target Campaign 7-29

8-1. Low-Earth Orbit J_2 Effect for West and East Shift, Prograde 8-4

8-2. Nodal Crossing Time vs. Eclipse. 8-7

8-3. Satellite Field of Regard Geometry 8-9

8-4. Walker "Streets of Coverage" Satellite Mass vs. Altitude 8-12

8-5. Walker "Streets of Coverage" Satellite Lifetime vs Altitude 8-13

8-6. Revisit Rate of Single Non-maneuvering Spacecraft 8-15

8-7 a-c. Revisit Time at Altitudes of 340 and 500 km 8-16

8-8 Propellant Use vs. Available Time at 310 and 500 km 8-18

8-9. Control authority at 300 km with BHT-8000 (A=0.5 mm/s^2). 8-20

8-10 a-d. Characteristic Comparison of Four Methods at 310 km Altitude 8-21

8-11 a-b. Time to Overflight and ΔV Use Comparison at 310 and 500 km 8-25

List of Tables

Table Page

2-1. Chemical vs. Electric Propulsion Characteristics 2-5

2-2. Comparison of Coplanar Orbital Transfers 2-26

5-1. Comparison of Two-Body vs High-Precision Propagators 5-18

5-2. Orbital Parameters after a Maneuver at Three Initial Altitudes 5-25

5-3. Comparison Summary of CP and EP 5-38

6-1. Comparison of Thrust-only and Thrust-Coast Maneuvers 6-27

7-1. Overflight Opportunities of a LEO Satellite in 3 Days 7-19

7-2. Comparison of Thrust-only and Thrust-Coast Maneuvers 7-23

7-3. Ten randomly selected Terrestrial Targets by Location and Order 7-27

8-1. Longitudinal Shift due to J_2 and Maneuvering 8-5

8-2. Walker Constellation at various Altitudes with 5-yr Design Life 8-11

8-3. Comparison of GeoEye-2 and Single Walker Satellite 8-14

OPERATIONALLY RESPONSIVE SPACECRAFT USING ELECTRIC PROPULSION

1 Introduction

Traditional space operations are characterized by large, highly-technical, long-standing satellite systems that cost billions of dollars and take decades to develop. Many branches of the U.S. government have recognized the problem of sustaining current space operations and have responded by heavily supporting research and development in a field known as Operationally Responsive Space (ORS). ORS research focuses on hardware, interfaces, rapid launch and deployment with the overall goal of reducing per-mission-cost down to $20 million (Wertz, 2007a: 5-7). Some research is also done in the area of orbit design to maximize the coverage time over specific areas (Kantsiper, 2007; Wertz, 2001, 2005, 2007b; Larrimore, 2005). However, there are few studies on the feasibility of maneuvering to different orbital planes in low-Earth orbit (LEO) using electric propulsion (EP) once an asset is launched (Alfano, 1982). Electric propulsion technology has been shelved due its low thrust and long transfer times. In fact, few studies exist overall for persistent satellite maneuvering beyond orbit maintenance (Guelman, 1999; Jean, 2003).

Reconsidering EP technology with today's state-of-the-art in electrical power generation and hardware, this capability could bring significant benefits for strategic and

tactical users alike, who need a responsive system based on changing requirements and rapid implementation. If it is possible for a user to task the re-positioning of a satellite in a timely and propellant-efficient manner such that a single asset can perform multiple maneuvers, then its mission can be modified to meet requirements based on emerging world events. The existing paradigm on maneuvering is that it is cost-prohibitive (Wertz, 2007b). In the case of chemical propulsion (CP), the presented analysis does support that view as is shown in Chapter 8. This paradigm and traditional space programs have to change and a transition to small, responsive, low-cost, and rapidly available systems must take place to meet the needs of space users including time-sensitivity.

This research proposes an EP system that could help transition to and stimulate renewed consideration for low-thrust orbit transfers for a wide variety of mission requirements. The feasibility of EP technology to perform slow, efficient orbit changes to modify a satellite's ground track to overfly any target on Earth is considered, and an algorithm is presented which could lead to an autonomous flight code to be implemented operationally. The work is presented in a scholarly format over the following chapters with the same content as published in several journal articles. The original motivation for this work comes from Newberry, who postulated that a maneuverable system is not only feasible but could meet the demands of 21st century warfare (Newberry, 2005: 47). After validating Newberry's results, an exhaustive reachability study is presented in Chapter 5 to show the impact on satellite maneuvering by modifying each parameter that defines the initial orbit. A critical building block is developed in the form of an equation which measures change as a result of maneuvering with respect to a non-maneuvering reference.

This equation is then used throughout this research to justify the feasibility of an EP system and how it compares to traditional space operations.

Many operational satellites are maneuverable, but they are designed to operate in 'static' parking orbits. The technology to maneuver efficiently is available and in use, but a concept of operation (CONOPS) needs to be developed to include how the system should be employed to achieve the desired effect to demonstrate its feasibility. Low thrust electric thrusters enable satellites already in orbit to perform slow, precise, and highly efficient station-keeping maneuvers. A typical CONOPS intends for the spacecraft to arrive at its orbital state and maintain its orbit, almost exclusively, for the life of the vehicle. Most spacecraft are designed in this manner so maneuvering is not considered (Newberry, 2005; Wertz, 2007). The current state-of-the-art for LEO satellites revolves around constellation design to maximize the coverage for an asset; hence most satellites are placed in polar, sun-synchronous or critically inclined orbits. Geosynchronous communication satellites use EP engines to move within their orbits to service different operational theatres such as Wideband Global SATCOM and Defense Satellite Communications System, but these maneuvers usually take weeks and perform a standard phasing maneuver. To harvest this potential, the CONOPS must be constructed around the assumption that these spacecraft do not necessarily have to operate within the orbit into which they were first launched. This research develops the necessary algorithm and tools to demonstrate that EP systems can maneuver significantly in a timely fashion to overfly any target within the satellite's coverage area. Although the algorithm is applicable to all orbital altitudes, it is mainly used to analyze LEO satellites in this dissertation. Performance characteristics are compared to and contrasted against

traditional systems to evaluate each technology's strengths and shortfalls. Chapters 4 through 8 are journal articles either published or under review for publication presented in a scholarly format.

Chapter 2 presents a body of pertinent research with the most applicable explained in further detail. The first section addresses continuous thrust maneuvers using EP and lays out the identified uses in industry and science. There are many studies addressing the benefits and drawbacks of using this technology to maneuver and it is clear that EP is becoming more common-place as the supporting power and thrust generation methods are advancing. Section two presents an evolution of orbit design. Since most designers plan constellations in a "static" manner, it is important that the orbital parameters are chosen carefully prior to launch to maximize the derived benefits based on a given mission. The discussion shows how, over time, the constellations became much smaller with larger body of knowledge, better simulation tools, and imposing the proper constraints to eliminate in-efficiencies. The third section offers the state-of-the-art for small, impulsive systems that maneuver to meet satellite observation and servicing missions. It is clear from these research projects that a satellite maneuvering capability is highly desirable. This dissertation will compare and contrast the proposed EP system with CP maneuvers to argue how the former can be beneficial to fulfilling these missions in a time-sensitive manner. Finally, section four draws from a large body of research in atmospheric (aero-assisted) maneuvers. It has been shown that aero-assisted systems can provide significant cost savings over purely impulsive ones especially for large orbital maneuvers.

Chapter 3 validates the work done by one of the strongest proponents of low-thrust, efficient satellite maneuvering. Chapter 2 presents a sampling of the body of work related to EP, in which Newberry stands out as an advocate for change to traditional space operations. Further he presents a viable alternative to traditional CP. His hypothetical spacecraft is able to change the overflight time – or as he calls it, time-over-target (TOT) – by 24 hours given seven days of lead-time. The significance is that an existing EP satellite system can be flexible and do so at a relatively low propellant cost. The initial results presented in Chapter 3 agree with Newberry's that with simple, in-plane, posigrade, continuous thrusting significant ground track changes are possible. The chapter continues to investigate the effect on maneuvering by varying each one of the six Classical Orbital Elements (COEs) individually and presents the results of the analysis. Newberry's findings are only the foundation for this work. New contributions present improved performance of a notional EP system, equations for accurately predicting EP in-plane and out-of-plane maneuvers, and an algorithm to affect target overflight using low, continuous thrust.

Chapter 4 postulates the implementation of a responsive orbit approach in four phases. This work was published in the Air and Space Power Journal in summer of 2011. The first phase shows that some currently operational satellites can modify their orbits significantly in an efficient manner simply by changing the CONOPS. The second phase incorporates moderate amounts of aerodynamic drag to the satellite for altitudes ranging between 300 and 700 km above the Earth's surface. Phases 3 and 4 are briefly discussed but the chapter does not provide any analysis. The writing was done during the initial phases of concept development and the direction changed to de-emphasize aero-assist

maneuvers. The reason is discussed briefly in Section 3.3. Nonetheless, the presented work is applicable and throughout this dissertation the concepts for satellite maneuvering become more defined whereas the performance results from the analysis improve significantly.

Chapter 5 presents methodology to quantify reachability of a satellite with CP and EP. Previous research does not address maneuvering satellites in this manner. This work was accepted for publication in the Journal for Spacecraft and Rockets and is scheduled for publication in fall 2012. The methodology is very different, although most results are identical so previous work is reproducible. Even Newberry's work is different in that it is limited to a specific class of highly elliptical orbits that only apply to very unique missions. After proving the feasibility of affecting meaningful orbital change with today's thruster technology, this chapter provides useful insights on initial orbits and quantifies maneuverability of both propulsion systems. The main contribution is the development of equations that can accurately predict how much an orbit can change using CP or EP based on available time, orbital altitude, and ΔV when compared to a non-maneuvering reference satellite with the same initial conditions.

Chapter 6 provides analytical solutions for in-plane and out-of-plane low thrust maneuvering satellites in low-Earth orbit to modify ground-track and change the time the spacecraft overflies a particular location within the orbit. This work is under review for publication in Acta Astronautica. To validate the solutions, a new approach is used in the problem formulation than in Chapters 4 and 5. An analytical time of overflight equation is derived, which is a cornerstone for determining the maneuver requirements to overfly specific terrestrial targets. Previously-developed algorithms are used to determine optimal

low thrust profiles. Five scenarios are analyzed to validate the developed analytical expressions. Two of them are in-plane, two out-of-plane, and the final scenario is a combination to change semi-major axis and right ascension of the ascending node simultaneously. Depending on the propellant consumed and the system's propellant budget, the process can be repeated multiple times to allow the spacecraft to maneuver. Although much of the literature presented in the introduction of Chapter 6 is somewhat related to the problem posed, it does not provide closed form solutions to the problem. Further, the reviewed literature does not consider the problem of a maneuvering satellite coinciding with a specific location within the orbit.

Chapter 7 presents the full algorithm developed to solve the problem posed in this dissertation. The work is under review for publication in the Journal for Spacecraft and Rockets. This chapter explains a method for accurately predicting in-plane maneuvers using EP to move the ground track over any desired terrestrial target regardless of initial satellite state and initial time. The necessary equation is developed in Chapter 6 and fully implemented here to compute the exact local time of, propellant consumption, and time required for overflight. Low-Earth satellites operating with EP face several challenges such as limited coverage, long revisit times, low thrust, and more drag and perturbing forces, which are discussed in this chapter. Conversely, low altitudes can be beneficial and allow smaller optical payloads, better resolution, smaller spacecraft, less expensive overall systems, and, for the purpose of maneuvering, more opportunities to overfly a specific ground target. It may also be important to understand the minimum amount of time required to achieve global reach or time to overflight that guarantees coverage of any target. Global reach times for multiple thrust levels and altitudes are analyzed and

presented. Finally, out-of-plane burn sequences are revisited to achieve right ascension of the ascending node (RAAN) and/or inclination changes while keeping orbital altitude constant.

Chapter 8 builds on previous work from Chapter 7 to compare an EP system to three conventional technologies for observing a terrestrial target. Two traditional methods (Walker constellations and single non-maneuvering satellites) are currently in operation and are used as baselines for the comparative study. Chemical maneuvers are the traditional method for orbital changes and are used extensively for orbit maintenance in LEO. The fourth method is a maneuvering satellite using highly efficient EP technology. This work is under review for publication in the Journal for Guidance, Navigation and Control. This chapter starts the discussion with some considerations for an EP system such as operational altitude, inclination, lighting conditions, viewable area, and power requirements. The majority of the work centers around designing comparable systems using the four observation methods based on Space Mission Analysis and Design models and equations. The notional systems are then compared side-by-side to show trade-offs between number of maneuvers, time to overflight, mission cost, and mission life. This chapter is the cumulation of all work done in the previous five chapters and provides a full picture of the potential capabilities of an EP maneuvering system.

The inevitable paradigm shift in the U.S. space program has begun. The future of conventional space operations must include small, cheap, responsive, and maneuverable assets that can be developed and launched in months rather than decades. Electric propulsion may present a viable solution to aid this paradigm shift. The presented algorithm and the supporting analysis are a significant step forward in understanding EP

maneuvers and under what circumstances this technology is most suitable to meet the mission requirements.

2 Literature Review

Many studies exist detailing the possible applications of the proposed responsive electric propulsion (EP) space system; however, none address the responsiveness achieved by modifying a satellite's ground track to arrive over a desired target at a user-defined time and altitude. This literature review attempts to survey and define the state-of-the-art of eight different research areas which provide the background for this study (see Figure 2-1). These areas are electric propulsion, benefits of EP missions, maneuvers, orbit design & hardware, survey missions, planetary fly-bys, aero-assist, and space plane. These subjects are vast and therefore only a selective sampling is presented here that is deemed most applicable. The eight areas are grouped into four categories of Continuous Thrust Maneuver, Operationally Responsive Space, Impulsive Thrust Maneuver, and Atmospheric Maneuver shown in Figure 2-1.

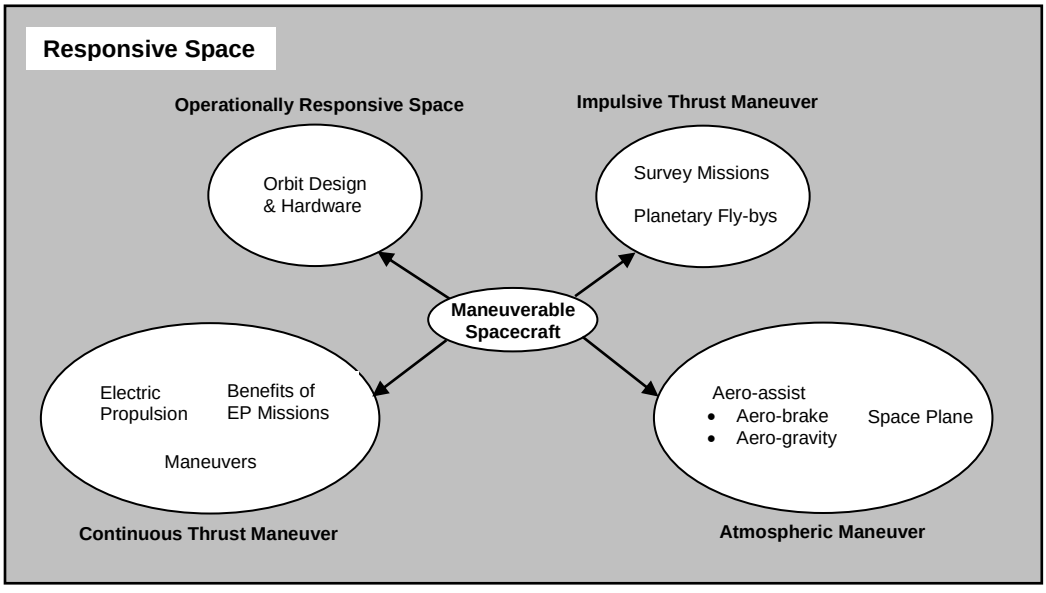

Figure 2-1. Responsive Space Literature Review Research Areas

The Impulsive Thrusting Maneuver has been researched extensively and is not generally used operationally for low-Earth orbit (LEO) maneuvering due to the prohibitive amount of propellant these maneuvers consume. Even so, recent research and real experiences show that in certain applications impulsive maneuvers are extremely applicable and when used in conjunction with planetary fly-bys and other creative maneuvers, such as lunar gravity assist, the amount of propellant used is significantly reduced when compared to traditional un-assisted maneuvers (Ocampo, 2003, 2005). This dissertation will make use of impulsive maneuvers as a stepping stone to comparing its performance to continuous thrust maneuvers.

2.1 Continuous Thrust Maneuver

2.1.1 Electric Propulsion.

Today's spacecraft mainly use two types of propulsion systems- chemical and electric (Saccoccia, 2000). Chemical propulsion (CP) is the first and earlier technology. Impulsive maneuvers rely on chemical reactions to produce thrust. Chemical propulsion systems are required to carry their propellant and oxidizer on-board due to the lack of an atmosphere in outer space, which translates into additional mass. The benefits of CP are the high thrust it produces and the resultant shorter trip times. It is also relatively simple to analyze and model maneuvers propelled by CP depending on the desired accuracy, because the maneuver occurs at a specific instance in time and adds energy to the system instantly rather than over a long period of time as in the case of EP. While there have

been numerous successful trials of various CP designs, the fundamental operation have remained the same. The combustion process is very complex and controlling the amount of thrust is inaccurate. The propellant types are solid and liquid. Solid propellants are used on large boosters to get the payload into orbit. Liquid propellants are on-board the spacecraft for orbital maneuvering, station-keeping and attitude control. A rocket engine requires a complicated system of tanks, valves, delicate control mechanisms and deals with highly flammable materials making it very dangerous.

Since the fifties and sixties, the United States and the Soviet Union developed EP thrusters for space applications. Since external power sources are required (mostly solar), the use of EP comes at the expense of power and mass (Saccoccia, 2002). This limited the application of EP on-board spacecraft until the 1990s as spacecraft power finally began to increase to meet the growing needs of communication satellites. With further advances in solar-power generation technology, these types of thrusters are widely used in industry today and are endorsed by NASA and the European Space Agency (ESA) for use in many space missions including deep-space, interplanetary probes, orbit raising, station-keeping, attitude control and other orbital changes (Saccoccia, 2000: 1-2).

Continuous thrust is safer, many times more efficient in propellant usage, and easier to control than CP; however, the thrust exerted is low resulting in long transfer times. The ESA puts forth significant effort to implement EP technologies for immediate use and to define requirements for future systems. There are four main application domains. In geosynchronous (GEO) communication satellites, it is used for station-keeping and orbit transfer. In addition, satellite designers have proposed uses of EP for drag compensation and attitude control LEO communication satellites. The other two areas where EP has

established a strong presence are inter-planetary and scientific and Earth observation missions. The low thrust it produces is suitable for very delicate maneuvers that require a high level of accuracy. At the same time, an EP system can affect significant changes in a spacecraft's position and orbit if sufficient time is available. The EP concept relies on positive and negative electric potential to accelerate ionized gas particles to very high speeds and ejecting those to create thrust. Studies show that propellants are ejected twenty times faster than traditional CP making it more efficient measured by the exit velocity of the propellant. The main consumable in EP is electricity. Since its power is derived from the sun, the energy is abundant and the system requires very little on-board propellant effectively saving more than 20 percent in initial launch mass of the spacecraft (Saccoccia, 2002: 9).

In selecting EP versus CP thrusters, high thrust is exchanged for high efficiency. CP systems vary widely in thrust and could provide forces into the mega-Newton range. The thrust-level generally increases with the mass of the system, yet the efficiency is specific to the engine. Propellant efficiency is commonly measured by specific impulse (I_{sp}). In a vacuum, I_{sp} is simply the ratio of propellant exit velocity and gravitational acceleration on the surface of the Earth. The higher the I_{sp}, the less propellant is consumed for the same thrust. EP engine characteristics are more consistent than those of CP. An increase in input electrical power increases both thrust-level and efficiency (Hall, 2010: 8-12). EP systems produce forces in the milli-Newtons but have very high propellant efficiencies. Table 2-1 provides some engine characteristics of current technology available in open sources (Busek, 2012).

Table 2-1. Typical Chemical vs. Electric Propulsion Characteristics

Engine Type	I_{sp} (s)	Thrust (N)	Mass (kg)	Power (W)	Efficiency (%)
Chemical	100-500	5 - 500	100	600	30
Electric	1000-3000	0.005 - 1.5	240	700 – 20,500	50-70

Transitioning to the theoretical modeling of EP maneuvers, Wiesel considers the problem of transferring from a low circular orbit to a higher one with very low, continuous thrust (Wiesel, 2003: 97-99). In LEO, an EP orbit transfer is often a spiral trajectory as the argument below shows. In this case, the orbit's semi-major axis (a) is increased to that of the desired orbit and the total two-body energy changes. The equation for energy of a two-body orbit is

$$\varepsilon = -\mu / (2a) \tag{2.1}$$

where $\varepsilon \equiv$ total specific mechanical energy and $\mu \equiv$ Earth's gravitational parameter. The change in energy with respect to time is simply the time-derivative of Equation (2.1)

$$\frac{d\varepsilon}{dt} = \frac{\mu}{2} a^{-2} \frac{da}{dt} \tag{2.2}$$

where $t \equiv$ time. The propulsion system does work to increase the energy of the satellite and along with it the semi-major axis. The work performed is the dot product between the acceleration ($\bar{A}$) and the velocity ($\bar{V}$) vectors given by:

$$\frac{d\varepsilon}{dt} = \bar{A} \cdot \bar{V} \tag{2.3}$$

This relation assumes that the mass of the system is constant. Although its mass does vary as propellant is consumed during propulsion, yet because propellant consumption is only a fraction of a percent of total vehicle mass over the maneuver time frames considered here, it is a reasonable assumption. The dot product of two vectors is maximized when they are aligned with each other. In other words, the spacecraft should thrust along its direction of travel (or reverse direction when going to a lower orbit). Due to the low thrust of EP, the vehicle will gain velocity very slowly, so the orbit will remain mostly circular thus resulting in a slow outward spiral trajectory.

It is important to predict the amount of time and propellant an EP maneuver consumes. To do that, Wiesel assumes that the velocity and acceleration vectors are aligned and the velocity is the instantaneous circular orbit velocity:

$$\begin{aligned} V &= \sqrt{\mu / a}, \\ \frac{d\varepsilon}{dt} &= A\left(\frac{\mu}{a}\right)^{\frac{1}{2}} = \frac{\mu}{2} a^{-2} \frac{da}{dt}. \end{aligned} \tag{2.4}$$

where $V \equiv$ magnitude of velocity vector and $A \equiv$ magnitude of acceleration vector. Rearranging this equation provides an expression for the time-rate-of-change of a, also known as the equation of motion of a:

$$\frac{da}{dt} = \frac{2}{\sqrt{\mu}} a^{3/2} A. \tag{2.5}$$

The variables a and t can be separated and each side integrated to yield a closed form solution of the problem:

$$\int_{a_0}^{a} \frac{da}{a^{3/2}} = \frac{2}{\sqrt{\mu}} A \int_{t_0}^{t} dt$$
$$a_0^{-1/2} - a^{-1/2} = \frac{A}{\sqrt{\mu}}(t - t_0) \tag{2.6}$$

The solution to Equation (2.6) provides the answers of how much time the maneuver takes (Equation (2.7.1)) and how much propellant it consumes (Equation (2.7.2)). Equation (2.6) can also be modified to estimate the amount of time it would take a spacecraft using EP to escape Earth's orbit (Equation (2.7.3)). To escape near-Earth gravitational pull, the satellite's orbit must become parabolic, which occurs when $a \rightarrow \infty$.

$$t - t_0 = \frac{\sqrt{\mu}}{A}(a_0^{-1/2} - a^{-1/2}) \tag{2.7.1}$$

$$\Delta V = A(t - t_0) = \sqrt{\frac{\mu}{a_0} - \sqrt{\frac{\mu}{a}}} \tag{2.7.2}$$

$$t_{escape} = \frac{1}{A}(t - t_0) \tag{2.7.3}$$

where $\Delta V \equiv$ change in velocity or propellant budget and the 0-subscripts denote initial conditions.

2.1.2 Cost Savings and Benefits of Electric Propulsion.

In the late eighties, interest in EP gained momentum as a cost-effective alternative to CP based on the number of research papers published. The cost to reach orbit is staggering, easily reaching tens to hundreds of millions of dollars depending on the required altitude and weight-class for the mission. The fundamental way of getting to and

staying in space has not changed since the advent of space flight, namely chemical rockets, so the associated cost have remained mostly the same. At best, the cost to reach LEO is $3,000 per kilogram. Launching into geostationary transfer orbit (GTO) is three times as costly as going to LEO and getting to the popular GEO costs an order of magnitude more (Larrimore, 2007: 2). Therefore, researchers started to look into using the highly efficient EP to get from GTO to GEO to save launch cost by downgrading to smaller rockets or increase the usable payload to orbit. The benefits of EP for orbit transfer and injection of GEO satellites are discussed and summarized in the following section.

A large amount of propellant is required for GEO spacecraft require to reach their operational orbit. They are usually launched into an elliptical GTO with apogee in the vicinity of GEO altitude. A significant amount of velocity change or delta-V (ΔV) is required to circularize the orbit, remove the inclination, and once on-station must provide the capability to maintain position and attitude for the life of the system. To do this with traditional CP requires considerable amounts of propellant. As a result, EP is widely used for on-station orbit maintenance operations today and could be extended to the orbit raising function as well (Forte, 1992). EP can increase the payload launch capacity of an Ariane launch vehicle by 250 kilograms or ten percent of its dry-mass and provide launch cost savings of $14M. Saccoccia concludes that EP for orbit-raising does not reduce launch cost due to the off-setting cost associated with the long delay of beginning the operational life of the payload (Saccoccia, 2002: 9). However, the additional payload capacity does provide flexibility for larger satellites or more propellant to significantly prolong the life of the system.

The main drawback preventing operational use of EP in the GTO-to-GEO transfer is the increased transfer times. Porte, Aubert and Buthion limit their transfer time in the study to six months and require the use of CP to initially raise the injection orbit's perigee. Fifteen years after Porte's paper, researchers claim transfer time reductions down to 60 days based on available EP technology and the option to start EP transfer immediately after launching into GTO (Dankanich, 2007: 9). Modeling and simulation show for a 10,000-lb modern XM satellite with 18 kW of on-board power, the GTO-to-GEO transfer time is less than 100 days. With the increased margin of mass opened up by the use of EP, one can add supplemental power to further reduce the transfer time. The launch cost savings also come back into play as the delay in operational utility is shortened significantly from six to only two months. Further advances in power generation would lower cost, mass, efficiency, and stowage volume of solar arrays and could make low-thrust transfers to GEO an even more attractive option. A number of scientific papers provide related analyses of the use of EP (Spitzer, 1995: 95-215; Gopinath, 2003; Duhamel, 1989; Vaughan, 1992; Kaufman, 1984; Jones, 1984).

2.1.3 Maneuvering Algorithms.

Guelman and Kogan are two of very few authors to consider minimum propellant flight profiles for low altitude, circular orbits to overfly a specific number of terrestrial targets in a given time period (Guelman, 1999: 313-321). Low altitudes provide significantly higher resolution or smaller payloads, but this advantage is often negated by the poor coverage and narrow swath widths of a low-flier. Their analysis indicates that

the application of EP to overfly desired targets is practical, because it combines high resolution with relatively short revisit times.

Guelman separates the problem into two steps – optimization and scheduling. Much like the algorithm applied in this dissertation, the control strategy is to modify the orbital period. There are discrete opportunities when a satellite can overfly terrestrial targets and those occur exactly when the rotating target coordinates cross the orbit plane. Therefore, a specific overfly time cannot be requested by the user unless there is a sufficiently long time period available or the intercept occurs by chance. The first step is to build a piecewise optimal trajectory that connects two sequential overfly points and results in an analytical solution. The second step is global optimization for the entire trajectory by choosing the proper passage times. Guelman uses the simulated annealing method (or SAM) for finding the global minimum fuel consumption. The method starts with an initial schedule and improves it by taking steps towards the optimum solution.

Low thrust maneuvering is effective and sustainable over an extended period of time. In Guelman's simulations, they consider a small spacecraft of 100 kg total mass, power input of 200 W, and an acceleration of no more than 1 mm/s^2. They demonstrate the overflight of 20 randomly selected sites over a period of 50 days and the associated propellant usage would allow a spacecraft with a modest initial propellant-mass-ratio to maneuver repeatedly and operate as long as 3 years. Doubling the number of overfly sites from 20 to 40 and keeping the collection period at 50 days increases propellant consumption by a factor of 60, whereas doubling the period from 50 to 100 days for 20 sites decreases propellant usage by a factor of 300. The take-away is that EP can be

effectively used to drastically reduce the revisit time of desired terrestrial targets for low orbit altitudes when compared to not maneuvering.

Jean and de Lafontaine further the research by adding atmospheric drag and geopotential effects up to J_2 to the previous models and introducing a new quartic guidance law to the cubic guidance used by Guelman (Jean, 2003: 1829-1844). They start in a sun-synchronous reference orbit and aim to always return to the reference after maneuvering. In essence, it is an in-plane phasing maneuver that starts at a sun-synchronous altitude, then the satellite thrusts in one direction to gain or lose altitude, and finally returns to the reference altitude by thrusting in the opposite direction. The position difference between the phasing satellite and a non-maneuvering reference satellite results in the shift of ground track (overflight time and position). The authors conclude that EP is practical in both maintaining a reference orbit by countering atmospheric drag and modifying the reference orbit to overfly a terrestrial target. Their end product is an autonomous algorithm that could be implemented on a spacecraft to take advantage of this technology.

The purpose of the on-board autonomous algorithm is to perform two functions without ground intervention – orbit maintenance and orbit transfer – with the goal to reduce the cost of additional ground resources to compute and execute orbital maneuvers. Low-thrust maneuvers require propagating the orbit and its perturbations over a long period of time. To avoid labor-intensive practices, the authors develop two guidance laws. The first is designed for orbit maintenance when no taskings are received and the spacecraft is maintaining its position by countering drag. The second is the main principle for the guidance algorithm to overfly user-specified ground targets by computing the

intersection between orbit plane and target longitude, and thereafter a time-history of the argument of latitude (u) of affect an overflight. Jean and de Lafontaine provide simulation results to demonstrate the application of both guidance laws.

2.2 Operationally Responsive Space

As discussed in Chapter 1, Operationally Responsive Space (ORS) is an important and related concept with the ultimate goal to reduce access-to-space costs and system development time. A number of orbit and constellation studies to maximize Earth coverage are available within ORS. The findings in the following section provide a good departure point in considering initial orbit characteristics that are suitable for a given mission. ORS however does not consider orbital changes in its fundamental design (Wertz, 2007a).

Battlefield commanders require persistent access to maintain the intelligence advantage over adversaries and a number of solutions are available. An expensive but small constellation of GEO satellites is commonly in use for Department of Defense systems such as Military Strategic and Tactical Relay (MILSTAR), Wideband Global SATCOM (WGS), Defense Satellite Communication System (DSCS), and Advanced Extremely High Frequency (AEHF). An alternative method is to use many smaller satellites in LEO to provide continuous coverage. Although the vehicle design is smaller and less complex and the cost to deploy each is significantly lower, the large number of required vehicles eliminates any cost advantages. The Iridium constellation has sixty-six satellites. As a result, ORS researchers have considered Highly Elliptical Orbits (HEO), circular Mid-Earth Orbits (MEO) and “streets of coverage” constellations as more cost

effective means to provide near equivalent coverage when compared to the two traditional methods – small GEO and large LEO constellations.

The problem of maximum coverage using the smallest satellite constellation was first extensively studied by Walker in the 1970s (Walker, 1977). His findings show that global coverage is optimized with multiple equally dispersed, circular orbits at the same inclination and altitude. Each orbital plane contains one or more satellites, which are then phased within that plane or between adjacent planes so that at least one satellite is in view from a location on the ground while the previous one moves out-of-view. AVM Dynamics' SC Modeler provides the graphics for two delta Walker constellations. The design requirement for Case 1 is continuous coverage for latitudes between N70° to S70° with a minimum ground elevation angle of 20°. This constraint is more restrictive and ensures that the satellite is not too close to the horizon to risk obscuration by buildings, mountains, and other obstacles. The AVM software determines that for an altitude of 1,400 km, the constellation requires 71 satellites each in its own plane, phased by 271° between satellites in adjacent planes, with a right ascension of the ascending node (RAAN) increment of 5° (Figure 2-2). The RAAN increment specifies the orientation of one plane with respect to the next. Case 2 uses an entirely different configuration. The design requirement is continuous coverage for latitudes between N90° to S90° (global coverage) with a minimum ground elevation angle of 20°. For the same altitude, the constellation requires 70 satellites in ten planes, phased by 17° within the plane and a RAAN increment of 27.5° (Figure 2-2).

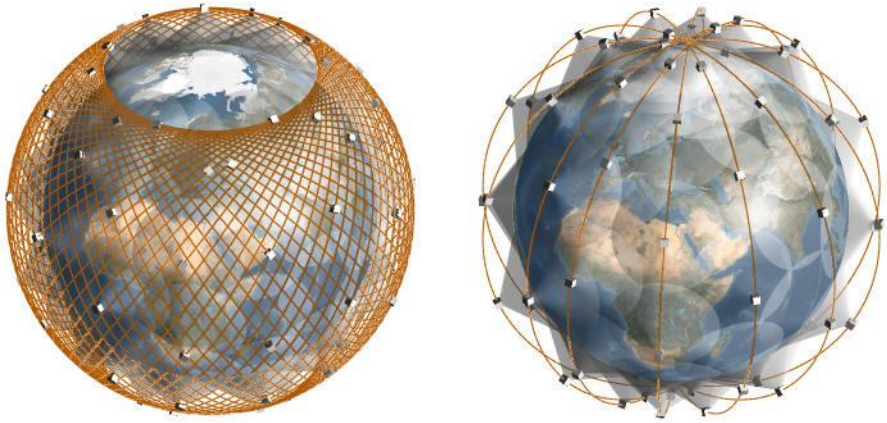

Figure 2-2. Walker Constellations (AVM Dynamics)

Case 3 is an example using higher altitude circular orbits to provide continuous coverage with a minimum of four visible satellites at any time to any point on Earth. The constellation is relatively small with 18 satellites, yet the altitude is significantly higher than the previous cases at 8,300 km. The minimum ground elevation angle is also relaxed to 0° to further reduce the constellation size. At this altitude and constraint, the 18 satellites are equally distributed in three planes, phased 20° within the plane and a RAAN increment of 120° (Figure 2-3). The last case, case #4, demonstrates a constellation of elliptical orbits providing continuous coverage with a minimum of four visible satellites at all times for high latitudes between N20° and N90°. The minimum ground elevation angle is 0°. Apogee altitude is 1,000 km and perigee is at 7,200 km. With these design factors, the constellation requires 18 critically inclined (see explanation below) satellites each in their own plane, phased by a third of their periods (the amount of time it takes the satellite to complete one revolution) and a RAAN increment of 20° (Figure 2-3).

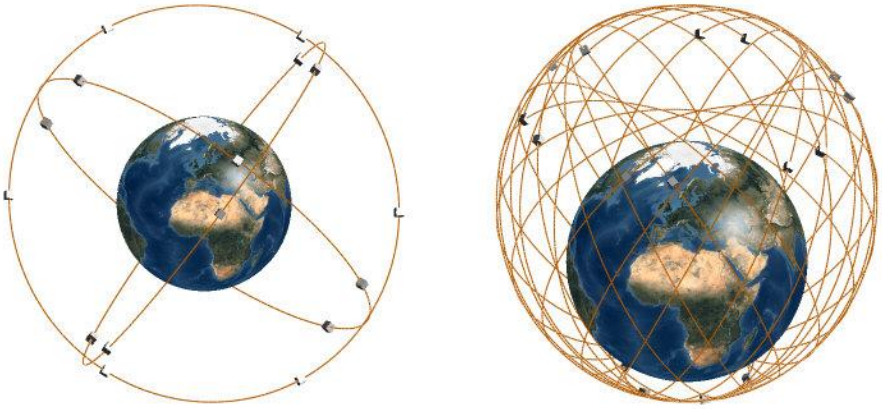

Figure 2-3. High Circular and Elliptical Constellations (AVM Dynamics)

These examples show how drastically different the constellation sizes can be based on altitude, minimum elevation angle and eccentricity. The following ORS studies aim to find orbit design parameters to further lower the number of required satellites while maintaining the same level of coverage.

Kantsiper *et al.* examine two HEO classes with three and four-hour periods populated with five to eight satellites to provide long dwell-times over a particular region (Kantsiper, 2007). The first orbit has a three-hour period, perigee altitude of 525 km and apogee at 7,800 km. This configuration is relatively easy to reach with a 400-kg spacecraft on a common Minotaur-IV launch vehicle. The second orbit is higher in altitude with a four-hour period, perigee at 700 km and apogee at 12,500 km. An example of an operational HEO is the Molniya orbit first used for Russian communication satellites. This unique orbit provides long dwell times over higher latitudes while the satellite is passing through its apogee. The orbital period is twelve hours of which almost eight are spent dwelling at high latitudes. Another characteristic of this orbit class is that it is critically inclined. It means that the location of perigee (argument of perigee or ω)

does not shift within the orbit over time due to Earth's oblateness (not being perfectly spherical – dominantly known as J_2 effects), in other words, a satellite can maintain apogee over the desired region. Based on Lagrange Planetary Equations, the argument of perigee changes as a result of J_2 at this rate over time (Wiesel, 2003: 141):

$$\dot{\omega} = -\frac{3nJ_2R^2}{2a^2(1-e^2)^2}\left(\frac{5}{2}\sin^2 i - 2\right) \tag{2.8}$$

where $\dot{\omega} \equiv$ time rate of change of argument of perigee, $n \equiv$ mean motion, $J_2 \equiv$ Earth's second dynamic form factor, R = radius of Earth, $e \equiv$ eccentricity, and $i \equiv$ inclination. This equation is zero when i = 63.4° or 116.6°, so at these two inclinations apogee of the orbit remains in place. These desirable characteristics of HEOs reduce the time that the satellite is away from its service area far north or south of the equator. Both HEOs under consideration in this study have these attributes.

The argument of perigee and period are the two design factors to maximize the coverage over a given theater while minimizing the number of satellites in the constellation. The study found that the four-hour orbit always requires a smaller constellation compared to the three-hour orbit with the penalty in the increased energy required to reach it. Furthermore, for latitudes greater than three degrees, the optimal argument of perigee for the lowest number of satellites required for continuous availability is ω = 270°. Below this latitude, the optimal ω is 180°. For orbits with a three-hour period, ω = 270° is optimal for all latitudes. Finally, comparing the constellation size between the two classes of orbits as it varies with latitude, above the latitude of 30°, the three-hour orbit only requires one more satellite than the four-hour

constellation. Thus depending on mission requirements, the lower orbit may warrant one more satellite in exchange for greater payload masses. The study concludes that with as little as three satellites, a four-hour HEO can provide uninterrupted coverage for high latitudes above 50°.

Wertz compares a circular Mid-Earth Orbit (MEO) to an elliptical MEO for persistent communications and finds that the former is a better choice (Wertz, 2007b). Since a small number of LEO satellites cannot provide persistent coverage as required by many missions and GEO satellites are too large and expensive, moderate altitude elliptical orbits are often advocated as a solution. The study explores the coverage, coverage flexibility, constellation size, impact on spacecraft design and overall system costs of these orbit classes and finds that circular MEOs are a better choice.

Starting at an altitude of 5,000 km, circular orbits are an alternative to elliptical MEOs, also known as Magic Orbits. Wertz compares orbits with the same apogee altitude since most of the communications occur at apogee which sizes the antenna and power systems. A circular MEO constellation creates a "streets of coverage" around the world with multiple satellites arranged in a single plane phased such that their Earth centered access angles overlap. The phasing angle is simply determined by dividing 360 degrees by the number of satellites in the constellation. The footprint of each satellite is then linked together to form a full orbital ring and coverage is persistent for a particular region of interest. With this "streets of coverage" approach, four to six satellites provide continuous coverage at an altitude of 8,000 km (dependent on latitude) and three to five at 15,000 km. These numbers are significantly lower than those for elliptical orbits with the same apogee.

From a vulnerability standpoint, orbit flexibility and radiation environment, an elliptical orbit is inferior to a comparable circular orbit. Altitude is the best defense against anti-satellite weapons. In order to reach a MEO asset, a launch vehicle must deliver a ΔV in access of 12 km/s. It is significantly more difficult to hit a target at that altitude. An elliptical orbit is vulnerable to attack at or near perigee when its altitude is in the LEO regions. Furthermore, the Magic Orbit must be critically inclined to keep the line of apsides constant within the orbital plane. In contrast, a circular orbit is not restricted to an altitude or inclination thus eliminating the potential failure mode of elliptical orbits when the critical inclination is not achieved. Lastly, the radiation environment is identically high for both types of orbits, so the trade is between the cost of radiation hardening and the savings of a smaller constellation and better coverage. Wertz concludes that with the exception of the larger payload of an elliptical orbit, a circular MEO is superior in the other trade spaces, especially in the reduction of the number of satellites required for the same coverage. The author provides further detail in his other publications (Wertz, 2001; Wertz, 2005).

Larrimore proposes a "streets of coverage" LEO constellation to provide partially continuous accesses to the mid-latitudes (Larrimore, 2005). This constellation design is not as commonly used as the Walker delta constellation (Iridium). Since GEO constellations require more powerful sensors due to the distance to a terrestrial target, this orbital altitude would be too costly to use for tactical missions. LEO constellations use smaller, less expensive, and simpler satellites but require a large number (scores) to provide the same coverage. The result is the same – too expensive. If the requirement for persistency is slightly relaxed, a "streets of coverage" circular LEO constellation of less

than ten satellites can provide several hours (up to 12) of continuous coverage per day. Larrimore lays out the process to select the optimal coverage constellation using an inclined orbit chain (Figure 2-4). The first step is to select the optimal long-term inclination for the target inclination. In general, satellite access is optimized when the orbit's inclination is slightly greater than the target's latitude for a standard satellite footprint. As this footprint reduces to zero, the optimal satellite inclination becomes the target latitude. For targets close to the equator, an equatorial orbital ring is ideal (inclination of 0°). For high-latitude targets, a polar orbit ring is optimal. The next step in Larrimore's process is to determine the number of spacecraft required. This quantity depends on the altitude of the constellation, the required dwell time over the target and the available mission budget. A "streets of coverage" chain a lower altitudes (250-500 km) requires more satellites (11-16), but they would be smaller, cheaper and less complicated. The dwell time is shorter as a percentage of total flight time.

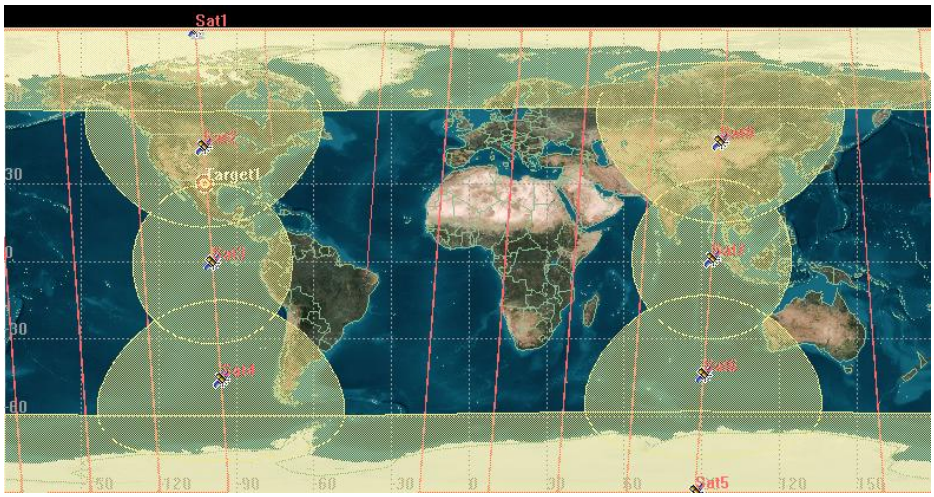

Figure 2-4. "Streets of Coverage" in Polar Orbit (Larrimore, 2005: 7)

In comparison, higher altitudes (800-1400 km) only require 6-8 spacecraft and provide longer dwell times of up to 50 percent of total flight time, but would cost more per spacecraft. As always, the trade-offs depend on the specific mission at hand. If the budget allows it, a second, complementary chain would provide continual coverage of a mid-latitude target (see Figure 2-5).

This section demonstrates that orbit and constellation design makes an enormous difference in the cost and scope of a mission. The original Walker constellations believed to be optimal in the 1970s require over seventy satellites to yield global coverage in LEO. With more knowledge and sophisticated modeling tools the mission requirements are modified (instead of a assuming blanket global coverage) to significantly reduce the number of required spacecraft in the constellation and still satisfy them. In some cases, very small constellations of three satellites may be sufficient to meet user needs.

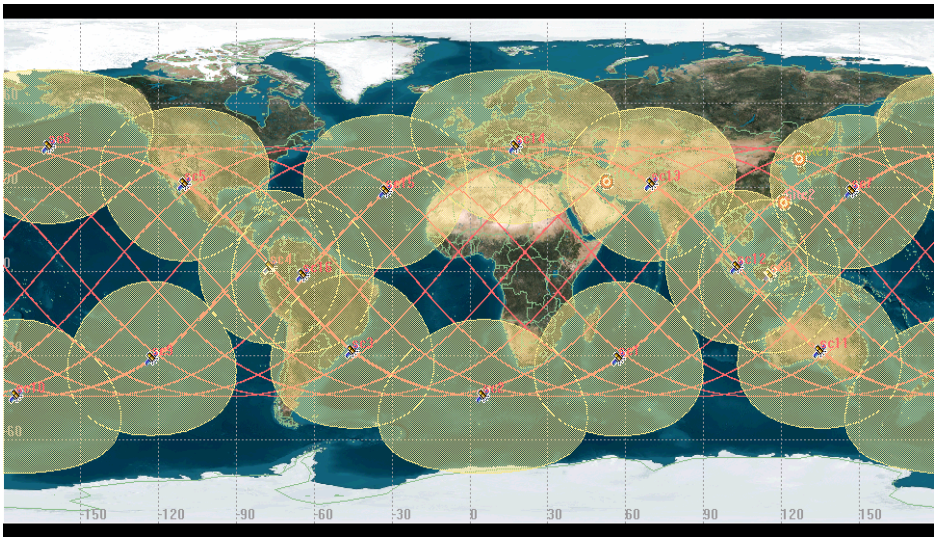

Figure 2-5. Multi-chained, inclined "Streets of Coverage" (Larrimore, 2005: 9)

2.3 Impulsive Thrust

2.3.1 Survey Missions.

In contrast to ORS, which focuses on non-maneuvering constellations, some missions use impulsive maneuvers to accomplish their objectives. Impulsive thrust maneuvers in the traditional sense use CP to change a satellite's position within its orbit or change the orbit altogether. The Orbital Express project, U.S. Air Force's Experimental Satellite System 11 (XSS-11), U.S. Army's Nanoeye, and the Repeated Intercept mission can be loosely grouped into survey missions that require proximity operations and orbital maneuvering.

Orbital Express is a Defense Advanced Research Projects Agency (DARPA) mission aimed at providing the capability to service and refill military spacecraft on orbit (Tether, 2003). This would not only prolong the service life of space assets, but also allow them to maneuver in unprecedented ways to evade detection and exploit the element of surprise of an adversary. The program's objective is to develop a cost-effective approach to autonomously service satellites in orbit. The system consists of two spacecraft - the Autonomous Space Transport Robotic Operations (ASTRO) vehicle is the unmanned service module and a prototype Modular Next-Generation Serviceable Satellite (NEXTSat). The project demonstrates several satellite servicing operations and technologies including rendezvous, proximity operations, station keeping, capture, docking, and most importantly propellant transfer and ORU (Orbit Replaceable Unit) transfer. These last two operations would greatly enhance the life expectancy of orbital

assets and help reduce the cost of space missions. A prime future military mission would be to replenish the propellant of reconnaissance satellites.

Autonomous rendezvous and docking systems could become a viable alternative to human-piloted missions in the next decade (Smith, 2007). Eight test series were conducted during the three-month mission in 2007. ASTRO and NEXTSat conducted approach and docking maneuvers from starting points up to 4.3 miles away. In order to come together, a series of proximity maneuvers were necessary. After rendezvous and docking, the two spacecraft swapped propellants and traded and installed batteries. This was the first unassisted component exchange in space history.

A similar program is the Air Force Research Laboratory's XSS-11 (AFRL, 2005). It is a new class of low-cost spacecraft (microsat) weighing approximately 100 kg to perform space servicing, diagnostics and maintenance as well as rendezvous, proximity operations, surveying and autonomous mission planning. In essence, the objectives of these programs are identical, but the implementation, in particular the propellant transfer, is different. The technology demonstrations were performed with nearby objects – NEXTSat in the case of Orbital Express and the expended rocket body for XSS-11. Neither of these systems have sufficient on-board propellant to service multiple satellites within their orbits. The notional system in this dissertation would be designed to maneuver significantly more within and outside its initial orbit and multiple times in its design life.

The Army Space and Missile Command (ARSTRAT) Technical Center commissioned a study on a low-cost, electro-optical imagery system designated as NanoEye (ARSTRAT, 2011). In 2012, this program was in its concept development

stage. ARSTRAT claimed that this maneuvering micro-satellite (using CP) could be tasked directly by tactical ground users who would receive desired images minutes later. The system would be designed as a light-weight vehicle with a dry mass of 20.6 kg and a propellant storage capacity of multiple times its dry mass. The primary objective of the research program is to demonstrate on-orbit maneuvering, tasking to image a desired ground target, and relaying the product back to the requesting user during the same satellite pass. NanoEye would be proliferated in large numbers and could provide submeter resolution imagery quickly at a relatively low cost. Figure 2-6 shows the concept configuration of NanoEye.

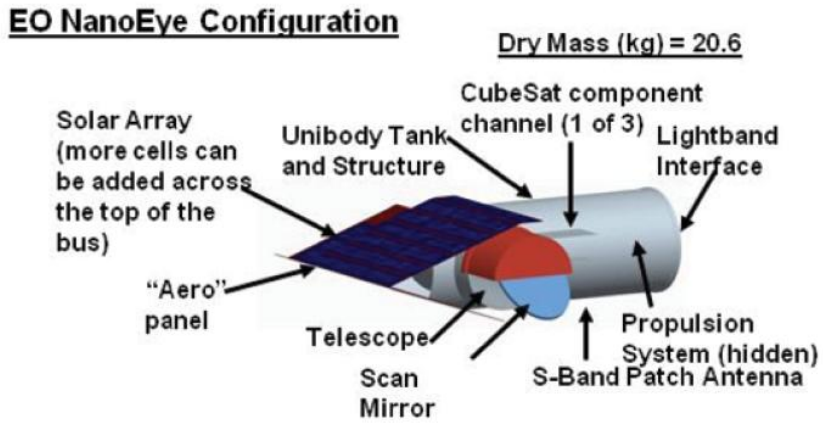

Figure 2-6. NanoEye Maneuvering, Electro-optical Satellite Concept (ARSTRAT)

Chioma examines the feasibility and operational usefulness of repeated intercepts (Chioma, 2004: 1-36). The concept requires that a microsat repeatedly fly past a target satellite once per orbit. This necessitates precise knowledge of the position of the two satellites and maneuvering in order to co-locate approximately after one revolution of the observing vehicle.

This mission allows the microsat to image a target from multiple perspectives and in various lighting conditions without requiring matched orbit planes. The principle drawback of this inspection method is the high rate of relative velocity at which the microsat is zooming by, but the advantages are the covert inspection of this method and the wide range of target satellites which are within the range of a single microsat. The asset would standby in a parking orbit until commanded to image a particular target. It initially performs a series of maneuvers to cause the first intercept. It does not need to launch into the same orbit plane or change its orbit to match the target. Thus its mission is not revealed at any time to those who may be watching. Furthermore since the velocity does not need to match the target's either, the microsat can image multiple targets in various orbits. Chioma offers an analysis that shows a microsat in an appropriate parking orbit would be in a position to repeatedly intercept any single target in LEO within 24 hours of command.

The repeated intercept mission is as much an orbit determination as it is an orbital maneuvering problem. This dissertation is not as concerned with the former but can apply some of the basic equations used by Chioma. Satellites experience perturbations due to air drag which can be modeled as an acceleration term opposite the direction of travel

$$\bar{a}_d = \frac{C_D S}{m} \frac{\rho^R V}{2} {}^R\bar{V} \tag{2.9}$$

where $\bar{a}_d \equiv$ acceleration vector due to drag, $C_D \equiv$ coefficient of drag, $S \equiv$ wetted vehicle surface area, $m \equiv$ satellite mass, $\rho \equiv$ atmospheric density, ${}^R V \equiv$ magnitude of relative velocity of satellite with respect to surrounding air particles (the barred version is the

corresponding vector quantity). Relative velocity is then defined as ${}^{R}\bar{V} = \bar{V} - \bar{V}_{atm}$, where the last term is the velocity of the local atmosphere which is assumed to rotate with the Earth according to

$$\bar{V}_{atm} = \bar{\omega}_{\oplus} \times \bar{R} \tag{2.10}$$

where $\bar{\omega}_{\oplus} \equiv$ angular velocity of the Earth and $\bar{R} \equiv$ inertial position vector of the satellite measured from the center of the Earth. The satellite's mass, area and coefficient of drag are often combined into a single term known as the ballistic coefficient:

$$B^{*} = \frac{C_D S}{m} \tag{2.11}$$

Further, the geopotential is a disturbing function to the satellite's two-body motion that causes significant effects in its orbit (Chioma, 2004: 22). If it is not included in the modeling the motion of LEO satellites, the errors can be large enough to cause the satellite to completely miss its intended target. These equations play a role in the development of the simulation model for low-thrust EP maneuvering.

2.3.2 Planetary Flyby (Lunar-Gravity Assist).

Since the seventies, researchers have investigated the idea of using momentum transfer between two bodies to insert a satellite into Earth's orbit (Ivashkin, 1971: 163-172). This is commonly known as planetary/lunar fly-by and can result in significant propellant savings when compared to inserting directly into the final orbit. This practical idea is based on the fact that the moon's mass is many times greater than that of the

satellite. As the satellite passes the moon, a momentum exchange occurs whereby the moon slows down and the satellite speeds up or vice versa. Since the moon is so massive compared to the satellite, the velocity loss from the exchange is miniscule while the much smaller satellite can speed up greatly. This maneuver is scalable and can be used to speed up (passing the Moon from behind its direction of travel) or slow down the satellite (passing the Moon in front). Studies have shown that it is almost as costly to go to geosynchronous orbit as it is to the moon. In fact it is cheapest to use a bi-elliptic transfer to go out to the moon, then return and use simple orbital maneuvers to enter a desired Earth orbit (such as geosynchronous). Vallado provides a detailed discussion on the different types of maneuvers and the following Table 2-2 for propellant consumption comparisons (Vallado, 2001: 305-322).

Table 2-2. Comparison of Coplanar Orbital Transfers

Type of Maneuver	Initial Altitude (km)	Final Altitude (km)	ΔV (km/s)	Transfer Time (hrs)
Transfer to Geosynchronous Orbit				
Hohmann	191.344	35781.35	3.935	5.256
One-tangent	191.344	35781.35	4.699	3.457
Bi-elliptic	191.344	35781.35	4.076	21.944
Transfer to Lunar Orbit				
Hohmann	191.344	376310.00	3.966	118.683
One-tangent	191.344	376310.00	4.099	83.061
Bi-elliptic	191.344	376310.00	3.904	593.9

These ΔV numbers represent a general case of going out to the moon and do not take into consideration the momentum exchange of a lunar fly-by. Such a maneuver would require the satellite to be collocated with the moon at the exact time the satellite reaches lunar altitude. Adding the additional free ΔV to the calculation will open up the possibilities to

performing high-cost maneuvers such inclination changes without expending on-board propellant (Ocampo, 2003: 173-179).

Mathur and Ocampo present an algorithm to quickly calculate the propellant cost of performing a change between two Earth-centered orbits using a single lunar fly-by (Mathur, 2010). The result can be compared to a direct orbit-to-orbit transfer for possible propellant savings. The algorithm aims to minimize the sum of the initial and final impulsive maneuvers to end up in the desired destination orbit. Starting in an arbitrary orbit, the first impulsive burn occurs at a time and location to assure that the satellite meets with the moon when it reaches the lunar orbit. The gravity assist experienced when satellite and moon meet is modeled as a free ΔV that modifies the return orbit. Finally, the second impulsive burn puts the satellite in its desired orbit. Figure 2-7 demonstrates the procedure.

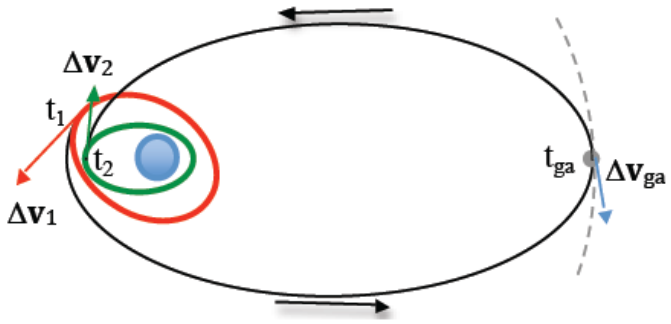

Figure 2-7. Diagram of Lunar Free Return (Mathur, 2010: 6)

Mathur presents three cases with different initial orbits and demonstrates graphically that the algorithm converges. To come to a solution quickly, this model sacrifices accuracy by using a simple two-body gravity model without perturbations. The research in this dissertation is similar in that there is a necessary transfer between two

arbitrary orbits, but the models need to include a higher level of fidelity to include Earth oblateness and air drag effects.

2.4 Atmospheric Maneuver

2.4.1 Space Plane.

NASA and the U.S. Air Force have been investing in maneuverable space vehicles for decades (Ward, 2000: 6-10). The initial focus was reusable launch vehicles (RLVs) to reduce cost. It evolved into space vehicles with aircraft-like maneuverability and these programs are still under development today. The Space Shuttle was the best operational example of a reusable space vehicle capable of re-entry and maneuvering in the atmosphere, however the cost of operating this inefficient, technically complex system was staggering. NASA advertised the average cost of a single Shuttle launch at $450 million, but other watchdog organizations placed the cost much higher at between $800 million to $1.6 billion per-mission depending on the accounting method (Pielke, 1993: 57). More recent efforts aim to demonstrate lower operational cost and center on the military and civilian capabilities of a maneuverable vehicle.

Starting in the early nineties, a series of DC- and X- programs sponsored by private and public sources developed the critical components that ultimately led to the SMV also known as the X-37 (Ward, 2000: 8). The McDonnell Douglas Delta Clipper Experiment (DC-X) flight-tested between 1993 and 1995 and demonstrated integration of RLV subsystems and the capability of relatively low-cost sub-orbital operations. The vehicle was never designed for orbital altitudes or velocities, but did multiple successful vertical

take-off and landing flights. Maintenance and refueling was done at the launch pad and resulted in unprecedented turn-around times. The advanced DC-X program overlapped this development from 1994-1996 and demonstrated the technologies and system design characteristics of quick-turnaround operations. In 1996, the system completed three test flights and showed that a nine-hour turn-around between flights was possible.

The X-33 was a joint NASA-Lockheed Martin program to demonstrate "aircraft-like" capabilities of RLVs. It was designed to use a longer, shallower re-entry profile and reduce heating compared to the Space Shuttle. The goal was to design and test a cost-effective single-stage-to-orbit rocket system and reduce the launch cost to LEO to $1,000 per pound. The program was terminated before this was achieved.

The X-34 served as a bridge between DC-XA and the X-33. It was designed as a single-engine rocket with even more aircraft-like features with short wings and a small tail surface. The technical objectives of the X-34 were sub-sonic and hypersonic autonomous flight and integration of composite materials and low cost avionics. Program components from these efforts contributed to the development of the U.S. Air Force SMV.

The SMV is a reusable space vehicle that deploys from an expendable launch vehicle, performs its mission on-orbit, returns to Earth and prepares for another mission. The SMV is designed as a flexible platform able to accommodate a wide variety of payloads with substantial on-orbit maneuver capabilities. In 2010 the Boeing X-37 Advanced Technology Vehicle began demonstration flights of this USAF SMV. It is designed to incorporate aircraft-like turn times and sortie rates as well as achieve a similar level of safety, reliability, operability, supportability, producibility, testability and

affordability. The vehicle is capable of undertaking four to six-month missions, can be rapidly recalled from orbit and would take less than 72 hours between missions (Arkin, 2000).

2.4.2 Aero-Assist.

Since the original aero-assisted orbital transfer studies in the early sixties, a number of studies and experiments explore the effects of re-entering Earth's atmosphere and how it can be used to benefit specific missions. There are five main categories of these maneuvers: aero-brake, aero-capture, aero-glide, aero-cruise, and aero-gravity assist (Wahlberg, 1985: 3-18; Mease, 1988: 7-33). An aerodynamic maneuver used to reduce the size of an orbit is termed aero-brake. One example is NASA's Mars Reconnaissance Orbiter which uses atmospheric drag to lower its orbit around the Red Planet naturally and thereby reducing the required on-board propellant (NASA, 2005). An aero-capture depletes enough energy to change a satellite's trajectory from hyperbolic to elliptic, hence capturing it in an orbit around an attracting planet/body. An aero-glide combines non-thrusting atmospheric flight with thrusting outside of the atmosphere to modify a satellite's orbit. An aero-cruise is an aero-glide maneuver with atmospheric thrusting. An aero-gravity assist combines a planetary fly-by with a portion of the profile inside the planet's atmosphere. Using the Earth's atmosphere to modify orbital elements can provide significant propellant savings compared to inducing the change with impulsive maneuvers.

Vinh and Shih present two potential uses of a multiple atmospheric skip trajectory to extend the range of a gliding vehicle and rotate the line of apsides (Vinh, 1997: 103-

112). The problem is posed using Hamiltonian mechanics to eliminate mathematical instabilities in the numerical integration and to simplify the iteration process during optimization. The results of these simplified equations are compared to those of the exact governing equations to find that they closely agree. Furthermore, to simplify the problem the basic assumptions are a non-rotating atmosphere and Earth is a point-mass, which eliminates all Earth-rotation rate components and effects due to Earth's oblateness. The assumptions are reasonable because the time periods in question are relatively short and these effects are negligible. Also, the specific geographic location is irrelevant in this problem so any long-term oblateness effects do not alter the results.

A set of standard equations of motion are transformed to suit the task of optimizing specific parameters using multiple skip trajectories. The non-dimensional variables of speed (u) and altitude (h) are

$$\begin{aligned} \mathrm{u} &= \frac{V^2}{g_0 r_0} \\ \mathrm{h} &= \frac{r - r_0}{r_0} \end{aligned} \tag{2.12}$$

where the zero subscript denotes the entry condition (or values at a reference altitude), $r \equiv$ distance of satellite to Earth's center, and $g \equiv$ Earth's gravitational constant. Earth's gravitational field and atmospheric density present the greatest uncertainties in the modeling of LEO satellites. These two parameters depend on many variables such as air temperature, pressure, mass density, and the geopotential; however both vary generally with altitude. The maximum lift-to-drag ratio is designated E^*. Vinh and Shih use E^* values between 0.75 and 1.75.

For a selected set of parameters the authors show how the range can be extended using multiple skip trajectories for a shallow and a steeper flight path angle. The results are intuitive. Shallow entry angles (γ_0 = -0.1°) allow a vehicle to skip back into space (essentially are grazing trajectories) and increase the range angle by almost 360 degrees or once around the Earth after each skip for the first few skips. Without adding any energy (i.e. thrusting) the velocity depletion will become significant enough to quickly consume the available energy and the vehicle is forced to re-enter and land on Earth. A steeper entry (γ_0 = -2.0°) results in more rapid velocity depletion and the altitude and range decrease significantly in each successive skip. Thus, the range is extended in either case, but how many times the system can skip out of the atmosphere greatly depends on the entry angle of the flight profile. Figure 2-8 shows the comparison of entry angles versus altitude and range.

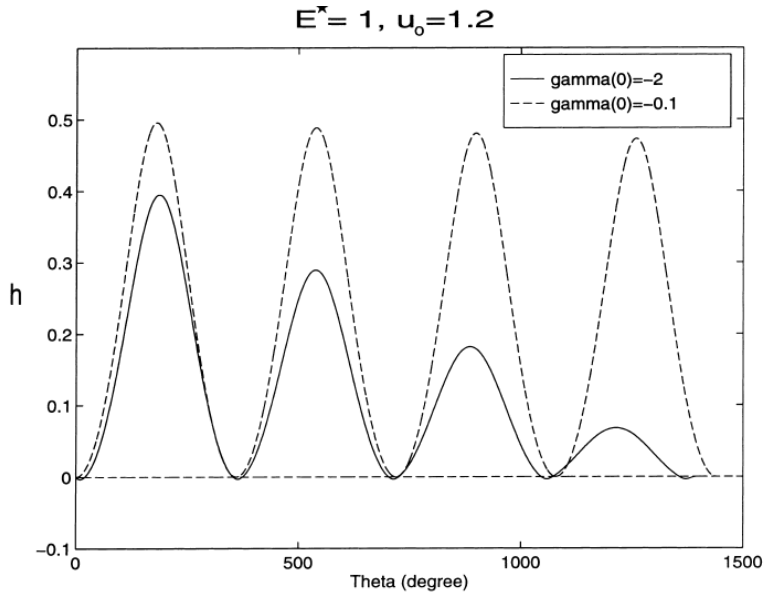

Figure 2-8. Multiple Skip Trajectory for Two Entry Angles (Vinh, 1997: 105)

Another propellant-saving application of aero-assisted flight is the rotation of perigee which is an in-plane maneuver. Considering an elliptical orbit, a pure propulsive maneuver to rotate the line of apsides (another way of saying rotation of perigee, α) is generally done at perigee. This maneuver requires a large amount of ΔV (Lawden, 1962: 323-351). Alternatively, a simple aero-assist scheme can provide cost saving for larger rotation angles. In fact, for $\alpha \geq 66.5°$, an aero-assisted drag-only maneuver consumes less propellant than a pure propulsive one. In this scheme, a small, retrograde thrust impulse applied tangentially at apogee lowers perigee sufficiently to speed up orbit decay. In time, the orbit circularizes and perigee can be chosen freely by applying a second posigrade impulse to raise apogee to its original value. Finally, a third small, posigrade impulse is applied at apogee to raise perigee out of the atmosphere to slow the rate of orbital decay. This effectively restores the initial orbit while rotating the line of apsides up to 180 degrees in either direction.

Furthermore, adding lift capacity to the satellite and applying multiple-skip trajectories, propellant savings are realized with a rotation angle as low as 20°. Figure 2-9 illustrates normalized ΔV for the pure propulsive, aero-assisted drag only and aero-assisted lifting maneuvers. The linear curve represents the normalized velocity increase to rotate perigee by α. The horizontal line is the drag-only ΔV input and it intersects with the first curve at $\alpha = 66.5°$ after which the latter maneuver is more propellant efficient. The last curve shows the ΔV requirement to rotate the line of apsides using the lifting maneuver.

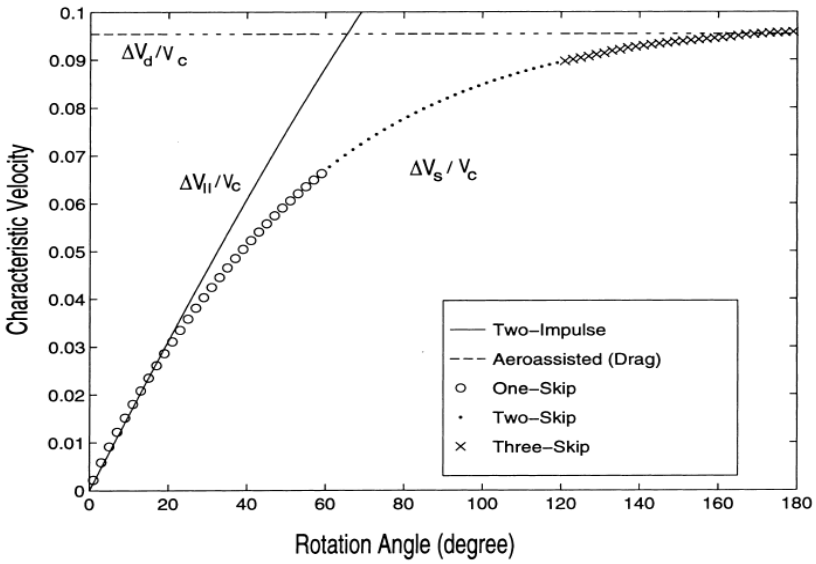

Figure 2-9. Characteristic Velocities vs. Rotation Angle (Vinh, 1997: 110)

For rotation angles below 20°, the propellant consumed for the maneuver is identical to a pure propulsive one, but propellant savings quickly increase for α-values greater than 20°. As α increases, the use of multiple skips further lowers the necessary ΔV expenditure.

Rao *et al.* approach the problem of aero-assisted orbit transfer from a propellant optimization point-of-view (Rao, 2008). The authors' motivation is that existing space capabilities are not operationally responsive, thus the ability to rapidly reposition an unmanned space vehicle can potentially bring benefits to military and civilian users. In order for a spacecraft to accomplish multiple distinct missions (or reposition), it is necessary to develop approaches to quickly design space missions and plan trajectories. Rao's goal is to develop a mission planning algorithm for thrusting aero-assisted orbit transfer using optimal control techniques to minimize the propellant consumed.

The optimization problem is set up in a conventional manner. Earth is spherical and not rotating, the satellite is assumed to be a point mass and thrust is impulsive. The propellant consumed is measured by the change of spacecraft mass

$$\Delta V = g_s I_{sp} \exp(m^+ / m^-) \tag{2.13}$$

where $g_s \equiv$ gravity at sea-level, $m^- \equiv$ mass of vehicle before the thrust impulse, and $m^+ \equiv$ mass of vehicle after the thrust impulse. The maneuver assumes a transfer between an initial equatorial, circular and a final inclined, circular orbit and is divided into three individual thrust impulses: (1) ΔV_1 de-orbit – to make the orbit elliptical and bring perigee into the atmosphere as it is first sensible by on-board instrumentation, (2) ΔV_2 re-orbit or boost – to set satellite on desired path after completing the atmospheric flight portion and (3) ΔV_3 circularize – to circularize the final orbit (Figure 2-10).

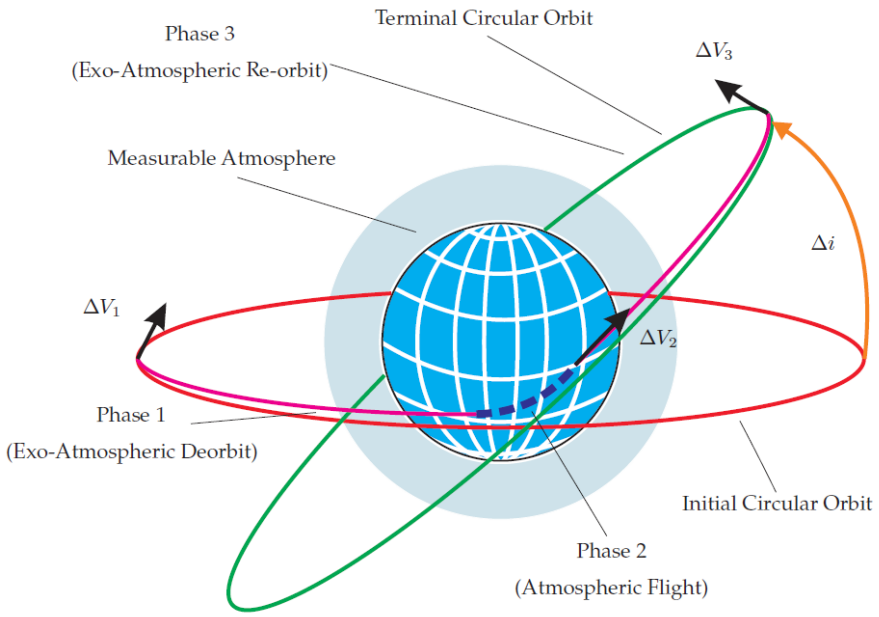

Figure 2-10. LEO to LEO Aero-assisted Orbital Transfer (Rao, 2008)

Darby finds that de-orbit and re-circularization phases require significantly less ΔV than the boost phase (Darby, 2010). The difference is two orders of magnitude where ΔV_1 and ΔV_3 range between 20 to 40 m/s while ΔV_2 is between 1000 to 3000 m/s. At these ΔV requirements, a conventional LEO satellite would only be capable of performing an aero-assisted inclination change once before its propellant is depleted. ΔV_2 is highly dependent on the magnitude of the inclination change. This is expected as the system trades the available kinetic energy (velocity) for a change in the orbital plane. The boost impulse essentially compensates for the velocity loss inside the atmosphere and adds it back to the system to maintain the orbit. The final result is a lower total ΔV, which is simply the sum of these three phases, as compared to making the change using CP.

The objective of Rao and Darby is to minimize total ΔV. Using a set of notional vehicle characteristics (mass, specific impulse, lift and drag coefficients, maximum heating rate, and surface area) and astrodynamic data (sea-level density, entry altitude, and velocity) the authors simulate aero-assisted orbit transfer maneuvers for different inclination changes while minimizing total ΔV. They compare the results to pure impulsive maneuvers and find that that the amount of propellant consumed in the latter increases significantly faster than that of aero-assisted ones. Only a small amount of inclination change ($\Delta i = 10°$) is necessary for an aero-assisted orbit change to outperform a pure impulsive one (Figure 2-11).

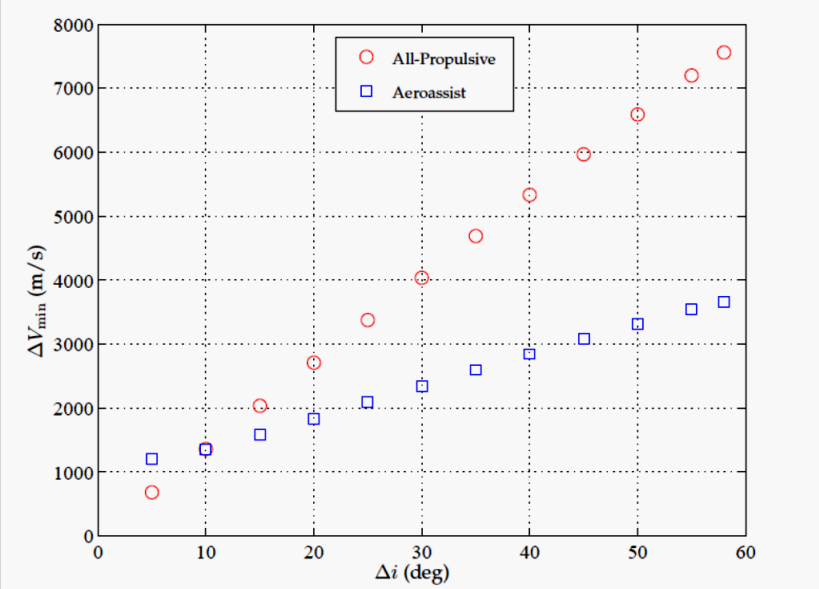

Figure 2-11. ΔV for Aero-assisted & Impulsive Transfer vs. Δi (Rao, 2008)

The field of aero-assisted orbit transfer holds enormous potential hence the numerous studies on this subject (Baumann, 2000: 457; Gogu, 2009: 927; Ross, 1998: 361; Zimmerman, 1998: 127). However, besides the Mars Reconnaissance Orbiter and a few isolated anomalies (rescue of AsiaSat-3/HGS-1 using a lunar fly-by (Ocampo, 2005: 232-253)) no operational system exists to tap the potential of atmospheric flight to modify the orbit of a space vehicle. The lack of operational examples signifies that there are still challenges in realizing this technology and the benefits do not outweigh the costs of such a system.

Previous work on related topics is vast, but none address low-thrust maneuvering to overfly specific ground targets. EP was developed in the 60s and has been a proven space technology for decades, yet the operational implementation is still very limited today. Orbit design and optimization based on specific missions is very useful and applicable. However, it is static and in a LEO environment it almost always necessitates a

constellation, which is expensive to deploy and cannot be rapidly reconstituted. Aero- and gravity-assist maneuvers can be creatively applied like the rescue of AsiaSat-3 or to make extraordinary changes to time-over-target or out-of-plane orbit changes, but these face great challenges in structural and vehicle design, especially in conjunction with low-thrust EP which requires a large amount of power. Gravity-assist maneuvers are not applicable to the mission of ground target overflight in a timely and responsive manner. The work in this dissertation considers the previous research summarized in this chapter and significantly improves upon what is currently available in literature.

3 Motivation

3.1 Newberry's Responsive Space System

Newberry analyzed the viability of a low-Earth orbit (LEO) electric propulsion (EP) system and its capability of changing time-over-target (TOT) by as much as 24 hours with seven days of lead-time (Newberry, 2005: 48). Time-over-target is defined as the time a spacecraft overflies a target. A change in TOT indicates that the same target is overflown at a different time. His hypothetical spacecraft weighs 500 kg and is equipped with a highly efficient, low-thrust engine. It is in a highly elliptical orbit (HEO) inclined at 85 degrees and a period of 2.7 hours. Newberry's motivation to investigate this problem provides the framework of the thesis presented in Chapters 1 and 2. The initial results show that with simple, in-plane, posigrade, continuous thrusting, significant ground track changes including a specific TOT are possible. The foundation of the analysis is that the vehicle overflies the same theater twice a day. This chapter reproduces Newberry's findings to validate the results since his work was not published in a peer-reviewed article. Reproducing the work aided the understanding of Newberry's process and capabilities of EP maneuvering. A large body of work followed these initial findings and is presented in the following chapters.

Interestingly, any odd divisor of a 24-hour period ensures that a satellite passes over the same area twice in one day, once in an ascending pass and again in a descending pass twelve hours later. For any odd divisor from 1 through 15, Satellite Tool Kit (STK)

simulations show that in fact the vehicle passes over the same longitude twice in a 24-hour period, while an even divisor of 24 hours does not.

Newberry also states that a satellite in HEO allows orbit adjustments with very low propellant consumption (on the order of tens of m/s) compared to circular orbits. Circular orbits are the least propellant efficient from which to make changes and such changes quickly shorten the lifespan of the vehicle. Yet proximity to Earth necessitates circularization of the orbit over time. Depending on the perigee altitude of the elliptical orbit, it can circularize very rapidly within a few revolutions. If the final circularized orbit is close enough to Earth, the orbit decays quickly and the satellite is forced to re-enter the atmosphere with devastating consequences unless the vehicle is designed to do so. Thus in order to utilize elliptical orbits there are three options: (1) orbit must be at a high altitude where air drag effects are minimal (perigee altitude above 700 km), (2) the amount of time spend in a lower elliptical orbit is short (3-5 revolutions), or (3) the satellite must thrust to counter drag forces. To investigate why HEOs are more efficient to maneuver from, the Lagrange Planetary Equations in force form can provide the answers (Wiesel, 2003b: 84-95):

$$\frac{da}{dt} = \frac{2e\sin\nu}{n\sqrt{1-e^2}}a_r + \frac{2a\sqrt{1-e^2}}{r}a_s \tag{3.1}$$

$$\frac{di}{dt} = \frac{r\cos(\omega+\nu)}{na^2\sqrt{1-e^2}}a_w \tag{3.2}$$

$$\frac{d\Omega}{dt} = \frac{r\sin(\omega+\nu)}{na^2\sqrt{1-e^2}\sin i}a_w \tag{3.3}$$

$$\frac{de}{dt} = \frac{\sqrt{1-e^2}\sin\nu}{na}a_r + \frac{\sqrt{1-e^2}}{na^2e}\left(\frac{a^2(1-e^2)}{r} - r\right)a_s \tag{3.4}$$

$$\frac{d\omega}{dt} = -\frac{\sqrt{1-e^2}\cos\nu}{nae}a_r - \frac{r\cot i\sin(\omega+\nu)}{na^2\sqrt{1-e^2}}a_w + \frac{\sqrt{1-e^2}}{nae}\left(1+\frac{r}{1+e\cos\nu}\right)\sin\nu a_s \quad (3.5)$$

$$\frac{dM_0}{dt} = -\frac{1}{na}\left(\frac{2r}{a} - \frac{1-e^2}{e}\cos\nu\right)a_r + \frac{3}{2}t\sqrt{\frac{\mu}{a^5}}\frac{da}{dt} - \frac{\sqrt{1-e^2}}{nae}\left(1+\frac{r}{a(1-e^2)}\right)\sin\nu a_s \quad (3.6)$$

where $a \equiv$ semi-major axis, $e \equiv$ eccentricity, $\nu \equiv$ true anomaly, $a_r \equiv$ radial acceleration component, $a_s \equiv$ tangential acceleration component perpendicular to a_r, $a_w \equiv$ out-of-plane acceleration component, $t \equiv$ time, $n \equiv$ mean motion, $r \equiv$ distance of satellite to Earth's center, $\omega \equiv$ argument of perigee, $\Omega \equiv$ right ascension of the ascending node, $i \equiv$ inclination, and $M_0 \equiv$ mean anomaly. The latter three of these six equations contain singularities when e is zero (circular orbit) along with the third equation listed here when i is zero (no inclination) and require proper expansions to eliminate the singularities (such as Delaunay equinoctal elements). To avoid this, this discussion is only limited to a, i and Ω, where $i \neq 0$. In order to numerically find the time rate of change of the classical orbital elements, it is necessary to use all six equations; however, looking at the first three alone provides valuable insight to understand Newberry's statement about propellant efficiency in circular versus elliptical orbits.

The first equation describes the time rate of change of the semi-major axis. Its magnitude increases with an orbit's eccentricity. Acceleration components in the radial and tangential directions affect this parameter while the out-of-plane component does not. The first term contains e in the numerator and the denominator. Clearly, if $e = 0$, there is no change in a as a result of radial acceleration; however, a changes indirectly as e increases due to a force in the radial direction. Hence these six equations of motion are described as coupled first order differential equations, where each element depends on

some or all of the other elements. The bottom line is an elliptical orbit ($e \neq 0$) increases the time rate of change of the semi-major axis as long as the vehicle experiences some radial acceleration.

Similarly, the second and third equations are also largest when the orbit is eccentric. Inclination and right ascension time rates of change have e in the denominator. Translated, this means the rate of change of i and Ω are smallest when the orbit is circular (e=0), but increases as it becomes more elliptical. The singularity due to a zero inclination is eliminated here, since the orbit is defined as near-polar (i = 85˚). Thus the statement that circular orbits are the least efficient to move in is generally true as these three Lagrange Planetary Equations yield greater changes in the orbital elements for elliptical compared to circular orbits.

Newberry's third statement is that low thrust EP systems are more attractive than high thrust CP systems because the total amount of possible orbit adjustments, or gas mileage, is increased by eight to ten times. This claim is supported by comparing the specific impulse (I_{sp}) or efficiency of existing ion propulsion versus liquid propellant engines. Legacy systems are able to achieve an I_{sp} between 100 and 500 seconds while Hall or Xenon Ion Propulsion Thrusters have an I_{sp} between 1000 and 4000 seconds. Simply based on these numbers, low thrust systems are eight to ten times more efficient and therefore yield more gas mileage when compared to a high thrust system.

Theoretically this means that EP is capable of changing its system's orbit multiple times compared to CP. The implementation of higher mass and more infrastructure inevitably reduces this number, but the bottom line is that the efficient system could

maneuver significantly more. The European Space Agency found that this number is even higher, as much as 20 times more efficient based on propellant use per unit of ΔV.

Newberry's final and most profound statement is that a low thrust system can achieve any TOT with a lead time of one week. The inner line of Figure 3-1 is the propellant use profile for a low-thrust EP system with respect to TOT change. The outer line depicts the same for a high-thrust CP system. On the x-axis, the TOT change is in hours. A positive TOT change indicates a later overflight time compared to the non-maneuvering reference, whereas a negative TOT change corresponds to an earlier arrival. The y-axis displays ΔV consumed in m/s. The low thrust system achieves a change in TOT of 1.8 hours when thrusting continuously for three days and expending an amount of propellant measured in ΔV of 170 meters per second. It is also apparent in the figure that a high-thrust system (CP) uses significantly less ΔV (100 m/s) yet the amount of propellant consumed measured by mass is higher due to the low I_{sp} of such systems. Electric propulsion's larger I_{sp} values effectively result in greater ΔV budgets.

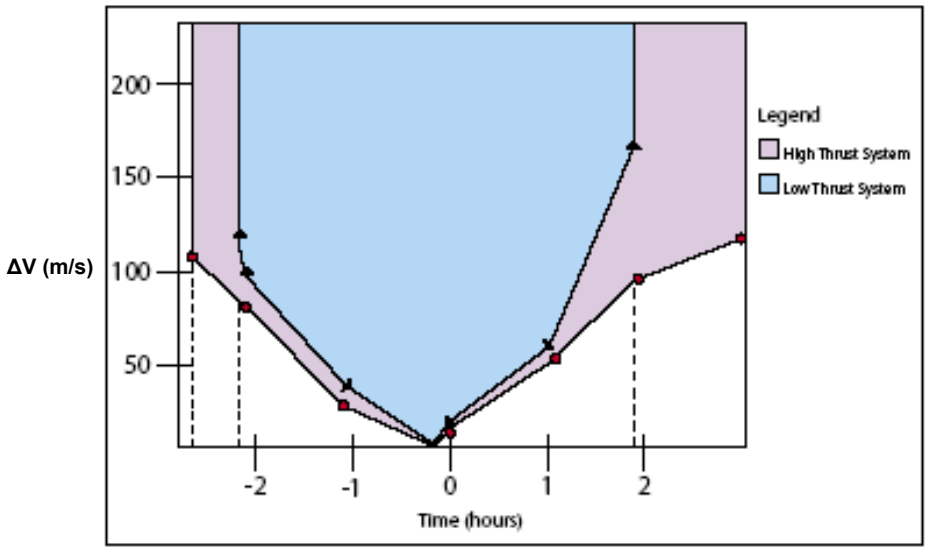

Figure 3-1. Time-over-Target (TOT) Control

Assuming a vehicle mass of 500 kg, the amount of thrust the engine is able to produce is almost 330 mN:

$$\Delta V = \frac{F}{m}t$$
$$F = \frac{170\text{m/s} \cdot 500\text{kg}}{259200\text{s}} = 327.9\text{mN} \tag{3.7}$$

where $F \equiv$ force. The simulations assume only half of this thrust level, but fortunately the change in TOT is linear as a function of thrust, so the results are applicable.

In Figure 3-2, Newberry shows that a typical operational asset that continuously thrusts with an EP engine over a seven-day period can change its orbit within the same orbital plane to produce a 24-hour time-over-target (TOT) change by controlling orbital period.

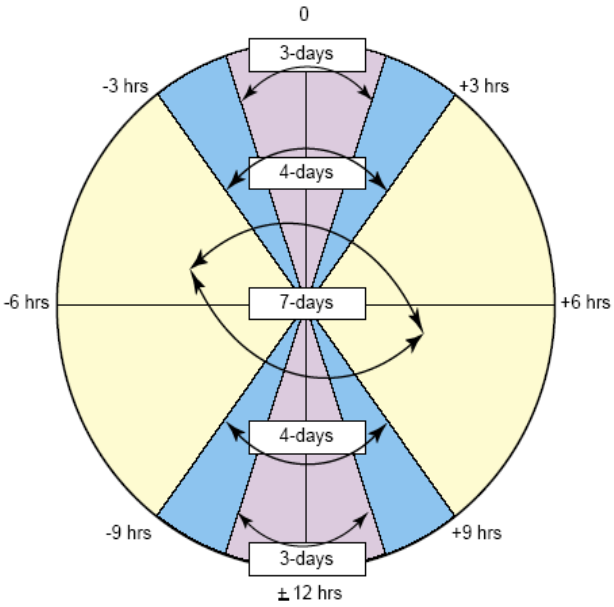

Figure 3-2. TOT Performance based on Lead Time (Newberry, 2005: 49)

The result is ground track alteration proportional to the lead time provided to adjust the orbit. A current asset that can maneuver in orbit using EP but not enter the denser atmosphere can reach any location on the Earth in seven days. Figure 3-2 is interpreted in the following manner. The outer numbers represent the amount of TOT change possible. At the 12-o'clock position, no maneuvering has been done and the TOT change is 0. This position is the reference. An equal distance to the left and right shows ±3 hours (hrs) attainable after 4 days of maneuvering, and it is signified by the inner arrow and the attached text box. After 7 days, the possible TOT is 6 hrs early or later compared to the reference (at 3 and 9 o'clock positions). Newberry argues that due to his problem setup, the satellite overflies each target twice per day exactly 12-hrs apart (at 12 and 6 o'clock positions). If maneuvering can change TOT by 12 hrs twice per day, a cumulative 24-hr change is possible. A simulation presented in this chapter for a satellite in a highly elliptical orbit (e = 0.5) with thrust levels between 60 and 150 mN can reproduce the results presented by Newberry and is summarized in Figure 3-3.

3.2 Initial Modeling & Analysis

The results from MATLAB and Satellite Tool Kit (STK) simulations confirm Newberry's findings. The problem setup starts with a circular orbit. Orbital altitude specifies the satellite's velocity (altitude 1000 km), inclination is arbitrarily set at 40°, at the initial time argument of perigee (undefined for circular orbits but stated here to expand to the elliptical case later) is 90°, argument of latitude is 0°, and RAAN is selected to put the vehicle over the desired target location. Two orbits are simultaneously

propagated forward in time. The first is a reference orbit without thrusting where all natural perturbations (third-body effects of sun and moon, higher order geopotential effects, and air drag) are included in the simulation. A second orbit is propagated using STK's Astrogator to include continuous low-thrust forces to model an EP system and the same natural perturbations. This assumes that the low thrust system is turned on at the initial time and its thrust vector is aligned with the velocity vector. The resulting trajectory is a spiral transfer as described in section 2.1.1. When the ground tracks of these two orbits cross the longitude line of the target location, the times are recorded. The difference of these times is the amount of change the propulsion system induced. This is termed the TOT control in the following graphs.

Figure 3-3 summarizes the TOT control of a circular orbit for five different low thrust levels (60, 82.5, 105, 127.5, and 150 mN).

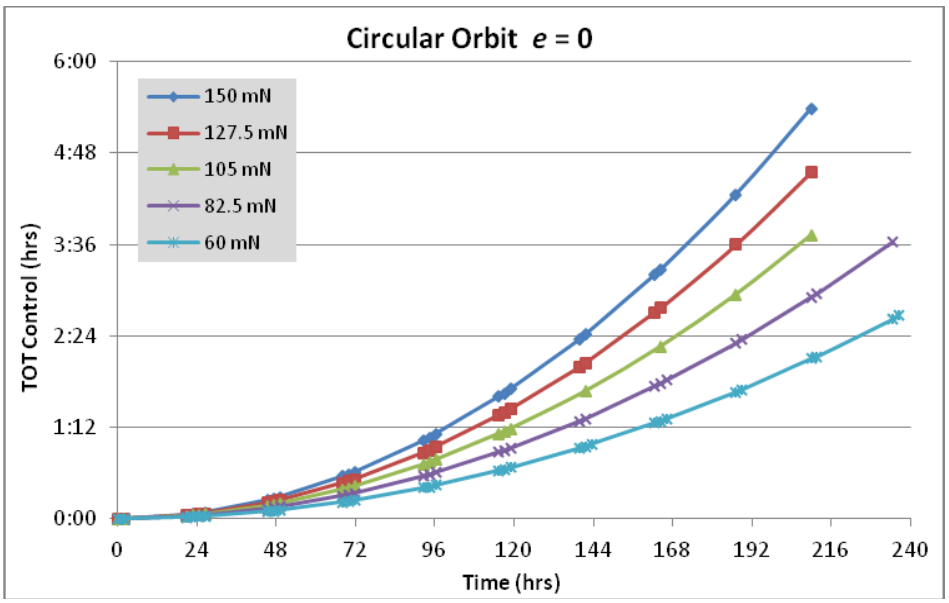

Figure 3-3. TOT Control vs. Time for a Circular Orbit (*e* = 0)

At the highest thrust level, the amount of time difference achievable is 35 minutes after three days of thrusting; 63 minutes after four days; and 196 minutes after seven days. Similarly at the lowest thrust level of 60 mN, the TOT difference is 14 minutes after three days and 120 minutes after seven days.

Figure 3-4 shows the change in TOT as a function of time for an elliptical orbit (e = 0.5). For this orbit, the in-plane thrust vector has radial and tangential acceleration components yet no out-of-plane component. The initial conditions are identical to the previous case with the exception of apogee altitude. After three days of thrusting at 150 mN, the TOT change is 50 minutes; 86 minutes after four days; and 270 minutes after seven days. These values are on average 39 percent higher than the circular case. The effective change in TOT is approximately half of those found in Newberry's analysis. It is no coincidence that the corresponding thrust levels are also roughly half. The unusual spikes in Figure 3-4 are only observed for this eccentricity and are outliers induced by the data collection methodology rather than a real physical phenomenon.

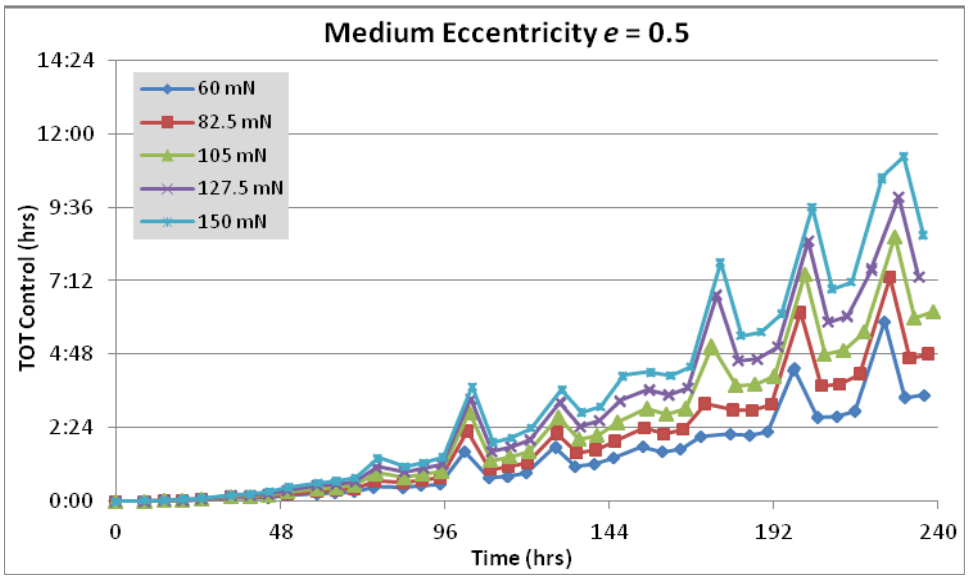

Figure 3-4. TOT Control vs. Time for an Eccentric Orbit (e = 0.5)

Figure 3-5 shows the same setup for an orbit of higher eccentricity (e = 0.7). After three days of thrusting at 150 mN, the TOT change is 58 minutes; 120 minutes after four days; and 300 minutes after seven days. These values are on average 69 percent higher than the circular case and 22 percent higher than the medium eccentricity case.

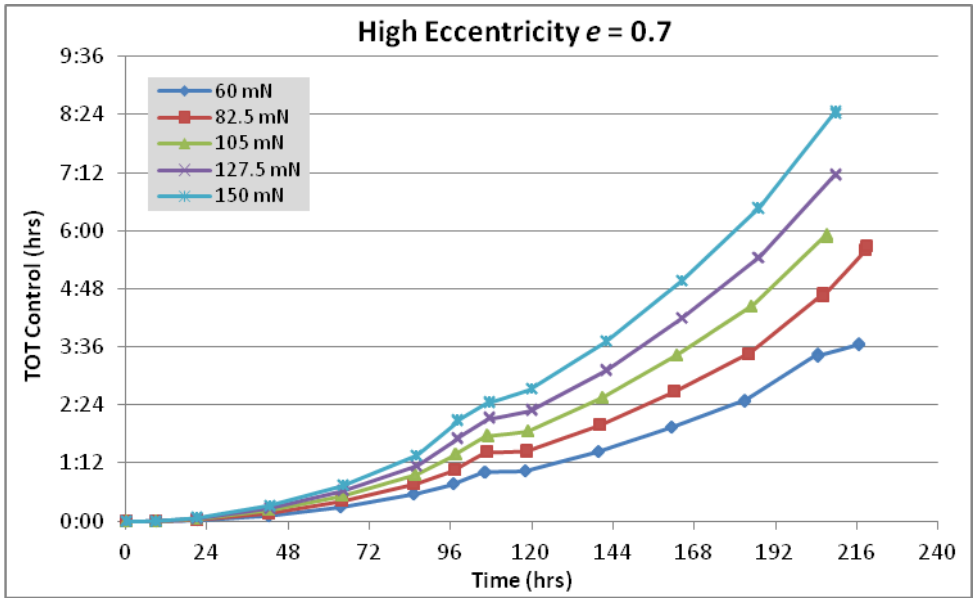

Figure 3-5. TOT Control vs. Time for an Eccentric orbit (e = 0.7)

The conclusion that an increasingly elliptical orbit is more efficient to maneuver from is consistent with Newberry's argument discussed in the previous section. A higher eccentricity does yield greater changes in TOT given the same elapsed time and thrust level. Although it is true that higher eccentricities lead to a greater TOT change, this is only accurate at perigee and for most the remaining orbit, the TOT change is in fact smaller than the circular case. This finding is further explained in section 5.4 Figure 5-7. Figure 3-6 displays the TOT control for the same 150-mN thrust for varying eccentricities.

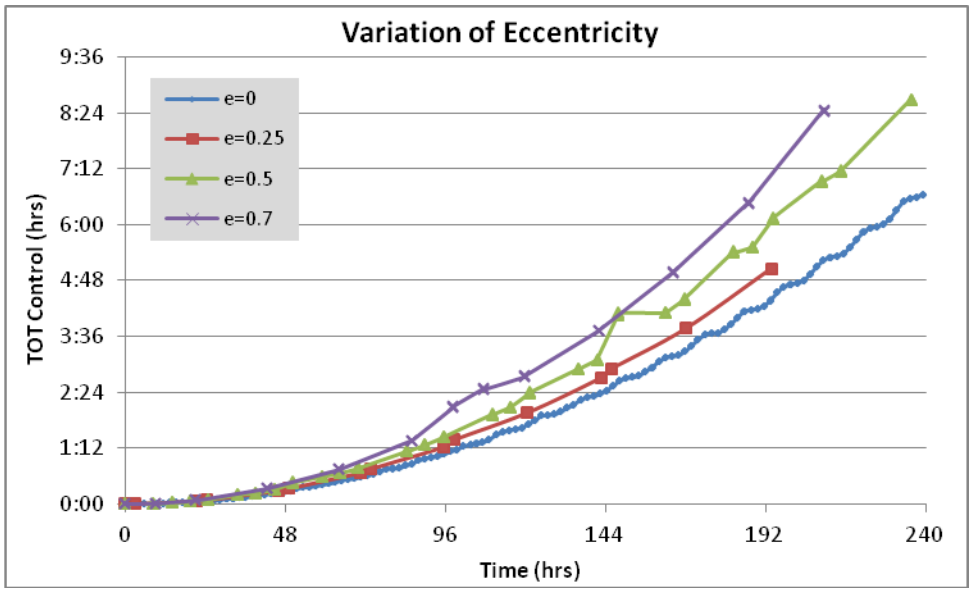

Figure 3-6. TOT Control vs. Eccentricity

Orbit plane orientation (defined by Ω) and the exact satellite location within the orbit (given by v or u) do not have an impact on TOT control using this measuring methodology. Since the reference and the thrusting orbits start with the same initial conditions, any change in these two parameters would be identically reflected in either orbit, there are no effects on the resulting time difference. To confirm this, Figures 3-7 and 3-8 plot TOT control against three different initial Ω and v values for an eccentric orbit (e = 0.5), respectively.

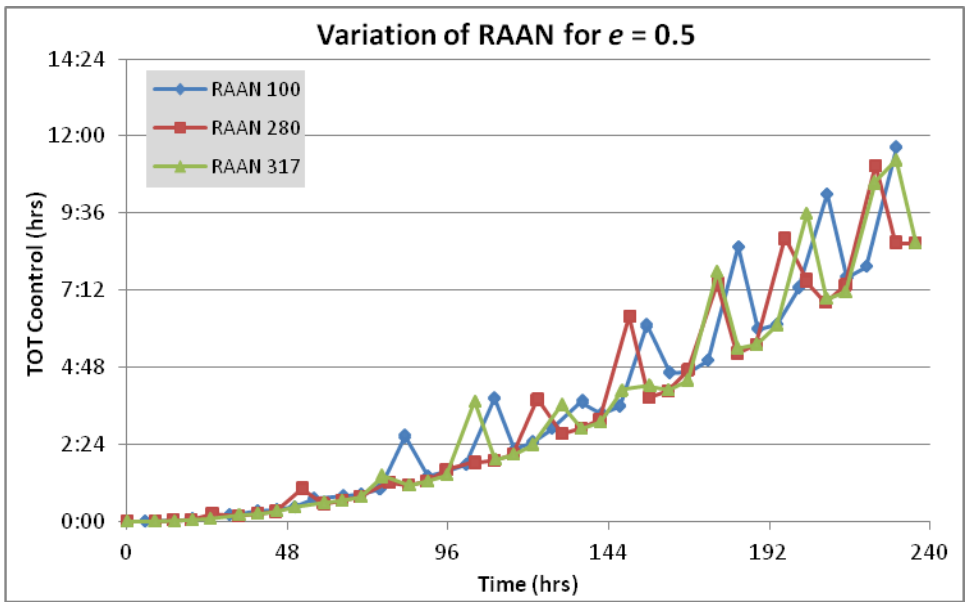

Figure 3-7. TOT Control vs. RAAN

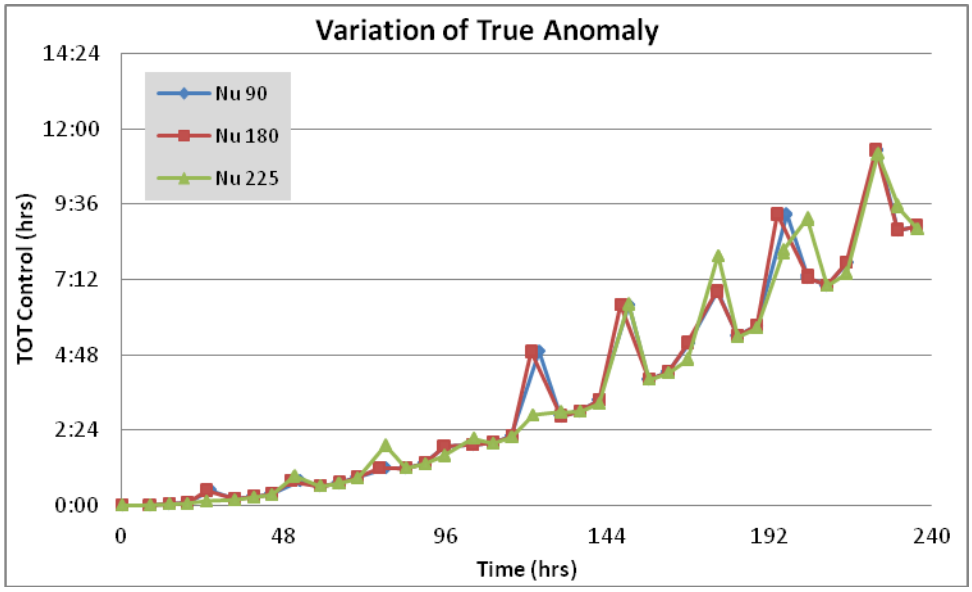

Figure 3-8. TOT Control vs. True Anomaly

Some minor differences are observable; however the trend is the same for these very different starting conditions. Although not shown here, the same principle applies to inclination.

There are some issues to consider with the proposed system. Eccentric orbits are problematic to work with because the amount of time spent at the lower altitudes is short thereby making most of the orbit useless for mission types in which a small range to target is critical. The proposed polar orbits also leave large areas of the globe uncovered, thus making many areas inaccessible without thrusting or requiring constant maneuvering.

In a highly eccentric orbit a satellite spends very little time (at high speeds) at perigee and most of its time a higher altitudes. Although this may not pose a problem for communications, it certainly does limit the amount of useful time for optical and radio frequency systems that require proximity to the planet's surface. Should it be necessary to change the geographic region surveyed by the satellite at low altitudes, the orbit needs to be re-oriented to move perigee over the particular area of interest requiring a substantial amount of propellant, shortening the vehicle's life by many months or even years. Using low-thrust EP may be a solution to this problem; however, orbit design should be the first consideration before advocating constant maneuvering. A tradeoff between propellant efficiency obtained by using higher eccentricity and propellant requirement to change the orbit's geographic perigee location is necessary to choose the proper orbit for the mission type.

A polar orbit can leave large areas of the globe uncovered. It allows a satellite to fly along certain longitude lines, therefore covering all regions along that longitude from the North to the South poles. However, there are large areas in-between the orbit passes that remain uncovered as a function of the orbit's period. The longer the period or the higher the satellite's altitude results in a larger uncovered area. Thus for some missions it would

be more beneficial to remain as close to the planet as possible without entering the atmosphere to avoid large energy losses and rapid orbit decay. Remaining close to the planet for an extended period of time also means sacrificing efficiency of an elliptical orbit as the orbit circularizes quickly at low altitudes. This trade-space must be explored to find a suitable middle-ground for the mission at hand.

In-plane thrusting changes four of the six orbital elements, but has no effect on the element that may have the greatest impact on TOT, namely the RAAN. The RAAN determines the orientation of the orbit with reference to the inertial Point of Aries. The rate of change of the RAAN is given by Equation (3.15) and it is also a function of eccentricity and inclination. Hence the two previous issues have bearing on how much or how fast the RAAN would change. Higher (or polar) inclinations and eccentric orbits favor a faster RAAN change. As with all orbital elements, the RAAN change is highly coupled with the other elements and therefore would also require tradeoffs for mission design. The trade study becomes very cumbersome and complicated when five of the six orbital elements are considered simultaneously, yet it is necessary in order to find the most efficient orbit to meet a set of user requirements.

3.3 Expanding the Idea of Responsive Space Systems

Most of Newberry's conclusions about a low-thrust, maneuverable system are verified in Chapters 3 and 4. TOT control can be very beneficial to the mission types Newberry mentions in his article, but also more traditional space missions can benefit. If a satellite's orbit can be effectively changed multiple times over its lifetime to evolve with constantly changing mission requirements, the cost to launch and operate spacecraft

can be significantly reduced. It would change the existing paradigm of static operations to a new, flexible way of operating in space.

This concept can provide more flexibility and faster response times by harnessing the potential aero-assisted flight of space systems. Although most space assets are not designed to re-enter the atmosphere, utilizing atmospheric drag to affect rapid change in a satellite's orbit could be feasible as shown by several studies addressed in Chapter 2. A change in the orbit translates into a change in the ground track and TOT. As Newberry points out, low thrust propulsion systems can effectively change TOT in a reasonable amount of time (seven days), but this magnitude of change is only possible for a restricted number of orbits (namely with selected orbital periods and highly elliptical). Since the goal is not to simply thrust most efficiently (i.e. direction aligned with velocity vector), but a combination of minimum time to overfly a ground target and least amount of propellant consumed in doing so, it may be beneficial to not constrain thrusting in this direction or even within this plane. Furthermore, a combination of out-of-plane, low-thrust and aero-assist profiles can result in even lower response times (higher TOT control) but expend more propellant and open the possibility for satellites to operate in a larger number of orbit classes.

This dissertation examines the combination of the proposed EP system with aero-assisted maneuvers, but concludes that current technology is not mature enough to overcome the challenges. Extraordinary maneuvers with much lower response times compared to EP are possible with CP. The cost for this responsiveness is a large amount of propellant. In most cases, a CP system could perform such a maneuver once. Similarly, even with aero-assist, Darby and Rao find that more than 50% of the on-board propellant

would be used up for a single maneuver (Darby, 2010). Alternatively, EP could be used as an efficient means to add the energy lost due the significant drag forces inside the atmosphere.

An analysis considering the power requirements, available acceleration, and propellant budgets quickly lead to the conclusion that an aero-assisted maneuver is extremely difficult to perform using today's technology. An observation mission using CP at an altitude of 280 km requires a propellant mass of 72,000 kg for a 5-yr lifecycle. The amount of drag at this altitude will deteriorate the orbit of a satellite within weeks. Switching to EP, after resizing the solar arrays to provide the amount of power required makes it infeasible to operate below 300 km since the available acceleration is insufficient to maintain the orbit. Increasing the altitude to slightly above 300 km changes the operating environment significantly.

The LEO altitudes of 300-500 km provide a favorable range for observation missions, which combine high resolution and responsiveness without the challenges of entering the atmosphere. In this altitude range, both CP and EP systems can maneuver effectively and static satellite systems can have 5 to 10-yr lifecycles with reasonable propellant budgets. A static satellite at 340 km carrying a 1-m resolution payload could operate for 5 years with a total wet mass of less than 1000 kg. At the same altitude, EP systems can effectively counter drag and have sufficient control authority to be responsive to evolving user requirements. Furthermore, the enormous area of the large solar arrays and higher velocities at lower altitudes act together to exponentially increase drag. Entering the atmosphere would create so much frictional heating on the spacecraft and its solar arrays such that it is unlikely the vehicle would survive. Using today's EP

technology, it would be more feasible, less costly, and safer to operate outside the atmosphere. As a result of these findings, the research in this dissertation turned away from aero-assisted maneuvers to focus on orbital parameters most beneficial for low-thrust maneuvers and the algorithm required to perform them.

An area of recommended future work is combining aero-assisted maneuvers with highly efficient EP to reduce the amount of propellant required in the boost phase, not in terms of ΔV but mass of propellant consumed. Provided the proper technology in solar arrays, power generation, and high thrust EP engines, it is conceivable that a combination CP-EP system may be the answer to bridge the gap from the concept to an operational aero-assist vehicle. A spacecraft in a 350 km parking orbit may use CP to lower its perigee to approximately 150 km and dip into the atmosphere, perform an extraordinary maneuver, and use highly-efficient EP to build up the lost energy and return to its original parking orbit. In the near-term, the proposed maneuverable EP satellite may provide the responsiveness, low-cost, and flexibility good enough to meet user requirements.

4 A Taskable Space Vehicle

4.1 Introduction

The use of space gives the United States distinct advantages in any battlefield environment, but the high cost of space operations increasingly jeopardizes these advantages. Although the U.S. pioneered much of the current space technology, declining budgets for space research, development, and operations leave our legacy systems vulnerable to adversaries around the world. Other nations formerly incapable of space exploitation are quickly learning to counter current U.S. space technologies at surprisingly low costs. In order to reduce the cost of deploying and maintaining a robust space capability, the Department of Defense (DOD) must change the status quo in space operations or risk losing its advantage. The US Strategic Command, National Aeronautics and Space Administration, Defense Advanced Research Projects Agency, and Air Force recognize the problem of sustaining the United States' edge in space despite declining budgets. Tasked with bridging the gap between available resources and operational needs, the Operationally Responsive Space (ORS) office envisions significant progress, but we should expand its vision. This article proposes a phased approach that will multiply the current ORS program (hereafter referred to simply as ORS) and increase US space capabilities; this approach harnesses the potential of the orbital and suborbital flight of space planes and existing satellites for repeatedly maneuvering and perform multiple missions.

Established in 2007 as a joint initiative of several agencies within the DOD, the ORS Office seeks to develop low-cost access to space via missions that are responsive to warfighters' needs. Access to space is not cheap; vehicle development and launch comprise the largest part of space expenditures. ORS strives to drive down the costs of both of those simultaneously so that we can prepare and launch a space vehicle within weeks at a fraction of current outlay for as little as a penny for every dollar currently spent for comparable missions (Wertz, 2007a: 4). At present, however, ORS focuses only on quickly preparing vehicles and launching them cheaply – it does not envision maneuverable space vehicles that could change their orbits to perform more than one mission during their service lives. According to Dr. James Wertz, an ORS proponent, "[Responsive space] cannot be achieved with already on-orbit assets. [It is] like hoping the bad guy will step into the path of a bullet which has already been shot." Using the same satellite for multiple missions by employing non-traditional, orbital change techniques can enhance responsiveness to warfighters' needs while reducing program costs even further.

Implementation of this new responsive orbit approach should proceed in four phases. The first phase will show that some currently operational satellites can modify their orbits significantly in an efficient manner simply by changing the concept of operations (CONOPS). The hardware for this technology already exists and is well-tested and understood. Such a system needs an electric propulsion system (gridded ion thruster or Hall Effect thruster) and a small satellite platform (weighing 500-1,000 kilograms). The second phase will apply moderate amounts of aerodynamic drag to the satellite, such as those experienced in the outer atmosphere for altitudes ranging between 150 and 700

kilometers (km) above the Earth's surface (known as thermosphere). In addition to a new CONOPS, electric propulsion, and a small platform, the third phase will demand a vehicle capable of manipulating aerodynamic forces (similar to the space shuttle and X-37). We find these three hardware components employed individually in spacecraft today. Therefore we need only a new CONOPS and the right combination of vehicle characteristics to turn an on-orbit satellite into a maneuverable space asset. The fourth and final phase will combine maneuverability with ORS concepts under development. Evolution of the first phase is under way, showing the potential of the responsive orbit concept. Future phases will progress as follows.

4.2 Operationally Responsive Space

The United States' present use of space drives a DOD space program that typically costs billions of dollars. Traditional space missions are strategic, durable (designed for 10- to 20-year lifecycles), inflexible, expensive ($100 million - $2 billion), highly capable, complicated, and hard to replace (Wertz, 2007a: 7). These characteristics are interrelated. Due to the considerable expense of launching spacecraft, designers make their systems highly capable and reliable. Those traits come at a premium cost and produce long lifecycles. Highly capable, reliable, and long-lasting systems must have redundancies for all components critical to their operation (almost the entire system) - and those redundancies add weight, which leads to greater launch expenditures. Clearly, this self-sustaining cycle creates ever-growing, supercapable spacecraft that cost billions of dollars and take a decade to build. This paradigm has become the defining

characteristic of space culture. Today's requirements for rapid reconstitution and assets responsive to unplanned threats and disasters necessitate additional space-acquisition models.

Current space missions often fall short of meeting the needs of warfighters. The systems demand long development times to mature and integrate the necessary technologies. By the time a system is ready to deploy, many of the electronic components are no longer state-of-the-art, so engineers must design new ones. The DOD cannot keep up with the demands of military operations (Berlocher, 2008). Users often wait several years beyond the originally planned delivery date before they finally receive a new asset whose intended purpose may have already changed. During the planning for Operation Desert Storm in September 1990, planners realized that existing satellite communications (SATCOM) capacity would not be sufficient to support the war effort; consequently, they urgently attempted to launch an additional Defense Satellite Communications System III spacecraft. That mission finally launched on 11 February 1992, missing the war by more than a year (Spires, 1998: 268). Designers produced the follow-on to that spacecraft, the Wideband Global SATCOM, as a commercial-off-the-shelf system because of advertised time savings in the acquisition schedule. When its development started in 2001, the launch was scheduled for the fourth quarter of 2003, yet the satellite did not attain operational orbit until 2008 (after a 7 October 2007 launch) - five years behind schedule (Wideband Gapfiller System, 2005). This delay caused critical communication shortages in the Pacific Command and Central Command theatres, resulting in up to 80 percent reliance on commercial assets at inflated costs to taxpayers.

ORS seeks a paradigm shift in space operations. In contrast to the latest methodology, ORS missions are designed to be tactical, short (intended for a one-year lifecycle), flexible (adaptable to mission need, timeline, and geographic region), cheap (less than $20 million), specialized (spacecraft provide a specific function and work with other spacecraft to achieve an objective, making the overall system less vulnerable to an attack), technologically simple, and immediately replaceable (Wertz, 2007a: 7-9). ORS emphasizes smaller satellites and launch vehicles; rapid, on-demand deployment; and quick availability of capabilities to users. Concepts under development will continue to rely on traditional, Keplerian orbits, meaning that each launched asset serves only a single purpose. Even a cursory comparison of a traditional mission and ORS shows that the latter is everything the former is not.

The ORS approach marks a significant shift in the US space culture. Stakeholders generally agree on the desirability of reducing mission cost and elevating responsiveness to user needs, but fulfilling those goals is difficult, requiring persistence and willingness to change the existing hardware, command and control, and testing norms. Hopefully, policy planners will acknowledge the benefits of transforming this culture and embrace new business rules, allowing rapid changes to give us the flexibility to meet user needs quicker and more efficiently.

ORS could offer even greater benefits if it included development of a maneuverable satellite, such as a small one in the 500-kg weight class, which can carry sufficient propellant onboard to perform multiple maneuvers (Newberry, 2005, 48). That is, the vehicle could perform an orbital change after completing one mission, thereby permitting retasking to carry out a new one. Assuming that the desired orbital changes were small,

the satellite could maneuver 15 times or more. One maneuver would reduce the number of required launches by 50 percent – three maneuvers, 75 percent. Regardless of the cost savings in hardware and testing that ORS might realize, launches will remain expensive, especially if we must launch a new satellite for each tasking. Therefore, a maneuverable satellite that we could retask on orbit multiple times could prove far less costly than the ORS version.

4.3 Meeting User Needs with a Maneuverable Asset

ORS optimistically presents a single, low-cost vehicle launched on demand and to the proper orbit within hours of tasking. This long-term vision of ORS has a target date of 2020. Assuming that such a vehicle exists and the launch capability and ground control segment are in place, the perennial shortage of available assets to meet operational user needs would expend any on-hand capability as quickly as it could be produced, thereby precluding a truly responsive system. Responsiveness is not limited to the space segment; quick launches can also improve the timeliness of meeting a new user need. Rapidly launching augmentation or replenishment spacecraft can prove essential to maintaining a specific capability. At present, spacecraft production follows a launch-on-schedule concept, but responsive vehicles must be prepared for launch-on-demand. An effective shift to the latter approach would require maintaining an inventory of war-reserve materiel, spacecraft, and associated launch vehicles at the launch sites (Doggrell, 2006: 49).

The ORS concept relies on the ability to launch rapidly from an available inventory to respond to developing crises. It might necessitate launching one satellite and positioning it to monitor a tsunami-devastated area in the Pacific one day and launching another to gather intelligence about a peasant uprising in Central Asia the next day. This capability requires having readily available spares prepared at a moment's notice for launch and operation. However, for the foreseeable future, operational needs will continue to far outpace the rate at which we can field new assets to meet those needs. As demonstrated by the previously discussed SATCOM scenarios, military capacity quickly diminishes as a consequence of supporting newly operational terrestrial and aerial systems that demand substantial bandwidth to transmit data between forward-deployed forces to command centers. In order to build up a responsive capacity (with available inventory), we need a different approach.

Complementing the ORS design with the ability of the space vehicle to maneuver via non-traditional (or novel) orbits would reduce the pressure of a high operations tempo and lower the required capacity. Maneuverability would enable a single satellite launched into low-Earth orbit to change its orbital plane sufficiently in a timely manner to respond to multiple world events or user requirements. In doing so, the satellite's on-orbit lifespan might decrease to less than the ORS program's current one-year standard, depending on how many different taskings the asset fulfills. Enabling a single vehicle to meet multiple user requirements could greatly reduce the need for repeated launches and thereby reduce cost by millions of dollars per vehicle.

Specifically, these proposed novel orbits would leverage aerodynamic forces of the Earth's atmosphere to change orbital parameters. Using simple technology developed

during the days of Gemini, Mercury, and Apollo, we can design a space vehicle to re-enter the atmosphere and use lift and drag to change its orbit by altering its flight-path, velocity, and altitude (Hicks, 2009: 239-241). In essence, the orbital space vehicle becomes akin to a suborbital spacecraft, behaving like an aircraft while inside the atmosphere. Based on multiple reentry profiles simulated using the equations of motion provided by Lt Col Kerry Hicks, a vehicle designed with sufficient lift capability can perform aircraft-like maneuvers such as climbing, diving, and rolling. This non-Keplarian part of the flight profile not only would enable a change in the orbit (the ground track required to fulfill a new operational objective), but also would add a degree of uncertainty for adversaries interested in tracking this vehicle. Thus, an adversary may be caught by surprise, having little or no prior warning of the vehicle coming overhead. The depth to which the satellite penetrates the atmosphere determines the control authority of the mechanisms put in place to modify orbital parameters. A deep atmospheric penetration can drastically change the orbit in ways that even high-thrust, liquid propellant rocket engines cannot because of the prohibitive amount of propellant expended by those engines.

A vehicle capable of entering and exiting the atmosphere unharmed by g-forces and heating due to atmospheric friction would certainly require some design changes. Since ORS strives to change the culture of space operations and architecture, it presents the perfect opportunity to take the idea further by considering novel approaches to increase flexibility and provide greater benefit to the effort with relatively simple modifications. The effects, controls, benefits, and dangers of re-entry have been well known since the early days of manned space flight. By carefully selecting features of a vehicle's design

we can greatly enhance its lift capability and, therefore, the aerodynamic control authority to modify its orbit. The result would be an expanded flight envelope and more operational flexibility.

The maneuverable vehicle concept, to a lesser extent for altitudes above 150 km, also applies to current operational satellites not designed with ORS capabilities. Atmospheric drag forces play a role in a satellite's orbit at or below an altitude of 700 km. The space shuttle and the International Space Station experience these constantly and must counter these forces to prevent orbital decay. The technology to allow satellites to maneuver is available and in use, but the CONOPS needs to change (phase one). Low thrust electric engines enable satellites already in orbit to perform slow, precise, and highly efficient station-keeping maneuvers. The current CONOPS intends the spacecraft to arrive at its orbital state and maintain its orbit, almost exclusively, for the life of the vehicle. Most spacecraft are designed in this manner so not much thought is given to powered flight and the potential it has. When necessary, these engines can move large satellites into orbits to serve different terrestrial theatres in the case of a geosynchronous system, or change the time a satellite arrives over a target (time over target [TOT]) for a low-Earth orbit system. To harvest this potential, the CONOPS must be built around the assumption that these spacecraft do not necessarily have to operate within the orbit into which they were first launched. Additionally, when we take into consideration the potential of the upper atmosphere to change a vehicle's orbit (even small drag forces can induce a noticeable change), a system that is already on-orbit can maneuver significantly to change its TOT or geographical location even without modifying vehicle characteristics.

4.4 Concept Design and Results

A small orbital change can affect the terrestrial ground track of a satellite. An asset without ORS hardware that continuously thrusts with an electric engine over a seven-day period can change its velocity within the same orbital plane enough to achieve a 24-hour TOT change by modifying the ground track (Newberry, 2005: 48). The ground track change is proportional to the lead time provided to change the orbital characteristics. In simple terms, the more time is available to implement a TOT change, the greater the magnitude of the potential change. In phase one and two of the research program, this result is achievable when the CONOPS of an existing system is modified to allow maneuvers to change TOT. Yet the response time is not comparable to the potential response time claimed by ORS systems under development. Ultimately, an ORS asset will be capable of reaching any location on earth within 45 minutes of launch and only nine hours following initial tasking (Wertz, 2007a: 9). However, this is only the ORS goal and is not yet a reality. A current asset that can maneuver in orbit using EP, but not enter the atmosphere (remain above an altitude of 122 km) can reach any location on earth at any specified TOT in seven days. In comparison, simulations show that a maneuverable asset designed with aerodynamic characteristics capable of leveraging atmospheric forces and out-of-plane maneuvers could reduce the period of time required to achieve the desired orbit by about 75 percent (i.e. from seven days to approximately two) as discussed in phase three. A little ingenuity can combine the atmospheric

maneuvers with an ORS satellite to provide a highly-responsive, effective, and inexpensive system capable of quickly responding to the threats the U.S. faces today.

An ORS asset is designed as a small, light satellite capable of maintaining attitude (pointing) and location (station-keeping). To make it maneuverable (phase four), it could be designed with both a small impulsive thrust (rocket) engine and a highly efficient electric thrust capability (such as a Hall Effect thruster). The impulsive thrust capability enables rapid, yet small changes in orbit and the continuous electric thrust can build up the energy to reach a stable parking orbit so that the process can be repeated. The design concept would involve launching such a satellite into a specific orbital plane to meet the requirements of the initial tasking. After completing its first mission, the vehicle would impulsively modify its orbit slightly to cause its perigee (point in its orbit closest to the earth's surface) to enter or "dip" into the atmosphere where the satellite could use aerodynamic forces to change its orbital plane to meet the requirements of the next tasking. Each time the vehicle performs such a maneuver, it loses energy. When the satellite reaches an energy level where orbital flight is on the verge of becoming unsustainable, simulations show that the continuous electric thrust system can efficiently raise the energy level enough to keep the vehicle in orbit. This process can be repeated until the satellite runs out of propellant for its propulsion system. A space plane equipped with the two types of engines described above (rocket & electric) would be capable of responding to multiple user taskings by using current technology – yet the knowledge of how to execute these maneuvers effectively is very limited. This design concept would strive to increase the number of taskings the system could fulfill by a factor of six compared to traditional low-Earth orbit assets equipped solely with chemical propulsion

since the efficiency (or gas mileage) of low-thrust electric engines is five to six times greater than that of high-thrust engines. Such a space plane could fulfill 15 or more taskings, meaning that 15 ORS missions could be completed with a single launch, and reducing the advertised mission cost significantly.

4.5 Conclusion

The current space culture of fielding large, expensive, and capable satellite systems is not sustainable and can neither satisfy the operational needs of U.S. warfighters nor keep up with threats posed by other space-faring nations. Much as conventional warfare must adapt to today's counterinsurgency demands, conventional space culture must adapt to today's space environment. New initiatives such as ORS and the research discussed in this article seek to adapt our space culture.

We should take a phased approach to expanding the current ORS concept. In phase one, a new CONOPS built around a different paradigm for an existing on-orbit asset can provide a test-bed for proving the feasibility to achieve significant TOT change using EP while staying outside the atmosphere. The required technology is already in use, well-tested, and understood. The cost would be relatively small since it does not require developing any new equipment. The second phase will incorporate aerodynamic forces in orbits as low as 122 km to open opportunities previously thought impossible due to vehicle and propellant constraints in order to enable greater flexibility and increased responsiveness to meet warfighter needs. The third phase will involve a new vehicle designed to enter the atmosphere, perform the desired orbital change and climb back into

space. The technology to create vehicle characteristics best suited to take advantage of lift and drag forces also exists and is well-studied. Yet the countless possibilities to change a satellite's ground track by using these aerodynamic forces are poorly understood so we need to conduct more research. It offers great potential to effect large-scale orbital changes at very low propellant costs, increasing the lifespan of a satellite (when compared to inducing the same amount of change using traditional chemical propulsion) and enabling it to fulfill 5-6 times as many taskings as current operational satellites that are not designed to maneuver significantly. The final phase would expand the scope of ORS to include maneuverability. Allowing a highly responsive, low cost system to perform multiple taskings during its operational lifespan would reduce the number of required satellite launches and enable us to have sufficient capability to make ORS a truly responsive system.

A paradigm shift in the U.S. space program is inevitable and has begun. Our future conventional space operations need to include small, cheap, responsive, and maneuverable space assets that we can develop and launch in months rather than decades.

5 Responsive Satellites through Ground Track Manipulation using Existing Technology

The space community has recognized the problem of sustaining current space operations and has responded by supporting research and development in technologies to reduce cost and schedule without sacrificing performance. One solution is maneuverable satellites. There are very few studies on maneuvering satellites in low-Earth orbit from a ground-track perspective. Operational responsiveness is achievable by changing the ground track; and thereby a geographical target location. The existing paradigm on maneuvering is that it is cost-prohibitive, thus orbit-changing maneuvers are done sparingly. This paper presents methodology to quantify reachability of a satellite with chemical and electric propulsion based on initial orbit, ΔV, and available maneuvering time. Initial orbit parameters are examined to determine which would yield the greatest benefit from maneuvering and the analysis shows that initial orbit orientation has no effect. These maneuvers are highly predictable and equations are formulated to become part of an algorithm that allows over-flight of user-specified ground targets. In sacrificing timeliness with electric propulsion, the system gains repeatability over chemical propulsion. Existing technology could maneuver a satellite significantly to change its ground track in a relatively short period of time and within standard propellant budgets.

Nomenclature

A = perturbing acceleration, km/s^2

a = semi-major axis, km

a_h = normal acceleration component, km/s^2

a_r = radial acceleration component in local-vertical, local-horizontal frame, km/s^2

a_θ = acceleration comp completing the right-handed coordinate system, km/s^2

D = terrestrial distance, km

$D_{100\text{km}}$ = distance at 100 km altitude, km

E = eccentric anomaly, rad

e = eccentricity

H = Haversine formula

h = angular momentum, km^2/s

i = inclination, degrees

M = mean anomaly

n = mean motion, rad/s

P = period of orbit, s

p = semi-latus rectum, km

R = distance from center of Earth, radius, km

$\bar{R}$ = radius vector, km

R_a = apogee radius, km

R_p = perigee radius, km

$R_\oplus$ = Earth's radius, km

r = Altitude, km

T = time since last perigee passage, s

t = time, min

Δt_m = time elapsed from beginning of the maneuver to target overflight, s

u = argument of latitude, rad

V = velocity, km/s

ΔV = velocity change, km/s

x, y, z = coordinates in Earth-Centered Fixed (ECF) coordinate frame, km

x_p, y_p, z_p = coordinates in perifocal coordinate frame, km

γ = angle between Earth-Centered Inertial (ECI) and ECF frames, rad

γ_g = Greenwich sidereal time, rad

ε = total mechanical energy, km^2/s^2

λ_{tgt} = target latitude, degrees

$\mu_\oplus$ = Earth's gravitational parameter, 3.98601 x10^5 km^3/s^2

v = true anomaly, rad

φ_{tgt} = target longitude, degrees

Ω = right ascension of the ascending node, degrees

ω = argument of perigee, degrees

$\omega_\oplus$ = Earth's angular velocity magnitude, rad/s

$\bar{\omega}_\oplus$ = Earth's angular velocity vector, rad/s

Superscripts

$^+$ = symbol with this superscript denotes value after a maneuver

$^-$ = symbol with this superscript denotes value before a maneuver

5.1 Introduction

TRADITIONAL space operations are characterized by large, highly technical, long-standing satellite systems that cost billions of dollars and take decades to develop (Wertz, 2007a: 4-7). To increase responsiveness, reduce development time, and maintain a robust, affordable space capability, the community must change this status quo in space operations or risk not being able to keep up with customer requirements (Spires, 1998: 268; Berlocher, 2008). This research presents new concepts to make current systems more responsive and timely to user requests and increase space capabilities by offering more flexibility; this approach could eventually allow repeated maneuvering and perform multiple missions on existing platforms with standard propellant budgets (Co, 2011b).

Repositioning a satellite for multiple missions by employing nontraditional, orbital-change techniques can enhance responsiveness to customer needs while drastically reducing program costs by eliminating multiple launches (Co, 2011a: 74-80). Maneuverability would enable a single satellite launched into low-Earth orbit (LEO) to change its orbit sufficiently in a timely manner to respond to multiple world events or user requirements. In doing so, the satellite's on-orbit life span might decrease depending on how many different taskings the asset fulfills. Enabling a single vehicle to meet multiple user demands could greatly lessen the need for additional launches to meet user taskings, thereby reducing cost by millions of dollars per vehicle (Larrimore, 2007: 2). Additionally, once the vehicle's propellant is depleted, the maneuverable asset could continue to provide service in the traditional manner until the payload fails or the satellite reenters the Earth's atmosphere.

Many operational satellites are maneuverable but they are designed to operate in static parking orbits. The technology to maneuver is available and in use, but is only applied to maintain the original static orbit (position and pointing) in most LEO operations. Occasionally, electric propulsion (EP) is used for orbit-raising, but not to change a satellite's over-flight position in the manner that would yield a responsive space capability as proposed in this research. High-thrust chemical propulsion (CP) engines are the traditional means to perform orbital changes and to maintain the final orbit once it is attained (Forte, 2002). Low-thrust EP engines enable satellites already in orbit to perform slow, precise, and highly efficient station-keeping maneuvers. Current concept of operations (CONOPS – document defining the user's operation of a system) intend for spacecraft to arrive at an orbital state and maintain the orbit, almost exclusively, for the life of the vehicle. The current state-of-the-art for LEO satellites focuses on constellation design to maximize the coverage for an asset rather than using a vehicle that could maneuver; hence most satellites are placed in polar, sun-synchronous or critically inclined orbits depending on the mission (Kantsiper, 2007a; Wertz, 2007b). To harvest the potential of maneuverability, the mission must be constructed around the assumption that these spacecraft do not necessarily have to operate within the orbit into which they were first launched. This research demonstrates that existing satellites can maneuver significantly to change their overflight location and provides a feasibility study by comparing the use of low-thrust, highly efficient EP to traditional CP in performing these types of maneuvers.

Many studies exist detailing the possible applications of an EP space system or a general maneuvering system; however, none address the responsiveness achieved by

modifying a satellite's ground track to arrive over a desired target. The majority of previous research revolves around long-duration orbit transfers (geosynchronous transfer) to save propellant and launch mass by using more efficient propulsion (Gopinath, 2003; Dankanich, 2007). Another class of research addresses survey missions that require rendezvous and proximity operations. The Orbital Express project, Experimental Satellite System 11 (XSS-11), and the Repeated Intercept mission are examples that use impulsive maneuvers to change a satellite's position within its orbit slightly to intercept another satellite (Tether, 2003: 5; Chioma, 2004: 1-36).

The quest for more responsive, less expensive, and more available space systems could benefit significantly if it included development of a maneuverable satellite, which can carry sufficient propellant on board to perform multiple orbital maneuvers. That is, the vehicle could perform an orbital change after completing one mission, thereby permitting re-tasking to carry out a new one if necessary. Assuming that the desired orbital changes were small (velocity change < 200 m/s), the satellite could maneuver 15 times or more given today's technology (Saccoccia, 2002: 9). One maneuver would reduce the number of launches by 50 percent since one satellite could address the needs of two different missions. Regardless of the cost savings in hardware and testing that research and technological advances might realize, launches will remain expensive for the foreseeable future, especially if a new satellite is launched for each tasking. Therefore, a maneuverable satellite that a user could re-task multiple times on orbit could prove far less costly than one that could not.

A small orbital change can affect the terrestrial ground track of a satellite. Newberry postulates that a typical operational asset that continuously thrusts with an EP

engine over a seven-day period can sufficiently change its orbit within the same orbital plane to produce a 24-hour time-over-target (TOT) change by modifying the ground track (see Figure 5-1). The ground track alteration is proportional to the lead time provided to adjust the orbit. A current asset that can maneuver in orbit using EP but not enter the denser atmosphere (the author limits the analysis for an altitude as low as 160 km) can reach any location on the Earth in seven days. The results are validated as part of the preliminary work of this paper.

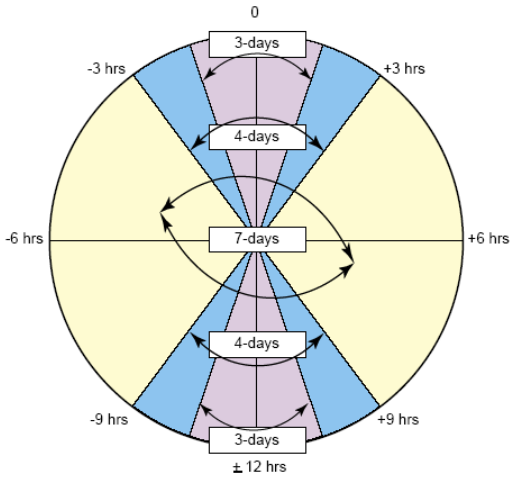

Figure 5-1. TOT Performance vs. Lead Time for Maneuvering (Newberry, 2005)

Newberry analyzes the viability of a LEO EP system and its capability of changing TOT. This hypothetical spacecraft weighs 500 kg wet and is equipped with a highly efficient (specific impulse of 1500 s), low-thrust (300 mN) engine. It is in a HEO inclined at 85 degrees and a period of 2.7 hours. In this configuration, the system could change its TOT by three hours after four days of maneuvering and six hours after seven days (Figure 5-1). The foundation of Newberry's analysis is based on the characteristic that the vehicle overflies the same theater twice a day. Given seven days of lead time, an EP

system could change the TOT by six hours ahead or behind at two opposing locations in the orbit and would cover a total TOT change of 24 hours, which is equivalent to global reach. The results of this paper confirm that with simple, in-plane, posigrade, continuous thrusting significant ground track changes are possible.

Previous research does not address maneuvering satellites as this paper does. Even Newberry's work is limited to a specific class of highly elliptical orbits that only apply to very unique missions. After proving the feasibility of affecting meaningful orbital change with today's thruster technology, this paper provides useful insights on initial orbits and quantifies maneuverability using CP and EP systems. It shows which initial Classical Orbital Elements (COEs) have the greatest impact on orbital changes due to maneuvering and quantifies their sensitivities. The main contribution is the development of equations that can accurately predict how much an orbit can change using CP or EP based on available time, orbital altitude, and ΔV when compared to a non-maneuvering reference.

5.2 System Models

There are two sets of the equations governing CP and EP motion of LEO satellites. The impulsive thrusting maneuver has been researched extensively and is not generally used operationally for LEO maneuvering due to the prohibitive amount of propellant these maneuvers consume. Even so, recent research shows that in certain applications, impulsive maneuvers are extremely applicable, such as survey missions, and when used in conjunction with planetary fly-bys (Ivashkin, 1971: 163-172) and other non-traditional maneuvers such as lunar gravity assist (Ocampo, 2003: 173-179; Mathur, 2010) the

amount of propellant used is significantly reduced when compared to traditional maneuvers.

The first set of equations model CP maneuvers. The standard two-body equation requires some mathematical manipulation to arrive at the solution to the restricted two-body problem, which describes the location of the satellite as a function of three of the six COEs and is used to propagate the position of a satellite to any point in time (Vallado, 2001: 49-106):

$$R = \frac{a(1-e^2)}{1+e\cos\nu} \tag{5.1}$$

$$n = \frac{2\pi}{P} = \sqrt{\frac{\mu}{a^3}} \tag{5.2}$$

$$M = nT \tag{5.3}$$

$$M = E - e\sin E \tag{5.4}$$

$$\nu = 2\arg\left(\sqrt{1-e}\cos\frac{E}{2}, \sqrt{1+e}\sin\frac{E}{2}\right) \tag{5.5}$$

Impulsive maneuvers are handled using common practices, assuming that the energy is added instantaneously. Prior to a maneuver, the total energy of a satellite is a combination of its kinetic and potential energy given by:

$$\varepsilon = -\frac{\mu_\oplus}{(2a)} = \frac{V^2}{2} - \frac{\mu_\oplus}{R}. \tag{5.6}$$

The velocity for general motion of a small mass around a larger one that is associated with Equation (5.6) is given as:

$$V = \sqrt{\frac{\mu_{\oplus}}{R}\left(2 - \frac{1-e^2}{1+\cos\nu}\right)} \tag{5.7}$$

The new energy value can be obtained by adding the ΔV of the maneuver to the original orbital velocity then substituting it into Equation (5.6) with the radius at which the maneuver was executed. The energy is necessary to compute the velocity of the satellite throughout the new orbit after maneuvering and the eccentricity. Propagating Equations (5.1)-(5.5) forward in time defines the location of the satellite. Assuming the added velocity is aligned with the velocity vector, these equations describe the process of calculating the new orbit after an impulsive maneuver:

$$V^{+} = V^{-} + \Delta V \tag{5.8}$$

$$\varepsilon^{+} = \frac{V^{+^2}}{2} - \frac{\mu_{\oplus}}{R^{-}} \tag{5.9}$$

$$e^{+} = \frac{R_a - R_p}{R_a + R_p}. \tag{5.10}$$

If the initial orbit prior to the maneuver is circular, the location where the thruster firing occurs becomes the perigee point of the new orbit if the thrust vector is aligned with the satellite's direction of travel. Similarly, this location becomes the new apogee point if the thrust is pointing in the opposite direction. If the original orbit is elliptical, standard practice is to perform the maneuver at the point of apogee or perigee for the highest propellant efficiency. Thus depending on the orbit prior to thruster firing, the location of

the maneuver may become the new apogee or perigee, yet the new eccentricity is simply a function of the new radii. This set of equations make up the equations of motion for the CP model.

The low thrust of an EP system results in small accelerations that perturb the orbit of the spacecraft. Gauss' form of the Lagrange Planetary Equations models the change over time in the COEs (a, e, i, Ω, ω, ν) in the following manner (Schaub, 2003: 522):

$$\frac{da}{dt} = \frac{2a^2}{h}\left(e\sin\nu a_r + \frac{p}{R}a_\theta\right) \tag{5.11}$$

$$\frac{de}{dt} = \frac{1}{h}\left(p\sin\nu a_r + \left((p+R)\cos\nu + Re\right)a_\theta\right) \tag{5.12}$$

$$\frac{di}{dt} = \frac{R\cos(\omega+\nu)}{h}a_h \tag{5.13}$$

$$\frac{d\Omega}{dt} = \frac{R\sin(\omega+\nu)}{h\sin i}a_h \tag{5.14}$$

$$\frac{d\omega}{dt} = \frac{1}{he}\left(-p\cos\nu a_r + (p+R)\sin\nu a_\theta\right) - \frac{R\sin(\omega+\nu)\cos i}{h\sin i}a_h \tag{5.15}$$

$$\frac{d\nu}{dt} = \frac{h}{R^2} + \frac{1}{he}\left(-p\cos\nu a_r + (p+R)\sin\nu a_\theta\right) \tag{5.16}$$

The three components of the perturbing acceleration in the local-vertical, local-horizontal (LVLH) frame are a_r, a_θ, and a_h, where a_r is the acceleration component in the radial direction, a_h is in the normal direction, and a_θ is in the direction completing the right-handed coordinate system. It is important to note that when the orbit is circular, a_θ is always aligned with the spacecraft's velocity vector, and when the orbit is elliptic it is aligned with the velocity vector only at perigee and apogee.

For most of this analysis it is assumed that the spacecraft's initial orbit is circular, the acceleration is small, ΔV is aligned with the spacecraft velocity, and the maneuver is coplanar so that the above equations are simplified. Equations (5.13) and (5.14) describe the orientation of the orbit plane and only the normal component of acceleration affects these values. Thus the coplanar maneuver assumption implies that there is no acceleration in the normal direction ($a_h = 0$). Since the total acceleration on the spacecraft is constant and one of its components is zero, the other two components can be written as functions of the total acceleration magnitude and a control angle describing the direction in which the acceleration is acting. The equations are further simplified with the assumption that the thrust vector is always aligned with the velocity vector and the control angle 90° in the velocity or anti-velocity direction. Since the spacecraft's orbit starts circular and the applied acceleration is very small, the orbit will remain quasi-circular throughout the maneuver resulting in a low-thrust spiral transfer when eclipses are not taken into consideration. Therefore Equation (5.15) for argument of perigee (or this component of argument of latitude) can essentially be ignored.

The Earth-shadow eclipses do pose some restrictions on how long the thrusters can operate uninterrupted in LEO. During eclipse, most current power systems do not generate enough electric current to thrust. At low altitudes eclipses make up almost 40% of the orbit and therefore significantly reduce the effective thrusting time. For example, in a 500-km altitude circular orbit, an EP system can thrust for 63% and coast for 37%. Within 24 hours of continuous thrusting, the orbit becomes slightly eccentric with e=0.007, which is equivalent to an orbit with a perigee that is 100 km lower than apogee.

Given sufficient time the orbit changes back to a circular orbit after every maneuver if the system does not compensate for air drag.

There are two other options to avoid terminating the thrust during eclipse. The first option is to maintain a carefully chosen sun-synchronous orbit which naturally keeps the sun visible from the satellite's perspective. This option would require following strict flight profiles, maintaining the initial and final orbital altitudes, or changing the inclination, all of which necessitate consumption of significant amounts of propellant. The second option could be a smaller spacecraft with a mass of 50-100 kg. Such a system would be required to operate on a smaller thruster, one that may be able to utilize batteries during eclipse. This option also provides power storage and generation challenges and severely limits the propellant capacity of the system. These are considerations for existing technology, but by no means do these preclude the possibility for low-thrust orbital maneuvers.

Finally, the following substitutions can be made:

$$h = \sqrt{\mu_{\oplus} a(1-e^2)} = \sqrt{\mu_{\oplus} a} \tag{5.17}$$

$$p = a(1-e^2) = a \tag{5.18}$$

$$r = a \tag{5.19}$$

$$a_r = 0 \tag{5.20}$$

$$a_\theta = A \tag{5.21}$$

After eliminating four of the six equations and plugging in Equations (5.17)-(5.21) where appropriate the final equations of motion for a low-thrust system become:

$$\frac{da}{dt} = \frac{2}{\sqrt{\mu_\oplus}} a^{3/2} A \tag{5.22}$$

$$\frac{d\nu}{dt} = \sqrt{\frac{\mu_\oplus}{a^3}}\,. \tag{5.23}$$

Equations (5.12), (5.22) and (5.23) are the equations of motion for an EP system thrusting to maximize the time-rate-of-change of *a*.

Metric: Terrestrial Distance.

Besides equations of motion and expressions of satellite locations from a ground track point-of-view there is one more metric needed to define the problem. To quantify the effects of a satellite maneuver, terrestrial distance (*D*) between two points on Earth defined by latitude and longitude is a suitable measure. To calculate it, the Haversine formula which gives great-circle distances between two points on a sphere defined by latitude and longitude (point 1 – λ_1, φ_1; point 2 – λ_2, φ_2) is used (Sinnott, 1984: 159). Fully expressed the Haversine formula is:

$$D = 2R_\oplus \arcsin\left(\sqrt{\sin^2\left(\frac{\varphi_2 - \varphi_1}{2}\right) + \cos\varphi_1 \cos\varphi_2 \sin^2\left(\frac{abs(\lambda_2 - \lambda_1)}{2}\right)}\right) \tag{5.24}$$

The entire portion inside the square root is designated as *H*. When using this formula, it becomes problematic if *H* exceeds the value 1 because the inverse sine of such values is undefined. Distance is only real for values from 0 to 1 and *H* approaches 1 for points on

opposite sides of the sphere, i.e. when the composite latitudinal and longitudinal separation is greater than 180 degrees. However, the problem setup avoids this scenario as described in the next paragraph.

The terrestrial distance is simply the arc length between two points and Equation (5.24) is *D* measured between the sub-satellite points of a non-maneuvering satellite in a reference orbit (simply reference for the rest of the paper) and a maneuvering one using CP or EP. The maneuvering algorithm is based on where the satellite is at the start of the simulation and the associated ground track for a non-maneuvering vehicle. Distance captures the changes of the new orbit with respect to the reference over time, i.e. the end-point difference in *D* between a non-maneuvering (no thrust) reference after four revolutions and a maneuvering case after the same amount of time (four revolutions of the reference). Figure 5-2 depicts how *D* is measured for three scenarios using EP. All cases start at the same initial time, state, and altitude.

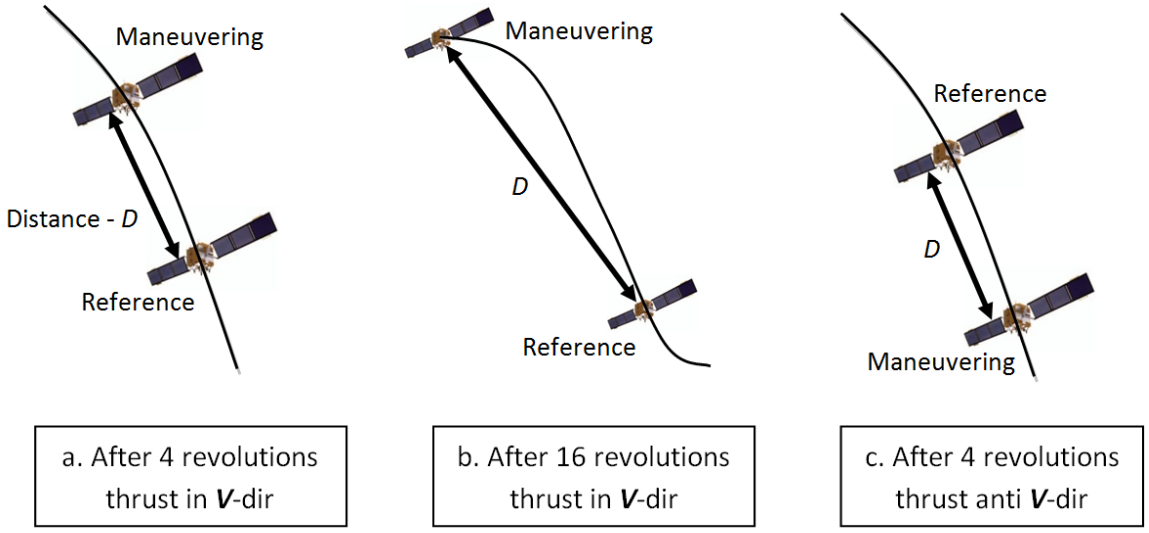

Figure 5-2 a-c. Distance between a Maneuvering Satellite and Reference

The distance is a function of ΔV and time as it grows as a result of continuous thrust input or simply with propagation after an impulsive input. Figure 5-2a shows *D* after four revolutions thrusting continuously in the velocity direction. The reference is slightly ahead on the ground track because the maneuvering satellite is adding energy, raising its orbit, and traveling at a lower mean motion. After 16 revolutions, *D* continues to grow due to propagation of the two satellites traveling at different speeds even if thrusting has ceased (Figure 5-2b). Figure 5-2c depicts *D* after four revolutions of thrusting in the anti-velocity direction. The analysis shows that thrusting in either direction results in almost the same *D* with an average error of 1.1%. The only difference is arriving over a target ahead instead of behind the reference.

5.3 Model Setup

After investigating multiple ways to set up the problem of a maneuvering satellite and its effects on ground track, which are not all shown here, methods are selected that allow data to be displayed in a meaningful manner. The use of the two-body model is justified since this setup compares all maneuvering cases to a reference orbit with the same starting conditions subject to the same governing equations. To justify it, the results from a high-fidelity model, which includes air drag (Jacchia-Roberts model), third-body effects (lunar and solar), solar radiation pressure, and geopotential perturbations (Joint Gravity Model 2) are compared against those of the two-body model (methodology in Appendix B). Thus whether a two-body or a higher precision model is used, the

maneuvering and reference cases experience the same perturbations thus negating the need for the more complicated model.

The CP two-body (TB) and the CP high-precision (HP) models are used to compare multiple cases at different altitudes (km) and ΔVs (km/s) over a 24-hour period to find that the difference in D is only a fraction of a percent in almost all cases. Nine test scenarios are set up to demonstrate the minute effect of these secondary forces, for the time period (24 hours) and altitudes (300-1000 km) in question, as measured by D (km). The reference cases are always subjected to the same forces, i.e. for the TB scenarios the reference satellite is only experiencing TB forces, whereas HP references are subjected to HP forces. There are three altitudes of 300, 500, and 1000 km, as well as three ΔVs of 0.01, 0.05, and 0.1 km/s. Each of the three altitudes is paired with the ΔV values one at a time for a total of nine cases. The thrust vector is always aligned with the velocity vector. Furthermore this analysis applies to thrusting in the velocity and anti-velocity direction. All CP cases start with a notional spacecraft with a mass of 1000 kg, cross sectional area of 10 m^2, and chemical propulsion with a 200-N thruster and specific impulse of 230 s. Table 1 summarizes the findings for a 24-hour period.

As expected, the average percent error is largest for low altitudes where both air drag and oblateness effects are most profound. With increasing altitude the observable error decreases from 1.23 percent at an altitude of 300 km, to 0.24 percent at 500 km, and 0.22 percent at 1,000 km. The second trend is also intuitive. At any given altitude the secondary forces acting on the satellite are identical, yet increasing ΔV translates into greater distances from the reference case given the same amount of time, thus resulting in a lower average percent error based on the way this measure is defined. From the data in

Table 1, it can be concluded that the use of the less complicated TB model does not affect the outcome of this particular study, thus it justifies neglecting secondary forces for the remainder of this paper.

Table 5-1. Comparison of Two-Body vs High-Precision Propagators

Altitude (km)	Δ*V* (km/s)	Average % Error	Max D Error (km)
300	0.01	1.23	63.8
	0.05	0.33	95.0
	0.10	0.29	138.1
500	0.01	0.24	11.4
	0.05	0.21	36.3
	0.10	0.18	48.0
1000	0.01	0.22	7.3
	0.05	0.18	31.7
	0.10	0.15	37.2

Most of this research is based on the comparison of a maneuvering satellite and one reference satellite with the same initial conditions. For instance, two satellites start with identical COEs. The reference case maintains that set of COEs throughout the simulation, whereas the maneuvering case changes via the CP or the EP model and thrusting. In a 24-hour period there are multiple opportunities to reach a desired target location – approximately 16 orbits multiplied by two for one on the ascending pass and one on the descending pass. Of course not all 32 opportunities are close to the desired target, but there are multiple opportunities that are close enough to represent a solution to the problem, i.e. those points on the orbital path that can be sufficiently changed using the available thrust from the CP or EP system to reach a target. There are also two options for the maneuver while maximizing the time-rate-of-change of *a*: (1) burn in the direction of

travel and thereby increasing the orbital radius and slowing down or (2) burn in the opposite direction to speed up. This setup provides solutions at terrestrial distances less than 20,000 km and thereby avoiding the floating point error of the Haversine formula.

Although it appears that a CP maneuver would change its COEs only once at the time of the maneuver and then maintain them (for the two-body model), the difference between the maneuvering and reference cases grows over time as the two satellites are traveling at different speeds and create greater distances as time passes. An EP maneuver is slightly more complex as energy is added slowly yet continuously for long periods of time, thus creating a different final orbit. The differences of these two propulsion systems are explored in this paper and it is shown that ground track manipulation, and therefore responsiveness and flexibility of space assets, is viable using today's widely-used technology.

5.4 Classical Orbital Elements' Effects on Maneuverability

In this section the effects of varying the length of thrusting period and the COEs on terrestrial distance for the two-body EP model are examined. The same problem setup as before is used and the scenario timeframe is kept at 24 hours. The inclination is 60 degrees so the ground track covers the majority of Earth's landmasses. The initial orbital parameters in this simulation are i = 60 degrees, a = 6878.14 km (altitude of 500 km), $\Omega=\omega+\nu=e=0$ degrees. For circular orbits ω and ν are undefined, so the argument of latitude (u) is used instead. This value is often written as $u=\omega+\nu$ and is defined as zero at the ascending node. For the thrusting period scenario, the amount of time thrusters are

firing is varied and then propagated via the EP model represented by Equations (5.12), (5.22), and (5.23) for the remaining time until at total of 24 hours has passed. The thruster set is capable of generating an acceleration of 1e-6 km/s^2 (i.e. thruster with 1 N of force and a system mass of 1,000 kg or any combination resulting in a similar acceleration). The cross sectional area is 20 m^2 to account for additional solar arrays as opposed to 10 m^2 for the CP cases.

Thruster characteristics are derived based on NASA's Deep Space 1 which was a mission in 1998 to demonstrate EP technology (Rayman, 2000: 475-487). The spacecraft's total mass was 486 kg with 81.5 kg of xenon propellant giving it a ΔV-budget of 4.5 km/s^2. The ion engine was made by L-3Comm and designated as the 30-cm NSTAR. It was capable of up to 0.1 N thrust with a specific impulse of 3280 s. The solar array weighed 55.6 kg with an approximate area of 13 m^2. Although Deep Space 1 was only capable to produce an acceleration of 2e-7 km/s^2 or one-fifth of the notional system selected in this paper, the actual acceleration is not important to the distance equations presented in later sections because the equations are scalable based on ΔV which in turn depends on acceleration.

These simulations show a satellite firing for one, six, twelve, and twenty-four hours then drifting for the remainder of the 24-hour period. Figure 5-3 summarizes the effect of varying the thrusting period graphically. It is apparent that the longer the thrusting period, the greater the slope of the distance curve, and so the length of the thrusting period establishes the rate of change for distance proportionally. After thrusting for one hour (or 2/3 of an orbit), the distance does not deviate much from the reference case. Thrusting for four orbits results in a distance of over 4,000 km after one day. After 12 hours of

continuous thruster activity or approximately eight orbits, the ground distance is almost 8,000 km. Finally, if the system thrusts continuously for 24 hours, which amounts to a ΔV of 0.087 km/s, it achieves slightly over 10,000 km. Similarly, if the thrusting period is 12 hours and the satellite could drift at the lower velocity until a distance of 10,000 km is achieved. At the established rate of change of D for a ΔV of 0.043 km/s (or 12 hours of thrusting) the system would need five hours longer or a total of 17 hours from thruster shut-off to achieve this distance. Thus the ΔV savings is 50 percent when thrusting 12 versus 24 hours just to save five hours to attain the same distance. The decision to do so would depend on the time sensitivity of the tasking.

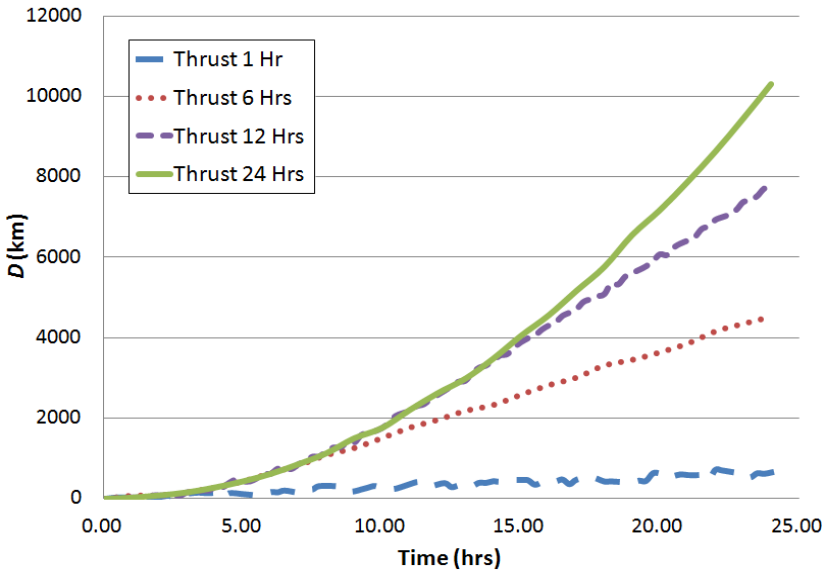

Figure 5-3. Effect of varying Thrusting Period on Distance

This section examines the effects different COEs have on distance. Once again, the same initial conditions are used for these scenarios, except only one COE is varied at a time to investigate its effect on distance. The ΔV used in these simulations is 0.043 km/s or thrusting continuously along the velocity vector for 12 hours using a 1-N thruster set

on a 1,000-kg spacecraft. The three orbital elements that have no bearing on the distance achievable through EP maneuvering are those that define the orbit's orientation, namely right ascension of the ascending node (RAAN), inclination, and argument of latitude. This observation is reasonable since the measure of interest is terrestrial distance between a maneuvering and reference satellite rather than user-specified points on the ground.

It is shown by varying initial inclination, argument of latitude, and RAAN that orbital plane orientation does not have any effect on distance. Figure 5-4 represents the effects of these three COEs on distance. To avoid redundancy, only the variation of initial inclination is shown as the other two COEs yield the same result. In fact, varying *u* for a circular orbit does not have an effect on terrestrial distance as well, much like the orbit plane orientation. Figure 5-4 displays the distances for three different inclinations of 10, 60 and 90 degrees. While the inclination is varied, all other initial COEs are kept constant for the three scenarios. The terrestrial distance between the maneuvering and reference satellites is mostly identical for the entire simulation period of 24 hours.

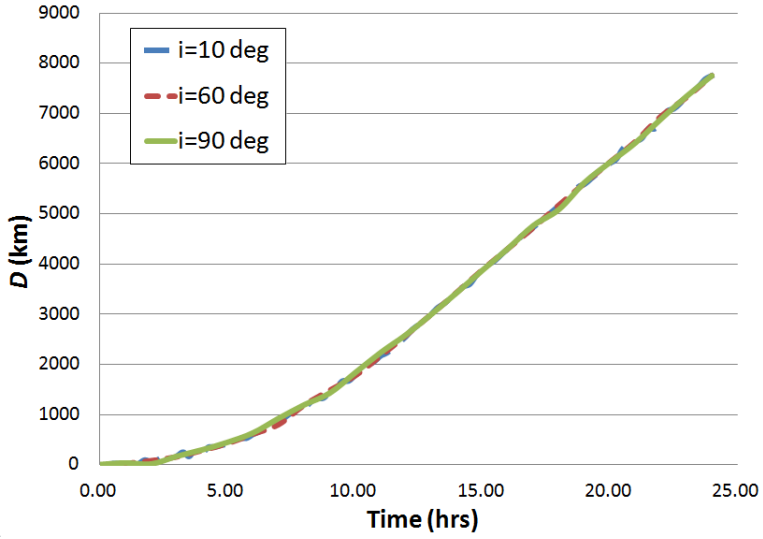

Figure 5-4. Effect of Varying Initial Inclination on Distance

With a ΔV of almost 0.05 km/s the resulting ground track distance is almost 8,000 km. Thus four of the six COEs have no quantifiable effect on distance measured in this manner.

To help visualize the scenarios, Figure 5 includes three slightly exaggerated depictions of the reference and maneuvering orbits. Initially, the reference and maneuvering orbits are perfectly aligned (Figure 5-5a). Thrusting commences immediately for 12 hours and Figure 5-5b shows the ground track difference at the end of the 12-hour thrusting period. The reference and maneuvering ground tracks are only slightly different for the first 12 hours of the simulation. The thrust is applied in the direction of travel aligned with the velocity vector, so energy is added raising the orbital altitude. A greater ΔV results in a higher altitude which in turn causes a slower velocity relative to ground and a faster rate of change in distance. This maneuver shifts the position of the satellite within the orbit to lag behind the reference. Simultaneously, the ground track is shifting westward as the Earth rotates underneath. Over the next 12 hours, the orbital position of the maneuvering vehicle lags behind further and the ground track is significantly different resulting in large ground track and TOT differences, depicted in Figure 5-5c.

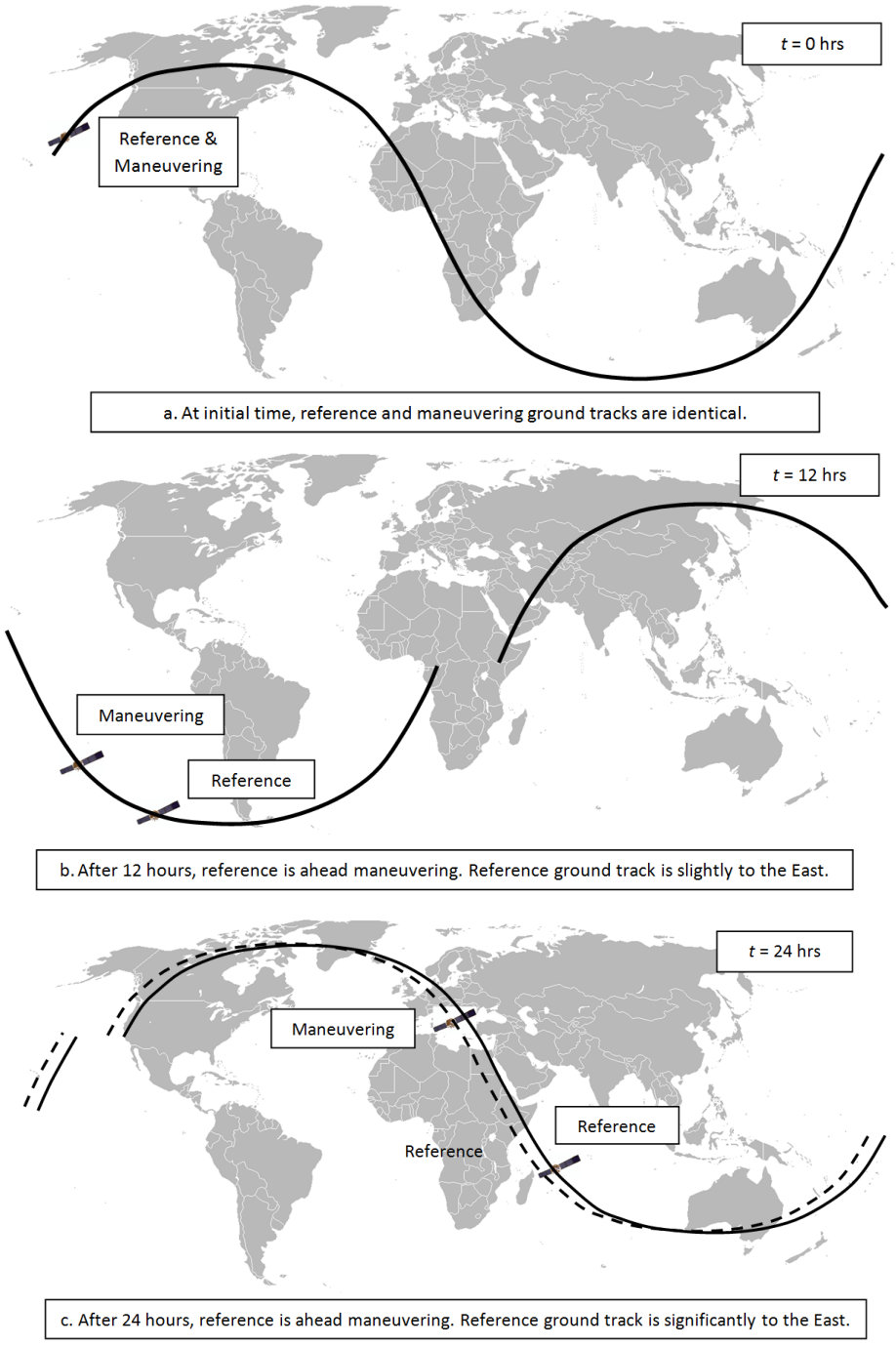

Figure 5-5 a-c. Ground Tracks of Maneuvering and Reference Satellites

The remaining two COEs of semi-major axis (or altitude) and eccentricity do affect terrestrial distance in interesting ways. Altitude is varied while keeping all other initial

COEs constant between scenarios. Cases are set up to evaluate the distances for three altitudes at 500, 1,000 and 1,500 km and the results are depicted in Figure 5-6.

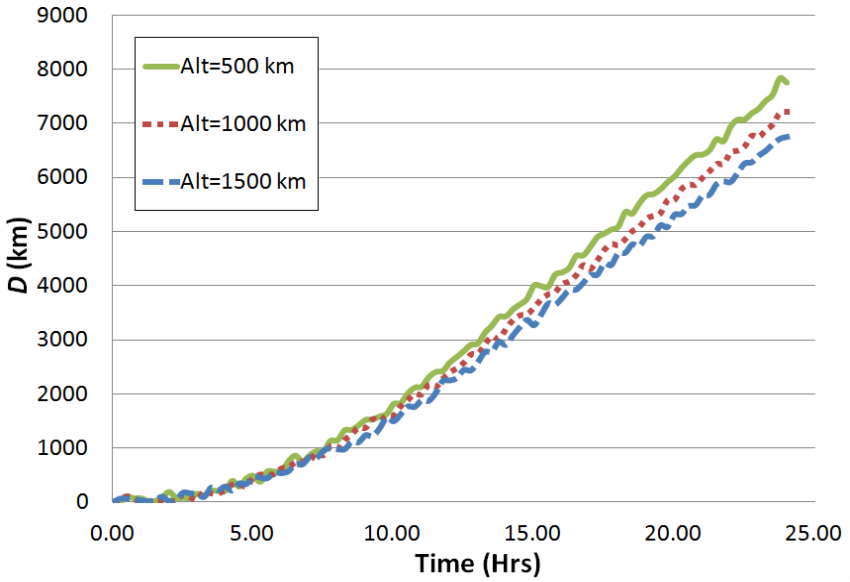

Figure 5-6. Effect of Varying Initial Altitude on Distance

The trend makes intuitive sense, however the reasoning is not as straightforward. At each of these four altitudes, the amount of ΔV added is identical, which ultimately results in a faster mean motion at lower altitudes (Table 5-2 last column). To demonstrate this, three cases of LEOs are included in Table 5-2 that experience the same amount of ΔV impulsively. The process involves several steps governed by Equations (5.1)-(5.8).

Table 5-2. Orbital Parameters after a Maneuver at Three Initial Altitudes

$V_{initial}$ (km/s)	$R_{initial}$ (km)	$\varepsilon_{initial}$ (km^2/s^2)	ΔV (km/s)	ε_{new} (km^2/s^2)	R_p (km)	a_{new} (km)	R_a (km)	Δa (km)	Δn (rad/hr)
7.61	6878.14	-28.98	0.043	-28.65	6878.14	6956.96	7035.77	78.82	**0.0675**
7.35	7378.14	-27.01	0.043	-26.70	7378.14	7465.75	7553.36	87.61	**0.0629**
7.11	7878.14	-25.30	0.043	-24.99	7878.14	7974.85	8071.56	96.71	**0.0589**

The demonstration starts with three circular orbits with velocities of 7.61, 7.35, and 7.11 km/s. The corresponding altitudes are 500, 1,000, and 1,500 km. All cases are subjected to a ΔV of 0.043 km/s, which is equivalent to thrusting with A=1e-6 km/s^2 for 12 hours. The resulting orbits become mildly elliptical. The change in mean motion is greater for lower altitudes, in other words, provided the same amount of ΔV, a satellite at a lower altitude moves even faster than it already does as a result of the maneuver. At the lowest altitude of 500 km the change in mean motion is 0.0675 rad/hr then it decreases to 0.0629 rad/hr at 1,000 km with the smallest Δn of 0.0589 rad/hr at 1,500 km. These numbers may seem small, but after 24 hours of drifting, the difference in distance between the lowest and highest altitudes is equivalent to over 1,300 km. It means at an altitude of 500 km, D is 1,300 km greater than at 1,500 km after thrusting for the same period of time. This effect is visible in Figure 5-6. The simulated difference in D is just over 1,000 km between the top (500 km altitude) and bottom (1,500 km altitude) curves at the end of the simulation period. Lower altitudes translate proportionally into greater distances.

Lastly, eccentricity causes the most interesting behavior for distance. Newberry also concludes that an increasingly elliptical orbit is more efficient to maneuver from. The higher eccentricity does yield greater changes in D given the same elapsed time and thrust level. However, this is misleading. The greater distances are only achievable at perigee when the satellite travels at the highest speed within the orbit, thus the greater D changes only apply for a small portion of the orbit. For the majority of time, the D change is less for any given scenario when compared to one with a lower eccentricity. Figure 5-7 displays the D control for varying eccentricities. The points where D difference is greatest within the orbit occur at perigee. It shows that increasing eccentricity results in

greater *D* control, but only in a limited sense. With increasing *e*, the curves become more distorted, where the spikes represent perigee and the greatest terrestrial distance, but a vehicle would only remain at that distance for a short period of time. A circular orbit actually has a greater average distance than a highly elliptical (HEO) case. The curve with the largest amplitude represents the distance for one such case (*e*=0.6). At perigee the distance spikes, dramatically surpassing the circular distance, but for most of the orbit, the HEO lags behind in distance. This orbit would only be practical for very specific missions. The low-amplitude curve represents the distance for a mildly eccentric case. For this case the distance fluctuates and grows with time, but the amplitude growth between periods is not drastic when compared to more eccentric cases. The average distance grows at the fastest rate for a mildly eccentric initial orbit and average distance grows slower as eccentricity increases.

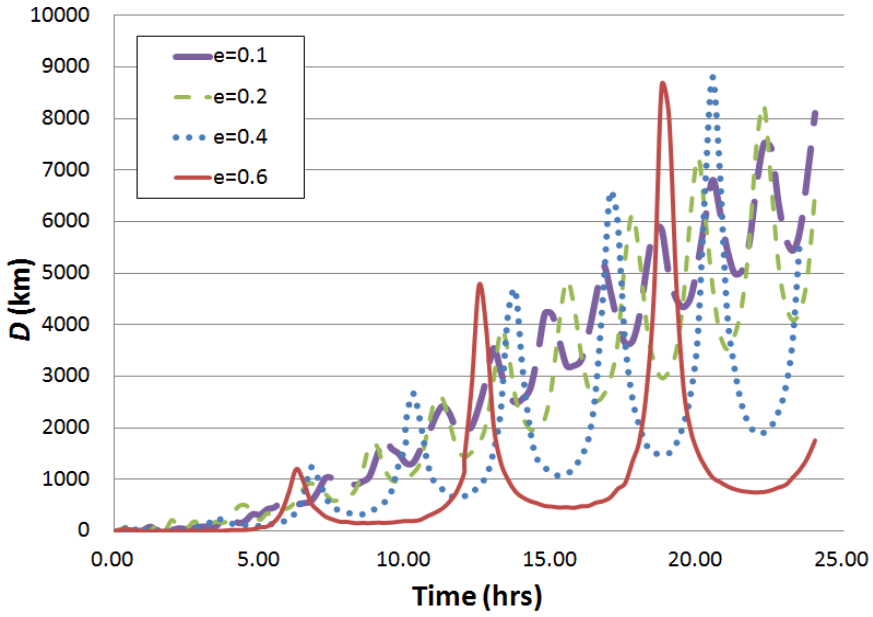

Figure 5-7. Effect of Varying Initial Eccentricity on Distance

The length of time EP thrusters are firing affects the rate of change of terrestrial distance most significantly and only two of the six initial COEs have any measureable effect on distance. Depending on altitude, an EP system capable of an acceleration of 1e-6 km/s^2 can achieve distances greater than 8,000 km when thrusting for 24 hours. This observation supports that it is feasible to maneuver significantly in LEO using EP. Further, initial altitude and eccentricity have profound effects on the achievable distances, which should be considered in mission planning. The next sections compare CP to EP systems and develop equations to accurately predict these ground distances.

5.5 Maneuverability with Chemical Propulsion Systems

The next task in developing an algorithm to place a satellite over a desired target is to formulate equations that predict how maneuvers affect achievable distances. The previous sections demonstrate that LEO satellites can be maneuverable and responsive from a ground track perspective. Global reach distances are possible in most cases in less than two days with ΔV expenditures within today's standard satellite propellant budgets. Examining one CP setup in this section and two EP setups in the next, equations are developed that predict the achievable terrestrial distance based on the equations of motion (Equations (5.1)-(5.10), (5.12), (5.22)-(5.23)). A prediction without a measure of accuracy is of little use, so an analysis of the accuracy is also included.

A series of orbital cases is examined using the CP model to develop the means to quickly calculate distance based on three parameters – time, altitude, and ΔV (Appendix C). The initial orbit is circular and inclined at 60 degrees. Analysis presented in the

previous section shows that the initial inclination does not have any bearing on the following distance equations. The notional propulsion system modeled here is a 200-N chemical thruster with a specific impulse of 230 s. The total system mass is 1,000 kg. The satellite thrusts impulsively at the initial time and propagates for 24 hours recording the distance measured from the non-maneuvering reference orbit in one-minute increments. This process is repeated for different altitudes and ΔVs. The resulting data are curve-fit and the errors associated with the predictions are quantified. Finally, the formula is used to calculate distances for different combinations of altitudes and ΔVs to validate that it is generally applicable as a component for a prediction algorithm. The equations are applicable to any thrust level and system mass as these are both embedded in ΔV.

Figure 5-8 shows that the curve fits for five altitudes are straight lines. The fluctuations are natural to the motion of the maneuvering and reference satellites as a result of the time lag between the two orbits. The ΔV in this case is 0.01 km/s. The previously used accuracy measure does not work uniformly here as it magnifies the error during the first 100 minutes of the simulations, but gets progressively better as time goes by and the distances become large with respect to the errors. For instance, initially D is zero and grows slowly. After 5 min D may be 2.5 km, but the predicted distance from the equation is 0.8 km. Thus error is 1.7 km and when normalized with D, the error is quite large at 68%, yet in reality the magnitude of the error is not significant for predicting achievable distances due to maneuvering over a 24-hour period. To better assess this measure, the maximum distance error is examined for the entire simulation period in each case. The conclusion is that the curve fits are suitable for distance predictions when the

time is greater than 100 minutes. The next step is to combine these five curves into one equation with an altitude adjustment factor.

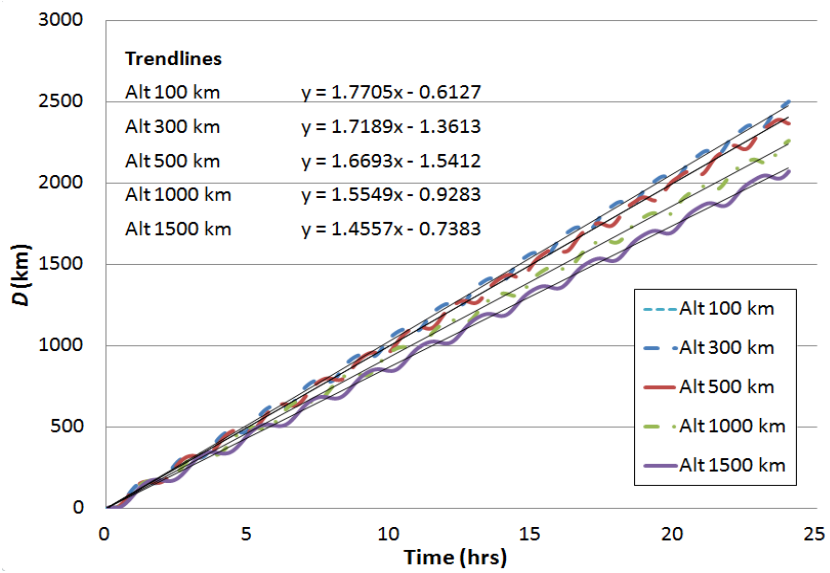

Figure 5-8. Distance Regression for ΔV of 0.01 km/s CP

The first equation (Equation (5.25)) is a simple linear regression with respect to t (in min) whereas the second equation (Equation (5.26)) is a combination of two variables (t and altitude, r in km). Both equations have units of km. Five curve fits are charted and the first one at an altitude of 100 km is selected as a reference:

$$D_{100km} = \frac{1.7705t}{1\,\text{min}} \tag{5.25}$$

Excluding the first 100 points, the accuracy of the fit is 2.4 percent. This exclusion is justifiable based on the definition of the accuracy measure. Since distances are initially small, any error is more pronounced in the beginning of the maneuver. The maximum distance error inside the first 100 points is only 15 km for an orbital altitude, r, of 100 km

and the accuracy increases almost three-fold when these are excluded. Using Equation (5.25), a scale factor is added to account for the altitude. To do so a ratio of the distance at any other altitude with respect to the reference is taken at every instance in time, i.e. $D_{300\text{km}}/D_{100\text{km}}$, and the average is computed while excluding the first 100 points. This leads to:

$$D_{Altitude} = \left(-0.0134 \frac{r}{100\text{km}} + 1.0081 \right) D_{100km} \tag{5.26}$$

When comparing the calculated results of Equation (5.26) to propagated data (considered truth data for this analysis) and excluding the first 100 points, this equation has an average accuracy of 3.9 percent. The final step is the inclusion of ΔV to this equation.

The analysis found that a simple scaling factor for ΔV is more accurate than subjecting the resulting distance values to the same process used above. Thus the case in which ΔV is 0.01km/s is used as the reference formula and simply scaled with a ΔV ratio:

$$D = \frac{\Delta V}{0.01\text{km/s}} D_{Altitude} \,. \tag{5.27}$$

The resulting formula is simpler and more accurate for different combinations of altitude and ΔV. Distances are predicted for nine additional cases (on top of the twenty cases used to derive this equation) with a worst case average accuracy of 3.3 percent. If the problem is restricted to low ΔVs of less than 0.1 km/s and a drift time of more than 100 minutes, the accuracy improves to 2.5 percent. These restrictions are reasonable because the goal is minimum propellant expenditure necessitating a greater amount of drift time. Even so,

distances of 10,000 km are realistic for a ΔV of 0.1 km/s and a drift time of approximately 11 hours. With the developed function, the amount of terrestrial distance can be predicted for any LEO circular orbit with three parameters – altitude, time, and ΔV – or better, if the over-flight of a certain ground target is desired, the equation can determine the time required to achieve it or the amount of ΔV expenditure for a CP system.

5.6 Maneuverability with Electric Propulsion Systems

The same analysis is repeated for an EP system (Appendix D). Two different EP setups are analyzed and compared to the CP performance. The initial orbit is circular inclined at 60 degrees. Once again, the initial inclination has no bearing on achievable distances. It is assumed that the propellant consumption for the EP system during each maneuver is very small compared to the total system mass such that the acceleration is determined by a ratio of the thrust and the initial system mass only. The notional EP thruster is capable of an acceleration of 1e-6 km/s^2 with a specific impulse of 1,500 s. Although the specific impulse is not used in the distance calculations, it is useful in determining the estimated propellant consumption over time based on expended ΔV.

The first set of maneuvers expends an equivalent amount of ΔV as the impulsive cases, namely 0.01, 0.05, and 0.1 km/s, over a period of time determined by the thrusters' acceleration. The maneuver starts at the initial time, thrusts for a specific period, and propagates for the remainder of time until a total of 24 hours has passed. The second set of maneuvers simply turns the thrusters on and allows them to fire continuously for the

entire 24-hour period. This process is repeated for different altitudes and ΔVs. A regression is applied to the resulting data to quantify the errors associated with the predictions. Finally, the formula is used to calculate distances for different combinations of altitudes and ΔVs to validate that it is generally applicable as a component for a prediction algorithm. The equations are applicable to any thrust level and system mass as these are both embedded in ΔV.

Figure 5-9 shows the curve fits for a ΔV of 0.01 km/s then propagating forward until a total time of 24 hours has passed at five altitudes. The fluctuations are natural to the motion of the maneuvering and reference satellites, but they are noticeably milder since the ΔV is added slowly and the resulting orbital change is a gradual outward spiral. The final orbit remains circular as opposed to eccentric when the ΔV is added instantly.

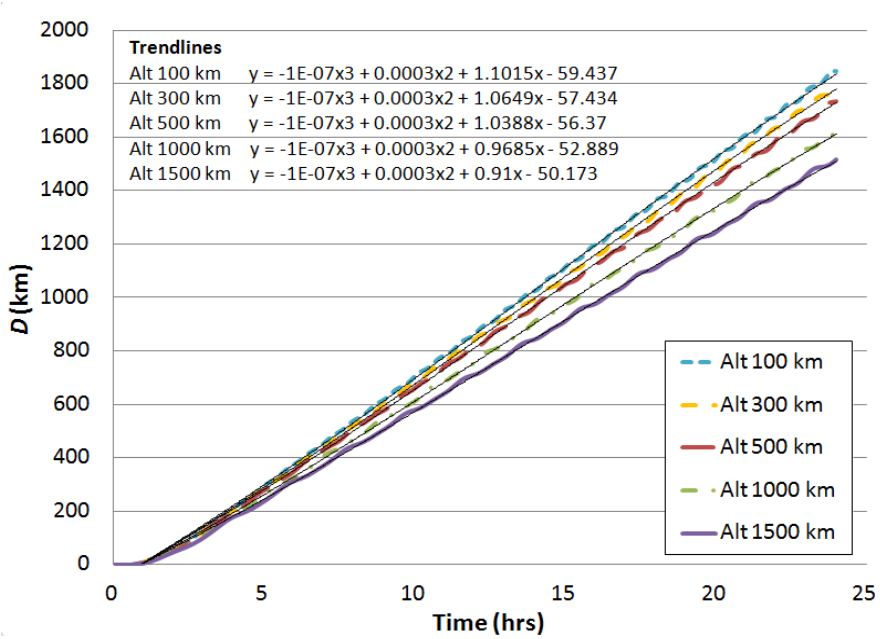

Figure 5-9. Distance Regression for ΔV of 0.01 km/s EP.

The ΔV of 0.01 km/s is added within the first 167 minutes of the maneuver (using a 1-N thruster set on a 1,000-kg system) followed by coasting for the remaining 1,273 minutes. This maneuver could achieve distances between 1,500 and 1,900 km within 24 hours depending on altitude. The next step is to combine these five curves into one equation with an altitude adjustment factor.

The first equation (Equation (5.28)) has units of km and is a third-order polynomial with one variable (t). Corresponding to an altitude of 100 km, the polynomial takes on the form of

$$D_{100km} = \frac{-1 \cdot 10^{-7} t^3}{1\text{min}^3} + \frac{3 \cdot 10^{-4} t^2}{1\text{min}^2} - \frac{1.102t}{1\text{min}} \tag{5.28}$$

This equation has an average accuracy of 2.4 percent based on percent error when the first 100 points are omitted. The maximum distance error for the simulation period is 32 km at an orbital altitude of 100 km. So regardless of which error measure is used, the equation is quite accurate. For low values of t (less than 100 min), the first term has little bearing on the distance, however, as time increases, the first term becomes significant (greater than 1,000 min). Using Equation (5.28) a scale factor is added to account for the altitude. This is accomplished by taking the ratio of the distance at another altitude with respect to the reference altitude. This leads to

$$D_{Altitude} = \left(-0.0107 \frac{r}{100\text{km}} + 1.0059 \right) D_{100km} \tag{5.29}$$

When compared to truth data, this equation has an overall worst average accuracy of 3.7 percent based on percent error after excluding the first 100 points. The accuracy decreases as altitude increases further away from 100 km. Therefore, the 1,500-km case (largest altitude) has the worst accuracy of 3.7 percent for the altitude range. The average error for points 200-300 is 5.6 percent and drops below 1.6 percent after the first 300 minutes and stays below this error for the remainder of time. The ΔV inclusion for this equation becomes problematic as discussed in the next paragraph.

The problem setup of varying the length of time the EP system is firing to achieve a specific level of ΔV does not allow for a simple scaling factor as before. Figure 5-3 in a previous section shows the distance curves for four values of ΔV. Since the acceleration of the thruster is 1e-6 km/s^2, the only way to vary ΔV is by the amount of time the thruster fires. There is no simple expression that can account for the different levels of ΔV since the relationship is very complex. If the previous ratio method is used, it will not yield a constant ratio that is suitable as a scaling factor. Figure 5-3 demonstrates the behavior of distance versus time. The slope continues to increase as long as the thrusters are firing. Once the desired ΔV is attained, the distance continues to grow at the rate of change at the time of thruster shut-off. Instead of finding an equation that accounts for time, altitude, and ΔV for this problem setup, the expressions are simply left as a function of time and altitude for several ΔV values. This same method is used to develop more equations and coded into an algorithm to determine an approximate ground track difference.

In this second set of EP maneuvers, the thruster remains on for the entire 24-hour period. The resulting distances are the largest the system can achieve within the allotted

time and it consequently uses the largest amount of ΔV. The purpose is to compare the maximum EP distance attainable with that of CP given the same time period. This process is repeated for different altitudes. A curve-fit of the resulting data provides equations which are analyzed to quantify the errors associated with the predictions. Since ΔV is added gradually, the curves are smooth and modeling the system's behavior is very accurate. Figure 5-10 shows the curve fits for continuous 24-hour thrusting at five altitudes. There are minimal fluctuations and the final orbit remains circular.

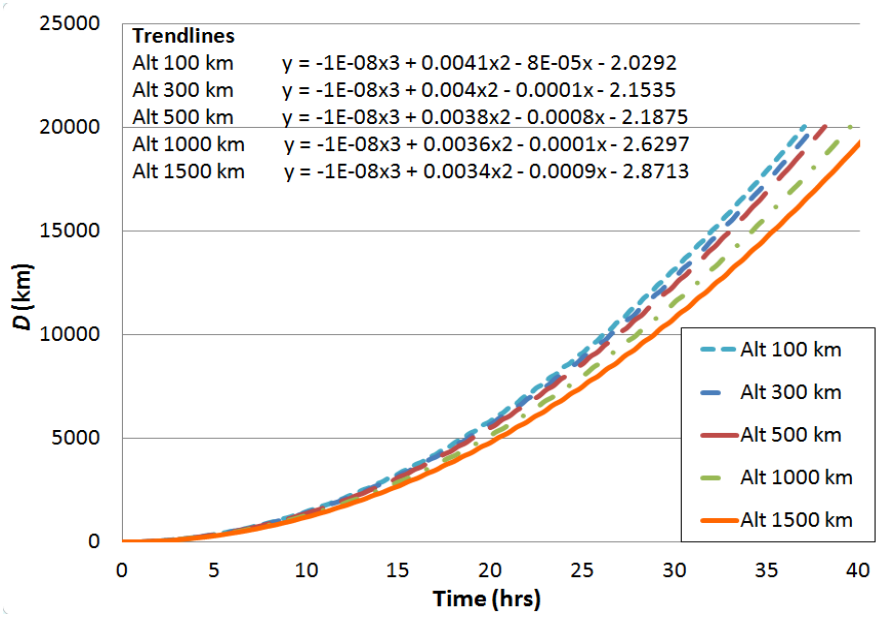

Figure 5-10. Distance Regression for Continuous Thrusting EP

The gradual increase of terrestrial distance with time is simply modeled using a third-order polynomial without loss of accuracy. Equation (5.29) is the reference case at an altitude of 100 km with a single variable (t). The remaining four curves closely follow the data, which allows for a highly-accurate relationship when combining the equations

into a single formula to account for altitude. As before, the reference equation is selected as:

$$D_{100km} = \frac{-1\cdot 10^{-8} t^3}{1\min^3} + \frac{4.1\cdot 10^{-3} t^2}{1\min^2} - \frac{8\cdot 10^{-5} t}{1\min} \tag{5.30}$$

When the first 100 points are omitted, the accuracy is 0.5 percent. The other equations modeling distances at altitudes of 300, 500, 1,000, and 1,500 km have negligible errors of no more than 1.5 percent. Following the same process as above, the altitude scaling factor is:

$$D_{Altitude} = \left(-0.0122 \frac{Altitude}{100} + 1.0046 \right) D_{100km}. \tag{5.31}$$

Excluding the first 100 points, this equation has an average accuracy of 1.1 percent. There is no need account for different values of ΔV here since the thrusting period, hence propellant consumption, remains constant between cases. Using this equation, the achievable terrestrial distances using EP can be predicted very accurately.

5.7 Comparison of CP vs. EP

The previous sections describe the development of a methodology to quantify terrestrial maneuver distances a satellite can achieve using CP and EP systems as a function of time, initial orbit, and ΔV. Using the resulting regression equations, either system can be effective in changing a LEO satellite's ground track enough to cover almost any point on Earth. Table 5-3 summarizes the findings for a sample case to demonstrate the difference between CP and EP maneuvers. The scenario starts as a

circular orbit at 500 km altitude inclined at 60 degrees. Using the presented problem setup the terrestrial distances resulting from three levels of ΔV at 0.01, 0.05, and 0.1 km/s are tabulated for both propulsion models. A CP maneuver affects ground distances of 2,365, 12,105, and 24,196 km, respectively. In comparison, an EP maneuver only achieves 1,735, 6,540, and 7,945 km or a fraction of CP when expending the same amount of ΔV. The reason for this gross difference is two-fold. A circular spiral transfer is less efficient because energy is used to raise the entire orbit to a higher altitude, whereas a CP maneuver makes the orbit eccentric, only raising the apogee altitude while leaving perigee at its original altitude. The second reason only pertains to the third case for a ΔV of 0.1 km/s. A CP maneuver expends the energy instantaneously, whereas the EP, at the level of thrust selected, does not have enough time within the first 24 hours to create enough ΔV. The selected system needs 100,000 seconds or 1.15 days to create a ΔV of 0.1 km/s, thus the distance would be greater (11,331 km) if the evaluation period is extended to allow the full ΔV expenditure.

Table 5-3. Comparison Summary of CP and EP

Maneuver Type	*ΔV* (km/s)	*D* (km)	Time to CP *D* (hrs)
CP - Impulsive Thrust	0.01	2365	
	0.05	12105	
	0.1	24196	
EP - Specific ΔV	0.01	1735	32
	0.05	6540	38.5
	0.1	7945	43.3
EP - Continuous Thrust	0.047	2365	13.1
	0.107	12105	29.7
	0.146	24196	40.6

Further, it is evaluated how long it would take the EP system to reach the same distance that the CP system can attain in 24 hours. It takes the EP model 32, 38.5, and 43.3 hours, respectively, to match the performance of CP at the three levels of ΔV.

Taking a different perspective, if the EP system thrusts continuously, the time to achieve the same performance as CP is less in exchange for larger ΔVs. Turning on the EP thrusters at the initial time and allowing them to fire continuously, the distance is 2,365 km after only 13.1 hours. This time savings of 45 percent comes at a ΔV expenditure of 4.7 times compared to that of CP. The system achieves 12,105 km in terrestrial distance in 29.7 hours, or 5.7 hours longer than CP, but uses twice as much ΔV. Finally, in 40.6 hours the distance is 24,196 km while expending 1.5 times more ΔV. Clearly, the more time there is available for the EP system to perform the maneuver the lower the ΔV expense.

5.8 Application

Equations (5.27), (5.29), and (5.31) allow users to determine general reachability, D, based on propellant consumption, altitude, and time. The distance equations are very accurate and predict the attainable ground separation as a result of maneuvering. For instance, if there is a requirement for the notional spacecraft at an altitude of 500 km to attain a distance of 9,000 km, Figure 5-10 shows that this is achievable in 25.5 hours. To achieve a greater distance requires either more time or acceleration greater than 1e-6

km/s^2. Similarly, given any combination of three of the four parameters, the forth one can be determined.

There are other practical applications for these distance equations. Consider a spacecraft at an altitude of 500 km with the same thruster characteristics described before. The reference ground track at the target time, t_f, is too far to the East from an equatorial target at λ=0° and φ=5°W to get useful images (Figure 5-11a). In order for the payload to achieve the user required resolution, the spacecraft must be almost directly over the target at t_f with an error margin of ±50 km. The reference ground track is 650 km from the target at t_f.

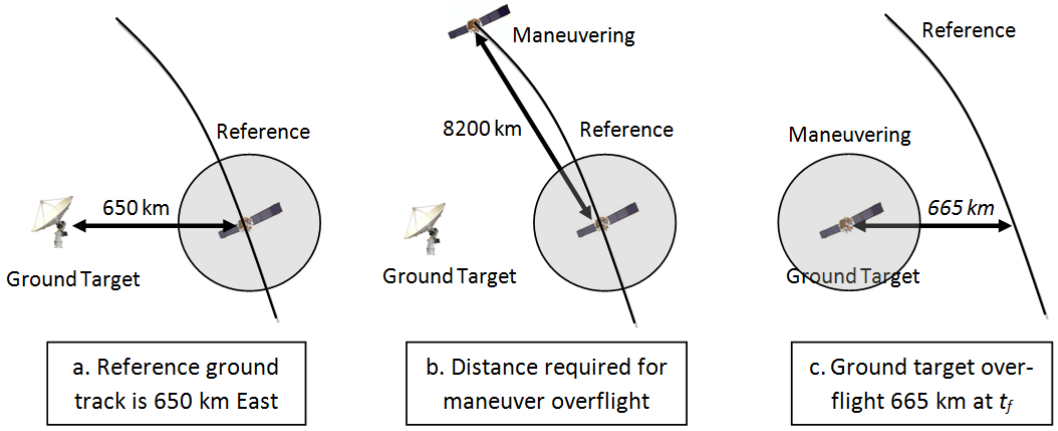

Figure 5-11 a-c. Distance Required to Move Reference Ground Track over Target

Based on the Earth's rotation rate, the difference in over-flight time is computed to be +18 min, which means the maneuvering satellite must pass over the Equator 18 minutes after the reference satellite does. The approximate *D* associated with 18 min of over-flight time difference is 8,220 km (circular orbital velocity of reference multiplied by 18 min). Using Equation (5.31), the maneuvering satellite can achieve a *D* of 8,220 km in

1460 min or slightly longer than a day (Figure 5-11b). Simulating this scenario with these inputs results in shifting the reference ground track westward by 665 km or just 15 km West of the target but within the allowed error margin (Figure 5-11c). The conclusion is that if the initial time, t_0, at which the maneuver begins is not 1460 min prior to t_f, then there is not enough time for this system to achieve the desired objective.

5.9 Conclusion

The analysis demonstrates that both chemical and electrical propulsion systems have potential for a satellite to be maneuverable and responsive. Distances in excess of 10,000 km are achievable within 24 hours with a ΔV of 0.05 km/s for chemical propulsion and within 27 hours with a ΔV of 0.1 km/s for electric propulsion. These distances and the ability to calculate the ΔV required to achieve a tasked overflight represent a novel capability for satellite operations.

This research shows the classical orbital elements that have the greatest impact on terrestrial distance for designing a suitable initial orbit. The elements designating the orbit plane's orientation and a spacecraft's location within the orbit, namely right ascension of the ascending node, inclination, argument of latitude (for circular orbits), argument of perigee, and true anomaly, have no effect on distance. Semi-major axis or altitude has a moderate effect. It is an inverse relationship, lowering the altitude results in greater distances. Eccentricity has the greatest effect. More eccentric orbits achieve much greater distances at perigee when compared to less eccentric ones, yet for the majority of the orbit the distances are smaller. Thus a less eccentric initial orbit results in the greatest average distance in a more consistent manner. Despite the findings, altitude and

eccentricity have to be chosen carefully based on the system's mission as each one imposes specific characteristics on the orbit.

Further, the presented terrestrial distance equations demonstrate a high level of accuracy in predicting a system's maneuvering capability. These equations are useful in determining the achievable terrestrial distance given the propellant budget, original orbit, and time available to reach a target. Similarly, given any combination of three input variables, the fourth one can be predicted. Provided the magnitude of the terrestrial distances current propulsion systems can achieve within 24 hours, it is concluded that existing technology with standard propellant budgets can maneuver significantly to respond to user needs in a timely fashion.

6 Optimal Low Thrust Profiles for Responsive Satellites

This study provides analytical solutions for in-plane and out-of-plane low thrust maneuvering satellites in low-Earth orbit to modify ground-track and change the time the spacecraft overflies a particular location within the orbit. To validate the solutions, previously-developed algorithms are used to determine optimal low thrust profiles. Responsive Space has become a buzz word in the space community; to achieve it requires new operational approaches. Besides fundamentally changing how access to space is attained, operational responsiveness is achievable by changing the satellite's ground track through maneuvering. An analytical time of overflight equation is derived, which is a cornerstone for determining the maneuver requirements to overfly specific terrestrial targets. In-plane maneuvers aligned with the velocity vector maximize the time-rate-of-change of the semi-major axis, but cannot change orbital plane orientation, namely inclination and right ascension of the ascending node. Out-of-plane maneuvers can change the latter two if executed in an alternating thrust pattern. The analysis confirms that in-plane maneuvers are far more effective in changing overflight time compared to out-of-plane ones. Current electric propulsion technology could change over-flight time up to 30 minutes with a 3-percent propellant expenditure within one day.

Nomenclature

A = perturbing acceleration magnitude, km/s^2

a = semi-major axis, km

a_0 = initial semi-major axis, km

a_h = normal acceleration component with respect to orbital plane, km/s^2

a_r = radial acceleration comp in local-vertical, local-horizontal (LVLH), km/s^2

a_θ = acceleration comp completing the right-handed coordinate system, km/s^2

e = eccentricity

h = angular momentum

$\hat{h}$ = normal component wrt orbital plane of the LVLH

i = inclination, degrees

m_0 = initial spacecraft mass, kg

$\dot{m}$ = mass flow rate, kg/s

Δm = change in mass due to maneuvering, kg

n = mean motion, rad/s

P = orbital period, s

p = semi-latus rectum, km

r = magnitude of radius vector, km

$\hat{r}$ = radial component of the local-vertical, local-horizontal frame

T = thrust magnitude, N

t = time, s

t_0 = initial time, s

t_f = final time, s

Δt = change in over-flight time, s

Δt_m = time elapsed from the beginning of maneuver to target overflight, s

$\boldsymbol{u}$ = thrust control vector, components in degrees

u = argument of latitude, degrees

u_0 = initial argument of latitude, degrees

u_1 = argument of latitude after thrust period, degrees

u_2 = final argument of latitude, degrees

ΔV = velocity change, km/s

x, y, z = coordinates in Earth-Centered Fixed (ECF) coordinate frame, km

γ = angle between Earth-Centered Inertial (ECI) and ECF frames, rad

γ_g = Greenwich sidereal time, rad

θ = out-of-plane thrust angle wrt $\hat{r}$-$\hat{\theta}$ plane, degrees

$\hat{\theta}$ = tangential component of the local-vertical, local-horizontal frame

λ_{tgt} = target latitude, degrees

$\mu_\oplus$ = Earth's gravitational parameter, 3.98601 x10^5 km^3/s^2

v = true anomaly, rad

φ_{tgt} = target longitude, degrees

ψ = in-plane thrust angle in $\hat{r}$-$\hat{\theta}$ plane, degrees

Ω = right ascension of the ascending node, degrees

ω = argument of perigee, degrees

$\omega_\oplus$ = Earth's angular velocity magnitude, rad/s

6.1 Introduction

OVER the past few years, research on responsive space has become more prevalent and the concept of low thrust orbital changes has been considered as a means to achieve it (Newberry, 2005: 46-49; Co, 2011a:74). A system that has the ability to respond to new taskings within days or hours could be a viable and less expensive alternative to rapid reconstitution and launch. Spacecraft which are able to maneuver multiple times throughout their lifetime to accomplish multiple missions to achieve responsiveness at the lowest cost are becoming more attractive. Allowing space assets to be re-tasked in this manner could significantly decrease the overall cost of maintaining space programs. The problem of minimum-propellant maneuvering using low-thrust electric propulsion to overfly a specific location within the orbit is considered. An analytical approach is followed to derive expressions for the change in time of arrival over a particular location within the osculating orbit, the change in inclination, and the change in right ascension of the ascending node (RAAN). Previously-developed algorithms are used to analyze five scenarios and validate the analytical expressions. Depending on the propellant consumed and the system's propellant budget, the process can be repeated to allow the spacecraft to maneuver multiple times.

One of the first published works on optimized spacecraft trajectories was Lawden's *Optimal Trajectories for Space Navigation* published in 1963 (Lawden, 1963). Lawden solved the problem of optimal impulsive maneuvers using calculus of variation methods. He presented analytical solutions of optimal thrust profiles for rocket trajectories and orbital transfer maneuvers. In his formulation he treated the Lagrange multipliers as

components of a "primer vector" whose behavior indicated the optimal direction of an impulsive thrust. Although Lawden did not consider low-thrust systems in solving the optimal control problem, his work is considered the foundation of optimal space trajectories and is a fundamental reference in a vast majority of the literature on this subject.

Marec first published *Optimal Space Trajectories* in France in 1973 (Marec, in English, 1979). Marec built on Lawden's work by including the consideration of using low-thrust propulsion systems, and referred to numerical results as opposed to purely analytical. His book served as a comprehensive compilation of all active research at that time and he included a variety of trajectory optimization problems. He started by providing a parametric optimization example using the popular Hohmann transfer to expose the shortcomings of parametric methods. He then discussed the use of functional optimization methods for optimal transfer problems using both impulsive thrust and continuous low thrust. Numerical methods have come a long way since Marec's book was published, and many applications to optimal control problems have been researched.

Optimal control methods have become more modernized and numerical solutions have become preferred over analytical solutions. However, analytical solutions have been derived for specialized cases. Wiesel and Alfano addressed the minimum-time transfer between two circular orbits using low thrust (Alfano, 1982; Wiesel, 1985: 155). The main assumption they made that allowed for a closed form solution is that the thrust magnitude is small enough that the orbit's semi-major axis and eccentricity remain fairly constant for a single revolution. The problem was separated into a fast timescale and a slow timescale version. The fast timescale problem was formulated to determine the small changes in the

orbital elements over one revolution, while maximizing the inclination change for a specified semi-major axis change. Solutions from the fast timescale problem were then used to solve the slow timescale problem over multiple revolutions, while taking into account the vehicle's change in mass. Wiesel used the method of variation of parameters to derive the differential equations that describe the behavior of the Classical Orbital Elements (COEs) perturbed by a small acceleration, which were used as a powerful tool for analysis in their minimum-time transfer problem (Wiesel, 2003). The shortcomings of using COEs are singularities for circular and equatorial orbits. One common method to avoid singularities is the use of Equinoctial elements.

Equinoctial elements have been used in spacecraft trajectory optimization. Kechichian used the non-singular set of elements to solve the optimal low-thrust rendezvous problem using continuous constant acceleration (Kechichian, 1996: 1-14). After formulating the problem, Kechichian used numerical methods to solve the Two-Point Boundary Value Problem (TPBVP). The problem is posed as a minimum time problem and solved using a quasi-Newton minimization algorithm. Rendezvous problems, like those of Kechichian are similar to the responsive maneuvers that are discussed in this paper. The main difference is that instead of the objective being to rendezvous with another spacecraft, it is to "rendezvous" with a location on an orbit that overflies a ground target. This paper presents scenarios with and without a final altitude constraint.

One of the most difficult parts of solving an optimal control problem is providing an initial guess for the solution. In his dissertation, Thorne formulated the minimum-time, continuous thrust orbit transfer problem, and used the shooting method to solve the

TPBVP (Thorne, 1996). The shooting method involves numerically integrating the equations governing the dynamics of the spacecraft and the Lagrange multipliers, which once again requires a guess for the initial conditions on the Lagrange multipliers. Thorne presented a method for modeling the initial values of the Lagrange multipliers. He first used numerical results from different scenarios to determine the functional relationship between the Lagrange multipliers and two different parameters - the radius of the final orbit and the constant acceleration acting on the spacecraft. Using analytical and empirical methods he derived approximate expressions that define the initial Lagrange multipliers, and analyzed their convergence. He then used these expressions as a reliable means of providing initial conditions on the Lagrange multipliers for the minimum-time continuous thrust orbit transfer.

Although much of the literature presented is somewhat related to the problem posed in this paper, it does not provide closed form solutions to a rather complex problem. Further it does not consider the problem of a maneuvering satellite coinciding with a specific location within the orbit. With the exception of the rendezvous problem presented by Kechichian, the literature described above does not take into account the position of the spacecraft at the end of the maneuver. Kechichian did account for the final position in order to complete the rendezvous but also incorporated a constraint that the final orbit must be the same as the initial orbit. This paper studies maneuvers where the spacecraft must reach a specific position within its orbit and its final altitude can be left unconstrained. The developed equations are then validated using examples of three classes of maneuvers – in-plane, out-of-plane, and a combination of the two.

6.2 System Models

The equations of motion for a spacecraft under a constant, low thrust can be simply written from Newton's second law using Classical Orbital Elements (COEs). Low thrust electric propulsion (EP) maneuvers result in small accelerations that perturb the orbit of the spacecraft. Gauss' form of the Lagrange Planetary Equations models the change over time in the COEs (*a, e, i,* Ω*, ω, ν*) (Schaub, 2003: 522):

$$\frac{da}{dt} = \frac{2a^2}{h}\left(e\sin\nu a_r + \frac{p}{r}a_\theta \right) \tag{6.1}$$

$$\frac{de}{dt} = \frac{1}{h}\left(p\sin\nu a_r + \left((p+r)\cos\nu + re\right)a_\theta \right) \tag{6.2}$$

$$\frac{di}{dt} = \frac{r\cos(\omega+\nu)}{h}a_h \tag{6.3}$$

$$\frac{d\Omega}{dt} = \frac{r\sin(\omega+\nu)}{h\sin i}a_h \tag{6.4}$$

$$\frac{d\omega}{dt} = \frac{1}{he}\left(-p\cos\nu a_r + (p+r)\sin\nu a_\theta \right) - \frac{r\sin(\omega+\nu)\cos i}{h\sin i}a_h \tag{6.5}$$

$$\frac{d\nu}{dt} = \frac{h}{r^2} + \frac{1}{he}\left(-p\cos\nu a_r + (p+r)\sin\nu a_\theta \right) \tag{6.6}$$

The disturbance acceleration vector can be written as a function of an acceleration magnitude, *A*, and two control angles, ψ and θ, which define the direction of the vector (Figure 6-1). In the Local-Vertical-Local-Horizontal (LVLH) frame, the angle ψ is measured from the $\hat{r}$ unit vector and lies on the $\hat{r}$-$\hat{\theta}$ plane, and θ measures the angle between the acceleration vector and the $\hat{r}$-$\hat{\theta}$ plane.

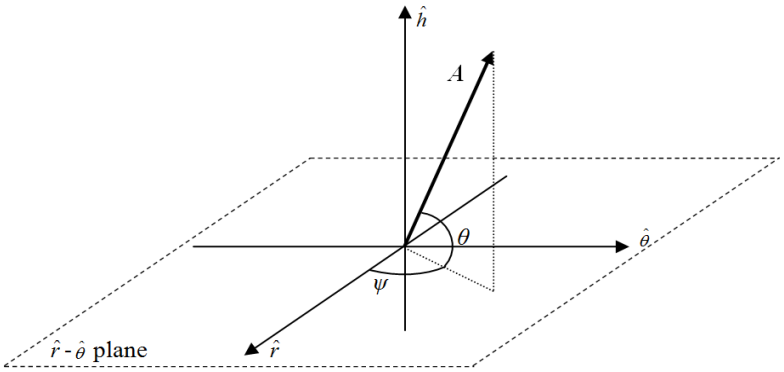

Figure 6-1. Acceleration Vector and Control Angles

The acceleration magnitude of the vehicle and each component of the acceleration vector are:

$$A = \frac{T}{m_0 + \dot{m}t} \tag{6.7}$$

$$a_r = A\cos\theta\cos\psi \tag{6.8}$$

$$a_\theta = A\cos\theta\sin\psi \tag{6.9}$$

$$a_h = A\sin\theta \tag{6.10}$$

The analysis is divided into two classes of maneuvers – in-plane and out-of-plane. Assuming that $\Delta m << m_0$ (for electric propulsion) the acceleration magnitude is a constant for the thrust periods considered. For in-plane maneuvers it is assumed that the initial orbit is circular and no out-of-plane thrust is applied ($\theta=0$). Equations (6.1)-(6.6) reduce to two equations for the Two Body Problem (TBP). Co *et al* provide reasoning for

the suitability of the use of the TBP for this problem setup (Co, 2011b: 12-13). Since all calculations are based on a maneuvering satellite with respect to a non-maneuvering reference satellite with the same initial conditions, both vehicles experience the same perturbing forces of the atmosphere and the geopotential. The simpler TBP allows for faster computation without sacrificing accuracy. To avoid the singularity, the rate of change of the true anomaly or argument of latitude, u, is replaced by the mean motion:

$$\frac{da}{dt} = \frac{2}{\sqrt{\mu_{\oplus}}} a^{3/2} A \sin\psi \tag{6.11}$$

$$\frac{du}{dt} = \sqrt{\frac{\mu_{\oplus}}{a^3}} \tag{6.12}$$

The initial semi-major axis, a_0, is known. The initial argument of latitude, u_0, is also known and assumed to be zero at the ascending node. The final argument of latitude is the target location within the circular orbit.

Out-of-plane maneuvers also allow for simplifications. It is assumed that the orbit is circular and there is no in-plane thrust, thereby making a and e constant and ω irrelevant. Equations (6.3)-(6.4) can be rewritten as

$$\frac{di}{dt} = \sqrt{\frac{a}{\mu}} \cos(nt) A \sin\theta \tag{6.13}$$

$$\frac{d\Omega}{dt} = \sqrt{\frac{a}{\mu}} \frac{\sin(nt)}{\sin i} A \sin\theta. \tag{6.14}$$

For Equation (6.13), the maximum t is one quarter of the period of the circular orbit and the total change in i for one revolution is simply $\frac{di}{dt}$ (where $t = P/4$) multiplied by four, because of the sign change of the cosine function at $u = 90°$ or $t = P/4$. Whereas Equation (6.14) can have a maximum t of one half the period of the circular orbit since the sign change for the sine function does not occur until $u = 180°$. Equations (6.11), (6.13), and (6.14) allow for thrust angle variations that maximize the time rate of change of the variables a, i, and Ω, respectively. This paper analyses the simple cases of considering each variable independently and then a more complex case that considers all three.

Defining Target Location.

The terrestrial overfly target is defined by latitude and longitude coordinates. The approach is to calculate the true anomaly required so that the orbit's ground track overflies that point on Earth. Using spherical geometry, the target latitude (λ_{tgt}) and longitude (φ_{tgt}) are converted to a position vector in the Earth-Centered-Fixed (ECF) coordinate frame using:

$$x = r\cos(\lambda_{tgt})\cos(\varphi_{tgt}) \tag{6.15}$$

$$y = r\cos(\lambda_{tgt})\sin(\varphi_{tgt}) \tag{6.16}$$

$$z = r\sin(\lambda_{tgt}) \tag{6.17}$$

This position vector is then converted into the Earth-Centered-Inertial (ECI) frame using a single 3-axis rotation through the angle γ, representing the location of the Prime Meridian:

$$\gamma = \gamma_g + \omega_{\oplus}\Delta t_m \tag{6.18}$$

where Δt_m is the difference between time of desired overflight and time at epoch. The final step is a standard 3-1-3 Euler angle rotation sequence through Ω, i, and ω, respectively, to transform the position vector into the perifocal frame, from which the true anomaly or argument of latitude can be easily calculated. This process assumes that at the desired overflight time the target will be on the plane of the orbit and consequently, the third component of the perifocal position vector will be zero. In order to fully solve the target overflight problem one would need to solve for the specific time that the target is in the plane of the orbit. For the purposes of this paper the target is defined as an arbitrary value of true anomaly that is to be reached with the understanding that future work can show how this value can be chosen to coincide with a desired ground target.

6.3 Analytical Solutions

Using Equations (6.11)-(6.12) allows the derivation of an analytical expression for the amount of time change of a non-maneuvering reference and the maneuvering satellite to arrive at a specified location within the orbits (argument of latitude) designated as Δt for in-plane maneuvers (change in time of overflight). The expected optimal control angle for an in-plane maneuver where a is unrestricted is $\pm 90^o$, because the acceleration is maximized to yield the largest possible time-rate-of-change of the semi-major axis. Plugging in the optimal control angle, $\psi = -90^o$, into Equation (6.11) gives:

$$\frac{da}{dt} = -\frac{2}{\sqrt{\mu}} a^{3/2} A \tag{6.19}$$

Separating variables allows for integration and solution for the maneuver duration:

$$t - t_0 = \frac{\sqrt{\mu}}{A}\left(a^{-1/2} - a_0^{-1/2} \right) \tag{6.20}$$

where *a* represents the final semi-major axis reached at the end of the maneuver. Equation (6.12) can then be used to change the independent variable of integration from time to argument of latitude:

$$\frac{da}{du} = -\frac{2}{\mu} a^3 A \tag{6.21}$$

Separating variables again allows for integration and solution for the final semi-major axis:

$$a = \left(\frac{1}{a_0^2} + \frac{4}{\mu} A(u - u_0) \right)^{-1/2} \tag{6.22}$$

where *u* represents the desired final argument of latitude. The solution for the final semi-major axis can then be used in Equation (6.20) and Δt can be calculated by:

$$\Delta t = (u - u_0)\sqrt{\frac{a_0^3}{\mu}} - \frac{\sqrt{\mu}}{A}\left[\left(\frac{1}{a_0^2} + \frac{4}{\mu} A(u - u_0) \right)^{1/4} - a_0^{-1/2} \right] \tag{6.23}$$

Equation (6.23) shows that Δt between a maneuvering and reference satellite is a function of the desired argument of latitude, acceleration, and initial semi-major axis. Therefore for any given circular orbit the larger the value of the desired argument of latitude, the larger the Δt will be. This Δt is critically important to determining when a maneuver must start provided specific vehicle characteristics, initial orbit, and a terrestrial target.

For out-of-plane maneuvers, the entire plane of the orbit is modified by changing i, Ω, or a combination of the two. Thus there is no Δt as a result of maneuvering. Changing i may have other purposes such as increasing the latitude range of a satellite and therefore the coverage area or aligning the orbit with a sun-synchronous inclination appropriate for the altitude. Conversely, changing Ω directly affects the ground track and can shift it East- or Westward to overfly a terrestrial target. Assuming A is constant, t_0 is zero, and $u(t_0)$ is zero (satellite at ascending node), Equations (13) and (14) can be solved analytically to yield

$$\Delta i = \sqrt{\frac{a}{\mu}} \sin(nt_f) \frac{A \sin\theta}{n} \tag{6.24}$$

$$\Delta\Omega = \sqrt{\frac{a}{\mu}} (1 - \cos(nt_f)) \frac{A \sin\theta}{n \sin i} \tag{6.25}$$

Both equations are used in portions when θ is constant and then added together for the duration of the maneuver. For instance, a RAAN-change thrusting maneuver performed over five revolutions would have ten thrust periods (twenty for inclination) where θ is constant. To change $\Delta\Omega$ most effectively, the thrust direction remains constant, directly out-of-plane between the ascending and descending nodes (constant portion) and then

changes to the opposite direction, or 180° directional change, between the descending and ascending nodes. The change in RAAN is added over the full simulation time to provide the net effect. Similarly, Δi maneuvers are performed in the same fashion but with each revolution divided into four portions because the directional change is shifted 90° from the nodes. These equations are not only useful in determining when to thrust to affect the desired orbital parameters, they also allow for quick and accurate computation of the magnitude of the changes. The following section uses optimal control and feedback control methods to validate Equations (6.23)-(6.25) and proves that these equations are accurate representations of numerical results.

6.4 Results and Discussion

This paper focuses on minimum propellant maneuvers to change the overflight time of a ground target. The magnitude of the acceleration is assumed constant, while its direction is treated as the control variable. With a constant acceleration and no throttling, the mass flow rate of the propulsion system will be constant; therefore minimizing the duration of the maneuver will also minimize the amount of propellant used. In his thesis, Zagaris develops two algorithms to produce trajectories for these maneuvers (Zagaris, 2012). The first algorithm he presents is developed through optimal control theory and uses pseudospectral methods to numerically solve the two-point boundary value problem and produce a solution. He formulates the optimal control problem for minimum time in-plane maneuvers using Euler-Lagrange theory, and applies the developed algorithm to a series of example maneuvers. The second algorithm he presents is developed through

Lyapunov theory and uses a Lyapunov based feedback control law. He shows that the two algorithms produce equivalent results for in-plane maneuvers and uses the feedback control algorithm to demonstrate out-of-plane maneuverability. These algorithms can be used to validate the analytical equations presented in the previous section.

Five test cases are run for this study – two in-plane cases with restricted and unrestricted final altitude, two out-of-plane cases to change i and Ω independently, and one that combines changing a and Ω. A target argument of latitude is chosen arbitrarily and the change in overflight time between the maneuvering spacecraft and a reference spacecraft is calculated. All four cases use a constant acceleration value of 1e-6 km/s^2, which is equivalent to 500 mN of thrust for a 500-kg spacecraft assuming that the change in mass during the maneuver is negligible compared to the total spacecraft mass. A date and time must be selected for the beginning of the maneuver to calculate the local sidereal time. All scenarios have a minimum altitude constraint of 200 km to avoid solutions that would cause collision with the Earth.

6.4.1 Scenario 1 – In-plane, Phasing Maneuver.

The spacecraft starts on a circular, polar orbit with a = 6,878 km, i = 90º, and $\Omega = u$ = 0º. The selected target argument of latitude is at 180º within the spacecraft's 15th orbit. The purpose of this scenario is simply to show that the optimal control algorithm works as expected, whereas scenarios 2-5 validate the derived equations. Figure 6-2 shows the optimal solution and Figure 6-3 shows the ground track of the reference spacecraft's final orbit and the ending positions of both the maneuvering and reference spacecraft. The semi-major axis decreases from 6,878 to 6,804 km then returns to the original value as it

is constrained to do by the problem setup. The control angle, ψ, starts at -88.9º, showing that the control angle will start in the anti-velocity direction and switch to end along the velocity direction at the same angle.

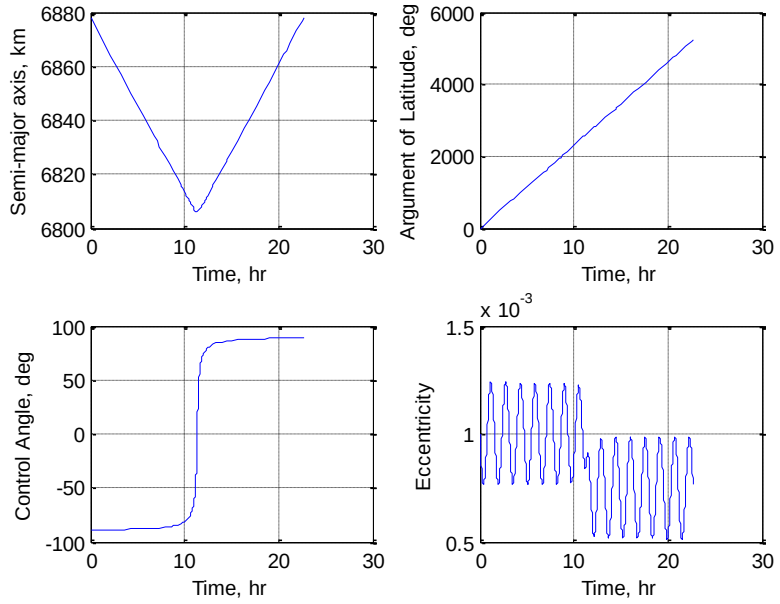

Figure 6-2. Control Inputs and States of Optimal Solution, Scenario 1

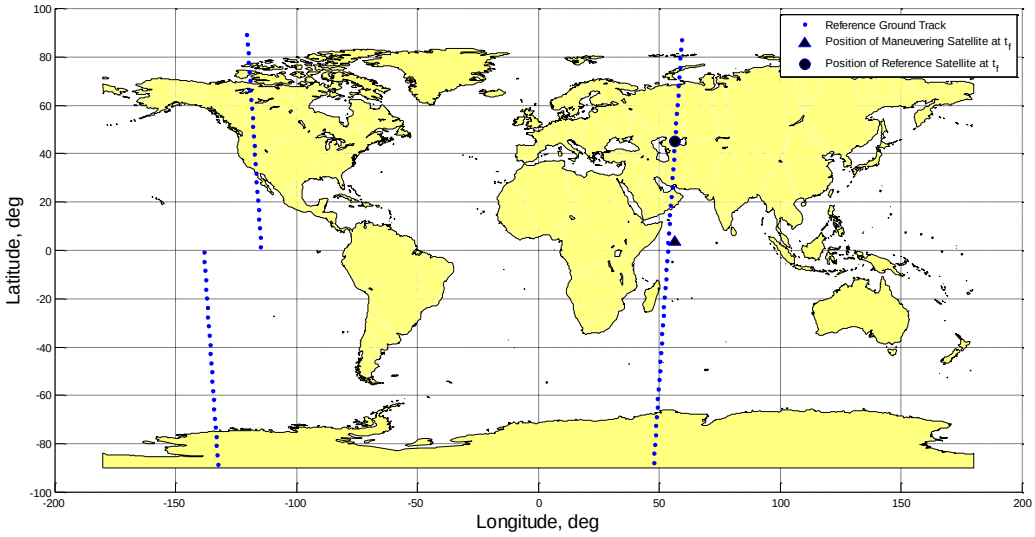

Figure 6-3. Ground Track and Target Location, Scenario 1

Argument of latitude behaves as expected. The eccentricity is small and grows slightly over a 24-hour period, but the behavior is cyclical and oscillates around the original value over time. Figure 6-3 clearly shows that the maneuvering spacecraft is much further ahead in time than the reference. It also shows that the maneuvering spacecraft has a small offset from the reference ground track. This offset is caused by the spacecraft's velocity changes throughout the maneuver. The changing velocity causes the orbital altitude to shrink temporarily, thus shifting ground track.

The final Mayer cost for this solution is 81,655 seconds. The ΔV is 0.082 km/s with a Δt of 11 minutes. By selecting a target almost a full 24 hours ahead in time, the Δt is on the order of minutes which yields the separation between spacecraft depicted in Figure 6-3.

6.4.2 Scenario 2 – In-plane, Unrestricted Maneuver.

In Scenario 2, the phasing maneuver constraint is removed to allow the spacecraft to end at an arbitrary altitude. Scenario 1 is repeated with the altitude constraint removed to observe the change in Δt. Figure 6-4 shows the optimal solution, and Figure 6-5 shows the ground track of the reference spacecraft's final orbit and the ending positions of both the maneuvering and reference spacecraft. These plots show that in order to gain the maximum amount of Δt the spacecraft must thrust constantly in the anti-velocity direction (or velocity direction when raising the orbit). This result is intuitive and shows that control algorithm works properly for constrained and unconstrained orbital maneuvering.

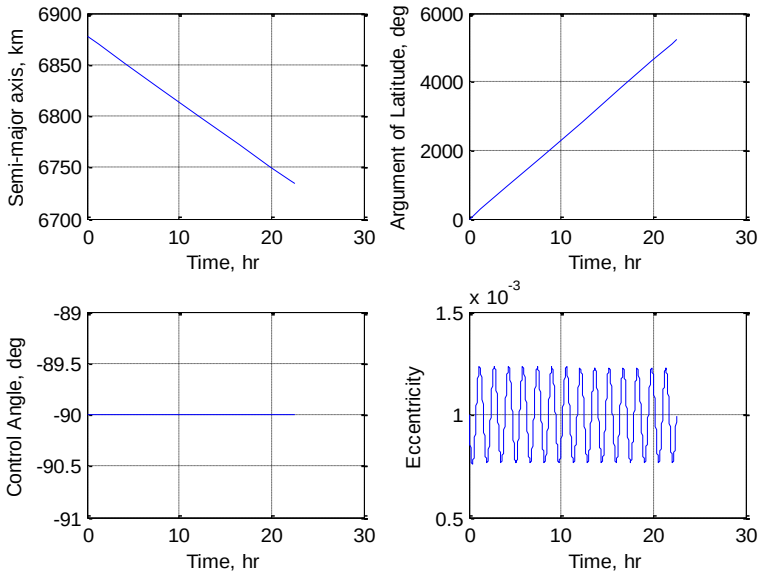

Figure 6-4. Control Inputs and States of Optimal Solution for Scenario 2.

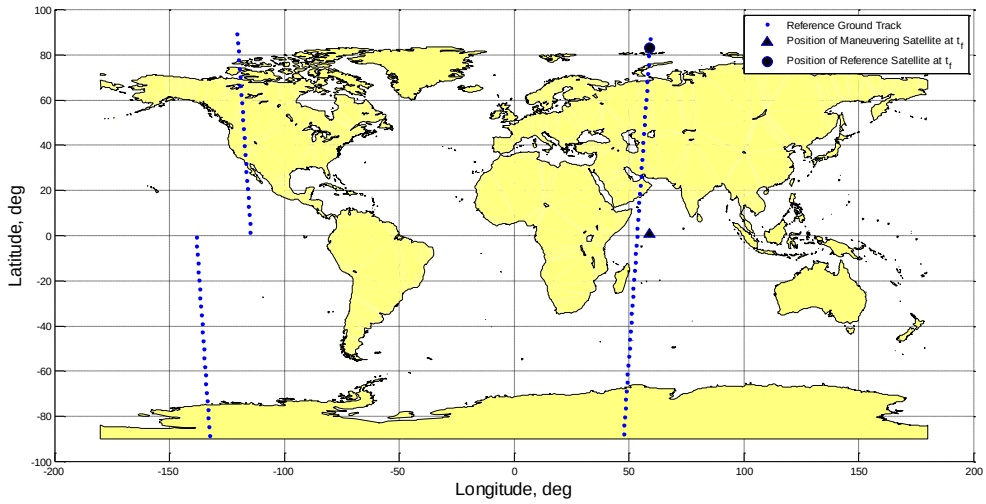

Figure 6-5. Ground Track and Target Location, Scenario 2

By removing the phasing maneuver constraint, the Δt is almost twice as large as the phasing maneuver with slightly less propellant consumed. The final Mayer cost for this solution is 81,011 seconds. The ΔV is 0.081 km/s with a Δt of 21.7 minutes. The two types of maneuvers presented in Scenarios 1-2 yield very different results, but the differences are logical and after some analysis become intuitive. Scenario 1 begins and

ends in the same orbit, only changing the overflight time. Scenario 2 is allowed to simply thrust continuously in the same direction to allow Δt to grow. The achievable Δt is larger due to removing the underlying requirement that the initial and final orbits are identical. This requirement necessitates that the spacecraft speeds up in one direction and at some point slows down to reverse the acceleration resulting in approximately half the achievable Δt. This is apparent in the S-shaped control angle profile in Figure 6-2.

The result from Scenario 2 can be used to validate the analytical expression for Δt shown in Equation (6.23). The desired value for the argument of latitude is 180 degrees within the 15th orbital period, which is equivalent to 29π radians. Plugging in $u=29\pi$ along with the initial conditions in Equation (6.23), the calculated Δt is 1302.3 seconds or 21.7 minutes. The calculated result matches the optimal result obtained through the optimal control algorithm.

6.4.3 Scenario 3 – Out-of-plane, Δi Maneuver

The third scenario presents an inclination change maneuver using the Lyapunov-based feedback control algorithm. The spacecraft starts on a circular, polar orbit with a = 6,878 km, $i = 90^{\circ}$, and $\Omega = u = 0^{\circ}$, and is commanded to decrease inclination over five orbital revolutions. It is again assumed that the spacecraft thrusts continuously throughout the maneuver. Figure 6-6 shows the resulting solution and Figure 6-7 shows the corresponding reference ground track along with the final positions of the reference and maneuvering spacecraft. The top left plot in Figure 6-6 shows that the semi-major axis of the orbit remains constant and the out-of-plane control angle flips between positive and negative 90° in order to build up inclination change. The bottom left plot shows the

decreasing inclination with a final value of 89.864°. The last plot shows the change in RAAN, which is cyclical in this case and does not experience any secular effects.

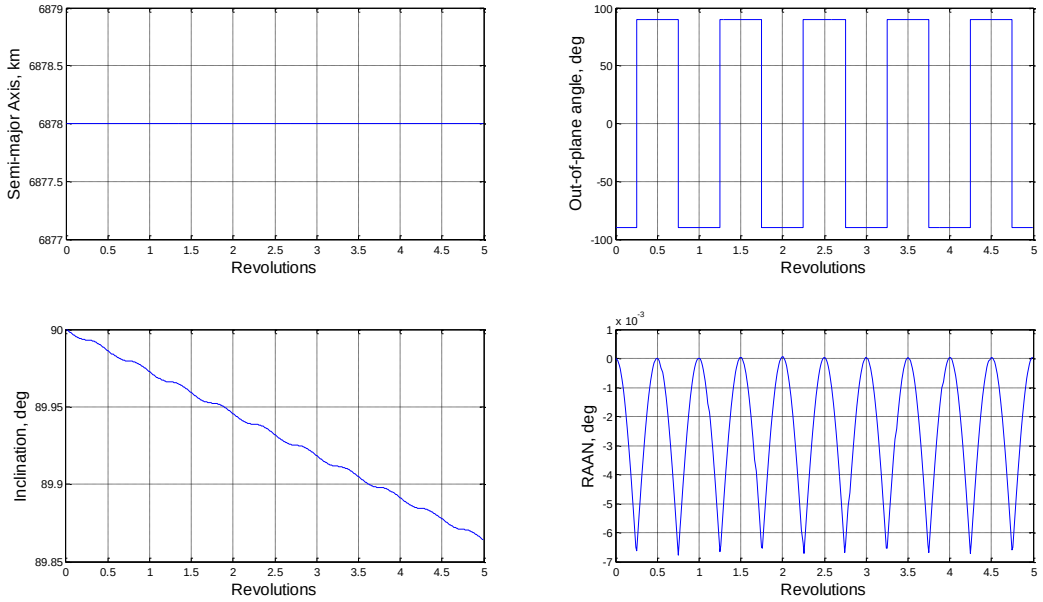

Figure 6-6. Control Angle and States, Scenario 3

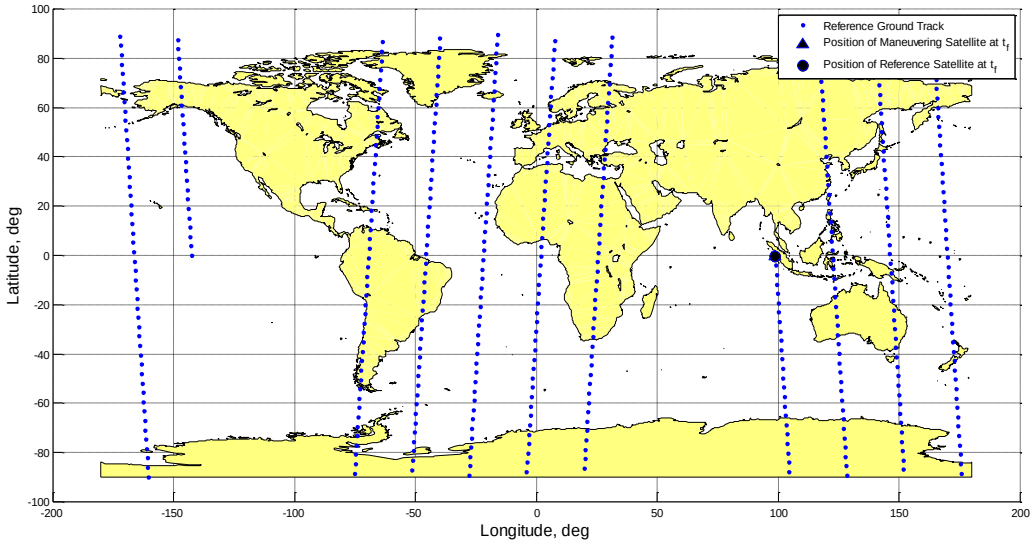

Figure 6-7. Ground Track and Final Positions, Scenario 3

The ground track in Figure 6-7 shows the two position markers on top of each other. Since the maneuver thrusts only out-of-plane, the orbit's mean motion does not change and therefore no Δt is created.

The result from Scenario 3 can be used to validate the analytical expression for Δi shown in Equation (6.24). Given the parameters of Scenario 3, the inputs for Equation (6.24) are computed as a = 6878 km, n = 0.001106783 rad/s, P = 5677 s, and $t_f = P/4$ = 1419 s. Inserting these values into the equation yields Δi = 0.0068 deg per quarter revolution or a Δi = 0.1360 deg for the whole maneuver. This value agrees with the inclination change calculated via the Lypunov feedback control algorithm, which is also depicted Figure 6-6.

6.4.4 Scenario 4 – Out-of-plane, $\Delta\Omega$ Maneuver.

The fourth scenario presents a RAAN change maneuver using the Lyapunov-based feedback control algorithm. The spacecraft starts on a circular, polar orbit with a = 6,878 km, $i = 90^o$, and $\Omega = u = 0^o$, and is commanded to increase RAAN over five orbital revolutions. Figure 6-8 shows the resulting solution and Figure 6-9 shows the corresponding reference ground track along with the final positions of the reference and maneuvering spacecraft. The top left plot in Figure 6-8 shows that the semi-major axis of the orbit remains constant. The top right plot shows that the out-of-plane control angle flips between positive and negative 90° in order to build up RAAN change. The bottom left plot shows the change in inclination, which is cyclical in this case and experiences no secular effects. The last plot shows the increasing RAAN with a final value of 0.136 degrees.

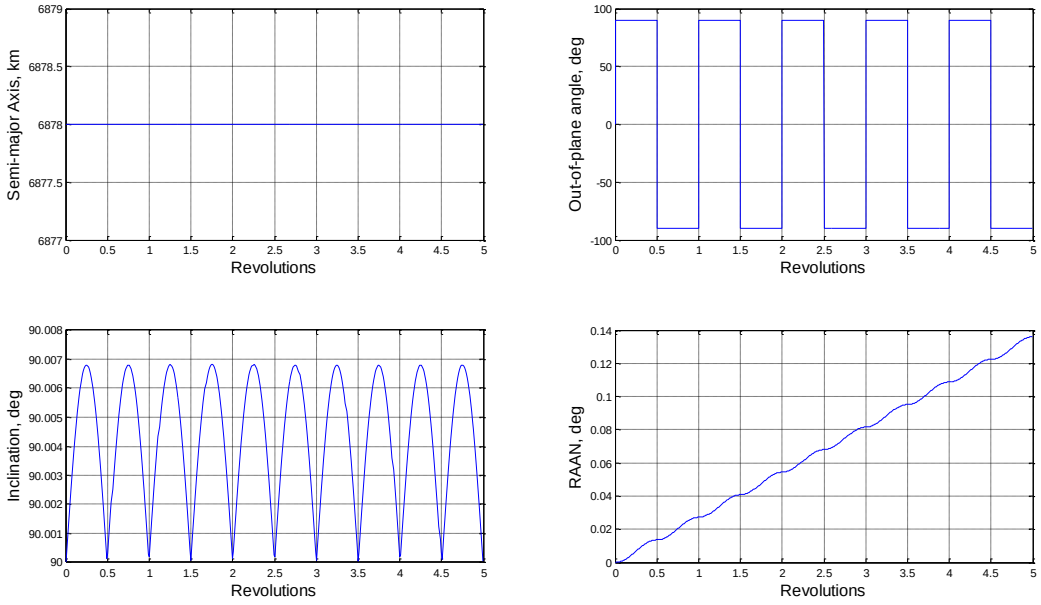

Figure 6-8. Control Angle and States, Scenario 4

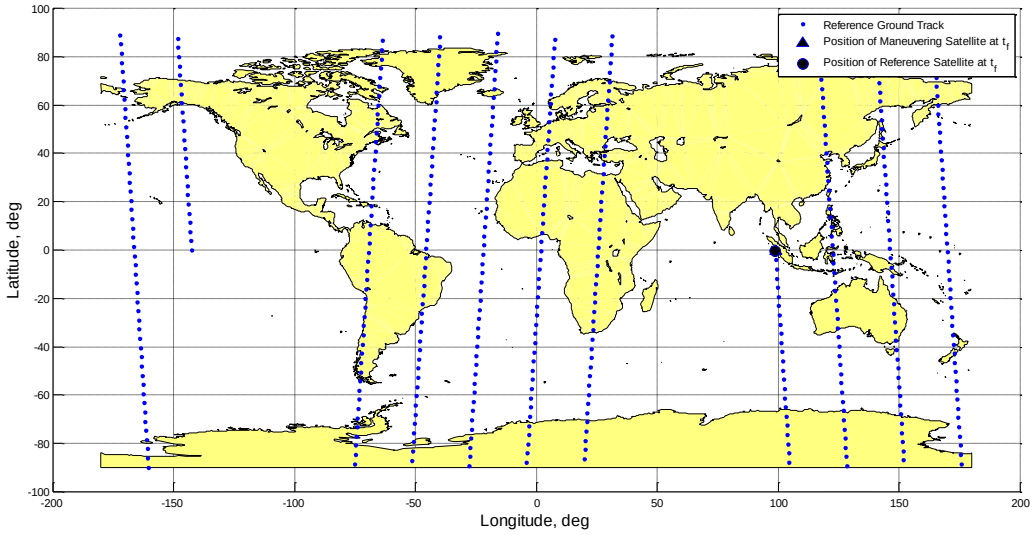

Figure 6-9. Ground Track and Final Positions, Scenario 4

The ground track in Figure 6-9 shows the two position markers on top of each other. As in Scenario 3, since the maneuver thrusts only out-of-plane the orbit's mean motion does not change and therefore no Δt is created.

The result from Scenario 4 can be use to validate the analytical expression for $\Delta\Omega$ shown in Equation (6.25). Given the parameters of Scenario 4, the inputs for Equation (6.25) are computed as a = 6878 km, n = 0.001106783 rad/s, P = 5677 s, and $t_f = P/2$ = 2838 s. Inserting these values into the equation yields $\Delta\Omega$ = 0.0136 deg per half revolution or a $\Delta\Omega$ = 0.1360 deg for the whole maneuver. This value agrees with the RAAN change calculated via the Lypunov feedback control algorithm, which is also depicted Figure 6-8.

6.4.5 Scenario 5 – Combination In-Plane and Out-of-plane Maneuver.

The fifth scenario is a combined semi-major axis and RAAN change maneuver to see the effect of out-of-plane maneuvering on Δt. The spacecraft starts on a circular, polar orbit with a = 6,878 km, i = 90º, and $\Omega = u$ = 0º. The Lyapunov-based feedback control algorithm is used to command a decrease in semi-major axis and an increase in RAAN. In order to maximize the amount of Δt achieved the controller is weighted more heavily toward decreasing the semi-major axis. Figure 6-10 shows the resulting solution and Figure 6-11 shows the corresponding reference ground track along with the final positions of the reference and maneuvering spacecraft. The top left plot in Figure 6-10 shows that the semi-major axis decreases to 6827.4 km. The top right plot shows that the out-of plane control angle flips between positive and negative 90°, but the transitions are slower than they are for Scenarios 3 and 4 causing a simultaneous decrease in semi-major

axis. The bottom left plot shows that the change in inclination is cyclical and the bottom right plot shows the increasing RAAN reaching a final value of 0.0198 degrees. The Δt achieved in this scenario is 153 seconds or 2.55 minutes. The final value of argument of latitude is 31.585 radians meaning that the maximum Δt based on Equation (6.23), with only in-plane thrusting, is 159 seconds. Therefore, by requiring an increase in RAAN the achievable Δt decreased by 6 seconds with a very small, but detectable RAAN change.

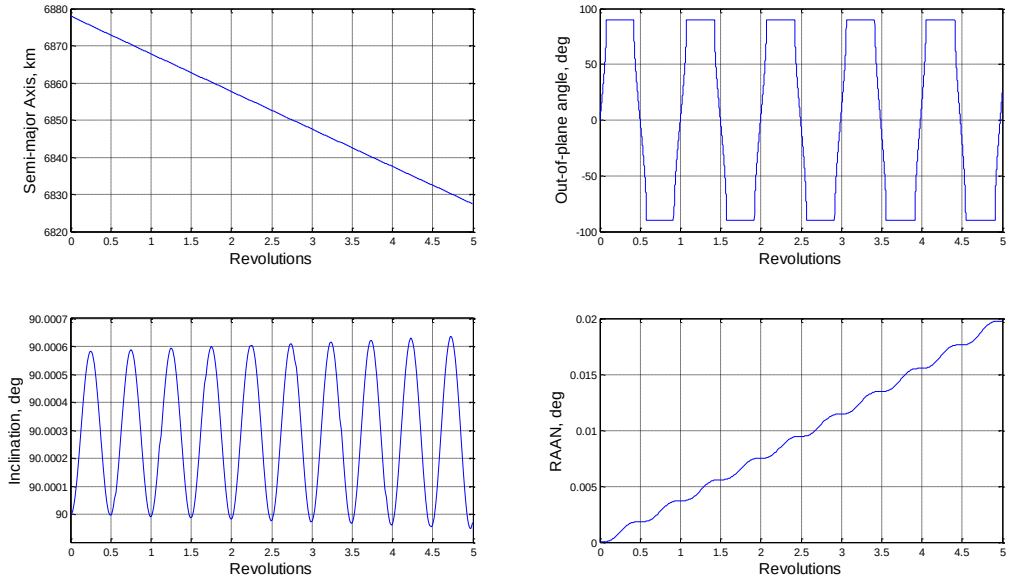

Figure 6-10. Control Angle and States, Scenario 5

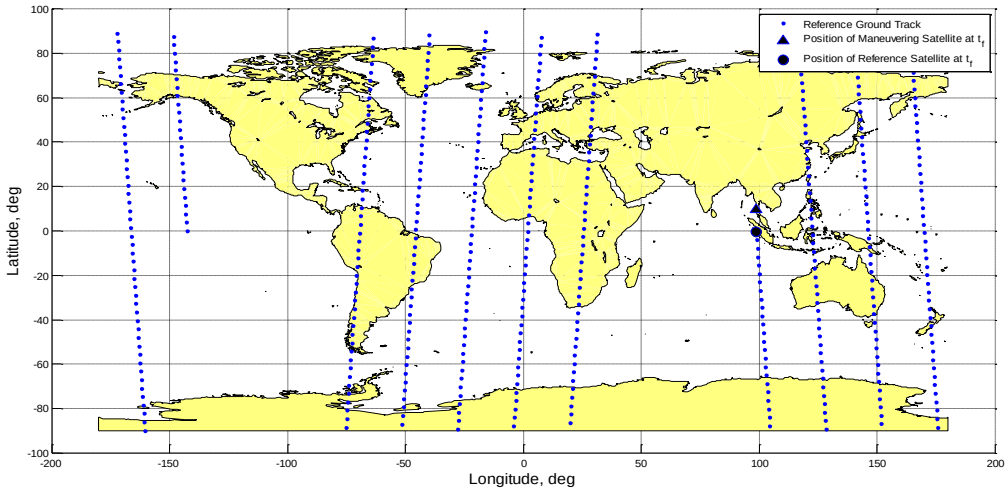

Figure 6-11. Ground Track and Final Positions, Scenario 5

`

The ground track in Figure 6-11 clearly shows the separation between the two spacecraft at the end of the maneuver, but the change in RAAN is too small to visually detect.

6.4.6 Thrust-Coast Maneuver.

To achieve simultaneous spacecraft position and terrestrial target location at the same time for over-flight requires careful consideration of timing, thus most maneuvers will not allow for a simple turn on-thrust-turn off maneuver, but requires consideration for a coasting period. Amending Equation (6.23) with a coast period can result in large propellant savings. Given a desired Δt and the amount of time available to achieve it, the new equation is used to determine the length of a thrust period and that of the subsequent coast period:

$$\Delta t = (u_2 - u_0)\sqrt{\frac{a_0^3}{\mu}} - \frac{\sqrt{\mu}}{A}\left[\left(\frac{1}{a_0^2} + \frac{4}{\mu}A(u_1 - u_0)\right)^{1/4} - a_0^{-1/2}\right] - (u_2 - u_1)\sqrt{\frac{a^3}{\mu}} \qquad (6.26)$$

Intuitively, a longer period of time available to achieve the target Δt results in the greater the propellant savings. However, Equation (6.26) shows that providing just twice the amount of time, three-quarters of propellant can be saved. Thus, thrusting upfront is always desirable to take advantage of the longest amount of coasting.

The following table summarizes the resultant propellant savings of a thrust-coast maneuver for an initial a = 7378 km compared to thrusting alone. Without the requirement of coinciding with specific terrestrial targets, thrusting continuously for one orbital period (see Table 6-1, row 1) yields a Δt of 8.1 s and a ΔV expenditure of 6.3 m/s.

Table 6-1. Comparison of Thrust-only and Thrust-Coast Maneuvers

Thrust-only Maneuver				Thrust-Coast Maneuver			
# of Revs	**Final *a* (km)**	**Thrust time (h)**	***Δt***	**Final *a* (km)**	**Time available (h)**	**Thrust time (h)**	**ΔV savings**
1	7365.4	1.75	8.1 s	7374.6	3.50	0.47	73 %
5	7315.5	8.82	3.3 min	7361.3	17.64	2.31	74 %
10	7254.6	17.75	13.3 min	7345.6	35.50	4.50	75 %
20	7137.1	35.98	52.0 min	7315.5	71.99	8.70	76 %

This maneuver represents the greatest Δt attainable with the propulsion system in the given amount of time. For the thrust-coast maneuver, the amount of available time is doubled while keeping Δt constant at 8.1 s, such that the thrusting period is greatly reduced from 1.75 hours to 0.47 hours and therefore results in significant propellant savings. Provided with 3.5 hours total maneuver time, the ΔV expenditure reduces to 1.7 m/s or a propellant savings of 73.1%. The remaining rows of Table 6-1 show the same calculations using Equation (6.26) for 5, 10, and 20 orbital periods with propellant savings between 73 and 76%.

6.5 Conclusion

Analytical expressions for the performance metrics Δt, Δi, and $\Delta\Omega$ are derived and presented. Previously developed algorithms are used to analyze five test scenarios and validate the results of the analytical expressions. With the derived expressions available, mission planners can quickly evaluate maneuvering effects and conduct trade studies to decide on a best course of action depending on the spacecraft's mission.

With a very small applied acceleration, it takes a long time to create a large enough change in the spacecraft's orbit. These maneuvers will be most effective when the spacecraft has a sufficiently long lead time on the target and is allowed to maneuver for a longer period of time resulting in a larger Δt. Any appreciable amount of ground-track change requires multiple orbits at the given magnitude of acceleration. By removing the constraint on the final altitude, the resulting Δt is almost twice as large. Removing the constraint also allows for a simple analytic solution describing the behavior of Δt with respect to different values of argument of latitude. As shown with the phasing maneuver, the larger the value of the final argument of latitude the larger the Δt achieved since the duration of the maneuver is longer.

Out-of-plane maneuvers are treated to show analytical solutions that are applicable without the use of cumbersome simulations or time consuming calculations. The derived equations quickly and accurately predict the amount of change in inclination and RAAN possible when provided with a level of thrust and vehicle characteristics. Out-of-plane thrusting does not result in Δt but can be useful to expand the spacecraft's coverage area, adjust the orbit for desirable natural characteristics such as sun-synchronous inclinations, or affect target arrival time. One of the five scenarios combines an in-plane with an out-of-plane maneuver to show changes in semi-major axis and the orbital plane can be achieved simultaneously in a deterministic manner.

Finally, if enough time is available, a thrust-coast combination should always be used for a Δt-maneuver for significant propellant savings. The maneuver should comprise of a thrust period up-front to achieve a final altitude and then take advantage of coasting to achieve the same Δt with significant propellant savings when compared to thrusting

alone. In all examined cases, given twice the amount of time, propellant savings of approximately 75 percent are realized.

7 Responsiveness in Low Orbits using Electric Propulsion

One promising option for space operational responsiveness is orbital maneuvering. In low orbit, a maneuverable spacecraft can provide valuable benefits such as better coverage properties, increased revisit times, selectable targets, and local overflight times. Such maneuvers are not common due to the high cost of chemical propulsion. The more recent paradigm of Operationally Responsive Space is to rapidly launch a small, inexpensive asset and use it in a short, disposable fashion. This concept relies on drastically reducing the cost of launch, yet it remains the most expensive piece, so additional cost savings can be realized by minimizing the need for launches. Electric propulsion has been considered as an efficient alternative to chemical propulsion. With technological advances, electric propulsion can provide responsiveness in a timely, propellant-efficient manner without requiring repeated launches to satisfy multiple missions. This study shows the control algorithm for a single low-Earth satellite equipped with the proper electric propulsion to overfly any target inside its coverage area in as little as 34 hours for 1.8 percent of its propellant budget. A comprehensive survey to quantify global reach requirements is provided and the optimal time and propellant solutions are explored. The results strongly support that electric propulsion could be a key enabler in responsive operations.

Nomenclature

A = perturbing acceleration magnitude, km/s^2

a = semi-major axis, km

a_h = normal acceleration component with respect to orbital plane, km/s^2

a_r = radial acceleration component in local-vertical, local-horizontal frame, km/s^2

a_θ = acceleration comp completing the right-handed coordinate system, km/s^2

e = eccentricity

h = angular momentum

$\hat{h}$ = normal comp wrt orbital plane of the local-vertical, local-horizontal frame

i = inclination, degrees

M = mean anomaly, rad

m_0 = initial spacecraft mass, kg

$\dot{m}$ = mass flow rate, kg/s

Δm = change in mass due to maneuvering, kg

n = mean motion, rad/s

p = semi-latus rectum, km

$\boldsymbol{r}$ = radius vector, components in km

r = magnitude of radius vector, km

$\hat{r}$ = radial component of the local-vertical, local-horizontal frame

T = thrust magnitude, N

t = time, s

t_0 = initial time, s

t_f = final time, s

Δt = change in over-flight time, s

u = argument of latitude, degrees

$\boldsymbol{V}$ = velocity vector, components in km/s

ΔV = velocity change, km/s

$\boldsymbol{x}$ = state vector in terms of Classical Orbital Elements

$\boldsymbol{x_0}$ = initial state vector in Classical Orbital Elements

γ = angle between Earth-Centered Inertial (ECI) and ECF frames, rad

γ_g = Greenwich sidereal time, rad

θ = out-of-plane thrust angle wrt $\hat{r}$-$\hat{\theta}$ plane, degrees

$\hat{\theta}$ = tangential component of the local-vertical, local-horizontal frame

λ = latitude, degrees

$\mu_\oplus$ = Earth's gravitational parameter, 3.98601 x10^5 km^3/s^2

ν = true anomaly, rad

φ = longitude, degrees

$\boldsymbol{\psi}$ = thrust control vector, components in degrees

ψ = thrust angle in $\hat{r}$-$\hat{\theta}$ plane, degrees

Ω = right ascension of the ascending node, degrees

ω = argument of perigee, degrees

$\omega_\oplus$ = Earth's angular velocity magnitude, rad/s

7.1 Introduction

Some of the main challenges of low-Earth satellites and electric propulsion (EP) are providing the desired coverage and the amount of time needed to achieve significant effects due to maneuvering (Wertz, 2007: 4; Larrimore, 2007: 2; Walker, 1977). Low-Earth satellites have much smaller swath widths and are traveling at higher velocities compared to those at greater altitudes therefore the coverage area is smaller and time is shorter compared to higher altitude orbits (Elachi, 1987: 393-404). Secondly, electric propulsion has very low thrust resulting in long periods of time to accumulate the effect. Furthermore, low altitudes also bring about "undesirable" perturbing forces such as higher atmospheric drag and larger effects due to the potential of the Earth's gravity field. Conversely, low altitudes allow for smaller optical payloads, better resolution, smaller spacecraft, less expensive overall systems, and, for the purpose of maneuvering, more opportunities to overfly a specific ground target.

Propulsive maneuvers have been used to maintain or to change a spacecraft's orbit, but due to the cost of conventional chemical propulsion, such maneuvers are rare. Maneuvers are often done only at the beginning or the end of a mission, because the benefits of maneuvering are not sufficient to justify the propellant cost. As a result, certain classes of orbits have become very popular and sometimes extremely congested. The orbits are geosynchronous for the hovering effect, sun-synchronous for the lighting effect, Molniya for the coverage effect, and repeating-ground-track (RGT) for the revisit effect. However, if the cost of maneuvering can be reduced for a small spacecraft such that it would be able to perform 40-50 orbital maneuvers during its mission life, then it

could be cost effective to re-task a satellite for a new application. Specifically, this paper focuses on changing the ground track of low-Earth orbit (LEO) satellites to directly overfly any desired targets within its coverage area (latitudinal coverage based on inclination).

A few researchers have explored the possible uses of EP for maneuvering. Newberry postulates that a typical operational satellite that continuously thrusts with an EP engine over a seven-day period can sufficiently change its orbit to produce a 24-hour time-over-target (TOT) change (Newberry, 2005: 48). In other words, given seven days the satellite changes its ground track so that it can overfly a desired target up 24 hours earlier or later. This maneuverability can only be achieved provided the spacecraft is in a highly-inclined, elliptical, and closed orbit, and visiting the same area twice a day (i.e. 24 hours divided by an odd integer).

Guelman and Kogan consider minimum propellant flight profiles for low altitude, circular orbits to overfly a specific number of terrestrial targets in a given time period (Guelman, 1999: 313-321). Their analysis indicates that the application of EP to overfly desired targets is practical. In their simulations, they demonstrate the overflight of 20 randomly selected sites over a period of 50 days and the associated propellant usage would allow a spacecraft with a modest initial propellant-mass-ratio ($m_{\text{propellant}}/m_{\text{total}} = 1/20$) to operate as long as 3 years. Using a Monte Carlo simulation, they quantify propellant consumption as a function of number of sites and available period. Doubling the number of overfly sites from 20 to 40 and keeping the period at 50 days increases propellant consumption by a factor of 60, whereas doubling the period from 50 to 100 days for 20 sites decreases propellant usage by a factor of 300. The take-away is that EP

can be effectively used to drastically reduce the revisit time of desired terrestrial targets for low orbit altitudes when compared to not maneuvering.

Jean and de Lafontaine further the research by adding atmospheric drag and geopotential effects up to J_2 to the previous models and introducing a new quartic guidance law to the cubic guidance used by Guelman (Jean, 2003: 1829-1844). They start in a sun-synchronous reference orbit and aim to always return to the reference after maneuvering. In essence it is a phasing maneuver that starts at a sun-synchronous altitude, then the satellite thrusts in one direction to gain or lose altitude, and finally returns to the reference altitude by thrusting in the opposite direction. The position difference between the phasing satellite and a non-maneuvering reference satellite results in the shift of ground track (overflight time and position). Co *et al.* explore optimal thrust profiles of such in-plane maneuvers and characterize the possible changes in ground track these can achieve given today's EP thrust levels as a function of available time (Co, 2011b). Jean and de Lafontaine also conclude that EP is practical in both maintaining a reference orbit by countering atmospheric drag and modifying the reference orbit to overfly a terrestrial target. Their end product is an autonomous algorithm that could be implemented on a spacecraft to take advantage of this technology.

The primary purpose of this paper is to present a method for accurately predicting in-plane maneuvers using EP and a general algorithm to change the ground track over a desired terrestrial target compared to a non-maneuvering reference. Once simplified, the equations of motion reduce to a few expressions with which the exact local time, propellant consumption, and time required for overflight can be computed. The complexity lies with the fact that the target is not stationary and the solutions change with

the initial state of the satellite, the specific date (location of the target in relation to the orbital plane), and the amount of time available. With only 24 hours available to reach a ground target, there may be only one solution. Increasing it to 48 hours may provide five. Knowledge of conventional impulsive maneuvers does not apply to EP. The highest propellant solution does not guarantee the shortest amount of time to reach the target. Further, the optimal time solution is not the same as the optimal propellant solution and both may change significantly given the available time. Similar to the findings of Guelman, provided with more time to achieve a desired overflight not only decreases the propellant consumption significantly, it also provides more opportunities to overfly the target hence a satellite can be overhead at more than one local time chosen by the user.

It is important to quantify the minimum amount of time required to achieve global reach (worst case scenario to overfly any desired point within the inclination band) for the available thrust level and initial orbit. The first part of the paper only considers in-plane maneuvering (orbital period) as the most effective and propellant-efficient way to change ground track. With this general information, a spacecraft can be sized for a given thruster and desired responsiveness; the algorithm will only need to be run for a specific period of time to guarantee a solution instead of an arbitrary period; and certain altitudes may be desired to coincide with target over-flight to ensure a repeated ground track or sun-synchronous orbit. Atmospheric drag and Earth's gravity field can be used to preposition a spacecraft prior to a maneuver through altitude control or to take advantage of desirable characteristics such as nodal regression.

Out-of-plane thrusting is another class of maneuvers that can affect ground track. This paper briefly examines the required out-of-plane burn sequence to achieve right

ascension of the ascending node (RAAN) and/or inclination change while keeping orbital altitude constant. As with chemical maneuvers, out-of-plane changes are very propellant-intensive and require a long period of time to accumulate for EP, but can be used to fine tune the orbit to affect time of arrival. Provided with a desired target and the available time to reach it, a combination of in-plane and out-of-plane thruster firings could simultaneously change altitude, RAAN, and/or inclination to cause an overflight. The possible effects of RAAN and inclination change are discussed and quantified.

7.2 System Model

The equations of motion for a spacecraft under a constant, low thrust can be simply written from Newton's second law. Low thrust EP maneuvers result in small accelerations that perturb the orbit of the spacecraft. Gauss' form of the Lagrange Planetary Equations models the change over time in the Classical Orbital Elements (COEs - a, e, i, Ω, ω, ν) (Schaub, 2003: 522):

$$\frac{da}{dt} = \frac{2a^2}{h}\left(e\sin\nu a_r + \frac{p}{r}a_\theta \right) \tag{7.1}$$

$$\frac{de}{dt} = \frac{1}{h}\left(p\sin\nu a_r + \left((p+r)\cos\nu + re\right)a_\theta \right) \tag{7.2}$$

$$\frac{di}{dt} = \frac{r\cos(\omega+\nu)}{h}a_h \tag{7.3}$$

$$\frac{d\Omega}{dt} = \frac{r\sin(\omega+\nu)}{h\sin i}a_h \tag{7.4}$$

$$\frac{d\omega}{dt} = \frac{1}{he}\left(-p\cos\nu a_r + (p+r)\sin\nu a_\theta\right) - \frac{r\sin(\omega+\nu)\cos i}{h\sin i}a_h \tag{7.5}$$

$$\frac{d\nu}{dt} = \frac{h}{r^2} + \frac{1}{he}\left(-p\cos\nu a_r + (p+r)\sin\nu a_\theta\right) \tag{7.6}$$

To keep the formulation general for inclusion of in-plane and out-of-plane maneuvers, the disturbance acceleration vector can be written as a function of an acceleration magnitude and two control angles, ψ and θ, which define the direction of the vector. In the Local-Vertical-Local-Horizontal (LVLH) frame, the angle ψ is measured from the $\hat{r}$ unit vector and lies on the $\hat{r}$-$\hat{\theta}$ plane, and θ measures the angle between the acceleration vector and the $\hat{r}$-$\hat{\theta}$ plane. The acceleration magnitude of the vehicle and each component of the acceleration vector are:

$$A = \frac{T}{m_0 + \dot{m}t} \tag{7.7}$$

$$a_r = A\cos\theta\cos\psi \tag{7.8}$$

$$a_\theta = A\cos\theta\sin\psi \tag{7.9}$$

$$a_h = A\sin\theta \tag{7.10}$$

Assuming that $\Delta m << m_0$ (for EP) the acceleration magnitude is a constant. Furthermore, if it is assumed that the initial orbit is circular. The majority of this study focuses on in-plane maneuvers where the out-of-plane thrust is zero ($\theta=0$) Equations (7.1)-(7.6) then reduce to two equations. For this part of the derivation, the two-body equations are sufficient since both the maneuvering and reference orbits are initially subjected to the same natural perturbations. Co *et al.* provide reasoning for the suitability of the use of

these simplified equations for this problem setup (Co, 2011b: 12-13). Perturbations of atmospheric drag and gravity field forces up to J_{50} are added in the global coverage analysis of this paper. To avoid the singularity, the rate of change of the true anomaly or argument of latitude, u, is replaced by the mean motion:

$$\frac{da}{dt} = \frac{2}{\sqrt{\mu_{\oplus}}} a^{3/2} A \sin\psi \tag{7.11}$$

$$\frac{d\nu}{dt} = \frac{du}{dt} = \sqrt{\frac{\mu_{\oplus}}{a^3}} \tag{7.12}$$

The initial semi-major axis, a_0, is known from the initial spacecraft state. The initial argument of latitude, u_0, is also known and can be assumed to be zero. The final true argument of latitude, u_f, is determined by the amount of time available to reach the target location.

The next step is to derive an analytical expression for the amount of change in over-flight time with respect to the reference orbit, Δt, attained for a given u_f. Inserting the optimal control angle, ψ = -90º, into Equation (7.11) gives:

$$\frac{da}{dt} = -\frac{2}{\sqrt{\mu}} a^{3/2} A \tag{7.13}$$

Separating variables allows for integration and solution for the maneuver duration:

$$t - t_0 = \frac{\sqrt{\mu}}{A}\left(a^{-1/2} - a_0^{-1/2}\right) \tag{7.14}$$

where *a* represents the final semi-major axis reached at the end of the maneuver. Equation (7.12) can then be used to change the independent variable of integration from time to argument of latitude:

$$\frac{da}{du} = -\frac{2}{\mu} a^3 A \tag{7.15}$$

Separating variables again allows for integration and solution for the final semi-major axis:

$$a = \left(\frac{1}{a_0^2} + \frac{4}{\mu} A(u - u_0) \right)^{-1/2} \tag{7.16}$$

where *u* represents the desired final argument of latitude. The solution for the final semi-major axis can then be used in Equation (7.14) and Δt can be calculated by:

$$\Delta t = (u - u_0) \sqrt{\frac{a_0^3}{\mu}} - \frac{\sqrt{\mu}}{A} \left[\left(\frac{1}{a_0^2} + \frac{4}{\mu} A(u - u_0) \right)^{1/4} - a_0^{-1/2} \right] \tag{7.17}$$

Equation (7.17) shows that Δt is a function of the desired true anomaly, acceleration, and initial semi-major axis. Therefore for any given circular orbit the larger the value of Δu, the larger the Δt will be.

Amending Equation (7.17) with a coast period provides the equation required to determine the amount of time needed for target over-flight given the initial satellite state, target location, and available thrust. The target location and initial state together provide the required Δt, the on-board propulsion provides the available *A*, so the solution of

Equation (7.18) is u_2 or equivalently the amount of time required for overflight. This equation is the critical piece to solving the target overflight problem using EP:

$$\Delta t = (u_2 - u_0)\sqrt{\frac{a_0^3}{\mu}} - \frac{\sqrt{\mu}}{A}\left[\left(\frac{1}{a_0^2} + \frac{4}{\mu}A(u_1 - u_0)\right)^{1/4} - a_0^{-1/2}\right] - (u_2 - u_1)\sqrt{\frac{a^3}{\mu}} \qquad (7.18)$$

7.3 Control Algorithm

With Equation (7.18) the remaining problem is to create an opportunity for the satellite ground track to intersect the target coordinates. To do so, the reference orbit is propagated forward using Keplerian motion amended with drag and geopotential perturbations. Within the propagation period, there will be multiple opportunities where the ground track is 'close' to the target, all of which are possible solutions to the problem. After taking into account the available thrust, the solution set is reduced by those close encounters that are not reachable within the required time of overflight. The closest encounter that is reachable by the continuously thrusting propulsion system is the minimum propellant solution. The soonest encounter that is reachable is the minimum time solution. This process is displayed as a flowchart in Figure 7-1.

At the beginning of the algorithm, the satellite state, time, and location of the Prime Meridian are arbitrary. A non-maneuvering initial satellite state is propagated forward in time using a high precision orbital model for approximately three days. This propagation time period depends on the altitude and thrust level of the spacecraft and normally does not need to exceed the global reach time to overflight. By definition this time to

overflight guarantees that any target will come within reach. The propagated data is sorted in ascending order by distance to target, such that the shortest distance is the first data point. All entries which are not solutions are eliminated. Assuming the remaining potential encounters are reachable with the available thrust, the data is sorted in ascending order by available time, such that the feasible solution with the shortest available time is now listed on top. From here the solution for minimum time or minimum propellant use is attainable.

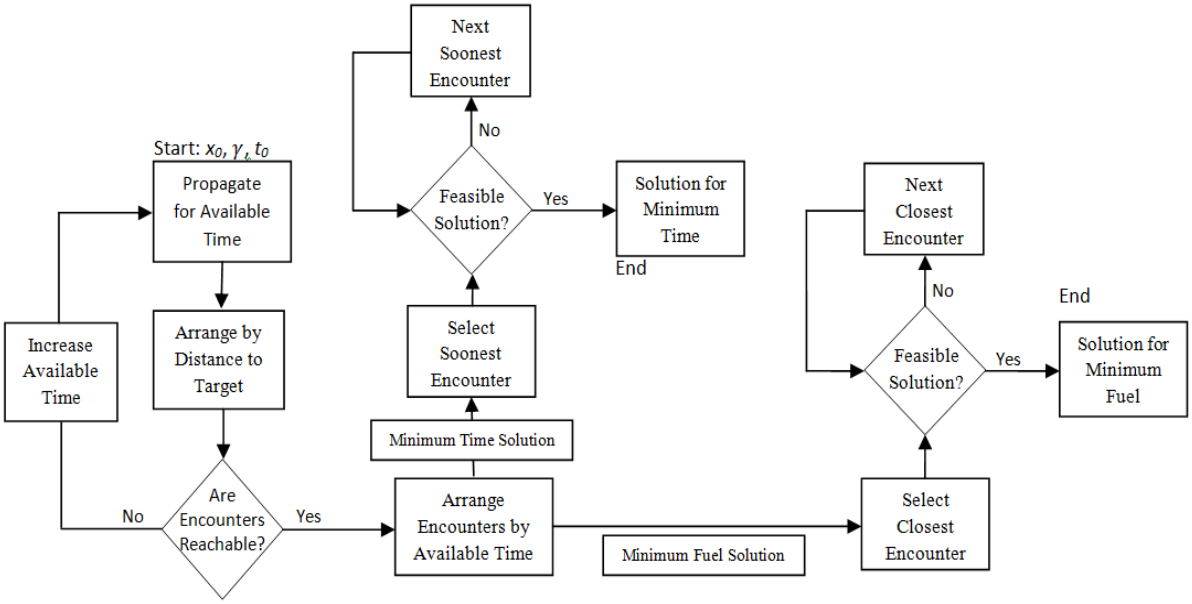

Figure 7-1. Flowchart to solve for Ground Target Overflight

The algorithm is best demonstrated by an example. Given a circular reference orbit at 500 kilometers, an arbitrary start date, a ground target, and a satellite with an EP system capable to providing an acceleration of 1 mm/s^2, the orbit is propagated forward for three days. Inside that period, there are 12 distinct solutions to affect an overflight. The minimum time solution occurs when the longitudinal separation between the

reference ground track and the target is 3.65 degrees with the target to the west. In other words, the orbital period must be adjusted such that the satellite will arrive earlier by Δt governed by the rotation rate of the Earth:

$$\Delta\varphi = \Delta t \cdot \omega_{\oplus} \tag{7.19}$$

If the orbit is posigrade and $\Delta t < 0$, the target lies to the west of the ground track and to the east for $\Delta t > 0$. The opposite is true for the retrograde orbit. Using Equation (7.19) to find the required Δt which is then used in Equation (7.18) to compute the total time period required comprised of a thrusting and drifting portion. The minimum time solution for this example occurs 22.25 hours after the initial time when the target is directly overflown using 70 m/s of ΔV. Following a similar process, the minimum propellant solution requires 69.4 hours (2.9 days) expending 11 m/s of ΔV. Figure 7-2 shows a generic depiction of shifting ground track by controlling Δt.

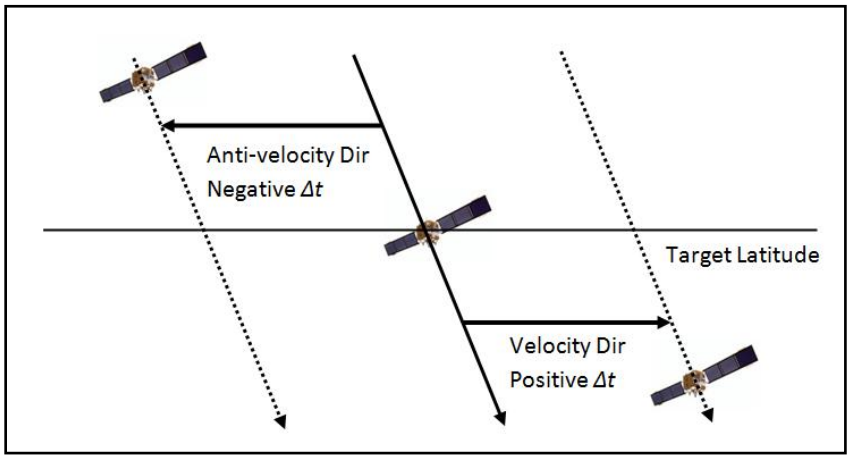

Figure 7-2. Control of Δt to Shift Ground Track

7.4 Global Reach

This section focuses on quantifying a measure for global reach. It is defined as the minimum amount of time required to guarantee that any terrestrial target within the service area can be overflown given an available thrust level and altitude. This is where the Earth gravity potential plays a significant role. The most significant effects come from zonal harmonics that describe the Earth's equatorial bulge, which most notably cause secular changes in Ω, ω, and M (Vallado, 2001: 602-610). The secular change in Ω due to zonal harmonics up to J_4 is:

$$\frac{d\Omega}{dt}_{\text{sec}} = -\frac{3J_2R_\oplus^2 n\cos(i)}{2p^2} + \frac{3J_2^2R_\oplus^4\cos(i)}{32p^4}\left(12-4e^2-(80+15e^2)\sin^2(i)\right) + \frac{15J_4R_\oplus^4\cos(i)}{32p^4}\left(8+12e^2-(14+21e^2)\sin^2(i)\right) \tag{7.20}$$

The magnitude of $\frac{d\Omega}{dt}_{\text{sec}}$ can be as large as nine degrees per day depending on inclination and altitude.

The geopotential effect combined with the change due to maneuvering using EP provides the required longitudinal shift of the ground track. The first effect always shifts ground track westward, whereas the second can move it in either direction. To reach the entire service area, the combined effect must cover the longitudinal separation between two subsequent passes in addition to adding one entire day to ensure that Earth's surface is completely covered. Figure 7-3 is a good visual aid. At the minimum time at which EP maneuvering can cover the separation between passes, that is 22-29° longitude, the

satellite could be on the first pass as depicted in Figure 7-3. However, the target is not close to the ground track at that time and requires two more passes to qualify as a close encounter. In this case, the minimum time to reach the target is prolonged by two orbital periods. Similarly, if the target is closest to the 15th pass, it would require an entire additional day to overfly the target. Hence adding one day is a conservative measure to ensure global reach. The likelihood that it would require this much time is low.

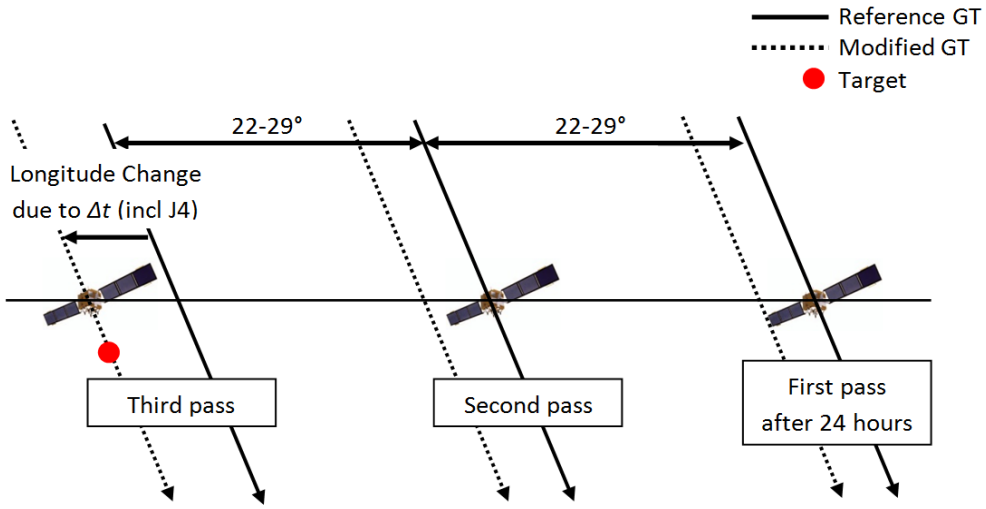

Figure 7-3. Target Overflight in a Subsequent Pass

Using this method, global reach can be computed for different altitudes and thrust levels. Figure 7-4 shows that the time required is not drastically different for various altitudes. The available thrust in this depiction is 1 mm/s^2, but provided there is more thrust, the time required for global reach is reduced and vice versa for lower thrust. However, the relationship is not linear hence the potential gains for increasing the level of thrust diminish after some point. The higher values in Figure 7-4 show the time required for global reach when only considering moving the ground track westward through maneuvering. The lower values take the ability to move the ground track in both

directions in account therefore reducing the time requirement across the board. The difference between the two lines is more pronounced for higher altitudes since the longitudinal separation between passes is greater compared to lower altitudes (29° versus 22°).

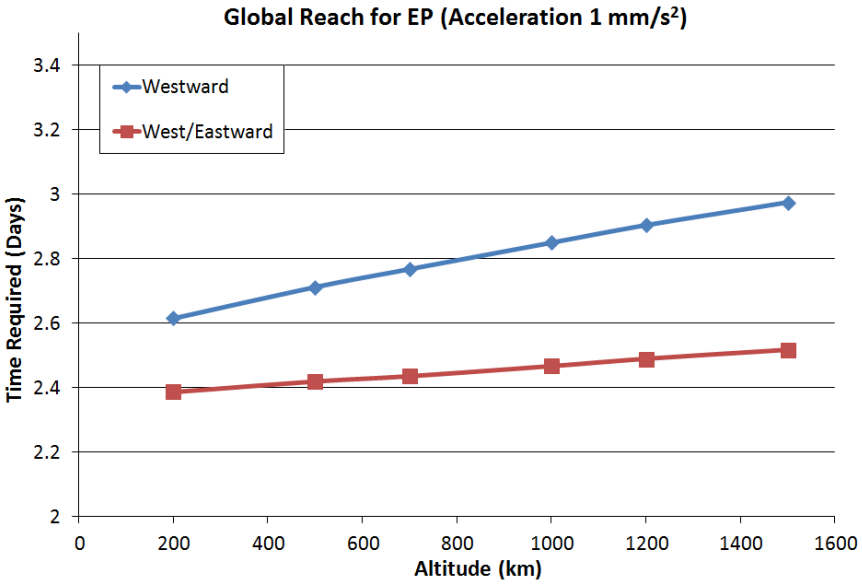

Figure 7-4. Global Reach for EP at Different Altitudes

7.5 Affecting Arrival Time

Selecting a specific arrival over a terrestrial target can be propellant-intensive and could require a long lead period using EP. One effective way to change the arrival time is to use the presented algorithm and allow a slightly longer lead time. If the available time is two days instead of one, the number of opportunities to affect an overflight increases significantly and hence more local overfly times are available. Figure 7-5 is a depiction of a scenario with one opportunity with one day of lead time and five opportunities when

the lead time is doubled. The increased number of opportunities is a result of more satellite passes and a larger control authority of the EP system given longer lead time.

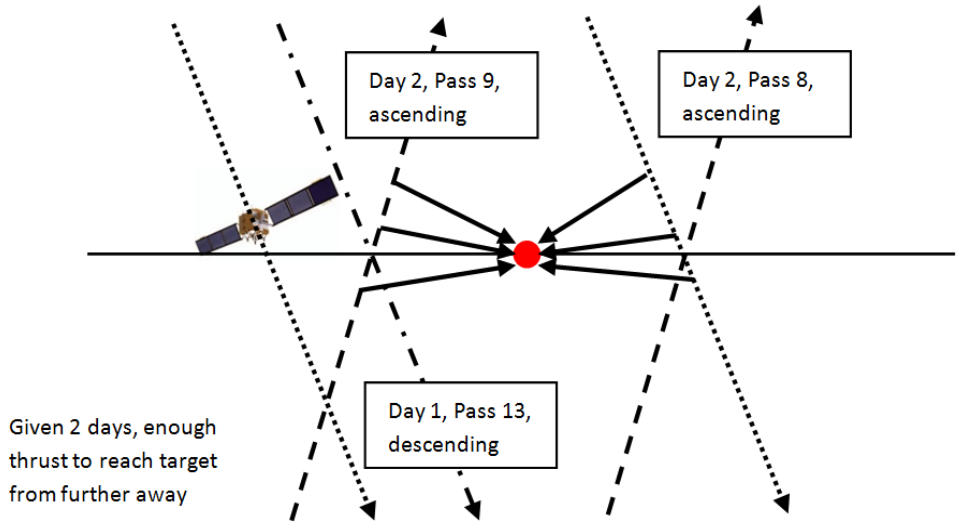

Figure 7-5. Arrival Times based on Opportunities

To demonstrate the arrival time concept, the example chosen is a satellite in a circular, 500-km orbit. The simulation is run for three days and using the algorithm of Figure 7-1, all close encounters are arranged first based on distance and then based on time to identify the rank order of potential overflights. Each overflight opportunity has a time range associated with it when the satellite enters and exits the window within which the propulsion system can reach the target. The initial date, satellite state, and target are arbitrarily chosen and not selected in any way to skew the results. Table 7-1 provides the results of the simulation. This example has twelve overflight opportunities in a 3-day timeframe. The window opens when the EP system has sufficient control authority to change the ground track by the required distance. Within the first day, there is only a

single opportunity. This number increases rapidly with the amount of available time; in two days there are five opportunities and in three days there are twelve. Although the time windows (left column) are spread out and often correspond to subsequent satellite passes, the actual overflight times are more bunched together. This is a result of timing satellite and ground target intercepts based on the Earth's rotation.

Table 7-1. Overflight Opportunities of a LEO Satellite in 3 Days

System Specifications		
Acceleration: 1 mm/s^2	*Start Date: 12/30/2011 17:00Z*	
Altitude: 500 km	*End Date: 01/02/2012 17:00Z*	
Target: Lat 30° Long 55°	*Initial Location: Lat 0° Long 7.194°*	
Opportunities		
Date & Time Window	*Distance*	*Overflight Time*
12/30/11 15:15	470 km	12/30/11 14:54 ± 15 sec
12/30/11 23:31-23:35	492-1147 km	12/30/11 23:59 ± 2.0 min
12/31/11 13:12-13:16	1298-1483 km	12/31/11 14:15 ± 2.5 min
12/31/11 14:50-14:58	404-1374 km	12/31/11 14:35 ± 4.5 min
12/31/11 16:34-16:38	1509-1790 km	12/31/11 15:09 ± 2.5 min
12/31/11 21:30-21:35	1458-2150 km	12/31/11 22:04 ± 3.0 min
12/31/11 23:08-23:21	521-2351 km	12/31/11 23:40 ± 7.0 min
01/01/12 00:47-01:01	1232-2406 km	12/31/11 23:59 ± 7.5 min
01/01/12 11:07-11:14	2820-3026 km	01/01/12 13:42 ± 4.0 min
01/01/12 12:44-13:01	1316-3100 km	01/01/12 13:56 ± 9.0 min
01/01/12 14:24-14:41	371-3144 km	01/01/12 14:15 ± 9.0 min
01/01/12 16:07-16:20	1495-3270 km	01/01/12 14:39 ± 7.0 min

7.6 Out-of-Plane Maneuvers

Traditionally out-of-plane maneuvers using chemical propulsion consume large amounts of propellant and there is no exception for EP systems. For a LEO satellite, the amount of change due to out-of-plane thrusting is approximately one-tenth of the change due to Earth's geopotential. The benefits of changing RAAN, inclination, or both are that a specific overflight time can be targeted and the maneuvers do not change the shape of

the orbit but only the orientation. If the same global reach concept is applied to RAAN change, the amount of time required to achieve it would be many times as long as in-plane maneuvers due to its limited control authority.

The analysis shows that certain regions of the orbit are more effective for out-of-plane thrusting than others. From Equation (7.4), the rate of change of RAAN can be integrated to compute the accumulated RAAN-change based on the amount of thrusting time. Assuming the acceleration vector is constant and t_0=0, Equation (7.4) becomes:

$$\Delta\Omega = \sqrt{\frac{a}{\mu}} \frac{A}{n \cdot \sin i} (1 - \cos(n t_f)) \tag{7.21}$$

The accumulated RAAN-change varies slightly as a result of altitude and is proportional to the amount of available acceleration. From Equation (7.4), it is clear that the largest amount of RAAN-change is achieved when the sine of the argument of latitude is unity, i.e. u = 90° and 270°. Furthermore, RAAN change can only be accumulated when the direction of the acceleration vector is switched at the nodes. In other words, to achieve pure RAAN change the acceleration vector should point 90° out of the orbital plane from the ascending to the descending node, then switch by 180° in the opposite direction from the descending to the ascending node. The same applies for inclination change, except rotated by 90°. Thus for pure inclination change, thrusting out-of-plane in one direction from ascending to descending nodes plus 90° and in the opposite direction to complete the orbit. A simultaneous change in both RAAN and inclination results when the acceleration direction is switched at any other point within the orbit.

Figure 7-6 shows the regions of maximum RAAN change due to out-of-plane thrusting where u = 90° and 270°. It is assumed that at the node, the argument of latitude is 0°. The effect on RAAN diminishes as u moves further away from these two regions. Figure 7-7 depicts the RAAN change as a function of thrusting time, where thrusting is centered on the two maximum regions. Increasing the thrusting time widens the region in which the satellite thrusts.

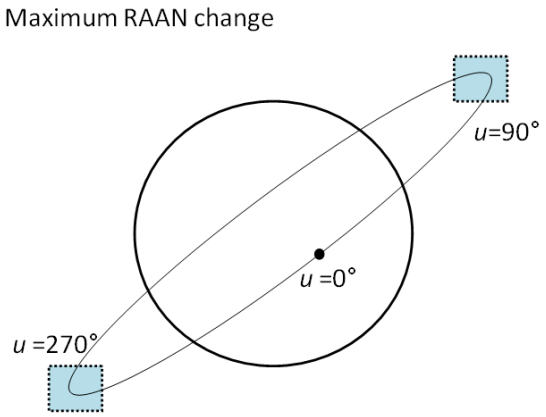

Figure 7-6. Regions of maximum RAAN Change from Out-of-plane Thrusting

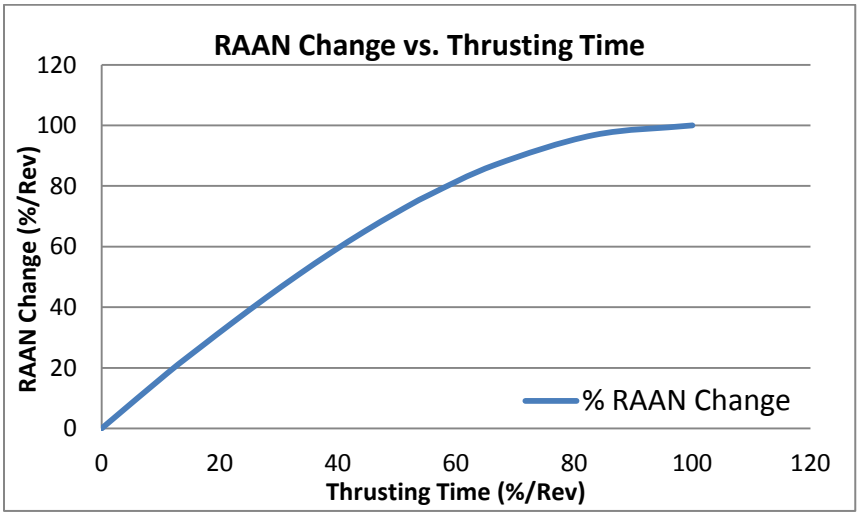

Figure 7-7. RAAN Change vs. Thrusting Time

Figure 7-7 shows that 50 percent of the RAAN change per revolution is accomplished by thrusting only 33 percent of orbital period. This effect diminishes rapidly when thrusting longer than half of the period. Should a combined in- and out-of-plane maneuver be considered, this information would be useful to determine what portion of the thrusting time to allocate each class of maneuver. For instance, if a combined altitude-RAAN change is desired, it may be beneficial to thrust purely out-of-plane for 40 percent of the orbit around the two maximum RAAN-change points, 20 percent at an angle of 45 degrees for a combined effect, and 40 percent purely in-plane.

7.7 Results and Discussion

The algorithm developed in this paper can be used to overfly any point on Earth regardless of the initial state, initial date, and available acceleration of the EP system. In most cases, any target on Earth can be reached within 1.5 days, but a worst case scenario is summarized in Figure 7-4 for different initial altitudes. When considering the full capability to move ground track East and Westward, in all cases, the terrestrial target can be overflown in less than 2.5 days as long as the acceleration is 1 mm/s^2 and the target is located within the satellite's coverage area. In some cases, the final altitude is drastically different after the maneuver and therefore the orbital characteristics are also different. Such a system would lend great flexibility to a user should a specific final altitude be desired, such that, for example, the orbit repeats its ground track daily. The key component of this algorithm is Equation (7.18).

7.7.1 Thrust-Coast Period.

Low thrust EP maneuvers can be accurately modeled and the effect for in-plane thrusting is governed by Equation (7.18). Much can be learnt from this equation such as the final altitude, length of thrust period, length of coast period, propellant consumption, and most importantly the change in time when a maneuvering satellite arrives at any given location within its orbit compared to a non-maneuvering reference. Intuitively, a longer period of time available to achieve the target Δt results in greater propellant savings. Furthermore, Equation (7.18) shows that providing just twice the amount of available time reduces propellant consumption by three-quarters. Table 7-2 summarizes the resultant propellant savings of a thrust-coast maneuver for an initial a = 7378 km compared to thrusting alone. The obvious conclusion is the longer the lead time, the better the propellant economy, but there is an embedded conclusion that thrusting upfront and allowing for the longest possible coast period results in a larger Δt.

Table 7-2. Comparison of Thrust-only and Thrust-Coast Maneuvers

Thrust-only Maneuver				**Thrust-Coast Maneuver**			
# of Revs	**Final *a* (km)**	**Thrust time (h)**	***Δt***	**Final *a* (km)**	**Time available (h)**	**Thrust time (h)**	**ΔV savings**
1	7365.4	1.75	8.1 sec	7374.6	3.50	0.47	73 %
5	7315.5	8.82	3.3 min	7361.3	17.64	2.31	74 %
10	7254.6	17.75	13.3 min	7345.6	35.50	4.50	75 %
20	7137.1	35.98	52.0 min	7315.5	71.99	8.70	76 %

7.7.2 Arrival Time.

Besides overflying a desired ground target, a user may find utility in a specific arrival time. In-plane thrusting alone cannot guarantee a specific time of arrival in a reasonable amount of time; to do so would require some out-of-plane maneuvers, namely RAAN change. Even then, it may be an unreasonable amount of time to achieve it with EP. Alternatively, in-plane maneuvers can provide multiple unique arrival time windows that may meet user requirements. The example summarized by Table 7-1 shows that the number of opportunities to arrive at a desired target increases rapidly as a function of available lead time. Given only one day, there is one opportunity, five in a two-day period, and twelve in three days. With enough lead-time, the EP system has enough control authority to reach any given target inside the coverage area from multiple close encounters; a number that continues to increase with available time.

A more costly option to affect target overflight is out-of-plane maneuvering. It is more costly because the amount of change in RAAN or inclination requires much more thrusting to accumulate any appreciable effect. Figure 7-8 summarizes the amount of daily change in RAAN (longitudinal) compared to the nodal regression due to J_2 and in-plane thrusting. At lower altitudes, out-of-plane maneuvers only account for 10 percent of the overall RAAN change per day. As the altitude increases and the J_2-effect decreases, the relative effect of such maneuvers increases to almost 20 percent. Nonetheless, the magnitude of this effect is small compared to the geopotential or the in-plane maneuvering effects. The main reason behind this phenomenon is that RAAN change is not secular, whereas altitude change propagates and grows the difference between the

maneuvering and reference cases over time. However small, out-of-plane EP maneuvers do have their place and utility to rotate the orbital plane and affect arrival time, but those are beyond the scope of this paper.

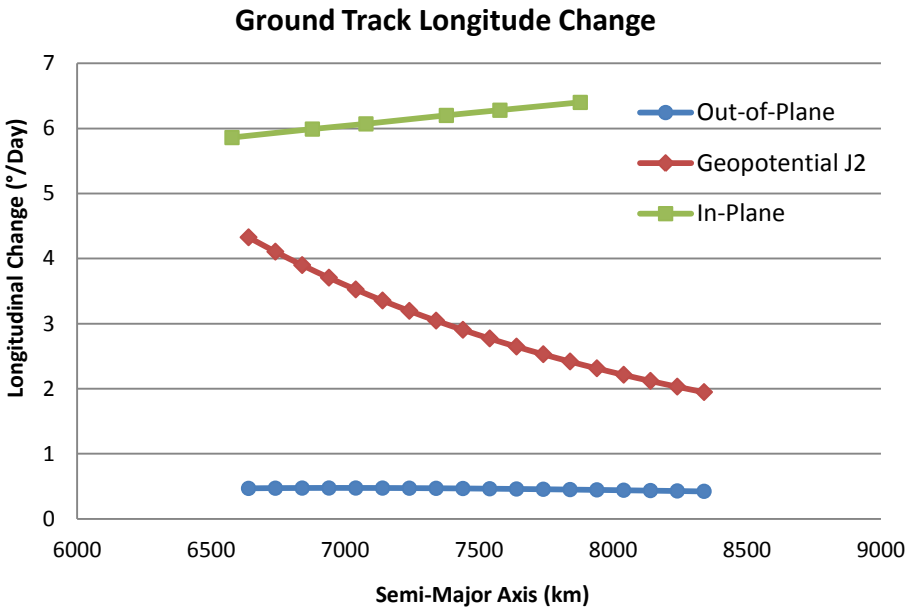

Figure 7-8. Longitudinal Change due to Maneuvering & Geopotential

7.7.3 System Life.

It is useful to quantify the amount of propellant consumed by EP maneuvers. Based on available data from Deep Space 1, a spacecraft with an initial wet mass of 500 kg, EP propellant budget of 100 kg, *Isp* of 3000 s, and available acceleration of 1 mm/s^2 is chosen for this analysis (Rayman, 2000: 475). Using the rocket equation the propellant budget is computed to be 6.5 km/s. The minimum amount of time for global reach is between 33 and 36 hours depending on initial orbital altitude. Thus for the worst case when the spacecraft is required to thrust the entire 36-hour period, the propellant consumption in terms of ΔV is 0.131 km/s or less than 2 percent of the total propellant

budget. Accounting for station-keeping, momentum dumping, and drag compensation, this nominal system could be able to perform over 40 tasked overflights continuously over a period of 100 days. More missions are possible if the required maneuvers do not drastically change the orbit as in the worst case scenarios presented. Spacecraft life could also be significantly longer if missions are not as frequent as it has been assumed here.

7.7.4 Operational Application.

Given today's operations tempo, users want high-quality space-derived products quickly and reliably. The developed algorithm can be responsive to such users provided suitable vehicle characteristics of a satellite. Using a vehicle with an EP capability of A = 1 mm/s^2, Isp = 3000 s, and continuous thrust for prolonged periods of time, surface area of less than 20 m^2, and a propellant storage capacity of 100 kg any target within the coverage area of the satellite is reachable within three days and often in much less time. Given an initial date of January 1, 2012 at 00:00:00 GMT with initial vehicle state vector of a = 6878 km, $e = \Omega = \omega = u = 0°$, $i = 98°$. The satellite is tasked to overfly a random target within the shortest amount of time (Appendix F). Once the ground track intersects the first target, the vehicle is tasked to overfly the next random target. This process is repeated until a total of ten randomly selected targets in a randomly selected order are overflown by the asset. Table 7-3 contains the randomly selected target list for ten national capitals throughout the world. Lighting conditions are not considered for this simulation.

All ten targets are overflown successfully within a period of 250 hours. Altitude constraints are put in place to avoid going below 300 km thereby risking significant

propellant use to counter air drag and going above 600 km in case the payload has technical distance limitations.

Table 7-3. Ten randomly selected Terrestrial Targets by Location and Order

Location	Latitude	Longitude
1. Washington, DC, USA	38° 53' N	77° 2' W
2. Berlin, Germany	52° 30' N	13° 25' E
3. Tokyo, Japan	35° 40' N	139° 45' E
4. Ottawa, Canada	45° 24' N	75° 43' W
5. Madrid, Spain	40° 26' N	3° 42' W
6. Moscow, Russia	55° 45' N	37° 36' E
7. Beijing, China	39° 55' N	116° 25' E
8. Canberra, Australia	35° 17' S	149° 8' E
9. Cairo, Egypt	30° 2' N	31° 21' E
10. Brazilia, Brazil	15° 48' N	47° 54' E

Figure 7-9 shows the semi-major axis variation from target to target. The plot clearly shows significant altitude degradation when the satellite is close to a = 6700 km. It is intentional that the initial and final altitudes are almost the same.

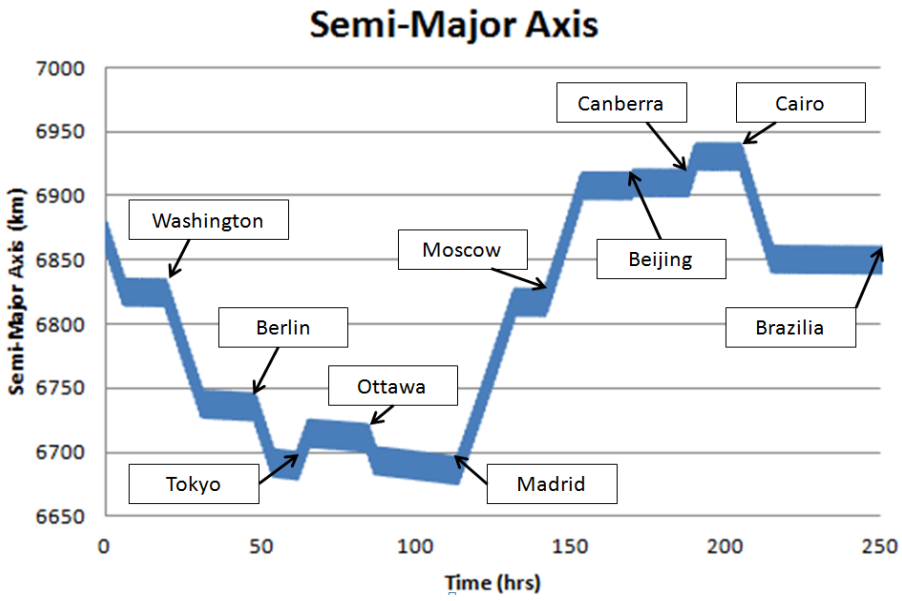

Figure 7-9. Semi-major Axis vs. Time for 10-Target Campaign

The overflight distance error for each instance is less than 1 km, meaning the target is directly at the sub-satellite-point. Each target overflight is achieved through a thrust period initially, shown by rapid increase or decrease in *a*, followed by a coast period that is almost constant in *a* except when the altitude decays due to drag (close to 300 km). The target is overflown at the end of each near-horizontal section and signified with a label. Each target acquisition is achieved in less than two days from the time each thrust period starts.

For the entire ten-and-a-half-day campaign the propellant consumption is less than 5 percent. The problem setup necessitates that each target overflight is comprised of a thrust and coast section because the timing of the Earth's rotation must be taken into consideration. As discussed, the existence of a coast period greatly reduces the amount of propellant consumed. The operational example presented is extreme as target requests may not be executed in such rapid succession in the real world. However, if the notional vehicle would maneuver continuously, it would be possible to overfly 200 targets over a six-month period. Allowing for some non-maneuvering time between overflight requests could potentially prolong the life of the satellite to between one and three years. The upper line in Figure 7-10 displays the cumulative ΔV of the system with the of target overflight marked by the arrows. The lower line is the fraction of propellant used assuming a propellant budget of 6.5 km/s.

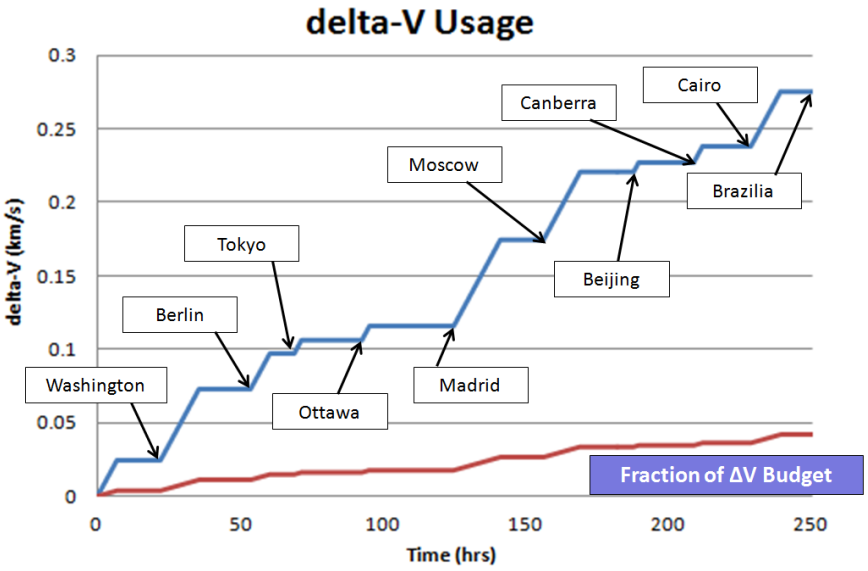

Figure 7-10. Propellant Consumption vs. Time for 10-Target Campaign

7.8 Conclusion

This paper presents the development of an algorithm to compute the requirements for an overflight of any terrestrial target (within the coverage area) using a single low-Earth orbiting satellite. A single equation that computes the time change between a maneuvering and reference ground track is the centerpiece of the algorithm. With it, it is possible to compute the thrust-coast maneuver to achieve a commanded overflight. Once achieved, the system can remain in the new orbit or perform another maneuver to fulfill a new mission. Provided a Deep Space 1 class vehicle using 1990s technology and 1 mm/s^2 of acceleration, one such vehicle can perform over 40 maximum ΔV maneuvers in the worst case. Even with low thrust, a worst case scenario in which the target is furthest away from the reference ground track can be reached in 2.5 days. Yet, realistically a target will not always require worst case maneuvers and simulations show that targets can be overflown in much less time with less propellant consumed. Electric propulsion is

capable of performing out-of-plane maneuvers as well and specific maneuvers sequences are required to affect changes in right ascension of the ascending node and inclination. Although small, these changes could be effective in fine-tuning an orbit without changing its shape. The findings support the feasibility of an electric, low-thrust propulsion system to perform orbital maneuvering to meet user requirements in a cost effective manner, reducing the requirement for costly launches.

8 Comparison of Electric Propulsion Maneuvers to Conventional Observation Missions

A polar, “Streets of Coverage” Walker constellation of three to nine satellites in low-Earth orbit can provide daily observation coverage of any terrestrial target latitude at a pre-selected local time. A single non-maneuvering, or static, satellite in a similar orbit at the correct altitude can cover any target in four to seven days. Maneuvering chemical and electric propulsion satellites provide more flexibility to user needs and can overfly any target in two days. Using Space Mission Analysis and Design concepts, a sample system is designed for four observation methods with equivalent satellite characteristics, so that a fair comparison is possible to evaluate the benefits and drawbacks of each technology. A proposed electric propulsion spacecraft is capable of responsive, repeated, and reliable target overflight at the same cost as a static satellite, while it is three times as responsive by sacrificing one third of its mission life. This work indicates that its higher propulsion efficiency is more effective for low altitude, maneuvering satellites. The maneuver ratio of an electric versus a chemical system is 5.3:1. Its responsiveness and mission life are inferior to that of a Walker constellation, but cuts total system cost by almost 70%.

Nomenclature

A	=	perturbing acceleration magnitude, km/s^2
a	=	semi-major axis, km
AP	=	aperture diameter, m
e	=	eccentricity
i	=	inclination, degrees
Res	=	resolution, m
SR	=	slant range, km
T	=	thrust magnitude, N
t	=	time, s
Δt	=	change in over-flight time, s
u	=	argument of latitude, degrees
ΔV	=	velocity change, km/s
ζ	=	wavelength in electromagnetic spectrum, μm
φ	=	latitude, degrees
μ	=	gravitational parameter, for Earth 3.98601 x10^5 km^3/s^2

8.1 Introduction

Non-maneuvering satellites and constellations have been the name of the space game since the early days of space exploration. The austere economic environment and enormous government debts have not prompted a decisive shift towards smaller space programs or significant changes in operations concepts. New threats in the international

environment may demand change as rapid reconstitution, lower launch cost, and greater flexibility take center stage. One major area of space operations is terrestrial observations, and alternative technologies could be beneficial to improving this field by reducing system cost, time to replace the asset, or time to observe the target of interest. The primary purpose of this paper is to compare four technologies for observing a terrestrial target using equivalent spacecraft design parameters. Two traditional methods are currently in operation and are used as baselines for the comparative study. One method is in research and development in programs such as the U.S. Air Force's X-37. The fourth method is a maneuvering satellite using highly efficient electric propulsion (EP) technology and it is currently not under operational consideration.

Co and Black explored the feasibility of satellite maneuvering using an EP system as an Operationally Responsive Space program (Co, 2011a: 74-80). The analysis showed that current thruster technology is not only capable of orbit maintenance (station-keeping and attitude control) but also of maneuvering smaller spacecraft in low-Earth orbit. The authors developed their analysis and tools to accurately predict low-thrust EP maneuvers and documented their findings in several articles which are referred to throughout this paper. Before discussing the details of the following comparative study, it is necessary to develop their concepts further and present some considerations for an EP system such as operational altitude, inclination, lighting conditions, viewable area, and power requirements.

Earth's first zonal harmonic (J_2) effect is more significant at lower altitudes and inclinations (Vallado, 2001: 614-616). Co *et al.* formulated Equation (8.1) which takes the propulsion system's thrust, initial altitude, and the amount of time available to

perform the maneuver into consideration to compute a change in time of overflight (Δt) of a terrestrial target as a result of maneuvering (Co, 2012a: 20):

$$\Delta t = (u_2 - u_0)\sqrt{\frac{a_0^3}{\mu}} - \frac{\sqrt{\mu}}{A}\left[\left(\frac{1}{a_0^2} + \frac{4}{\mu}A(u_1 - u_0)\right)^{1/4} - a_0^{-1/2}\right] - (u_2 - u_1)\sqrt{\frac{a^3}{\mu}} \qquad (8.1)$$

where the subscripts denote initial (0 – at the beginning of the maneuver), intermediate (1 – thrusting stops and coasting begins), and final (2 – at the time of target overflight) conditions. To demonstrate this concept, assume the Earth is not rotating. A satellite overflies target A at some time t_1. Thrusting tangentially, in-plane, and in the direction of travel, raises the altitude and the satellite directly overflies target A at a later time (after t_1). Thrusting in the opposite direction has the reverse effect in that target A is now overflown at an earlier time. Since the Earth is rotating 360° every sidereal day, the Δt actually causes the overflight location to shift westward when raising the altitude and eastward when lowering it. For prograde orbits, the J_2 favors westward and counters eastward motion as depicted in Figure 8-1.

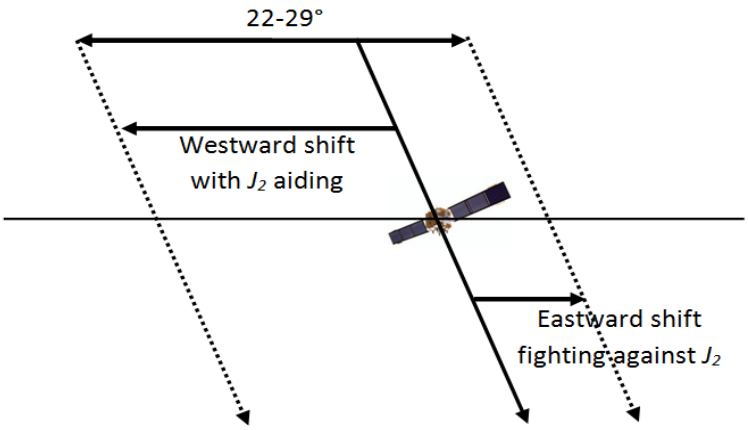

Figure 8-1. Low-Earth Orbit J_2 Effect for West and East Shift, Prograde

The solid line is the reference ground track of a non-maneuvering spacecraft. If the Earth had no axial rotation and the J_2 effect was negligible, this line would be static and the satellite would have a repeating ground track. Maneuvering would only change the time the spacecraft reaches the target latitude (horizontal line). However, since both Earth's rotation and J_2 are realities, the dotted lines are the new ground tracks for a maneuvering system. The westward shift is more pronounced for this prograde low-Earth orbit as compared to the eastward shift as a result of J_2. Table 8-1 numerically shows the longitudinal shift ($\Delta\lambda$) due to nodal regression (J_2) and maneuvering for two altitudes and four inclinations. At an altitude of 300 km, the Earth's rotation shifts the ground track westward by 22.7° during the period of a circular orbit. Nodal regression is more significant at lower inclinations with 6.499° per day at i=40° and reducing to -0.985° at i=96.7° (sun-synchronous).

Table 8-1. Longitudinal Shift due to J_2 and Maneuvering

Altitude (km)	Inclination (°)	Nodal Reg (°/day)	West Δλ (°/day)	East Δλ (°/day)	East/West Δλ (°/day)
300	40	6.499	12.385	-0.613	11.772
	60	4.240	10.126	1.646	11.772
	90	0.000	5.886	5.886	11.772
	97.4	-0.985	4.901	6.871	11.772
500	40	5.860	11.831	0.111	11.942
	60	3.830	9.801	2.141	11.942
	90	0.000	5.971	5.971	11.942
	96.7	-0.985	4.986	6.956	11.942

Assuming the spacecraft's EP is capable of a constant acceleration of 1 mm/s^2, the longitudinal shift of the ground track as a result of maneuvering is 5.886° per day in either direction. The trends are similar for a circular orbit at 500 km. The longitudinal

separation between ground tracks is 24°, $\Delta\lambda$ due to maneuvering is slightly greater at 5.971° per day in either direction, and J_2 has a lesser overall effect.

Although the J_2 effect on nodal regression is more pronounced at lower altitudes and at lower inclinations, there is an unexpected zero-net-effect on reachability when considering the ability to raise and lower the altitude of an EP spacecraft. Table 8-1 shows that the westerly $\Delta\lambda$ is significantly larger than that for the eastward shift, however, the net east/west effect remains the same at twice the $\Delta\lambda$ induced by the propulsion system regardless of inclination and altitude. Thus, this begs the questions of why not maneuver to only raise the altitude or select a higher initial orbit and take advantage of the "free" J_2 support. The ability to maneuver and shift the ground track east and west is more desirable, because a target may just be slightly to the east of the non-maneuvering reference and it would take less time and energy to affect an overflight. Furthermore, even without considering payload altitude constraints, a higher altitude results in greater longitudinal separations between passes (i.e. 24° at 500 km versus 22.7° at 300 km) such that it takes just over two days for global reach at an altitude of 500 km compared to 1.9 days at 300 km. Since J_2 has no net impact on reachability, it allows the selection of any inclination for orbit design. This characteristic becomes important when considering lighting conditions of an operational orbit.

Solar flux is extremely important for an EP system reliant on solar energy. A low-thrust, highly efficient EP spacecraft is only effective for maneuvering if it can be utilized nearly continuously over a one- to two-day period. If there is insufficient solar energy or eclipses become too long in duration, EP thrusting must cease and the amount of time to reach a target overflight is extended. Thus, an orbit with the most amount of sun exposure

is ideal and essential for a maneuvering EP system. Nodal regression plays a favorable role. A sun-synchronous orbit (SSO) is often selected for electro-optical satellites due to the daily constant sun angles at a given time. However, a simple SSO is not enough for the proposed system, but rather a dawn-to-dusk SSO with a nodal crossing time of 0600L or 6:00am local is more suitable. Analysis shows that it is more beneficial to be close 0600L since the total eclipse time throughout the year and maximum eclipse duration are both shortest. Higher altitudes also help in reducing total eclipse time. At an altitude of 1500 km, the percentage of time a satellite spends in eclipse is effectively zero in dawn-to-dusk SSO. Figure 8-2 shows ten nodal crossing times and the associated percentage of time a satellite spends in eclipse in a 400-km orbit.

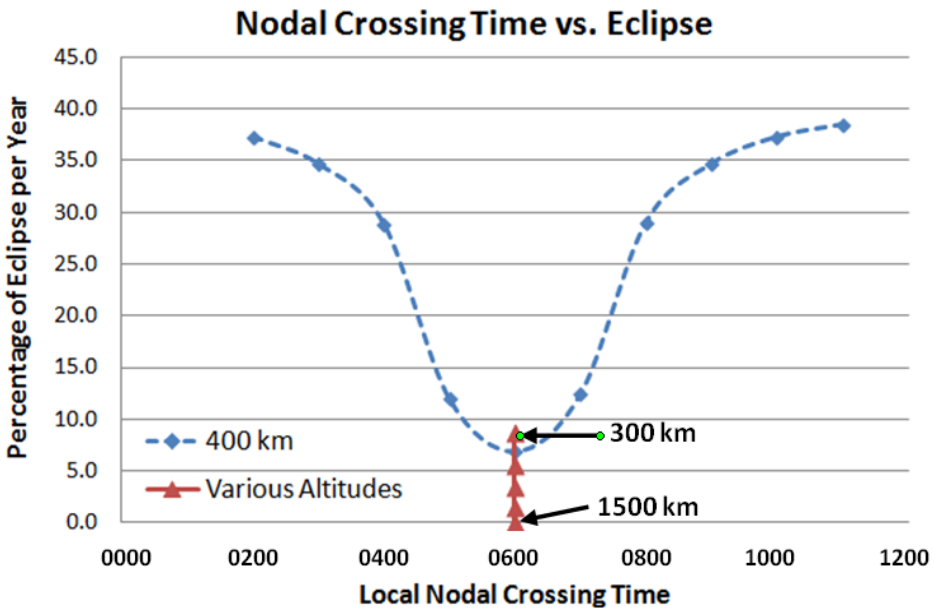

Figure 8-2. Nodal Crossing Time vs. Eclipse.

The minimum eclipse percentages are 8.7 and 6.9 at 300 km and 400 km, respectively. Earth's 23.5°-tilt from the Plane of the Ecliptic is not only responsible for terrestrial

seasons, but it also makes it impossible to avoid eclipse in low-Earth orbit. Therefore, a dawn-to-dusk SSO with a nodal time of 0600L is most desirable for an EP system. Another consideration is that the proposed satellite is designed to change its altitude constantly, so maintaining an SSO is impractical unless propellant-intensive inclination changes are incorporated. Co *et al.* analyzed the effect of a standard eclipse on a continuous, low-thrust EP spacecraft and concluded that after one day of thrusting with approximately 16 interruptions results in a slightly elliptical orbit with an altitude difference of 100 km between apogee and perigee (Co, 2011c: 9). Even so, the operational orbit design can minimize the eclipse times to allow the desired responsiveness of a maneuvering system. The next considerations are power requirements and payload sizing.

An electric propulsion spacecraft requires a fine balance between payload sizing, power requirements, operational altitude and lifetime. Standard payload sizing methods for observation systems take the electromagnetic wavelength, required resolution, and the distance to the target in consideration to compute the diameter for the aperture (Larson, 2004: 264). Using Plank's and Wien's Laws, the wavelength, ζ, at which an object emits the maximum energy from reflected sunlight is 0.483 μm (visible spectrum). This wavelength applies to electro-optical observation systems and does not need to be adjusted for atmospheric absorption. The worst allowable resolution (*Res*) is arbitrarily selected as 1 m and will remain a standard requirement throughout this paper. Similarly, the minimum elevation angle as depicted in Figure 8-3 common in literature is 60°, which determines the slant range (*SR*) based on satellite altitude. Equation (8.2)

determines the minimum required aperture size for an electro-optical payload to meet resolution requirements given any *SR* determined by altitude:

$$AP = \frac{0.00244 \cdot \zeta \cdot SR}{Res} \tag{8.2}$$

where the constant converts input units to the proper output unit for aperture (m), such that the inputs are entered in their standard forms. Wavelength is entered in units of micrometers, *SR* in kilometers, and *Res* in meters. Thus the driving factor is altitude which affects aperture size, mass, power consumption, spacecraft structure, lifecycle, and cost. All these factors are considered in the system design section of this paper.

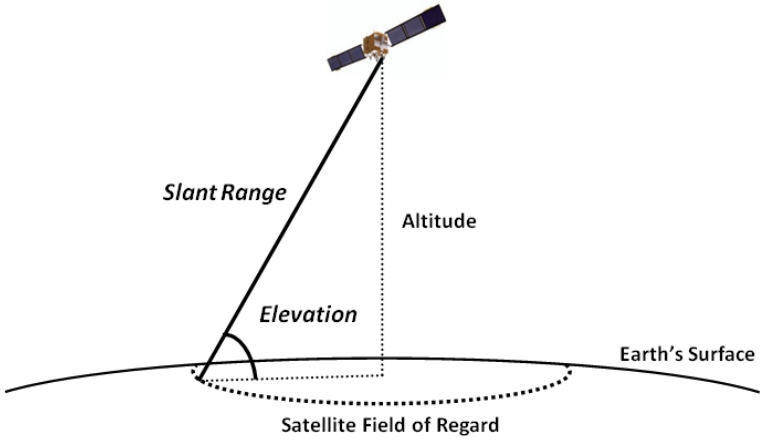

Figure 8-3. Satellite Field of Regard Geometry

Electrical power is a key component to the success of an EP system. Current Hall Effect (HET) and Ion thrusters require enormous amounts of power (Hall, 2010: 8-12). A commercially available Busek HET designated as BHT-8000 requires 8 kW and produces 512 mN of thrust at a specific impulse of 1900 s. Several other thrusters are available, but

characteristics from this thruster are used for the upcoming EP analysis. An appropriately sized solar array with similar specifications as NASA's Deep Space 1 spacecraft (specific power 45 W/kg and 200 W/m^2) would have an area of 42.5 m^2 and a mass of 190 kg. Habraken *et al* compiled 200 solar array research documents in October 2000 showing space-qualified cell technologies capable of specific power ratings of 340 W/m^2 and 90 W/kg with efficiencies of 25% (Habracken, 2000). In other words, more capable solar array technologies are available and could cut both size and mass of the proposed solar array in half. Regardless, it is critical that increased atmospheric drag considerations are made for the EP system in the analysis.

8.2 Traditional Missions vs. Electric Propulsion

This section presents analysis for three traditional observation methods using satellites and the proposed EP system. Proper considerations are made to maintain a meaningful and fair comparison between the different methods. The following paragraphs discuss the design, cost, and lifecycle of a Walker constellation (Walker), a single non-maneuvering satellite (Single Static), a single maneuvering CP satellite (Single CP), and a single maneuvering EP satellite (Single EP).

8.2.1 Walker Constellation.

A polar Walker constellation of three to nine satellites in a single plane could provide coverage of any target latitude on Earth at a pre-selected local time (Appendix G). This is similar to the "Streets of Coverage" constellation discussed by Larrimore

(Larrimore, 2007). The number of required satellites is driven by altitude. With a required resolution of 1 m and a minimum target-to-satellite elevation of 60°, a number of design parameters are adjusted based on altitude and a total mission cost is determined using the Space Mission Analysis and Design (SMAD) computation method. The resolution constraint dictates that for the worst-case it does not exceed 1 m anywhere within the field of regard, which means that the sub-satellite resolution is significantly better (0.75 m for this elevation angle). Table 8-2 provides design characteristics of a single satellite in such a Walker constellation with a design life of 5 years.

Table 8-2. Walker Constellation at various Altitudes with 5-yr Design Life

Altitude (km)	# of SC	Aperture (m)	PL Mass (kg)	ΔV (m/s)	Dry Mass (kg)	Prop Mass (kg)	Total Mass (kg)	Const Cost (M$)
283	9	0.445	46.7	11900	1283	72183	73466	N/A
300	8	0.47	55.6	3270	578	1180	1758	720
310	8	0.49	61	2922	540	919	1459	703
320	8	0.5	68	2585	518	730	1248	694
330	8	0.52	74	2269	506	589	1095	666
340	7	0.53	81	1978	503	483	986	600
350	7	0.55	88	1716	507	402	909	601
370	7	0.58	104	1305	532	297	829	611
394	7	0.62	125.9	933	579	216	795	630
491	6	0.77	243.7	307	921	101	1022	651
651	5	1.02	568	182	1928	123	2051	875
974	4	1.53	1902	249	5952	526	6478	1475
2015	3	3.17	16843	0	46408	0	46408	7198

The design can be optimized for constellation cost (highlighted). The only variable is altitude whereas other inputs of resolution, elevation angle, lifetime, launch vehicle type, number of satellites per launch, and satellite subsystem characteristics are held

constant. The altitude range is selected first based on the number of satellites required for "Streets of Coverage" and then fine-tuned to find the lowest constellation cost. At an altitude of 340 km, seven satellites are necessary. Each spacecraft has a payload with a 0.53-m aperture, payload mass of 81 kg, dry mass of 503 kg, propellant mass of 483 kg (for a ΔV budget of 1978 m/s), and total system mass of 986 kg. The cost for the seven-satellite constellation is $600M. The lowest altitude analyzed is 283 km, where the required number of spacecraft is nine. Although the aperture is relatively small, the amount of drag is so significant that the satellite must carry an infeasible amount of propellant to provide a ΔV budget of 11.9 km/s for five years of operation. A higher altitude requires not only a larger aperture, but also the supporting structure and maintenance mechanisms add mass and, to some extent, propellant to the system. Figure 8-4 displays the component and total masses of a single satellite in the constellation with respect to altitude (Appendix G, G-8).

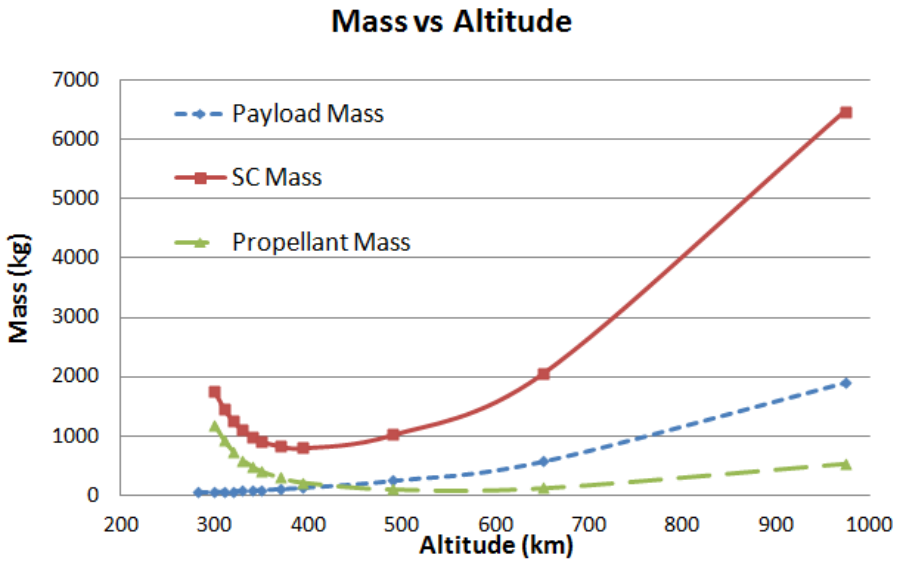

Figure 8-4. Walker "Streets of Coverage" Satellite Mass vs. Altitude

The trend initially decreases with altitude as less propellant is required to counter drag despite the larger payload. After an altitude of 400 km, the payload mass increases at a faster rate requiring more structural support and thus outpacing any propellant savings gained through a sparser atmosphere.

A similar behavior can be observed by analyzing system lifetime as depicted in Figure 8-5. Lifetime significantly impacts mass below an altitude of 400 km. At higher altitudes, the propellant savings quickly diminish and above 500 km the system lifetime has little to no impact on mass.

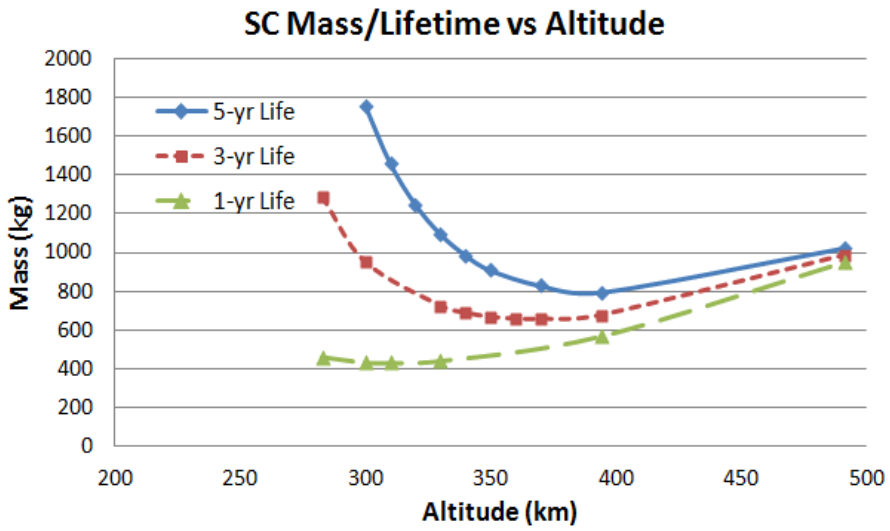

Figure 8-5. Walker "Streets of Coverage" Satellite Lifetime vs Altitude

8.2.2 Single Non-Maneuvering Satellite.

Commercial companies such as GeoEye use single non-maneuvering spacecraft for imagery like those available through Google. GeoEye-2 is the industry's cutting edge and provides the highest commercially available resolution at 0.34 m. Table 3 provides a comparison between GeoEye-2 and a Walker satellite discussed in the previous section

(Appendix H). There are several similarities but the model used in this paper has less sophisticated optics, therefore providing a lower resolution. GeoEye-2 is far superior in both nadir resolution and off-nadir imaging angles. The difference in total mass is made up by increasing the propellant mass for the single Walker, which would inevitably lengthen the design life. The revisit rate is one day longer for the single Walker.

Table 8-3. Comparison of GeoEye-2 and Single Walker Satellite

	GeoEye-2	Single Walker
Orbital Altitude	681 km	651 km
Nodal Crossing	1030L	1000L
Aperture	1.1 m	1.02 m
Propellant Mass	453 kg	123 kg
Total Mass	2540 kg	2015 kg
Design Life	7 years	5 years
Revisit Rate	3 Days	4 Days
Off-Nadir Imaging	60°	28.4°
Nadir Resolution	0.34 m	0.75 m

To compare Single Static to the other three methods requires investigating its revisit rate. The revisit rate in this paper is defined as the amount of time required for a satellite to overfly every point on Earth at least once. The analysis measures revisit time at various altitudes. Although a higher altitude increases swath width, the revisit time does not necessarily decrease with it. Figure 8-6 shows revisit time as a function of altitude. The data can be separated into two groups – in-sync and out-of-sync. When the period of the satellite is in-sync, its motion is in-tune with Earth's rotation and the J_2 effect and the result is very little to no overlap in ground tracks. The end effect is a significantly lower revisit time. The in-sync altitudes are at 310, 500, 640, and 783 km and the associated

revisit times are 7, 5, 4, and 4 days, respectively. Conversely, the period is out-of-sync at altitudes of 340 and 550 km with revisit times of 23 days.

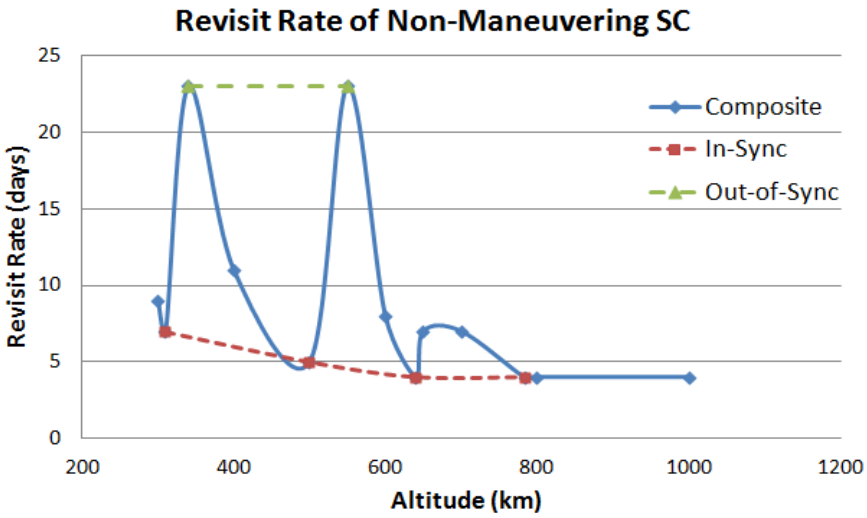

Figure 8-6. Revisit Rate of Single Non-maneuvering Spacecraft

The data shows that a small change in altitude can have a large effect on revisit time. Figure 8-7 depicts ground coverage for a single non-maneuvering satellite, where each line represents a pass. Only the descending passes are counted as the ascending ones are usually on the night-side. The first picture (Figure 8-7a) shows gaps between each pass. At an altitude of 340 km the period is out-of-sync. There are several lines grouped in threes. The lines furthest east in each group are one of 16 orbits during the first day. The second set of lines in the middle of each pack represents the second day and so on. After three days, there are gaps between each pass. Figure 8-7b shows that the entire globe is covered after 23 days. The close-up shot reveals that each pass is overlapped multiple times. Thus in reality, the time required to revisit a terrestrial target may not take 23 days, but to cover the entire world at least once does require that amount of time.

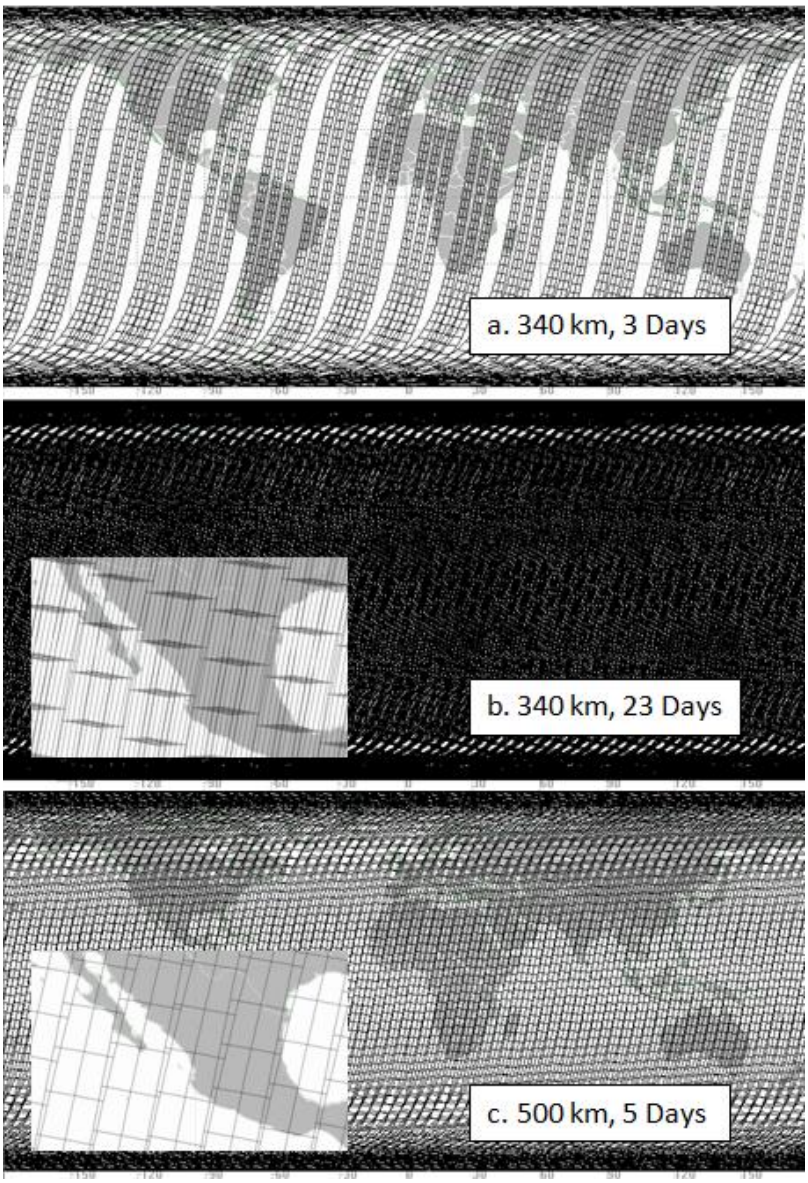

Figure 8-7 a-c. Revisit Time at Altitudes of 340 and 500 km

For an in-sync orbit, the revisit rate is only five days at an altitude of 500 km. Figure 8-7c depicts a wider swath for each pass and the overlap is minimal. Therefore, the selected operational altitude is critical for a non-maneuvering satellite to ensure the shortest revisit times.

8.2.3 Single Maneuvering Satellite (Chemical).

A system much like the X-37, a maneuvering satellite using chemical propulsion (CP), could overfly a desired terrestrial target with great flexibility. Limiting the maneuvers to in-plane, tangential burns only, a CP spacecraft performs a phasing maneuver to change its ground track to affect an overflight. The propellant consumption for a single change can be extremely high depending on the amount of time available to carry it out. If the target over-flight is required within one orbital period, 90% of the propellant budget would be consumed. On the other hand, if the available time is two days, the propellant consumption would be 5.3%. Given two days, each maneuver shortens the spacecraft life by 97 days (0.265 years) on orbit. Figure 8-8 summarizes this relationship.

For a meaningful comparison, the analysis uses the same propellant budget as Walker (Appendix I). As a result, a maneuvering CP satellite is only feasible at certain lower altitudes. The phasing maneuver starts and ends at the same orbital altitude, therefore it is important to select the proper altitude with the lowest revisit rate. Based on the analysis of the previous section, the altitudes for which the orbital period is in-sync are 310, 500, 640, and 783 km. To maintain identical mass and ΔV characteristics as Walker, the propellant budget decreases significantly with altitude thereby making it infeasible for CP maneuvers at higher altitudes. At 310 km, the total propellant budget is 2.922 km/s which allows extraordinary maneuvers such as affecting a target overflight in less than 100 minutes after thrusters are fired, but consumes most of the propellant in a single maneuver. At 500 km, such maneuvers are not possible without adding more

propellant or allowing more time and thereby resizing the entire system. A CP maneuver cannot be done at this altitude unless there are 16 orbital periods available to achieve a single overflight. At that altitude and given two days, a single maneuver still consumes over 50% of the propellant budget. Figure 8-8 demonstrates these relationships.

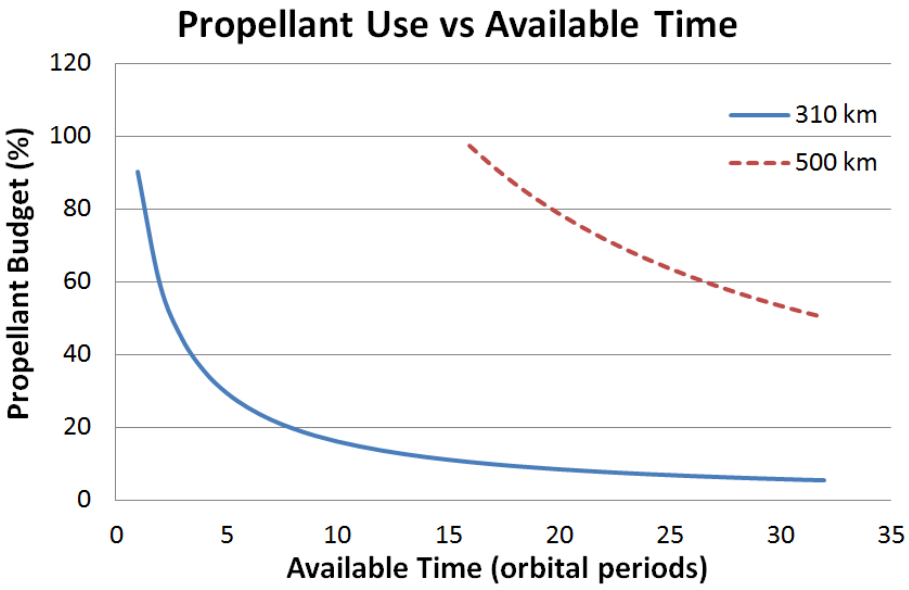

Figure 8-8 Propellant Use vs. Available Time at 310 and 500 km

Although CP maneuvers can be very capable, the propellant consumption for extraordinary maneuvers is prohibitive. With the same vehicle characteristics established for the Walker constellation, the only feasible operational altitude is 310 km. Sacrificing responsiveness significantly reduces propellant use. Given the longer response time of two days and on average one maneuver per month, the system could be operational for approximately 14 months or 23% of the 5-year design life of the Walker constellation.

8.2.4 Single Maneuvering Satellite (Electric).

A new system concept that is currently not in operational use but has much potential is maneuvering in low-Earth orbit using EP. Co and Black developed an algorithm to consistently compute the amount of time and propellant required to affect overflight of any terrestrial target within the satellite's coverage area using EP (Co, 2012b: 9-12). Some considerations and challenges of EP are discussed in the beginning of this paper. Using the same characteristics as the Walker constellation, the EP system must be adjusted for the increased power demand, drag, and associated mass increase for a fair comparison (Appendix J). Thus, the overall mass and ΔV budgets are changed to account for EP operations, both of which counter the efficiency gain of such a system. Significantly larger solar arrays add mass (190 kg) and ΔV to counter the enormous amount of drag when compared to a CP spacecraft. The simulation uses 4 km/s of ΔV for EP for every 1 km/s for CP. Power determines how much thrust and therefore control authority is available to the system.

Control authority is the amount of change achievable with the available thrust to propel the spacecraft. Using Equation (8.1), it is possible to calculate the magnitude of Δt based on thrust, altitude, and the amount of time available. This value in turn translates linearly into longitudinal change of the ground track ($\Delta\varphi$). Thus a large Δt allows greater reach of the satellite as a result of maneuvering. After one day of thrusting in either direction (increasing or decreasing altitude) using the Busek BHT-8000 with an effective acceleration of 0.5 mm/s^2, $\Delta\lambda$ is 2.98° at an altitude of 300 km and 3.00° at 400 km. Further, Co and Black only considered nadir overflights in their analysis, thereby

restricting the spacecraft to only see sub-satellite points. This paper expands the field of view of the spacecraft up to an angle of 60° (see Figure 8-3) therefore expanding the satellite's longitudinal reach by 1.47° in either direction at 300 km and 1.93° at 400 km. The total control authority of this EP satellite, measured in $\Delta\varphi$, is between 8.90° and 9.86° per day for the altitude range in question as depicted in Figure 8-9. It follows that global reach is achievable in 2.5 and 2.3 days at altitudes of 300 and 400 km, respectively.

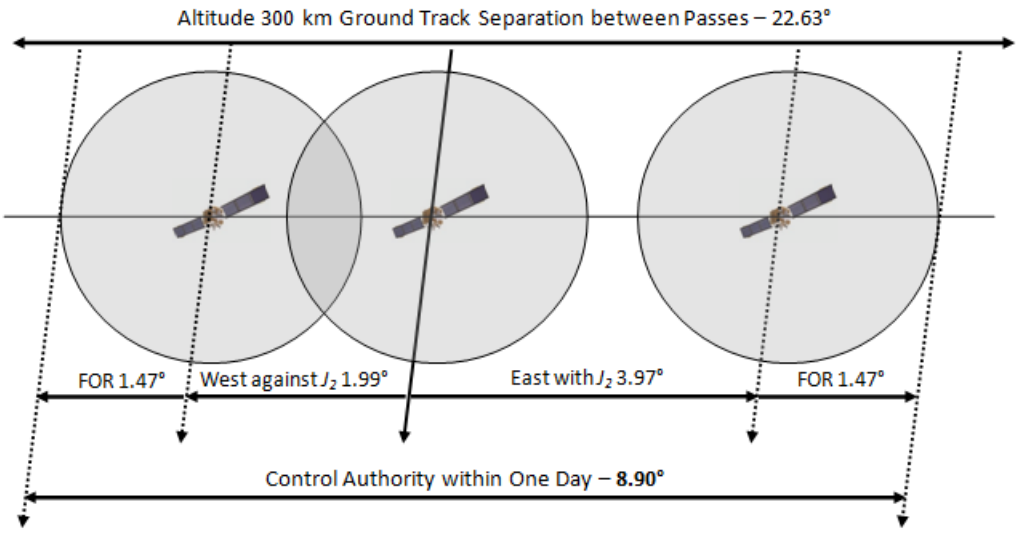

Figure 8-9. Control authority at 300 km with BHT-8000 (A=0.5 mm/s^2).

8.3 Compare and Contrast

This section discusses the four presented methods in a side-by-side fashion to point out their advantages and disadvantages. The Walker constellation is the baseline. At the in-synch altitude of 310 km, eight satellites are required to provide daily overflight of all targets within the coverage area of the orbital inclination. A Walker constellation in a

sun-synchronous orbit with a nodal crossing time of 1000L overflies every equatorial target at 10:00am local time and can cover every other spot on Earth once a day. No maneuvers are necessary except for station-keeping and attitude control. The Single Static spacecraft similarly performs no maneuvers to change its orbit. A Single CP satellite can perform 14 max-$\Delta\varphi$ maneuvers, which means to reach any target within its coverage area, at a rate of once per month. This number takes propellant use for maneuvers and station-keeping into account. The frequency of maneuvers is up or down adjustable and the relationship is inversely proportional. The CP maneuvers are allowed 32 orbital periods or 2 days to accomplish the overflight. A proposed Single EP system can perform 38 max-$\Delta\varphi$ maneuvers at the same rate of once per month. Using the algorithm developed by Co and Black, 2.5 days guarantee global reach, yet most targets come within reach in 2 days. Figure 8-10a depicts this comparison graphically.

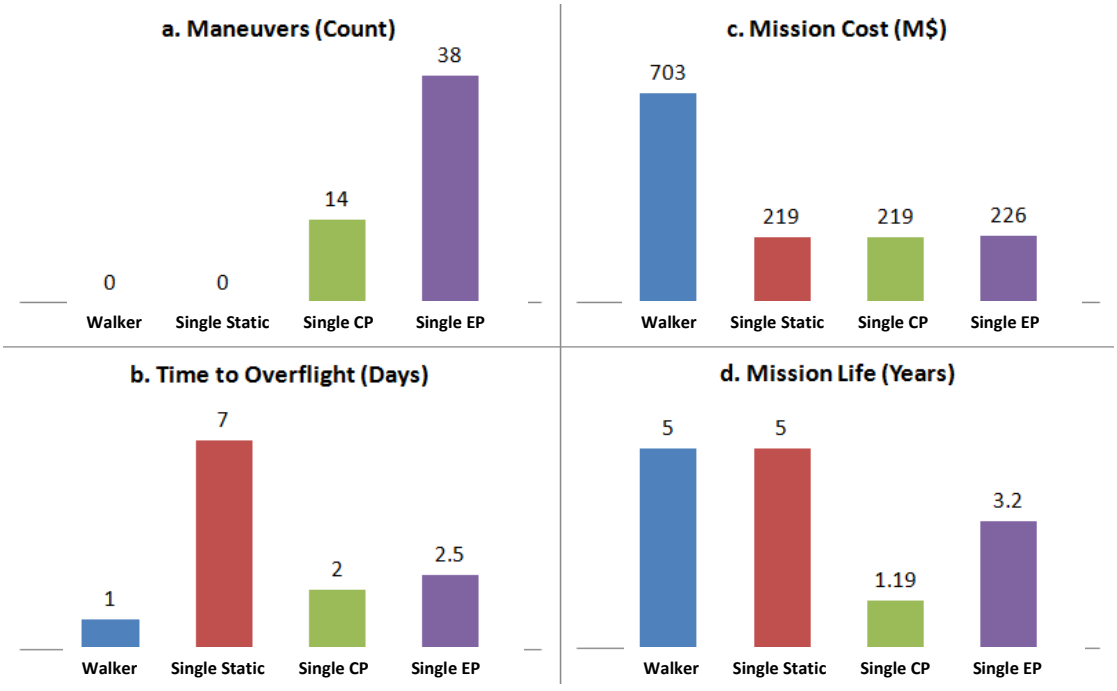

Figure 8-10 a-d. Characteristic Comparison of Four Methods at 310 km Altitude

The second bar graph (Figure 8-10b) is denoted Time to Overflight instead of revisit rate because this term only applies to Walker and Single Static in this setup, since Single CP only has a 2-day revisit rate if it maneuvered every two days instead of once a month. Changing this rate increases the number of possible maneuvers but shortens the mission life of the system. Similarly, Single EP could have a revisit rate of 2.5 days if it maneuvered continuously, otherwise it should be denoted Time to Overflight for accuracy. Walker is setup to revisit daily so the time to reach any target is no more than one day. Single Static revisits every target once in seven days without maneuvering only at the in-sync altitude of 310 km. Even slight deviations of 30 km from this altitude could drastically increase the revisit rate of the Single Static. Thus the highest revisit rate is achieved by the constellation, followed by the maneuvering satellites, and trailed by the static one.

The third bar graph (Figure 8-10c) shows a comparison of system cost. Naturally, the Walker constellation of eight satellites with four Falcon 9 launches at $50M each is the most costly of the four systems. Based on the SMAD estimation method, the space segment makes up $338M, launch $200M, and operations and maintenance $165M for the 5-year lifecycle totaling $703M. In the space segment, the cost is further broken down into $80M for the first satellite, which includes research and development costs and $258M for the remaining seven units. The Single Static and Single CP systems share the same cost because it is the same spacecraft. Single Static is one satellite taken from the Walker constellation. At an altitude of 310 km, the payload aperture size remains constant at 0.49 m and a mass of 61 kg. All other characteristics are kept the same such as design life of 5 years, propellant budget of 2922 m/s, and total system mass of 1459 kg.

Differences in cost result from no purchase of additional units beyond the first, one instead of four Falcon 9 launches, and less operations and maintenance cost. The total system cost for the Single Static is $219M. For comparison purposes, Single CP shares the same characteristics as Single Static with an engine efficiency of 300 s. The concept of operation for Single CP allows the spacecraft to maneuver using a combination of its four chemical thrusters beyond station-keeping and attitude control, thereby depleting the ΔV budget more rapidly and shortening mission life. Lastly, Single EP is slightly more costly at $226M. The more efficient Hall-Effect thruster with a specific impulse of 2000 s reduces the propellant mass drastically, hence reducing total system mass and size. However, the significantly higher power requirement of 8.5 kW versus 600 W for the Single CP necessitates massive solar arrays. To account for that, 200 kg are added to the estimated dry mass for a 42.5-m^2 array (assuming a specific power of 200 W/m^2 and 45 W/kg). Furthermore, larger solar arrays have another side effect – more drag. To account for drag, the propellant budget is quadrupled compared to that of Single CP and the propellant mass adjusted accordingly. The total system mass is lower at 1171 kg and the cost is comparable to Single Static and Single CP.

The final bar graph (Figure 8-10d) compares the length of mission life for each system. Walker and Single Static both have a design life of 5 years. Their propellant budgets are sized to account for station-keeping and attitude control as well as a small amount of ΔV for end-of-life (EOL) operations. Without maneuvering, the 5-year design life is the baseline for comparison. Assuming Single CP maneuvers once per month, it is capable of 14 maneuvers before depleting most of its propellant. Orbit maintenance and EOL operations are accounted for in this figure. Thus, the system life of Single CP is 14

months or 1.19 years. Similarly, Single EP also maneuvers at a rate of once per month. The ΔV budget and efficient thrusters allow it to maneuver 38 times before depleting its propellant for a total system life of 38 months or 3.2 years.

A single, maneuvering electric propulsion spacecraft is capable of responsive, repeated, and reliable target overflight at the same cost of a single non-maneuvering satellite by sacrificing one-third of its mission life. The restriction is that at these figures, Single EP can only perform a maneuver once per month. More frequent maneuvers are possible by adding a second spacecraft and leveraging the launch capacity of the Falcon 9 and effectively cutting the launch cost in half. A second Single EP satellite would cost $55M and its addition could increase maneuvers, reduce time to overflight, and lengthen mission life. The responsiveness of the Single EP is 2.5 times slower than Walker and mission life is shorter by 36%, but the total system cost is less than a third. Comparing the Single EP to the Single CP, cost and response time are almost identical but Single EP can perform almost 3 times the number of maneuvers and mission life is 170% longer. The Single Static is almost 3 times less responsive than Single EP with a 50% longer mission life. However, Single Static revisits every seven days whereas Single EP may not revisit a target at all until the next maneuver the following month. Each system has benefits and limitations. Therefore, it is not fair to make a determination on system superiority as it dependents strongly on the mission requirements.

The comparison can also be made from a propellant use versus response time point-of-view. Another perspective is offered in the following analysis by adding a different altitude at 500 km. Figure 8-11 displays the Time to Overflight as a function of percentage of the propellant budget used on a logarithmic scale at 310 and 500 km. Given

the available ΔV, Single CP can perform extraordinary maneuvers with Time to Overflight in as little as one orbital period or 91 minutes. However, it can only perform this maneuver once. With a more reasonable Time to Overflight of two days, Single CP can perform at least 14 maneuvers at an interval of once per month. Hence the CP maneuvers are labeled "Fastest, Costly". The next shortest Time to Overflight is Walker with a revisit rate of one day and no maneuvers. The propellant use during this time period is 0.05% of the budget, but the system cost is the highest at $704M. Single EP is slower at 2.5 days and given twice the amount of time, the propellant use reduces to 25% for the same maneuver. These efficient EP maneuvers consume 1% of the propellant budget for a 2.5-day Time to Overflight. Lastly, Single Static is the slowest with a revisit rate of seven days and consumes 0.27% of its propellant for orbit maintenance.

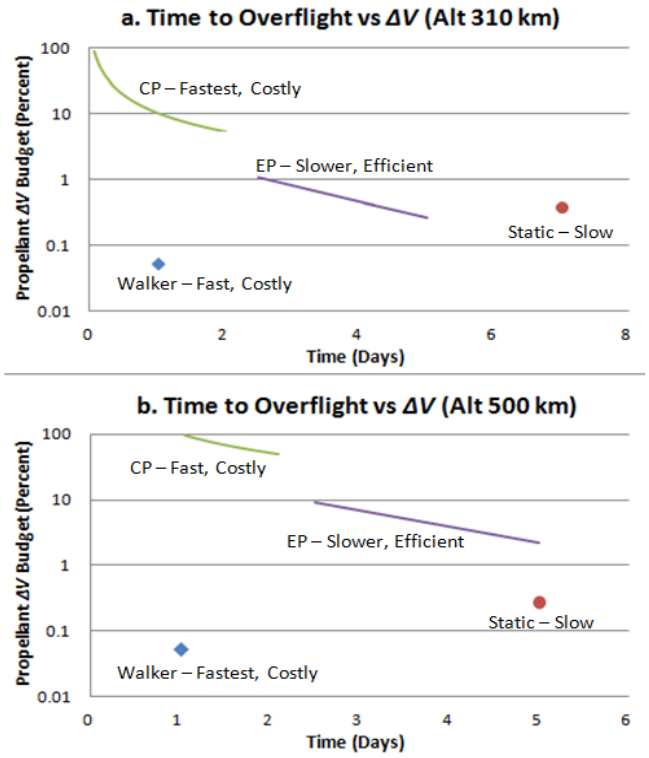

Figure 8-11 a-b. Time to Overflight and ΔV Use Comparison at 310 and 500 km

The ΔV consumption paints a different picture at 500 km (Figure 8-11b). At this altitude, the propellant budget is significantly smaller, so the Single CP cannot perform extraordinary maneuvers. The shortest time required to complete a CP maneuver is just over one day using up over 97% of the propellant. Even given two full days to complete the maneuvers, the consumption is 50%. Therefore, a maneuvering satellite at 500 km with a ΔV budget of 307 m/s is very propellant-intensive unless much longer time periods are allowed to overfly a desired target. Time to Overflight and propellant use are not affected for Walker, but the constellation has two fewer satellites at the higher altitude. Single EP is affected significantly by altitude. Due to the smaller ΔV budget, each maneuver consumes almost 9% of propellant, therefore allowing fewer taskings. Lastly, Single Static has a significantly shortly revisit rate at five days as long as the altitude remains at 500 km.

The Time of Overflight comparison clearly distinguishes EP and CP maneuvers and provides some interesting facts. Single CP can reach targets quickly at extremely high propellant costs allowing it to only perform a few maneuvers. Further, only lower altitudes are feasible when keeping the vehicle characteristics consistent with the other three systems (except vehicle mass), unless more propellant is added or responsiveness is sacrificed. Single EP can perform many more maneuvers than Single CP. Within a short time frame (i.e. continuous maneuvers), the ratio is 5.3 EP to 1 CP for equivalent systems as a direct result of the greater efficiency of EP systems. The non-maneuvering system's propellant consumption is very low, but interestingly, at 310 km the Single EP ΔV consumed (when five days of Time to Overflight is available) is lower than Single Static while achieving target overflight a full two days sooner. Regardless of which perspective

is used for analysis, it is difficult to ignore the important potential an EP system holds for the described application.

8.4 Conclusion

This paper presents a comparative analysis for an overflight of any terrestrial target (within the coverage area) between four satellite systems – namely a Walker constellation, a single non-maneuvering, a single maneuvering CP, and a single maneuvering EP spacecraft. Most importantly, the equations for predicting EP maneuvers are a key component that made this study possible. The introduction further develops previous concepts and discusses suitable orbit types for a proposed EP system and how to overcome known challenges.

The analysis of EP and CP system reveals that higher efficiency, despite lower thrust, is more effective and feasible for a low-Earth orbit satellite designed for repeated maneuvering. After accounting for a much larger power subsystem and increased drag, the ratio of EP to CP maneuvers is 5.3:1 for equivalent systems. This means that the higher efficiency of an EP versus a CP system does not translate one-to-one into the number of possible maneuvers. An EP system maneuvers in a spiral motion and carries larger solar arrays which induce more drag, both of which reduce efficiency. Thus, even though the *Isp* ratio may be 10:1 from electric to chemical, an EP system can maneuver 5.3 times for each chemical maneuver. To shorten the revisit rate, there are only a handful of altitudes at which a static or maneuvering CP system can operate effectively (i.e. 310, 500, 640, 783 km), greatly restricting flexibility. Furthermore, given the smaller

propellant budgets at higher altitudes as a result of less drag, chemical maneuvering at 500 km is very propellant-intensive, thereby restricting the operational domain further.

Benefits and drawbacks for static and maneuvering satellites are also presented in measurable terms, which provide insight for designers to select a suitable technology to meet mission needs. The analysis describes the trade-offs between mission life, cost, and responsiveness. A Walker constellation may be a fast method to acquire a target, but requires many satellites on orbit and launches to get them there. It would not be suitable if the requirement is rapid reconstitution. A maneuvering CP satellite is the most responsive system, able to reach a target as quickly as 90 minutes, but it can only do this once due to high propellant consumption. Thus, if the requirement is cost-effectiveness, this method is infeasible. A proposed EP system can provide flexibility of target overflight in a more persistent manner (compared to Single CP), more responsively (compared to Single Static), and for a lower cost (compared to Walker). However, EP is neither the fastest nor the least costly method and it sacrifices mission life for maneuverability. Therefore, for given a set of mission requirements, an electric, low-thrust propulsion spacecraft to perform orbital maneuvering for Earth observation may provide the right solution for a combination of cost effectiveness, responsiveness, and flexibility.

9 Conclusion

The current space culture of fielding large, expensive, and capable satellite systems is not sustainable and cannot satisfy the operational responsiveness desired by space users. Much as conventional warfare must adapt to today's counterinsurgency demands, conventional space operations must adapt to today's space environment. New initiatives such as Operationally Responsive Space and maneuvering satellites can help transition space culture to meet modern demands. The thesis of this dissertation provides one possible solution with highly efficient, maneuvering satellites to meet users' evolving requirements by overflight of selected ground targets.

The idea to overfly ground targets is not new; however, it is not done operationally in a repeated and sustained manner due to the high cost of maneuvers. Many operational satellites are maneuverable but they are designed to operate in 'static' parking orbits. The technology to maneuver efficiently is available and in use, but a concept of operation needs to be developed to include how the system should be employed. This concept of operations requires a new technology which provides the engineering and mathematical model to predict the specific maneuvers needed to achieve a target overflight given any initial conditions of time and spacecraft location and vehicle characteristics such as available thrust, dimensions, and mass. Low thrust electric engines enable satellites already in orbit to perform slow, precise, and highly efficient station-keeping maneuvers. The current CONOPS intends for the spacecraft to arrive at its orbital state and maintain its orbit for the life of the vehicle. Most spacecraft are designed in this manner so maneuvering is not considered. Using today's electric propulsion technology, it is

demonstrated in this dissertation that repeated maneuvers are not only feasible, but can also be responsive, timely, and inexpensive. No previous research provides the mathematical model or algorithm to achieve low-thrust maneuvering for target overflight with little to no restrictions.

Newberry analyzes the viability of a low-Earth orbit (LEO) electric propulsion (EP) system and its capability of changing time-over-target (TOT). Time-over-target is defined as the time a spacecraft overflies a ground target expressed in local time or GMT. A change in TOT indicates that the same target is overflown at a different time. Newberry's concept requires the orbit to be highly elliptical, inclined at 85 degrees, and above LEO altitudes. His simulations show that with simple, in-plane, posigrade, continuous thrusting, significant ground track changes including a specific TOT are possible. The foundation of the analysis is that the vehicle overflies the same ground target twice a day, which provides two opportunities to change TOT. The most effective in-plane change of satellite position is modifying the semi-major axis. Since the spacecraft can optimally thrust in or directly opposite the direction of travel, that is to speed up or slow down, this then provides Newberry with four options to change TOT on any given day. The argument is based on this specific highly-elliptical orbit to achieve the 24-hour TOT change within seven days of maneuvering. If the spacecraft is in any other orbit, the analysis is not valid. There is no such restriction or requirement for the work presented in this dissertation.

Guelman and Kogan consider minimum propellant flight profiles for low altitude, circular orbits to overfly a specific number of terrestrial targets in a given time period (Guelman, 1999: 313-321). Low altitudes provide significantly higher resolution or

smaller payloads, but this advantage is often negated by the poor coverage and narrow swath widths of a low-flier. Their analysis indicates that the application of EP to overfly desired targets is practical, because it combines high resolution with relatively short revisit times. The authors separate the problem into two steps – optimization and scheduling. Much like the algorithm applied in this dissertation, the control strategy is to modify the orbital period. There are discrete opportunities when a satellite can overfly terrestrial targets and those occur exactly when the rotating target coordinates cross the orbit plane. Therefore, a specific overfly time cannot be requested by the user unless there is a sufficiently long time period available or the intercept occurs by chance. The first step builds a piecewise optimal trajectory that connects two sequential overfly points and results in an analytical solution. The second step is global optimization for the entire trajectory by choosing the proper passage times. In their simulations, they consider a small spacecraft of 100 kg total mass, power input of 200 W, and an acceleration of no more than 1 mm/s^2. They demonstrate the overflight of 20 randomly selected sites over a period of 50 days and the associated propellant usage would allow a spacecraft with a modest initial propellant-mass-ratio to maneuver repeatedly and operate as long as 3 years. Their shortfalls are that they do not consider any perturbations by assuming a two-body dynamics and they require that a target list is known ahead of time such that an optimization flight profile is possible. Over sufficiently long periods of time (i.e. 50 days), the perturbations are large enough to cause significant ground track and position changes of the satellite. By not considering these effects, the error is likely to be large enough to miss target overflight all-together. Furthermore, the requirement that a list of 20 targets is known ahead of time eliminates the flexibility and timely response to user

requests. With an orbital altitude of approximately 800 km and a high resolution payload (such as GeoEye), no maneuvering is necessary for a revisit rate of three days, that is any terrestrial target can be imaged within three days. The algorithm in this dissertation is compatible with any dynamics model from the basic two-body to the most complex and there are no restrictions of prior knowledge of a target list.

Jean and de Lafontaine further Guelman's research by adding atmospheric drag and geopotential effects up to J_2 to the previous models and introducing a new quartic guidance law. They start in a sun-synchronous reference orbit and aim to always return to the reference after maneuvering. In essence it is a phasing maneuver that starts at a sun-synchronous altitude, then the satellite thrusts in one direction to gain or lose altitude, and finally returns to the reference altitude by thrusting in the opposite direction. The position difference between the phasing satellite and a non-maneuvering reference satellite results in the shift of ground track (overflight time and position). The authors conclude that EP is practical in both maintaining a reference orbit by countering atmospheric drag and modifying the reference orbit to overfly a terrestrial target. Their end product is an autonomous algorithm that could be implemented on a spacecraft to take advantage of this technology. The restrictions are that the spacecraft must perform a phasing maneuver and that it relies on atmospheric drag to return to its original orbital altitude. As discussed in Chapter 6, a phasing maneuver is not an efficient way to repeatedly change ground track and affect a target overflight, because propellant is used to first increase the orbital altitude and more propellant is used to return to the starting altitude. In Jean's case, atmospheric drag is used for the latter portion of the maneuver, which trades propellant savings for responsiveness. A sample simulation shows that a target overflight is

achieved within 13 days. The authors do not comment on how large a ground track change they achieved or if 13 days would provide global reach. Although their algorithm is very useful for maintaining a sunsynchronous orbit, it lacks responsiveness. The algorithm presented in this dissertation is not restricted to phasing maneuvers and achieves global reach in 2.5 days with today's available EP technology.

The remainder of this chapter summarizes the findings discussed in Chapters 5 through 8, which provide the mathematical model and algorithm for repeated low-thrust maneuvers with little to no restrictions. An extensive analysis demonstrates that both chemical and electrical propulsion systems have potential for a satellite to be maneuverable and responsive. Distances in excess of 10,000 km are achievable within 24 hours with a velocity change (ΔV) of 0.05 km/s for chemical propulsion and within 27 hours with a ΔV of 0.1 km/s for electric propulsion. These distances and the ability to calculate the ΔV required to achieve a tasked overflight represent a novel capability for satellite operations. Terrestrial distance equations are developed and used to demonstrate a high level of accuracy in predicting a system's maneuvering capability. These equations are useful in determining the achievable terrestrial distance given the propellant budget, original orbit, and time available to reach a target.

Analytical expressions for the performance metrics of change in Time of Overflight (or Time over Target, Δt), inclination (Δi), and right ascension of the ascending node (ΔRAAN, $\Delta\Omega$) are derived and presented for electric propulsion (EP) maneuvers. These expressions are:

$$\Delta t = (u_2 - u_0)\sqrt{\frac{a_0^3}{\mu}} - \frac{\sqrt{\mu}}{A}\left[\left(\frac{1}{a_0^2} + \frac{4}{\mu}A(u_1 - u_0)\right)^{1/4} - a_0^{-1/2}\right] - (u_2 - u_1)\sqrt{\frac{a^3}{\mu}} \tag{9.1}$$

$$\Delta i = \sqrt{\frac{a}{\mu}}\sin(nt_f)\frac{A\sin\theta}{n} \tag{9.2}$$

$$\Delta\Omega = \sqrt{\frac{a}{\mu}}(1-\cos(nt_f))\frac{A\sin\theta}{n\sin i} \tag{9.3}$$

Previously developed algorithms are used to analyze several test scenarios and validate the analytical expressions. With the derived expressions available, mission planners can quickly evaluate maneuvering effects and conduct trade studies to decide on a best course of action depending on the spacecraft's mission. These efficient maneuvers can be effective but may require slightly longer lead times of 2-2.5 days to reach any target within its coverage area. Out-of-plane maneuvers also have analytical solutions for predicting the effects of low-thrust maneuvers, but are shown to be significantly less effective for the timely overflight problem. The derived equations quickly and accurately predict the amount of change in inclination and RAAN possible when provided with a level of thrust and vehicle characteristics. Equation 9.1 is the cornerstone of the algorithm presented in Chapters 7 and 8 and represents an important contribution that made the remainder of the analysis possible.

The most significant contribution of this dissertation is the development of an algorithm to compute the requirements for an overflight of any terrestrial target using a single low-Earth orbiting satellite. A single equation that computes the time change between a maneuvering and reference ground track is the centerpiece of the algorithm.

With it, it is possible to compute the thrust-coast maneuver to achieve a commanded overflight. Once achieved, the system can remain in the new orbit or perform another maneuver to fulfill a new mission. The algorithm as it is currently used may not generate the most time or propellant efficient maneuver, because it blends both metrics to provide propellant efficiency and timeliness. It is not possible to achieve the optimal solution for each metric simultaneously as one trades for the other, but a blend as it is used in this algorithm can satisfy both metrics without being the optimal solution. Using current technology, one such vehicle can perform approximately 40 maximum ΔV maneuvers in the worst case. Even with low thrust, a worst case scenario in which the target is furthest away from the reference ground track can be reached in 2.5 days.

Lastly, a comparative analysis for an overflight of any terrestrial target as it could be done with four different space observation systems – namely a Walker constellation, a single non-maneuvering, a single maneuvering chemical propulsion (CP), and a single maneuvering EP spacecraft – is performed. Each notional system is developed with equivalent characteristics and then compared to point out benefits and drawbacks for each technology. The work on EP and CP system reveals that higher efficiency, despite lower thrust, is more effective and feasible for a low-Earth orbit (LEO) satellite designed for repeated maneuvering. After accounting for a much larger power subsystem and increased drag, the ratio of EP to CP maneuvers is 5.3:1 for equivalent systems.

Operational altitude plays a critical role. To shorten the revisit rate, there are only a handful of altitudes at which a static or maneuvering CP system can operate effectively (i.e. 310, 500, 640, 783 km), greatly restricting flexibility. Furthermore, given the smaller propellant budgets at higher altitudes as a result of less drag, chemical maneuvering at

500 km is very propellant-intensive, thereby restricting the operational domain further to a single altitude of 310 km. The notional EP system could operate well between 300 and 400 km providing users with almost 40 maneuvers for tasked overflights at a rate of once per month and a slightly shorter system life of 3.2 years (vs. 5 years).

Returning to the motivation of this work to find an alternative system capable of lowering cost, complexity, acquisition and deployment time, and time to target overflight, electric propulsion is a feasible, proven, and powerful solution. This technology is neither the fastest nor the least expensive and it sacrifices mission life for maneuverability, however, for the given set of mission requirements, an electric, low-thrust propulsion spacecraft to perform orbital maneuvering for target overflight provides the right capability for a combination of cost effectiveness, responsiveness, and flexibility with some operational restrictions.

A. Appendix A – Nomenclature

$\bar{A}$ = acceleration vector

A = perturbing acceleration, km/s^2

a = semi-major axis, km

a_0 = initial semi-major axis, km

a_h = normal acceleration component, km/s^2

a_r = radial acceleration comp in local-vertical, local-horizontal (LVLH), km/s^2

a_θ = acceleration comp completing the right-handed coordinate system, km/s^2

AP = aperture diameter, m

D = terrestrial distance, km

$D_{100\text{km}}$ = distance at 100 km altitude, km

E = eccentric anomaly, rad

e = eccentricity

g_s = gravity at sea-level, m/s^2

H = Haversine formula

h = angular momentum, km^2/s

$\hat{h}$ = normal component wrt orbital plane of the LVLH frame

i = inclination, degrees

M = mean anomaly, rad

m_0 = initial spacecraft mass, kg

$\dot{m}$ = mass flow rate, kg/s

Δm = change in mass due to maneuvering, kg

m^- = mass of vehicle before thrust impulse, kg

m^+ = mass of vehicle after thrust impulse, kg

n = mean motion, rad/s

P = orbital period, s

p = semi-latus rectum, km

R = distance from center of Earth, radius, km

$\overline{R}$ = inertial position vector of satellite measured from Earth's center, km

R_a = apogee radius, km

R_p = perigee radius, km

$R_\oplus$ = Earth's radius, km

r = distance of satellite to Earth's center, km

$\hat{r}$ = radial component of the local-vertical, local-horizontal frame

Res = resolution, m

SR = slant range, km

T = thrust magnitude, N

t = time, s

t_0 = initial time, s

t_f = final time, s

Δt = change in over-flight time, s

Δt_m = time elapsed from beginning of maneuver to target overflight, s

$\boldsymbol{u}$ = thrust control vector, components in degrees

u = argument of latitude, degrees

u_0 = initial argument of latitude, degrees

u_1 = argument of latitude after thrust period, degrees

u_2 = final argument of latitude, degrees

u = speed, km/s

$\bar{V}$ = velocity vector

V = velocity, km/s

ΔV = change in velocity or propellant budget, km/s

${}^{R}V$ = magnitude of relative velocity with respect to surrounding air particles, km/s

α = angle of line-of-apsides rotation, degrees

γ_0 = flight path angle at atmospheric entry, degrees

γ_g = Greenwich sidereal time, rad

ε = specific total mechanical energy, km^2/s^2

ζ = wavelength in electromagnetic spectrum, μm

θ = out-of-plane thrust angle wrt $\hat{r}$ - $\hat{\theta}$ plane, degrees

$\hat{\theta}$ = tangential component of the local-vertical, local-horizontal frame

λ = latitude, degrees

λ_{tgt} = target latitude, degrees

μ = gravitational parameter, for Earth 3.98601 x10^5 km^3/s^2

ν = true anomaly, rad

ρ = atmospheric density, kg/m^3

φ = longitude, degrees

φ_{tgt} = target longitude, degrees

$\boldsymbol{\psi}$ = thrust control vector, components in degrees

ψ = in-plane thrust angle in $\hat{r}$-$\hat{\theta}$ plane, degrees

Ω = right ascension of the ascending node, degrees

ω = argument of perigee, degrees

$\omega_{\oplus}$ = Earth's angular velocity magnitude, rad/s

$\bar{\omega}_{\oplus}$ = Earth's angular velocity vector, rad/s

B. Appendix B – 2-Body Assumption

In Chapter 5, the analysis is mostly based on the 2-Body dynamics assumption to reduce the complexity and the processing time. The following appendix shows the analysis done to validate the assumptions made. Satellite Tool Kit and Microsoft Excel are the main software tools utilized. Since impulsive maneuvers (CP) are more coarse and less accurately predictable compared to continuous thrust (EP), the analysis is done using the former method.

1. Set up maneuvering scenario in STK (start date is arbitrary, but chosen to be 7/18/2011 1600 GMT)
2. Add a non-maneuvering reference satellite ($a = 6678.14$ km, $i = 60°$, $e = 0$, $\Omega = \omega = \nu = 0°$) using a high precision propagator (HPOP, SGP4 or J4)
3. Add a maneuvering satellite with the same initial conditions using Astrogator with a ΔV of 0.01 km/s
4. Propagate for 24 hours (column C in spreadsheet on page B-2)
5. Get LLA (latitude, longitude, altitude) report and export to Excel (columns D and E for reference; columns G and H for maneuvering)
6. Use distance equation (Chapter 5, Eq. (24)) to compute ground distance between reference and maneuvering satellites (column I)
7. Change reference and maneuvering satellite propagators to TwoBody, propagate for 24 hours and export LLA report to Excel
8. Use Chapter 5, Eq. (24) to compute ground distance between reference and maneuvering satellites (column J)
9. Compute error between reference and maneuvering data set for HPOP and TwoBody propagators (column K and L)
10. Repeat steps 1-9 for different altitudes (500, 1000 km)
11. Repeat steps 1-10 for different ΔVs (0.05, 0.1 km/s), once done, there should be a total of 9 comparisons

A	B	C	D	E	F	G	H	I	J	K	L
longitude of a maneuvering satellite after an impulse and then coasting for the remaining time (total time period is 24 hrs). **Validation of 2-Body Model versus HPOP.**	dV=0.01 km/s	Time (UTCG)	RLat (deg)	RLon (deg	Time (min	Lat (deg)	Lon (deg)	Distance (KM)	TB Distance (KM)	Delta Distance (KM)	Delta %
		4:00:00 PM	0.067	-175.966	0	0.067	-175.966	0	0	0	N/A
Maneuvering satellite		4:01:00 PM	3.532	-174.226	1	3.537	-174.223	0.648046036	0.555594257	0.092451779	0.142662
Using STK's Astrogator		4:02:00 PM	6.993	-172.471	2	7.002	-172.466	1.14281643	1.14281643	0	0
Initial State: i=60 deg, alt=300 km, om=Om=nu=0		4:03:00 PM	10.445	-170.686	3	10.458	-170.678	1.689628572	1.68963003	1.45813E-06	8.63E-07
e = 0		4:04:00 PM	13.882	-168.856	4	13.899	-168.846	2.176800172	2.176800172	0	0
a = 6678.14 km		4:05:00 PM	17.301	-166.964	5	17.321	-166.951	2.617304171	2.617308129	3.9583E-06	1.51E-06
dV = Varied		4:06:00 PM	20.694	-164.992	6	20.717	-164.977	2.995817516	3.091287967	0.095470451	0.031868
Maneuver: Impulsive		4:07:00 PM	24.056	-162.92	7	24.081	-162.902	3.326774887	3.42023933	0.093464443	0.028095
Propagate: 86400s		4:08:00 PM	27.378	-160.724	8	27.406	-160.704	3.686798689	3.64857779	0.038220899	0.010367
Characteristics		4:09:00 PM	30.654	-158.38	9	30.682	-158.356	3.868154259	3.812175475	0.055978784	0.014472
Dry mass: 700 kg		4:10:00 PM	33.873	-155.856	10	33.901	-155.83	3.93110184	3.93110184	0	0
Drag area: 10 sq m		4:11:00 PM	37.022	-153.119	11	37.049	-153.091	3.897509535	3.929021098	0.031511563	0.008085
Fuel mass: 300 kg		4:12:00 PM	40.088	-150.128	12	40.114	-150.099	3.800294807	3.716392247	0.083902561	0.022078
Ion engine: Thrust 200N, Isp 230s		4:13:00 PM	43.053	-146.839	13	43.077	-146.809	3.614043425	3.53268971	0.081353715	0.02251
		4:14:00 PM	45.897	-143.2	14	45.917	-143.17	3.214582123	3.159109737	0.055472386	0.017256
Reference satellite		4:15:00 PM	48.593	-139.154	15	48.608	-139.127	2.593035441	2.721017459	0.127982018	0.049356
Using STK's TwoBody		4:16:00 PM	51.11	-134.644	16	51.121	-134.62	2.074273204	2.074126791	0.000146413	7.06E-05
Initial State: i=60 deg, alt=300 km, om=Om=nu=0		4:17:00 PM	53.41	-129.612	17	53.416	-129.596	1.252848232	1.252679399	0.000168833	0.000135
e = 0		4:18:00 PM	55.451	-124.015	18	55.453	-124.01	0.38583133	0.385766018	6.53128E-05	0.000169
a = 6678.14 km		4:19:00 PM	57.184	-117.833	19	57.181	-117.843	0.688803859	0.741878629	0.053074769	0.077054
		4:20:00 PM	58.557	-111.089	20	58.551	-111.12	1.918075234	1.917160866	0.000914368	0.000477
		4:21:00 PM	59.521	-103.865	21	59.515	-103.922	3.283611114	3.281277268	0.002333847	0.000711
		4:22:00 PM	60.037	-96.306	22	60.034	-96.392	4.787884388	4.78326793	0.004616458	0.000964
		4:23:00 PM	60.082	-88.613	23	60.085	-88.73	6.497045201	6.429157169	0.067888032	0.010449
		4:24:00 PM	59.654	-81.011	24	59.666	-81.157	8.308363606	8.279740828	0.028622778	0.003445
		4:25:00 PM	58.771	-73.707	25	58.796	-73.88	10.35017532	10.27927883	0.070896495	0.00685
		4:26:00 PM	57.47	-66.861	26	57.512	-67.055	12.49868391	12.43820392	0.06047999	0.004839
		4:27:00 PM	55.8	-60.565	27	55.861	-60.775	14.765083	14.69193698	0.073146017	0.004954
		4:28:00 PM	53.811	-54.853	28	53.894	-55.076	17.29492896	17.15559537	0.139333583	0.008056
		4:29:00 PM	51.552	-49.713	29	51.659	-49.944	19.90107952	19.80865478	0.092424746	0.004644
		4:30:00 PM	49.069	-45.104	30	49.2	-45.341	22.57182866	22.54471696	0.027111694	0.001201
		4:31:00 PM	46.399	-40.971	31	46.557	-41.213	25.53512439	25.50768059	0.027443799	0.001075
		4:32:00 PM	43.575	-37.256	32	43.761	-37.501	28.56721233	28.45942974	0.10778259	0.003773
		4:33:00 PM	40.624	-33.901	33	40.839	-34.149	31.75231782	31.64161763	0.11070019	0.003486
		4:34:00 PM	37.568	-30.855	34	37.813	-31.105	35.01528163	34.87155399	0.143727636	0.004105
		4:35:00 PM	34.426	-28.069	35	34.701	-28.323	38.4188087	38.30479212	0.114016583	0.002968
		4:36:00 PM	31.211	-25.505	36	31.517	-25.762	41.87084278	41.81136905	0.059473735	0.00142

Summary

Altitude (km)	delta-V (km/s) 0.01	0.05	0.1
300	Avg % Error: 1.23% Max *D* Error: 63.8 km	Avg % Error: 0.33% Max *D* Error: 95.0 km	Avg % Error: 0.29% Max *D* Error: 138.1 km
500	Avg % Error: 0.24% Max *D* Error: 11.4 km	Avg % Error: 0.21% Max *D* Error: 36.3 km	Avg % Error: 0.18% Max *D* Error: 48.0 km
1000	Avg % Error: 0.22% Max *D* Error: 7.3 km	Avg % Error: 0.18% Max *D* Error: 31.7 km	Avg % Error: 0.15% Max *D* Error: 37.2 km

C. Appendix C – CP Reachability

In Chapter 5, the baseline analysis uses CP maneuvers with the 2-Body assumption. The reachability is quantified using Satellite Tool Kit and Microsoft Excel. After defining some basic vehicle characteristics, a single impulsive maneuver is simulated at the initial time and then propagated for 24 hours. The accumulated distance of the maneuvering satellite is measured with respect to the reference. The data is used to formulate equations predicting reachability of a CP maneuvering satellite measured by ground distance.

1. Set up maneuvering scenario in STK (start date is arbitrary, but chosen to be 6/22/2011 1600 GMT)
2. Add a non-maneuvering reference satellite (a = 6478.14 km, i = 60°, e = 0, $\Omega = \omega = \nu = 0°$) using TwoBody propagator
3. Add a maneuvering satellite with the same initial conditions using Astrogator with a ΔV of 0.01 km/s
4. Propagate for 24 hours (column C in spreadsheet on page C-2)
5. Get LLA (latitude, longitude, altitude) report and export to Excel (columns D and E for reference; columns F and G for maneuvering)
6. Use distance equation (Chapter 5, Eq. (5.24)) to compute ground distance between reference and maneuvering satellites (column I)
7. Graph the data and apply linear regression fit for each set
8. Resultant equation is a prediction of distance as a result of an impulsive maneuver, use equation to compute distance with respect to time
9. Use D_{100km} equation (Chapter 5, Eq. (5.25)) to compute predicted ground distance between reference and maneuvering satellites (column J)
10. Compute error between simulated and computed data (column K and L)
11. Repeat steps 1-10 for different altitudes (300, 500, 1000, 1500 km)
12. Repeat steps 1-11 for different ΔVs (0.05, 0.1, 0.15 km/s)

A	B	C	D	E	F	G	H	I	J	K	L
		Time	Lat (deg)	Lon (deg)	MLat (deg)	MLon (deg)	Time (min)	Distance (KM)	Calculated Distance (KM)	Delta %	Delta D (KM)
		16:00:00	0.066	-150.34	0.066	-150.34	0	0	14.98	N/A	14.98
Maneuvering satellite		16:01:00	3.694	-148.507	3.699	-148.504	1	0.648015479	11.288508	16.4201	10.6404925
Using STK's Astrogator		16:02:00	7.317	-146.656	7.326	-146.651	2	1.142627274	8.006728	6.0073	6.86410073
Initial State: i=60 deg, perigee=100 km, om=Om=nu=0		**Data not displayed**									
e = 0		18:00:00	34.328	-23.519	35.689	-24.791	120	190.5829841	211.8473	0.11158	21.2643159
a = 6478.14 km		18:01:00	30.967	-20.843	32.384	-22.044	121	194.2712636	213.6178	0.09959	19.3465364
dV = 0.01		18:02:00	27.542	-18.366	29.012	-19.509	122	198.1030022	215.3883	0.08725	17.2852978
Maneuver: Impulsive		18:03:00	24.064	-16.054	25.584	-17.151	123	202.0444663	217.1588	0.07481	15.1143337
Propagate: 86400s		18:04:00	20.545	-13.876	22.111	-14.939	124	206.0186428	218.9293	0.06267	12.9106572
Characteristics		18:05:00	16.99	-11.807	18.601	-12.844	125	210.1013284	220.6998	0.05044	10.5984716
Dry mass: 700 kg		18:06:00	13.41	-9.824	15.062	-10.844	126	214.0756064	222.4703	0.03921	8.39469356
Drag area: 10 sq m		18:07:00	9.808	-7.906	11.501	-8.917	127	218.2751195	224.2408	0.02733	5.96568049
Fuel mass: 300 kg		18:08:00	6.192	-6.034	7.923	-7.044	128	222.4171318	226.0113	0.01616	3.5941682
CP: Thrust 200N, Isp 230s		18:09:00	2.567	-4.19	4.334	-5.208	129	226.6516008	227.7818	0.00499	1.13019918
		18:10:00	-1.061	-2.359	0.739	-3.391	130	230.7107964	229.5523	0.00502	1.15849644
Reference satellite		18:11:00	-4.688	-0.522	-2.857	-1.578	131	234.9023746	231.3228	0.01524	3.57957456
Using STK's TwoBody		18:12:00	-8.308	1.336	-6.449	0.249	132	238.9489514	233.0933	0.02451	5.85565137
Initial State: i=60 deg, perigee=100 km, om=Om=nu=0		**Data not displayed**									
Eccentricity: e=0		15:50:00	-10.986	37.535	8.779	26.061	1430	2537.94692	2531.2023	0.00266	6.74462004
a = 6478.14 km		15:51:00	-14.581	39.473	5.192	27.905	1431	2541.822191	2532.9728	0.00348	8.84939132
		15:52:00	-18.154	41.481	1.598	29.725	1432	2545.465911	2534.7433	0.00421	10.7226113
		15:53:00	-21.698	43.583	-1.998	31.538	1433	2548.95741	2536.5138	0.00488	12.4436104
		15:54:00	-25.205	45.802	-5.592	33.359	1434	2552.181228	2538.2843	0.00545	13.8969281
		15:55:00	-28.666	48.164	-9.178	35.207	1435	2555.004835	2540.0548	0.00585	14.9500354
		15:56:00	-32.072	50.702	-12.75	37.096	1436	2557.892637	2541.8253	0.00628	16.0673367
		15:57:00	-35.409	53.451	-16.304	39.046	1437	2560.378189	2543.5958	0.00655	16.7823887
		15:58:00	-38.664	56.455	-19.834	41.077	1438	2562.723672	2545.3663	0.00677	17.3573723
		15:59:00	-41.818	59.76	-23.331	43.21	1439	2564.971584	2547.1368	0.00695	17.8347841
		16:00:00	-44.849	63.424	-26.79	45.47	1440	2567.00706	2548.9073	0.00705	18.0997602

The data of importance on page E-2 is in the final two columns (K and L). Due to the way the error measure is computed, the percentage error is initially very large although the distance error is only a few kilometers. This continues to be the case for the first 100 data points. After 125 min (or the first 125 data points), the percentage error drops below 5% and continues to decrease. At the end of the simulation period, the error is less than 20 km in physical terms for an achieved distance of over 2500 km. The percentage error is below 1%.

Further, the final equation accounting for time, altitude, and ΔV (Chapter 5, Eq. (5.27)) is validated for accuracy. Different combinations of altitude and ΔV are inserted into the equation and compared to simulated STK data. The findings show that overall error is less than 3% in all cases.

D. Appendix D – EP Reachability

In Chapter 5, the analysis expands to include EP maneuvers under the 2-Body assumption. The reachability is quantified using Satellite Tool Kit and Microsoft Excel. After defining some basic vehicle characteristics, a thrusting period is begins at the initial time and continues until the desired amount of ΔV is expended. Then the scenario is propagated for 24 hours. The accumulated distance of the maneuvering satellite is measured with respect to the reference. The data is used to formulate equations predicting reachability of a EP maneuvering satellite measured by ground distance.

1. Set up maneuvering scenario in STK (start date is arbitrary, but chosen to be 6/22/2011 1600 GMT)
2. Add a non-maneuvering reference satellite (a = 6478.14 km, i = 60°, e = 0, $\Omega = \omega = \nu$ = 0°) using TwoBody propagator
3. Add a maneuvering satellite with the same initial conditions using Astrogator
4. Select continuous maneuver and add an engine model by duplicating one of the models in the STK database; specify thrust (ex. 1 N) and I_{sp} (2000 s) only by selecting the duplicated model; use this custom model for the following scenario
5. Enter the length of the trusting period; for a 1-N thruster and a 1000-kg wet mass satellite, the acceleration is 1e-6 km/s^2; at this acceleration, the thrusting period is 10000 s for a ΔV of 0.01 km/s (50000 s for 0.05 km/s and 100000 s for 0.1 km/s)
6. Propagate for a total of 24 hours (column C in spreadsheet on page C-2)
7. Get LLA (latitude, longitude, altitude) report and export to Excel (columns D and E for reference; columns F and G for maneuvering)
8. Use distance equation (Chapter 5, Eq. (5.24)) to compute ground distance between reference and maneuvering satellites (column I)
9. Graph the data and apply linear regression fit for each set
10. Resultant equation is a prediction of distance as a result of an impulsive maneuver, use equation to compute distance with respect to time

11. Use D_{100km} equation (Chapter 5, Eq. (5.28)) to compute predicted ground distance between reference and maneuvering satellites (column J)

12. Compute error between simulated and computed data (column K and L)

13. Repeat steps 1-12 for different altitudes (300, 500, 1000, 1500 km)

14. Repeat steps 1-13 for different ΔVs (0.05, 0.1, 0.15 km/s)

A	B	C	D	E	F	G	H	I	J	K	L
		Time	MLat (deg)	MLon (deg)	Lat (deg)	Lon (deg)	Time (min)	Distance (KM)	Calculated Distance (KM)	Delta %	Delta D (KM)
		16:00:00	0.067	-175.966	0.067	-175.966	0	0	-59.437	N/A	59.437
Maneuvering satellite		16:01:00	3.695	-174.133	3.695	-174.133	1	0	-58.3352001	N/A	58.3352001
Using STK's Astrogator		16:02:00	7.317	-172.282	7.317	-172.282	2	0	-57.2328008	N/A	57.2328008
Initial State: i=60 deg, peri=100 km, om=Om=nu=0		**Data not displayed**									
e = 0		17:40:00	46.061	-164.544	46.311	-164.172	100	39.9107	53.613	0.343323	13.7022682
a = 6478.14 km		17:41:00	48.866	-160.274	49.104	-159.853	101	40.5482	54.7717699	0.350781	14.223549
dV = 0.01 (thrust for 10000 s)		17:42:00	51.473	-155.49	51.695	-155.012	102	41.2322	55.9310792	0.356491	14.6989101
Maneuver: Continuous		17:43:00	53.837	-150.129	54.038	-149.588	103	41.8752	57.0909273	0.363358	15.2156855
Propagate: Until Distance Achieved		**Data not displayed**									
Characteristics		21:00:00	11.988	-78.205	9.691	-76.831	300	296.226	295.313	0.003083	0.91338513
Dry mass: 700 kg		21:01:00	8.39	-76.313	6.075	-74.96	301	297.549	296.5677099	0.003298	0.98129041
Drag area: 10 sq m		21:02:00	4.78	-74.461	2.45	-73.118	302	298.887	297.8228392	0.003562	1.06464898
Fuel mass: 300 kg		21:03:00	1.164	-72.629	-1.178	-71.286	303	300.193	299.0783873	0.003712	1.11418019
EP: Thrust 1N, Isp 1500s		21:04:00	-2.455	-70.804	-4.805	-69.449	304	301.478	300.3343536	0.003793	1.14348276
		21:05:00	-6.07	-68.967	-8.425	-67.59	305	302.722	301.5907375	0.003737	1.13119075
Reference satellite		21:06:00	-9.676	-67.102	-12.033	-65.692	306	303.966	302.8475384	0.003679	1.11842806
Using STK's TwoBody		21:07:00	-13.268	-65.192	-15.622	-63.736	307	305.108	304.1047557	0.003288	1.00317729
Initial State: i=60 deg, peri=100 km, om=Om=nu=0		**Data not displayed**									
Eccentricity: e=0		20:20:00	-31.386	-41.686	-46.449	-25.059	1700	2198.52	2188.813	0.004417	9.7102914
a = 6478.14 km		20:21:00	-34.729	-38.991	-49.234	-20.716	1701	2198.31	2190.06729	0.003751	8.24640394
		20:22:00	-37.993	-36.054	-51.813	-15.849	1702	2198.12	2191.321159	0.003092	6.79652279
		20:23:00	-41.16	-32.826	-54.143	-10.396	1703	2198.04	2192.574607	0.002487	5.46681867
		20:24:00	-44.211	-29.255	-56.172	-4.313	1704	2198.03	2193.827634	0.001914	4.20712548
		20:25:00	-47.118	-25.279	-57.843	2.408	1705	2198.26	2195.080238	0.001448	3.18396919
		20:26:00	-49.85	-20.833	-59.097	9.714	1706	2198.58	2196.332418	0.001021	2.24518727
		20:27:00	-52.37	-15.851	-59.883	17.48	1707	2199	2197.584176	0.000642	1.41237833
		20:28:00	-54.629	-10.275	-60.163	25.506	1708	2199.79	2198.835509	0.000434	0.95550367
		20:29:00	-56.578	-4.067	-59.923	33.542	1709	2200.67	2200.086417	0.000267	0.58726873
		20:30:00	-58.156	2.769	-59.175	41.336	1710	2201.83	2201.3369	0.000223	0.49209432

E. Appendix E – Global Coverage

In Chapter 7.4, the discussion turns to EP maneuvers and the time required for them achieve global reach. In this amount of time, the satellite can reach any target inside its coverage area from any starting position and time. It is effectively the time to overflight measure that can be compared to the revisit rate of a non-maneuvering spacecraft.

This analysis makes use of two things – 1. Maneuvering and 2. Nodal regression. The control authority of a system is determined by the thrust of its propulsion, the initial state, and the amount of time to overflight. The amount of control as a result of maneuvering is accurately computed using Chapter 7, Eq. (18). Nodal regression is a function of altitude and inclination and it is characterized by Chapter 7, Eq. (20). The following graphs summarize the effects of both components measured by longitudinal change (ΔLong) per day. For EP maneuvers, the control authority increases with altitude and available thrust and can be as much as12.5°/day for the systems under consideration.

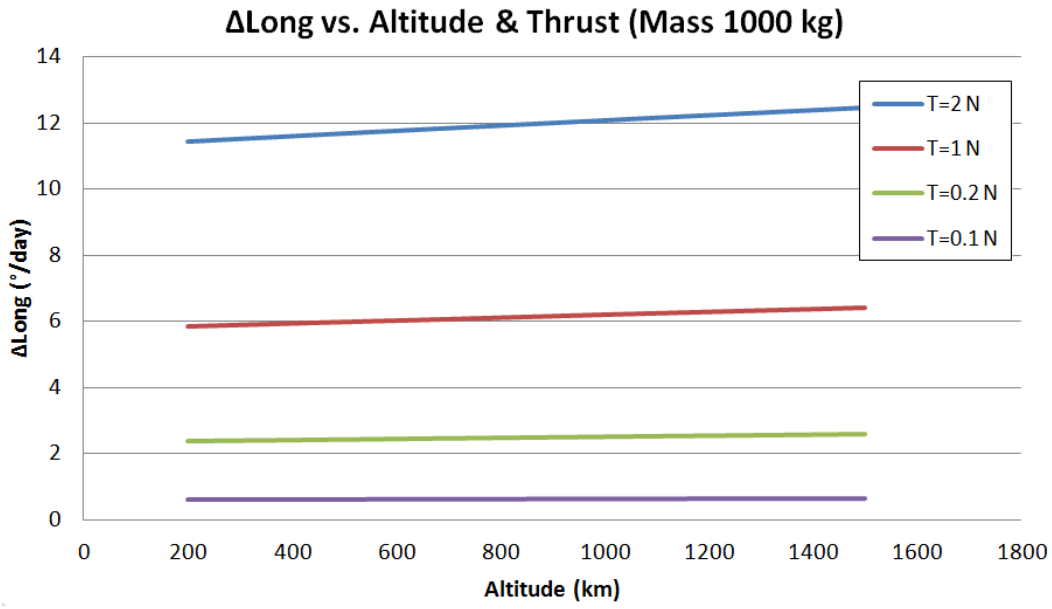

Nodal regression can also be quite significant and can change the node (or the longitude of the satellite ground track) by as much as 5-9° per day.

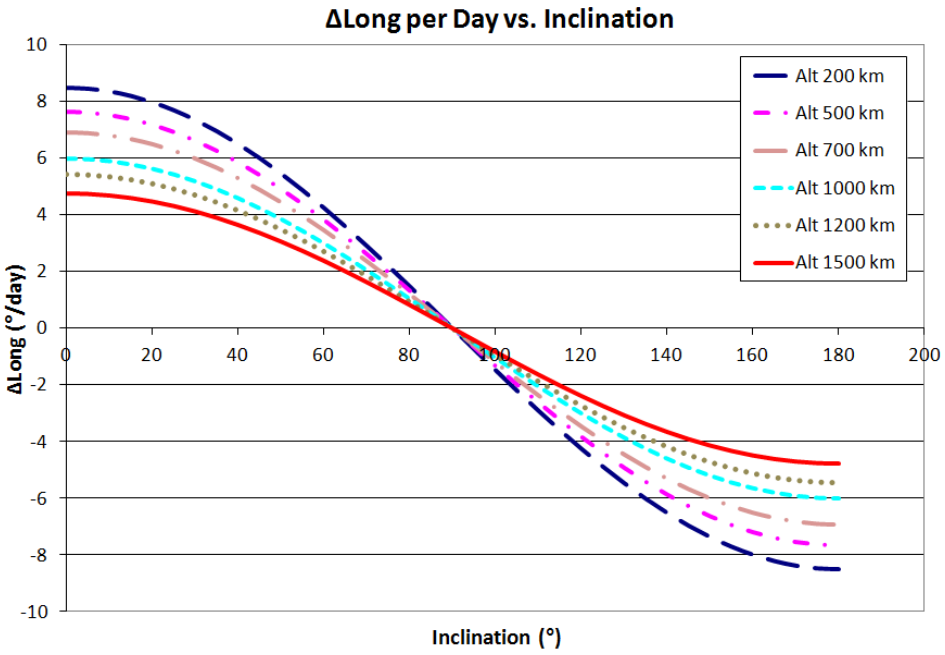

The following process is used to determine the amount of time required for global coverage:

1. Select an appropriate thrust level to determine the acceleration (A=1e-6 km/s^2 used)
2. Establish time available for target overflight (column C in spreadsheet on E-3)
3. Compute Δt using Chapter 7, Eq. (18) (every other column starting with D)
4. Compute $\Delta Long$ using Chapter 7, Eq. (19) (every other column starting with E)
5. Compute $\Delta Long$ (nodal regression) using Chapter 7, Eq. (20)
6. Combine the two effects to determine total $\Delta Long$ per day
7. Divide into longitudinal separation between orbital passes at the selected altitude

C	D	E	F	G	H	I	J	K	L	M	N	O
	Altitude 200 km		Altitude 500 km		Altitude 700 km		Altitude 1000 km		Altitude 1200 km		Altitude 1500 km	
Tavail (hrs)	Δt (min)	ΔLong (deg)	Δt (min)	ΔLong (deg)	Δt (min)	ΔLong (deg)	Δt (min)	ΔLong (deg)	Δt (min)	ΔLong (deg)	Δt (min)	ΔLong (deg)
2	1.66E-01	4.16E-02	1.70E-01	4.26E-02	1.72E-01	4.32E-02	1.76E-01	4.41E-02	1.78E-01	4.47E-02	1.82E-01	4.56E-02
3	3.73E-01	9.36E-02	3.82E-01	9.57E-02	3.87E-01	9.71E-02	3.95E-01	9.91E-02	4.01E-01	1.00E-01	4.09E-01	1.02E-01
4	6.63E-01	1.66E-01	6.78E-01	1.70E-01	6.88E-01	1.72E-01	7.02E-01	1.76E-01	7.11E-01	1.78E-01	7.25E-01	1.82E-01
5	1.03E+00	2.59E-01	1.06E+00	2.65E-01	1.07E+00	2.69E-01	1.10E+00	2.75E-01	1.11E+00	2.78E-01	1.13E+00	2.84E-01
6	1.49E+00	3.73E-01	1.52E+00	3.82E-01	1.54E+00	3.87E-01	1.58E+00	3.95E-01	1.60E+00	4.00E-01	1.63E+00	4.08E-01
7	2.02E+00	5.07E-01	2.07E+00	5.19E-01	2.10E+00	5.26E-01	2.14E+00	5.37E-01	2.17E+00	5.44E-01	2.21E+00	5.55E-01
8	2.64E+00	6.62E-01	2.70E+00	6.77E-01	2.74E+00	6.87E-01	2.80E+00	7.01E-01	2.83E+00	7.10E-01	2.89E+00	7.24E-01
9	3.34E+00	8.37E-01	3.41E+00	8.56E-01	3.46E+00	8.68E-01	3.53E+00	8.86E-01	3.58E+00	8.98E-01	3.65E+00	9.15E-01
10	4.12E+00	1.03E+00	4.21E+00	1.06E+00	4.27E+00	1.07E+00	4.36E+00	1.09E+00	4.42E+00	1.11E+00	4.50E+00	1.13E+00
11	4.98E+00	1.25E+00	5.09E+00	1.28E+00	5.16E+00	1.29E+00	5.27E+00	1.32E+00	5.34E+00	1.34E+00	5.44E+00	1.36E+00
12	5.92E+00	1.48E+00	6.05E+00	1.52E+00	6.14E+00	1.54E+00	6.26E+00	1.57E+00	6.35E+00	1.59E+00	6.47E+00	1.62E+00
13	6.94E+00	1.74E+00	7.09E+00	1.78E+00	7.19E+00	1.80E+00	7.34E+00	1.84E+00	7.44E+00	1.86E+00	7.58E+00	1.90E+00
14	8.04E+00	2.01E+00	8.22E+00	2.06E+00	8.33E+00	2.09E+00	8.50E+00	2.13E+00	8.62E+00	2.16E+00	8.78E+00	2.20E+00
15	9.22E+00	2.31E+00	9.42E+00	2.36E+00	9.55E+00	2.40E+00	9.75E+00	2.44E+00	9.88E+00	2.48E+00	1.01E+01	2.52E+00
16	1.05E+01	2.63E+00	1.07E+01	2.68E+00	1.09E+01	2.72E+00	1.11E+01	2.78E+00	1.12E+01	2.81E+00	1.14E+01	2.87E+00
17	1.18E+01	2.96E+00	1.21E+01	3.03E+00	1.22E+01	3.07E+00	1.25E+01	3.13E+00	1.27E+01	3.17E+00	1.29E+01	3.24E+00
18	1.32E+01	3.32E+00	1.35E+01	3.39E+00	1.37E+01	3.44E+00	1.40E+01	3.51E+00	1.42E+01	3.55E+00	1.45E+01	3.62E+00
19	1.47E+01	3.69E+00	1.51E+01	3.77E+00	1.53E+01	3.83E+00	1.56E+01	3.90E+00	1.58E+01	3.96E+00	1.61E+01	4.03E+00
20	1.63E+01	4.09E+00	1.67E+01	4.18E+00	1.69E+01	4.23E+00	1.72E+01	4.32E+00	1.75E+01	4.38E+00	1.78E+01	4.46E+00
21	1.80E+01	4.50E+00	1.83E+01	4.60E+00	1.86E+01	4.66E+00	1.90E+01	4.76E+00	1.92E+01	4.82E+00	1.96E+01	4.91E+00
22	1.97E+01	4.93E+00	2.01E+01	5.04E+00	2.04E+01	5.11E+00	2.08E+01	5.22E+00	2.11E+01	5.29E+00	2.15E+01	5.39E+00
23	2.15E+01	5.39E+00	2.20E+01	5.50E+00	2.23E+01	5.58E+00	2.27E+01	5.70E+00	2.30E+01	5.77E+00	2.35E+01	5.88E+00
24	2.34E+01	5.86E+00	2.39E+01	5.99E+00	2.42E+01	6.07E+00	2.47E+01	6.20E+00	2.50E+01	6.28E+00	2.55E+01	6.40E+00
25	2.53E+01	6.35E+00	2.59E+01	6.49E+00	2.63E+01	6.58E+00	2.68E+01	6.72E+00	2.71E+01	6.80E+00	2.77E+01	6.93E+00
26	2.74E+01	6.86E+00	2.80E+01	7.01E+00	2.84E+01	7.11E+00	2.89E+01	7.26E+00	2.93E+01	7.35E+00	2.99E+01	7.49E+00
27	2.95E+01	7.39E+00	3.01E+01	7.55E+00	3.06E+01	7.66E+00	3.12E+01	7.82E+00	3.16E+01	7.92E+00	3.22E+01	8.07E+00
28	3.17E+01	7.94E+00	3.24E+01	8.12E+00	3.28E+01	8.23E+00	3.35E+01	8.40E+00	3.39E+01	8.51E+00	3.46E+01	8.67E+00
29	3.39E+01	8.51E+00	3.47E+01	8.70E+00	3.52E+01	8.82E+00	3.59E+01	9.00E+00	3.64E+01	9.11E+00	3.70E+01	9.29E+00
30	3.63E+01	9.10E+00	3.71E+01	9.30E+00	3.76E+01	9.43E+00	3.84E+01	9.62E+00	3.89E+01	9.74E+00	3.96E+01	9.93E+00
31	3.87E+01	9.70E+00	3.96E+01	9.92E+00	4.01E+01	1.01E+01	4.09E+01	1.03E+01	4.15E+01	1.04E+01	4.22E+01	1.06E+01
32	4.12E+01	1.03E+01	4.21E+01	1.06E+01	4.27E+01	1.07E+01	4.36E+01	1.09E+01	4.41E+01	1.11E+01	4.50E+01	1.13E+01

F. Appendix F – Target Overflight

The purpose of this dissertation is to develop an algorithm to reliably affect target overflight repeatedly, globally, and responsively. All work culminates in the following process. The task is to overfly ten randomly selected targets. At the time of overflight of the first target is also the receipt of the tasking for the second, so this is not an optimization of the order of overflight but a demonstration of how well this algorithm works to satisfy its intended purpose. Since global coverage is achievable within three days for most low-Earth orbit satellites with common EP characteristics, the initial propagation period of three days is standard.

1. Set up maneuvering scenario in STK (start date is arbitrary, but chosen to be 1/1/2012 2400 GMT)
2. Add a non-maneuvering reference satellite ($a = 6878.14$ km, $i = 97°$, $e = 0$, $\Omega = \omega = \nu = 0°$) using HPOP propagator
3. Propagate for 3 days
4. Get LLA (latitude, longitude, altitude) report and export to Excel (columns B and C)
5. Enter target coordinates for first desired overflight
6. Compute absolute difference between satellite and target lat-lon (columns D and E)
7. Compute the basic norm (column F)
8. Compute distance to target using Chapter 5, Eq. (18) (columns G)
9. Compute solutions by subtracting the required Δt from the possible Δt (Chapter 6, Eq. (23)), all negative solutions are not feasible
10. Sort data in ascending order based on solution
11. Eliminate all data points that are not solutions (i.e. acceleration insufficient to reach target in the available time, or solution is negative)
12. Sort remaining data in ascending order based on available time, this is the fastest feasible solution that allows target overflight in the shortest amount of time

13. Use available time and initial conditions to compute the thrusting vs. coasting period (Chapter 7, Eq. (18)) to find ΔV required for the maneuver and the final satellite state

14. Repeat steps 1-13 using the final state from step 13 as the new initial state

For the maneuver campaign discussed in Chapter 7.7.4, the following table summarizes the time, ΔV, and ΔV % required for each one of the ten maneuvers. On average one maneuver requires slightly longer than one day, 35 m/s of ΔV or 0.5% of the total propellant budget.

Maneuver	**Time (s)**	**ΔV (m/s)**	**ΔV %**
1	79425	24.47	0.003765
2	113677	48.473	0.007457
3	55019	24.21	0.003725
4	91140	14.975	0.002304
5	91140	91.14	0.014022
6	115208	75.198	0.011569
7	115200	49.873	0.007673
8	75555	1.293	0.000199
9	71761	11.102	0.001708
10	71761	11.102	0.001708
Total	**879886**	**351.836**	**0.054129**
Average	**1.01 days**	**35.1 m/s**	**0.5 %**

G. Appendix G – Walker Constellation

Fit to Screen

Orbit Dynamics

Return to Navigator

Circular orbit altitude	310.000	310.000	km	***Atmospheric Perturbations***					
Semimajor axis		6688.137	km	Drag coefficient				3.13	
Inclination		96.71	deg	Ballistic coefficient Calculate BC	57.56	*57.56*	57.56		kg/m^2
Eccentricity		0.0000		Atmospheric scale height			51.2		km
Perigee altitude		N/A	km						
Apogee altitude		N/A	km		Min	Mean	Max		
				Atmospheric density	6.37E-12	1.59E-11	3.33E-11		kg/m^3
Repeating ground tracks									
Number of orbits				Change in semi-major axis	-1.805E+02	-4.495E+02	-9.430E+02		km/yr
Number of days Calculate SMA				Change in eccentricity	N/A	N/A	N/A		per day
				Orbit lifetime	2.835E-01	1.138E-01	5.426E-02		years
Basic Dynamics									
Orbit period		90.72	min						
Orbit revolutions per day		15.87	revs/day	***Gravitational Perturbations***					
Orbit energy		-29.80	km^2/sec^2	Node precession rate - J2	9.856E-01	deg/day			
Average orbit angular velocity		1.1543E-03	rad/sec	Node precession rate - Moon	2.487E-05	deg/day			
Average ground velocity		7.36	km/sec	Node precession rate - Sun	1.133E-05	deg/day			
				Total node precession rate	9.856E-01	deg/day			
Satellite velocity (circular)		7.720	km/sec						
Escape velocity (circular)		10.918	km/sec	Node spacing	-22.68	deg/rev			
				Sun synchronous inclination	96.71	deg			
Satellite velocity (at perigee)		N/A	km/sec						
Escape velocity (at perigee)		N/A	km/sec	Perigee rotation rate - J2	N/A	deg/day			
				Perigee rotation rate - Moon	N/A	deg/day			
Satellite velocity (at apogee)		N/A	km/sec	Perigee rotation rate - Sun	N/A	deg/day			
Escape velocity (at apogee)		N/A	km/sec	Total perigee rotation rate	N/A	deg/day			

Fit to Screen

Orbit Geometry

					General Coverage Characteristics - Circular Orbit (or at Perigee)		
Circular orbit altitude		310.000	km		Planet angular radius	72.49	deg
Perigee altitude		N/A	km		Maximum eclipse time	36.53	min
Apogee altitude		N/A	km		Maximum planet central angle	17.51	deg
Inclination		96.71	deg		Range to horizon	2012.597	km
Orbit period		90.72	min		Swath width for overlapping equatorial coverage	22.52	deg
					Swath width	3.04	deg
Minimum elevation angle	60.00	60.00	deg		Swath width	338.808	km
Maximum nadir angle		28.48	deg		Field of regard	56.96	deg
					Slant range to edge of swath	355.233	km
Target latitude		0.0	deg		Instantaneous access area	9.015E+04	km^2
Target longitude			deg		Area access rate	2.494E+03	km^2/sec
Instantaneous longitude of the ascending node			deg				
					Target Viewing - Circular Orbit (or at Perigee)		
					Latitude of the orbit pole	-6.71	deg
					Longitude of the orbit pole on the current pass		deg
					Maximum elevation angle	90.00	deg
					Minimum distance to target	310.000	km
					Maximum angular rate	85.61	deg/min
					Maximum azimuth range	180.00	deg
					Maximum time in view	0.77	min
					Average time in view	0.61	min

Fit to Screen

ΔV Budget

Return to Navigator

Maneuver and Maintenance ΔV		2783.1	m/s	*Total ΔV*		2922.3	m/s	
Elements of the ΔV Budget:								
Orbit Transfer				Percent of ΔV for attitude control		5.0%		
Parking orbit burn		0.0	m/s	Attitude control ΔV		139.2	m/s	
Operational orbit burn		0.0	m/s					
Altitude Maintenance (LEO)		2721.3	m/s					
Stationkeeping (GEO)		0.0	m/s					
Rephasing		0.0	m/s					
Spacecraft Disposal		61.8	m/s					

Mapping and Pointing Budgets

Geometry				*Error Sources*				*Errors* Mapping (km)	*Errors* Pointing (deg)
Altitude		310.000	km	Spacecraft Position Errors					
Planet angular radius		72.49	deg	Along-track	1.0	1.0	m	0.001	0.000
				Cross-track	1.0	1.0	m	0.001	0.000
Elevation angle		60.00	deg	Radial	1.0	1.0	m	0.001	0.000
Nadir angle		28.48	deg						
Planet central angle		1.52	deg	Orientation Errors					
Slant range to edge of swath		355.233	km	Azimuth	0.0010	0.0010	deg	0.003	0.000
				Nadir Angle	0.0010	0.0010	deg	0.007	0.001
Latitude of the target		0.00	deg						
				Other Errors					
				Target altitude	10.0	10.0	m	0.006	N/A
				Spacecraft clock	0.0000	0.0000	sec	0.000	0.000
						Total (RSS):		0.010	0.001

Fit to Screen

Launch Vehicle Information

Return to Navigator

Select Desired Launch Vehicle: Falcon 9

Spacecraft loaded mass	**1427.5**	**kg**

Performance

Mass to orbit		
LEO (low inclination)	**9287.0**	**kg**
LEO (polar or SSO)	**7348.0**	**kg**
GTO	**4540.0**	**kg**
GEO	**1350.0**	**kg**
Available inclinations		
Minimum	**28.5**	**deg**
Maximum	**101.0**	**deg**
Injection accuracies		
Apogee location	**130.0**	**km**
Perigee location	**10.0**	**km**
Inclination	**0.10**	**km**
Flight rate	**8**	**per year**

Reliability experience

Reliability	**100.0%**	
Total flights	**2**	
Successes	**2**	
Partial failures	**0**	
Total failures	**0**	
Down time - last failure	**N/A**	**months**
Down time - average	**N/A**	**months**
Launches since last failure	**N/A**	

Environment

Payload compartment - diameter	**5.2**	**m**
Payload compartment - cylinder length	**6.6**	**m**
Payload compartment - cone length	**4.8**	**m**
Axial acceleration	**6.0**	**g's**
Lateral acceleration	**2.0**	**g's**
Fundamental axial frequency	**25.0**	**Hz**
Fundamental lateral frequency	**15.0**	**Hz**

Estimated Launch Price	**50.0**	**$M**

Fit to Screen

Observation Payload - Optics

Return to Navigator

Altitude		310.000	km	Angular radius of the planet	72.49	deg
Elevation angle		60.00	deg	Swath width	3.04	deg
Nadir angle		28.48	deg	Swath width	338.808	km
				Max range	355.233	km
Angular field of view		56.96	deg	Object plane radius	1.52	deg
				Object plane radius	169.404	km
Wavelength		4.830E-07	m			
Ground resolution at nadir	0.75	0.75	m	Ground resolution at max range	0.99	m
Angular resolution		2.419E-06	rad			
Pixel size		5.000E-06	m	Pixel ground resolution at nadir	0.75	m
Pixel quality factor		1.000		Pixel angular resolution	2.419E-06	rad
				Number of pixels	410886	
Aperture diameter		0.487	m	F Number	4.243	
Focal length		2.067	m	Numerical aperture	0.118	
Image plane radius		1.121	m	Magnification	6.667E-06	

Fit to Screen

System Inputs for Cost Estimation

Mass Estimates (with margin)				**Other Spacecraft Information**				
Payload mass		73.6	kg	Type of payload	Visible Light			
Spacecraft bus dry mass		466.1	kg					
ADCS		22.0	kg	Type of attitude control	Three-axis			
C&DH		11.4	kg	Pointing accuracy	0.010	0.010	deg	
Power		86.6	kg	Pointing knowledge		0.001	deg	
Propulsion		188.0	kg					
Structure		142.9	kg	Number of thrusters		4		
Thermal		9.4	kg					
TT&C		5.7	kg	Data storage capacity		#########	Mb	
Propellant mass		887.9	kg	Downlink data rate		3000.00	Kbps	
				Number of spacecraft	8	8		
Physical Dimension Estimates								
Spacecraft volume		14.275	m^3					
Solar array area		4.675	m^2	**Launch Information**				
Aperture diameter		0.487	m	Number of launches	4	4		
				Cost per launch		50.0	$M	
Power Estimates								
Payload power (with margin)		169.8	W	**Operations Information**				
BOL power		1263.5	W	Mission duration		5	yrs	
EOL power		1113.3	W	Number of FTEs		233		
Average power		588.7	W	FTE - burdened rate		160.0	$K	
Battery capacity		26.7	A-hr	Learning curve slope		95.0%		

Fit to Screen

Summary of the Mission Design

Return to Navigator

Orbit Dynamics		
Semimajor Axis (a)	6688.137	km
Eccentricity (e)	0.0000	
Inclination (i)	96.71	deg
Orbit Period	90.72	min
Estimated Satellites per Orbit Plane	8	

Orbit Geometry		
Minimum Elevation Angle	60.00	deg
Field of Regard	56.96	deg
Swath Width	3.04	deg

Maneuver Characteristics		
Rephasing		
Number of maneuvers		
Rephasing angle per maneuver		deg
Time to complete maneuver		days
ΔV per maneuver		m/s
Lifetime ΔV requirement		m/s
Drag		
Annual ΔV to maintain altitude	544.26	m/s
Lifetime ΔV requirement	2721.30	m/s

Budget Information		
Lifetime ΔV Requirement	2922.27	m/s
RSS Mapping Error	0.01	m

Observation Payload Information		
Resolution at nadir	0.75	m
Resolution at max range	0.99	m
Payload Size		
Aperture Diameter	0.49	m
Mass	61.30	kg
Peak Power	141.50	W
Average Power	141.50	W
Size of one square image	31.2 x 31.2	km
Images collected per orbit	118	
Surface area imaged per orbit	13577730.6	km^2
Image size (scanning sensor)	1488475.8	Mb
Download size	175640141.9	Mb

Downlink Communication Information		
Frequency	2.29	GHz
Data Rate	3.000E+06	bps
Link Margin	3.09	dB

Satellite Information		
Estimated Dry Mass	539.59	kg
Estimated Propellant Mass	887.91	kg
Estimated Total Mass	1427.49	kg
Estimated Peak Power	588.73	W
Estimated Average Power	588.73	W

Cost Information (FY00 - $M)				
Lifecycle Cost	Total	Space Segment	Launch	Ops & Maint
USCM Model	$703.6	$338.1	$200.0	$165.5
Small Satellite Model	$741.1	$375.6	$200.0	$165.5
Space Segment Cost	RDT&E	First Unit	Add'l Units	
USCM Model	$50.0	$44.1	$258.2	
Small Satellite Model	$53.7	$47.5	$278.1	

For the comparison in Chapter 8, three system lifecycles are considered – 1, 3, and 5 years. The design summary for a 5-yr lifecycle is formally discussed in the chapter. The following tables are for the 3-yr and 1-yr lifecycle. It is noteworthy that with the reduction of system life, there are significant savings in propellant and total system mass; however, the total system is not significantly different. Despite the propellant and mass reductions, the number of satellites remains the same at seven or even increase to eight and the number of launches is steady, resulting in total system cost savings of less than 10% in exchange for a lifecycle reduction of 80%.

3-yr Lifecycle

Altitude (km)	# of SC	Aperature (m)	PL Mass (kg)	ΔV (m/s)	Dry Mass (kg)	Prop Mass (kg)	Total Mass (kg)	Const Cost (M$)
283	9	0.445	46.7	3062	454	832	1286	743
300	8	0.47	55.6	2416	418	533	951	625
330	8	0.52	74	1579	424	301	725	629
340	7	0.53	81	1358	434	255	689	572
350	7	0.55	88.3	1166	449	219	668	578
360	7	0.57	96.1	1011	467	192	659	586
370	7	0.58	104.3	876	488	169	657	594
394	7	0.62	125.9	625	547	130	677	616
491	6	0.77	243.7	233	910	75	985	647
651	5	1.02	568	174	1926	117	2043	874
974	4	1.53	1902	249	5951	526	6477	1475
2015	3	3.17	16843	0	46408	0	46408	7198

1-yr Lifecycle

Altitude (km)	# of SC	Aperature (m)	PL Mass (kg)	ΔV (m/s)	Dry Mass (kg)	Prop Mass (kg)	Total Mass (kg)	Const Cost (M$)
283	9	0.445	46.7	1449	283	180	463	612
300	8	0.47	55.6	1072	302	133	435	551
310	8	0.49	61	913	317	115	432	558
330	8	0.52	74	663	353	89	442	575
394	7	0.62	125.9	280	517	52	569	644
491	6	0.77	243.7	157	900	49	949	836
651	5	1.02	568	167	1924	112	2036	873
974	4	1.53	1902	248	5951	524	6475	1475
2015	3	3.17	16843	0	46408	0	46408	7198

Fit to Screen

Summary of the Mission Design

Return to Navigator

Orbit Dynamics			**Observation Payload Information**			**Cost Information (FY00 - $M)**				
Semimajor Axis (a)	6688.137	km	Resolution at nadir	0.75	m	***Lifecycle Cost***	Total	Space Segment	Launch	Ops & Maint
Eccentricity (e)	0.0000		Resolution at max range	0.99	m	USCM Model	$219.4	$91.3	$50.0	$78.1
Inclination (i)	96.71	deg				Small Satellite Model	$228.2	$100.1	$50.0	$78.1
			Payload Size							
Orbit Period	90.72	min	Aperture Diameter	0.49	m	***Space Segment Cost***	RDT&E	First Unit	Add'l Units	
Estimated Satellites per Orbit Plane	8		Mass	61.30	kg	USCM Model	$50.0	$44.1	$0.0	
			Peak Power	141.50	W	Small Satellite Model	$53.7	$47.5	$0.0	
			Average Power	141.50	W					
Orbit Geometry										
Minimum Elevation Angle	60.00	deg	Size of one square image	31.2 x 31.2	km					
Field of Regard	56.96	deg	Images collected per orbit	118						
Swath Width	3.04	deg	Surface area imaged per orbit	13577730.6	km^2					
			Image size (scanning sensor)	1488475.8	Mb					
			Download size	175640141.9	Mb					
Maneuver Characteristics			**Downlink Communication Information**							
Rephasing			Frequency	2.29	GHz					
Number of maneuvers			Data Rate	3.000E+06	bps					
Rephasing angle per maneuver		deg	Link Margin	3.09	dB					
Time to complete maneuver		days								
ΔV per maneuver		m/s	**Satellite Information**							
Lifetime ΔV requirement		m/s	Estimated Dry Mass	539.59	kg					
			Estimated Propellant Mass	887.91	kg					
Drag			Estimated Total Mass	1427.49	kg					
Annual ΔV to maintain altitude	544.26	m/s	Estimated Peak Power	588.73	W					
Lifetime ΔV requirement	2721.30	m/s	Estimated Average Power	588.73	W					
Budget Information										
Lifetime ΔV Requirement	2922.27	m/s								
RSS Mapping Error	0.01	m								

Fit to Screen

Summary of the Mission Design

Return to Navigator

Orbit Dynamics			Observation Payload Information			Cost Information (FY00 - $M)				
Semimajor Axis (a)	6688.137	km	Resolution at nadir	0.75	m	*Lifecycle Cost*	Total	Space Segment	Launch	Ops & Maint
Eccentricity (e)	0.0000		Resolution at max range	0.99	m	USCM Model	$219.4	$91.3	$50.0	$78.1
Inclination (i)	96.71	deg				Small Satellite Model	$228.2	$100.1	$50.0	$78.1
			Payload Size							
Orbit Period	90.72	min	Aperture Diameter	0.49	m	*Space Segment Cost*	RDT&E	First Unit	Add'l Units	
Estimated Satellites per Orbit Plane	8		Mass	61.30	kg	USCM Model	$50.0	$44.1	$0.0	
			Peak Power	141.50	W	Small Satellite Model	$53.7	$47.5	$0.0	
			Average Power	141.50	W					
Orbit Geometry										
Minimum Elevation Angle	60.00	deg	Size of one square image	31.2 x 31.2	km					
Field of Regard	56.96	deg	Images collected per orbit	118						
Swath Width	3.04	deg	Surface area imaged per orbit	13577730.6	km^2					
			Image size (scanning sensor)	1488475.8	Mb					
			Download size	175640141.9	Mb					
Maneuver Characteristics			**Downlink Communication Information**							
Rephasing			Frequency	2.29	GHz					
Number of maneuvers			Data Rate	3.000E+06	bps					
Rephasing angle per maneuver		deg	Link Margin	3.09	dB					
Time to complete maneuver		days								
ΔV per maneuver		m/s	**Satellite Information**							
Lifetime ΔV requirement		m/s	Estimated Dry Mass	539.59	kg					
			Estimated Propellant Mass	887.91	kg					
Drag			Estimated Total Mass	1427.49	kg					
Annual ΔV to maintain altitude	544.26	m/s	Estimated Peak Power	588.73	W					
Lifetime ΔV requirement	2721.30	m/s	Estimated Average Power	588.73	W					
Budget Information										
Lifetime ΔV Requirement	2922.27	m/s								
RSS Mapping Error	0.01	m								

Fit to Screen

Summary of the Mission Design

Return to Navigator

Orbit Dynamics		
Semimajor Axis (a)	6678.137	km
Eccentricity (e)	0.0000	
Inclination (i)	96.67	deg
Orbit Period	90.52	min
Estimated Satellites per Orbit Plane	8	

Orbit Geometry		
Minimum Elevation Angle	60.00	deg
Field of Regard	57.05	deg
Swath Width	2.95	deg

Maneuver Characteristics		
Rephasing		
Number of maneuvers		
Rephasing angle per maneuver		deg
Time to complete maneuver		days
ΔV per maneuver		m/s
Lifetime ΔV requirement		m/s
Drag		
Annual ΔV to maintain altitude	667.68	m/s
Lifetime ΔV requirement	3338.41	m/s

Budget Information		
Lifetime ΔV Requirement	3567.22	m/s
RSS Mapping Error	0.01	m

Observation Payload Information		
Resolution at nadir	0.75	m
Resolution at max range	0.99	m
Payload Size		
Aperture Diameter	0.47	m
Mass	55.60	kg
Peak Power	128.30	W
Average Power	128.30	W
Size of one square image	29.7 x 29.7	km
Images collected per orbit	122	
Surface area imaged per orbit	13162385.9	km^2
Image size (scanning sensor)	1395507.6	Mb
Download size	170251922.4	Mb

Downlink Communication Information		
Frequency	2.29	GHz
Data Rate	3.000E+06	bps
Link Margin	3.09	dB

Satellite Information		
Estimated Dry Mass	457.67	kg
Estimated Propellant Mass	847.20	kg
Estimated Total Mass	1304.87	kg
Estimated Peak Power	505.78	W
Estimated Average Power	505.78	W

Cost Information (FY00 - $M)				
Lifecycle Cost	Total	Space Segment	Launch	Ops & Maint
USCM Model	$689.2	$326.6	$200.0	$162.6
Small Satellite Model	$914.8	$552.1	$200.0	$162.6
Space Segment Cost	RDT&E	First Unit	Add'l Units	
USCM Model	$47.1	$38.8	$227.6	
Small Satellite Model	$66.8	$68.0	$398.2	

Bibliography

AFRL, Space Vehicles Directorate. *XSS-11 Micro Satellite*. AFD-070404-108, no date [2005] http://www.kirtland.af.mil/shared/media/document/AFD-070404-108.pdf.

Alfano, S. *Low Thrust Orbit Transfer*. MS Thesis. Graduate School of Engineering and Management, Air Force Institute of Technology (AU), Wright-Patterson, AFB OH, 1982 (ADA).

Arkin, William M. "Air Force Seeks to Power Space Maneuver Vehicle," *Defense Daily*, 31 May 2000.

ARSTRAT, Technical Center. *NanoEye*. Technical factsheet, no date [2011] http://www.smdc.army.mil/FactSheets/NanoEye.pdf.

Baumann, H. and Oberle, H. "Numerical Computation of Optimal Trajectories for Coplanar, Aeroassisted Orbital Transfer," *Journal of Optimization Theory and Applications*, Vol. 107, No. 3: 457-479 (December 2000).

Berlocher, G. "Military Continues to Influence Commercial Operators," Satellite Today, 1 September 2008 http://www.satellitetoday.com/military/milsatcom/Military-Continues-To-Influence-Commercial-Operators_24295.html.

Busek Space Propulsion. *Hall Effect Thruster Systems*. Natick MA, no date [2012] http://www.busek.com/technologies__hall.htm.

Chioma, Vincent J. *Navigation Solutions to enable Space Superiority through the Repeated Intercept Mission*. Air Force Institute of Technology (AU), Wright-Patterson AFB OH, September 2004 (ADA).

Co, T. and Black, J., "A Taskable Space Vehicle: Realizing Cost Savings by Combining Orbital and Suborbital Flight", *Air & Space Power Journal*, Volume XXV, No. 2: 74-80 (Summer 2011).

Co, T., Zagaris, C., and Black, J. "Responsive Satellites through Ground Track Manipulation using Existing Technology," *AIAA Space 2011 Conference and Exposition*, AIAA-2011-7262. Long Beach, CA (September 2011).

Co, T., Zagaris, C., and Black, J. "Responsive Satellites through Ground Track Manipulation using Existing Technology," *accepted for publication in AIAA Journal for Spacecraft and Rockets*, AIAA-2011-10-A32263: 9 (November 2011).

Co, T., Zagaris, C., and Black, J. "Optimal Low Thrust Profiles for Responsive Satellites," *Submitted to Acta Astronautica*, Submission Reference #AA-D-12-00391 (April 2012).

Co, T. and Black, J. "Responsiveness in Low Orbits using Electric Propulsion," *Submitted to AIAA Journal for Spacecraft and Rockets*, AIAA-2012-04-A32405: 9-12 (April 2012).

Darby, Christopher L. and Rao, Anil V. "Minimum-Propellant Low-Earth Orbit Aero-assisted Orbital Transfer of Small Spacecraft," *Journal of Spacecraft and Rockets*, Vol. 48, No. 4: 618-628 (2011)

Dankanich, John W. "Electric Propulsion Performance from Geo-transfer to Geosynchronous Orbits," *30th International Electric Propulsion Conference*. Florence: September 2007.

Doggrell, L. "Operationally Responsive Space, A Vision for the Future of Military Space," *Air & Space Power Journal*, Vol. 20, no. 2 (Summer 2006).

Duhamel, T. "Implementation of Electric Propulsion for North-South Station-Keeping on the EUROSTAR Spacecraft," *AAS/AIAA Astrodynamics Conference*, AIAA 89-2274. Stowe VT: Aug 1989.

Elachi, C. *Introduction to the Physics and Techniques of Remote Sensing*. New York: Wiley, 1987.

Forte, F., Siant Aubert, P., and Buthion, C. "Benefits of Electric Propulsion for Orbit Injection of Communication Spacecraft," *14th AIAA International Communication Satellite Systems Conference*. Washington: March 1992.

"Wideband Gapfiller System," *GlobalSecurity.org*, 10 April 2005 http://www.globalsecurity.org/space/systems/wgs-schedule.htm.

Gogu, C., Matsumura, T., Haftka, R., and Rao, Anil V., "Aeroassisted Orbital Transfer Trajectory Optimization Considering Thermal Protection System Mass," *Journal of Guidance, Control and Dynamics*, Vol. 32, No. 3: 927-938 (May 2009).

Gopinath, N. S. and Srinivasamuthy, K. N. "Optimal Low Thrust Orbit transfer from GTO to Geosynchronous Orbit and Stationkeeping using Electric Propulsion System," *54th International Astronautical Congress*, IAC-03-A.7.03. Bremen Germany: September 2003.

Guelman, M. and Kogan, A. "Electric Propulsion for Remote Sensing from Low Orbits," *Journal of Guidance, Control, and Dynamics*, Vol. 22, No. 2: 313-321 (1999).

Habraken, S., Defise, J., Collette, J., Rochus, P., D'Odemont, P., and Hogge, M., "Space Solar Arrays and Concentrators", *51st International Astronautical Congress*. Rio de Janeiro: October 2000.

Hall, Timothy S. *Orbit Maneuver for Responsive Coverage using Electric Propulsion*, Air Force Institute of Technology (AU), Wright-Patterson AFB OH, March 2010 (ADA).

Hicks, Kerry D. *Introduction to Astrodynamic Reentry*. AFIT/EN/TR-09-03. Wright-Patterson AFB OH, Graduate School of Engineering and Management (September 2009).

Ivashkin, V.V. and Typitsin, N. N. "Use of the Moon's Gravitational Field to Inject a Space Vehicle into a Stationary Earth-Satellite Orbit," *Cosmic Res*, Vol. 9, No. 2: 163-172 (1971).

Jean, I. and de Lafontaine, J. "Autonomous Guidance and Control of an Earth Observation Satellite Using Low Thrust," *Advances in the Astronautical Sciences*, Vol. 116, Part 3, No. AAS 03-617: 1829-1844 (2003).

Jones, R. M. "Comparison of Potential Electric Propulsion Systems for Orbit Transfer," *Journal of Spacecraft and Rockets*, Vol. 21, No. 1 (Jan 1984).

Kantsiper, Brian L., Stadter, Patrick A., and Stewart, Pamela L. "ORS HEO Constellations for Continuous Availability," *5th Responsive Space Conference*. Los Angeles: April 2007.

Kaufman, H. R. and Robinson, R. S. "Electric Thruster Performance for Orbit Raising and Maneuvering," *Journal of Spacecrafts and Rockets*, Vol. 21, No. 2 (Mar 1984).

Kechichian, J. A., "Optimal Low-Thrust Rendezvous Using Equinoctial Orbit Elements", Acta Astronautica, Vol. 38, No. 1: 1-14 (1996).

Larrimore, Scott C. "Partially Continuous Earth Coverage from a Responsive Space Constellation," *5th Responsive Space Conference*. Los Angeles: 2007.

Larson, W. and Wertz, J. *Space Mission Analysis and Design* (3rd Edition), El Segundo CA: Microcosm Press, 2004.

Lawden, D. F. *Optimization Techniques*, ed. G. Leitmann. New York: Academic Press, 1962.

Lawden, D. F. *Optimal Trajectories for Space Navigation*, London: Butterworth, 1963.

Marec, J.-P. *Optimal Space Trajectories*, Oxford: Elsevier Scientific Publishing Company, 1979.

Mathur, R. and Ocampo, Cesar A. "An Algorithm for Computing Optimal Earth Centered Orbit Transfers via Lunar Gravity Assist," *AIAA/AAS Conference*. Toronto: August 2010.

Mease, K. D. "Aeroassisted Orbital Transfer: Current Status," *The Journal of the Astronautical Sciences*, Vol. 36, No. ½: 7-33 (1988).

NASA, Jet Propulsion Laboratory. *Mars Reconnaissance Orbiter*. Pasadena CA. No date [2005] http://marsprogram.jpl.nasa.gov/mro/mission/overview/.

Newberry, R. "Powered Spaceflight for Responsive Space Systems," *High Frontier*, Vol.1, No. 4: 46-49 (Summer 2005).

Ocampo, Cesar A. "Transfers to Earth Centered Orbits via Lunar Gravity Assist," *Acta Astronautica*, 52: 173-179 (2003).

Ocampo, Cesar A. "Trajectory Analysis for the Lunar Flyby Rescue of AsiaSat-3/HGS-1," Annals of N.Y. Academy of Science, 1065: 232-253 (2005).

Pielke, Roger A., Jr. "Space Shuttle Value Open to Interpretation," *Aviation Week*, 26 July 1993: 57.

Rao, Anil V., Scherich, Arthur E., and Cox, S. "A Concept for Operationally Responsive Space Mission Planning Using Aeroassisted Orbital Transfer," *6th Responsive Space Conference*. Los Angeles: Apr 2008.

Rayman, M.D., Varghese, P., Lehman, D.H., and Livesay, L.L. "Results from the Deep Space 1 Technology Validation Mission," *Acta Astronautica*, 47: 475-487 (2000).

Ross, I. and Nicholson, J. "Optimality of the Heating-Rate-Constrained Aerocruise Maneuver," *Journal of Spacecraft and Rockets*, Vol. 35, No. 3: 361-364 (May 1998).

Saccoccia, G., Gonzales del Amo, J., and Estublier, D. "Electric Propulsion: A Key Technology for Space Mission in the New Millenium," *ESA Bulletin 101*: 1-2 (February 2000).

Saccoccia, G. "Electric Propulsion," *ESA Publications Division*, BR-187: 9 (July 2002).

Schaub, H. and Junkins, J. L. *Analytical Mechanics of Space Systems*. Reston VA: American Institute of Aeronautics and Astronautics Press, 2003.

Sinnott, R. W. "Virtues of the Haversine," *Sky and Telescope*, Vol. 68, No. 2: 159 (1984).

Smith, R. "Look Ma! No (Human) Hands!," *NASA Space News*. 5 Mar 2007 http://science.nasa.gov/science-news/science-at-nasa/2007/05mar_nohands/.

Spires, David N. *Beyond Horizons: A Half Century of Air Force Space Leadership*, rev. ed. Peterson AFB, CO: Air Force Space Command in association with Air University Press, 1998.

Spitzer, A. "Near Optimal Transfer Orbit Trajectory Using Electric Propulsion," *AAS/AIAA Spaceflight Mechanics Conference*, AAS Paper 95-215. Albuquerque NM, 1995.

Tether, T., Director Defense Advanced Research Projects Agency. Statement to the House Armed Services Committee. 5. Washington, March 2003.

Thorne, J. D., *Optimal Continuous-Thrust Orbit Transfers*. Graduate School of Engineering and Management, Air Force Institute of Technology (AU), Wright-Patterson AFB OH, 1996 (ADA).

Vallado, D. *Fundamentals of Astrodynamics and Applications* (2nd Edition). El Segundo CA: Microcosm Press, 2001.

Vaughan, C. E. and Cassady, R. J. "An Updated Assessment of Electric Propulsion Technology for Near-Earth Space Missions," *28th AIAA Joint Propulsion Conference*, AIAA 92-3202. Nashville TN: Jul 1992.

Vinh, Nguyen X. and Shih, Y. "Optimum Multiple Skip Trajectories," *Acta Astronautica*, Vol 41, No 2: 103-112 (1997).

Walberg, G. D. "A Survey of Aeroassisted Orbit Transfer," *Journal of Spacecraft and Rockets*, Vol. 22, No. 1: 3-18 (1985).

Walker, J. G. "Continuous Whole-Earth Coverage by Circular-Orbit Satellite Patterns," RAE Technical Report 77044, 1977.

Ward, John E. "Reusable Launch Vehicles: Rethinking Access to Space," Air War College, Center for Strategy and Technology. Occassional Paper No. 12. Maxwell AFB AL, May 2000.

Wertz, James R. *Mission Geometry; Orbit and Constellation Design and Management*. El Segundo CA: Microcosm Press, 2001.

Wertz, James R. "Coverage, Responsiveness, and Accessibility for Various 'Responsive Orbits'," *3rd Responsive Space Conference*. Los Angeles: April 2005.

Wertz, James R. *Responsive Space Mission Analysis and Design*. El Segundo CA: Microcosm Press, 2007.

Wertz, James R. "Circular vs. Elliptical Orbits for Persistent Communications," *5th Responsive Space Conference*. Los Angeles: April 2007.

Wiesel, W.E. and Alfano, S. "Optimal Many-Revolution Orbit Transfer", *Journal of Guidance, Control, and Dynamics*, Vol. 8, No. 1: 155-157 (1985).

Wiesel, William E. *Spaceflight Dynamics* (3rd Edition). Beavercreek OH: Aphelion Press, 2003.

Wiesel, William E. *Modern Astrodynamics*. Beavercreek OH: Aphelion Press, 2003.

Zagaris, C. "Trajectory Control and Optimization for Responsive Spacecraft", MS Thesis, Graduate School of Engineering and Management, Air Force Institute of Technology, Wright-Patterson AFB OH, March 2012 (ADA).

Zimmerman, F. and Calise, A. J. "Numerical Optimization Study of Aeroassisted Orbital transfer," *Journal of Guidance, Control, and Dynamics*, Vol. 21, No. 1: 127-133 (Jan-Feb 1998).

Vita

Thomas C. Co is a Major Select in the U.S. Air Force studying at the Air Force Institute of Technology, Wright-Patterson AFB, OH. His study areas are in Orbital Mechanics and Space Operations with a focus on maneuverable satellites. Prior to starting his assignment at AFIT, he held several technical and leadership positions in the Air Force.

His last duty station was Schriever AFB, CO. He was the Operations Flight Commander of the 3rd Space Operations Squadron responsible for all crew operations to maintain a fleet of communication satellites – DSCS and WGS. He supervised 60+ personnel, both officers and enlisted, for day-to-day operations. His other assignments there were Chief of Engineering and WGS Engineering Officer,

At Edwards AFB, CA, Captain Co was in charge of operational testing for the B-2 Avionics Midlife Improvement. He led a team of operational fliers, developmental testers, and contractor engineers to provide a critical upgrade to the bomber fleet to extend its life to 2050. Prior to that, he was stations at Los Angeles AFB, CA during his initial flight training. He holds a private pilot license for small, single engine aircraft.

Captain Co completed his Master's (2002) and Bachelor's (2001) in Aerospace Engineering at the University of California, Irvine. He also has a Bachelor's degree in International Studies from the same university. He spent one year in Sydney, Australia as an exchange student at the University of Sydney. Captain Co is fluent in three languages and has basic in-country training for a forth. He is assigned to the Air Force Research Laboratory upon completion of his doctorate.

REPORT DOCUMENTATION PAGE		Form Approved OMB No. 0704–0188

1. REPORT DATE (DD–MM–YYYY)	2. REPORT TYPE	3. DATES COVERED (From — To)
13-09-2012	Dissertation	Sept 2009 – Sept 2012

4. TITLE AND SUBTITLE	5a. CONTRACT NUMBER
Operationally Responsive Spacecraft Using Electric Propulsion	5b. GRANT NUMBER
	5c. PROGRAM ELEMENT NUMBER
6. AUTHOR(S)	5d. PROJECT NUMBER
Co, Thomas C., Captain, USAF	5e. TASK NUMBER
	5f. WORK UNIT NUMBER
7. PERFORMING ORGANIZATION NAME(S) AND ADDRESS(ES) Air Force Institute of Technology Graduate School of Engineering and Management (AFIT/ENY) 2950 Hobson Way WPAFB OH 45433-7765	8. PERFORMING ORGANIZATION REPORT NUMBER AFIT/DS/ENY/12-01
9. SPONSORING / MONITORING AGENCY NAME(S) AND ADDRESS(ES) Intentionally left blank	10. SPONSOR/MONITOR'S ACRONYM(S)
	11. SPONSOR/MONITOR'S REPORT NUMBER(S)

12. DISTRIBUTION / AVAILABILITY STATEMENT

APPROVED FOR PUBLIC RELEASE; DISTRIBUTION IS UNLIMITED

13. SUPPLEMENTARY NOTES

The views expressed in this dissertation are those of the author and do not reflect the official policy or position of the United States Air Force, Department of Defense, or the U.S. Government.

14. ABSTRACT

A desirable space asset is responsive and flexible to mission requirements, low-cost, and easy to acquire. Highly-efficient electric thrusters have been considered a viable technology to provide these characteristics; however, it has been plagued by limitations and challenges such that operational implementation has been severely limited. The technology is constantly improving, but even with current electric propulsion, a spacecraft is capable of maneuvering consistently and repeatedly in low-Earth orbit to provide a responsive and flexible system. This research develops the necessary algorithm and tools to demonstrate that EP systems can maneuver significantly in a timely fashion to overfly any target within the satellite's coverage area. An in-depth analysis of a reconnaissance mission reveals the potential the proposed spacecraft holds in today's competitive, congested, and contested environment. Using Space Mission Analysis and Design concepts along with the developed algorithm, an observation mission is designed for three conventional methods and compared to the proposed responsive system. Analysis strongly supports that such a spacecraft is capable of reliable target overflight at the same cost as non-maneuvering ones, while it is three times as responsive in terms of time-to-overflight by sacrificing one third of its mission life. An electric versus a chemical system can maneuver 5.3 times more. Its responsiveness and mission life are slightly inferior to that of a Walker constellation, but cuts total system cost by almost 70%.

15. SUBJECT TERMS

Maneuvering satellites, Operationally Responsive Space, Orbital Mechanics, Electric propulsion, Novel orbits

16.SECURITY CLASSIFICATION OF: **Unclassified**			17. LIMITATION OF ABSTRACT	18. NUMBER OF PAGES	19a. NAME OF RESPONSIBLE PERSON
a. REPORT	b. ABSTRACT	c. THIS PAGE	UU	280	Dr. Jonathan T. Black
U	U	U			19b. TELEPHONE NUMBER (Include Area Code) (937) 255-6565, ext 4578 (jonathan.black@afit.edu)